

Non-Abelian anyons and topological quantum computation

Chetan Nayak

*Microsoft Station Q, University of California, Santa Barbara, California 93108, USA
and Department of Physics and Astronomy, University of California, Los Angeles, California
90095-1547, USA*

Steven H. Simon

Atcatel-Lucent, Bell Labs, 600 Mountain Avenue, Murray Hill, New Jersey 07974, USA

Ady Stern

*Department of Condensed Matter Physics, Weizmann Institute of Science, Rehovot
76100, Israel*

Michael Freedman

Microsoft Station Q, University of California, Santa Barbara, California 93108, USA

Sankar Das Sarma

Department of Physics, University of Maryland, College Park, Maryland 20742, USA

(Published 12 September 2008)

Topological quantum computation has emerged as one of the most exciting approaches to constructing a fault-tolerant quantum computer. The proposal relies on the existence of topological states of matter whose quasiparticle excitations are neither bosons nor fermions, but are particles known as non-Abelian anyons, meaning that they obey non-Abelian braiding statistics. Quantum information is stored in states with multiple quasiparticles, which have a topological degeneracy. The unitary gate operations that are necessary for quantum computation are carried out by braiding quasiparticles and then measuring the multi-quasiparticle states. The fault tolerance of a topological quantum computer arises from the nonlocal encoding of the quasiparticle states, which makes them immune to errors caused by local perturbations. To date, the only such topological states thought to have been found in nature are fractional quantum Hall states, most prominently the $\nu=5/2$ state, although several other prospective candidates have been proposed in systems as disparate as ultracold atoms in optical lattices and thin-film superconductors. In this review article, current research in this field is described, focusing on the general theoretical concepts of non-Abelian statistics as it relates to topological quantum computation, on understanding non-Abelian quantum Hall states, on proposed experiments to detect non-Abelian anyons, and on proposed architectures for a topological quantum computer. Both the mathematical underpinnings of topological quantum computation and the physics of the subject are addressed, using the $\nu=5/2$ fractional quantum Hall state as the archetype of a non-Abelian topological state enabling fault-tolerant quantum computation.

DOI: [10.1103/RevModPhys.80.1083](https://doi.org/10.1103/RevModPhys.80.1083)

PACS number(s): 05.30.Pr, 03.67.Lx, 03.67.Pp, 73.43.-f

CONTENTS

I. Introduction	1084	4. A fractional quantum Hall quantum computer	1101
II. Basic Concepts	1085	5. Physical systems and materials considerations	1102
A. Non-Abelian anyons	1085	D. Other proposed non-Abelian systems	1103
1. Non-Abelian braiding statistics	1085	III. Topological Phases of Matter and Non-Abelian Anyons	1106
2. Emergent anyons	1089	A. Topological phases of matter	1107
B. Topological quantum computation	1090	1. Chern-Simons theory	1107
1. Basics of quantum computation	1090	2. TQFTs and quasiparticle properties	1109
2. Fault tolerance from non-Abelian anyons	1092	B. Superconductors with $p+ip$ pairing symmetry	1113
C. Non-Abelian quantum Hall states	1094	1. Vortices and fermion zero modes	1113
1. Rapid review of quantum Hall physics	1094	2. Topological properties of $p+ip$ superconductors	1115
2. Possible non-Abelian states	1096	C. Chern-Simons effective field theories, the Jones polynomial, and non-Abelian topological phases	1117
a. $5/2$ state	1097	1. Chern-Simons theory and link invariants	1117
b. $12/5$ state	1098	2. Combinatorial evaluation of link invariants and quasiparticle properties	1119
c. Other quantum Hall states	1099		
3. Interference experiments	1099		

D. Chern-Simons theory, conformal field theory, and fractional quantum Hall states	1121
1. The relation between Chern-Simons theory and conformal field theory	1121
2. Quantum Hall wave functions from conformal field theory	1123
a. Wave functions from CFTs	1124
b. Quasiparticle braiding	1124
c. The Laughlin state	1125
d. Moore-Read Pfaffian state	1126
e. Z_3 Read-Rezayi state (briefly)	1127
E. Edge excitations	1128
F. Interferometry with anyons	1131
G. Lattice models with P, T -invariant topological phases	1134
IV. Quantum Computing with Anyons	1137
A. $\nu=5/2$ qubits and gates	1137
B. Fibonacci anyons: A simple example that is universal for quantum computation	1138
1. Structure of the Hilbert space	1139
2. Braiding Fibonacci anyons	1140
3. Computing with Fibonacci anyons	1141
4. Other theories	1142
C. Universal topological quantum computation	1142
D. Errors	1144
V. Future Challenges for Theory and Experiment	1146
Note added in proof	1149
Acknowledgments	1149
Appendix: Conformal Field Theory for Nonexperts	1149
1. OPE	1149
2. Conformal blocks	1150
3. Changing bases	1150
4. The chiral boson	1151
References	1151

I. INTRODUCTION

In recent years, physicists' understanding of the quantum properties of matter has undergone a major revolution, precipitated by surprising experimental discoveries and profound theoretical revelations. Landmarks include the discoveries of the fractional quantum Hall effect and high-temperature superconductivity, and the advent of topological quantum field theories. At the same time, new potential applications for quantum matter burst on the scene, punctuated by the discoveries of Shor's factorization algorithm and quantum error correction protocols. Remarkably, there has been a convergence between these developments. Nowhere is this more dramatic than in topological quantum computation, which seeks to exploit the emergent properties of many-particle systems to encode and manipulate quantum information in a manner that is resistant to error.

It is rare for a new scientific paradigm, with its attendant concepts and mathematical formalism, to develop in parallel with potential applications, with all of their detailed technical issues. However, the physics of topological phases of matter is not only evolving alongside topological quantum computation but is even informed by it. Therefore this review must necessarily be rather sweeping in scope, introducing the concepts of non-

Abelian anyons and topological quantum computation, their interconnections, and how they may be realized in physical systems, particularly in several fractional quantum Hall states. [For a popular account, see [Collins \(2006\)](#); for a slightly more technical one, see [Das Sarma, Freedman, *et al.* \(2006\)](#).] This exposition will take us on a tour extending from knot theory and topological quantum field theory to conformal field theory and the quantum Hall effect to quantum computation and all the way to the physics of gallium arsenide devices.

The body of this paper is composed of three parts: Secs. II–IV. Section II is rather general, avoids technical details, and aims to introduce concepts at a qualitative level. Section II should be of interest, and should be accessible, to all readers. In Sec. III we describe the theory of topological phases in more detail. In Sec. IV, we describe how a topological phase can be used as a platform for fault-tolerant quantum computation. The second and third parts are probably of more interest to theorists, experienced researchers, and those who hope to conduct research in this field.

Section II.A.1 begins by discussing the concept of braiding statistics in $2+1$ dimensions. We define the idea of a non-Abelian anyon, a particle exhibiting non-Abelian braiding statistics. Section II.A.2 discusses how non-Abelian anyons can arise in a many-particle system. We then review the basic ideas of quantum computation and the problems of errors and decoherence in Sec. II.B.1. We explain in Sec. II.B.2 how non-Abelian statistics naturally leads to the idea of topological quantum computation, and explain why it is a good approach to error-free quantum computation. In Sec. II.C, we describe the non-Abelian quantum Hall systems which are the most likely arena for observing non-Abelian anyons (and hence for producing a topological quantum computer). Section II.C.1 gives a review of quantum Hall physics. Section II.C.2 introduces non-Abelian quantum Hall states. This section also explains the importance of numerical work in this field for determining which quantum Hall states are non-Abelian. Section II.C.3 describes some of the proposed interference experiments which may be able to distinguish Abelian from non-Abelian quantum Hall states. Section II.C.4 shows how qubits and elementary gates can be realized in a quantum Hall device. Section II.C.5 discusses some of the engineering issues associated with the physical systems where quantum Hall physics is observed. In Sec. II.D we discuss some of the other, non-quantum-Hall, systems where it has been proposed that non-Abelian anyons (and hence topological quantum computation) might occur.

Sections III and IV are written to be accessible to the broadest possible audiences, but they might be somewhat harder going than Sec. II. Section III introduces the theory of topological phases in detail. Topological quantum computation can become a reality only if some physical system “condenses” into a non-Abelian topological phase. In Sec. III, we describe the universal low-energy, long-distance physics of such phases. We also discuss how they can be experimentally detected in the

quantum Hall regime, and when they might occur in other physical systems. Our focus is on a sequence of universality classes of non-Abelian topological phases, associated with $SU(2)_k$ Chern-Simons theory, described in Sec. III.A. The first interesting member of this sequence, $k=2$, is realized in chiral p -wave superconductors and in the leading theoretical model for the $\nu=5/2$ fractional quantum Hall state. Section III.B shows how this universality class can be understood with conventional BCS theory. In Sec. III.C, we describe how the topological properties of the entire sequence of universality classes (of which $k=2$ is a special case) can be understood using Witten's connection between Chern-Simons theory and the Jones polynomial of knot theory. In Sec. III.D, we describe an alternate formalism for understanding the topological properties of Chern-Simons theory, namely, through conformal field theory. The discussion revolves around the application of this formalism to fractional quantum Hall states and explains how non-Abelian quantum Hall wave functions can be constructed with conformal field theory. The Appendix gives an introduction to conformal field theory. In Sec. III.E, we discuss the gapless edge excitations which necessarily accompany chiral [i.e., parity- (P -) and time-reversal- (T -) violating] topological phases. These excitations are useful for interferometry experiments, as discussed in Sec. III.F. Finally, in Sec. III.G, we discuss topological phases that do not violate parity and time-reversal symmetries. These phases emerge in models of electrons, spins, or bosons on lattices which could describe transition metal oxides, Josephson junction arrays, or ultracold atoms in optical lattices.

In Sec. IV, we discuss how quasiparticles in topological phases can be used for quantum computation. We first discuss the case of $SU(2)_2$, which is the leading candidate for the $\nu=5/2$ fractional quantum Hall state. We show in Sec. IV.A how qubits and gates can be manipulated in a gated GaAs device supporting this quantum Hall state. We discuss why quasiparticle braiding alone is not sufficient for universal quantum computation and how this limitation of the $\nu=5/2$ state can be circumvented. Section IV.B discusses how topological computations can be performed in the simplest non-Abelian theory that is capable of universal topological quantum computation, the so-called Fibonacci anyon theory. In Sec. IV.C, we show that the $SU(2)_k$ theories support universal topological quantum computation for all integers k except $k=1, 2, 4$. In Sec. IV.D, we discuss the physical processes that will cause errors in a topological quantum computer.

Finally, we conclude in Sec. V. We discuss questions for the immediate future, primarily centered on the $\nu=5/2$ and $12/5$ fractional quantum Hall states. We also discuss a broader set of questions relating to non-Abelian topological phases and fault-tolerant quantum computation.

II. BASIC CONCEPTS

A. Non-Abelian anyons

1. Non-Abelian braiding statistics

Quantum statistics is one of the basic pillars of the quantum mechanical view of the world. It is the property that distinguishes fermions from bosons: the wave function that describes a system of many identical particles should satisfy the proper symmetry under the interchange of any two particles. In three spatial dimensions and one time dimension $[(3+1)D]$ there are only two possible symmetries—the wave function of bosons is symmetric under exchange while that of fermions is antisymmetric. One cannot overemphasize, of course, the importance of the wave function symmetry, which is the root of the Pauli principle, superfluidity, the metallic state, Bose-Einstein condensation, and a long list of other phenomena.

The limitation to one of two possible types of quantum symmetry originates from the observation that a process in which two particles are adiabatically interchanged twice is equivalent to a process in which one of the particles is adiabatically taken around the other. Since, in three dimensions, wrapping one particle all the way around another is topologically equivalent to a process in which none of the particles move at all, the wave function should be left unchanged by two such interchanges of particles. The only two possibilities are for the wave function to change by a \pm sign under a single interchange, corresponding to the cases of bosons and fermions, respectively.

We can recast this in path integral language. Suppose we consider all possible trajectories in $3+1$ dimensions which take N particles from initial positions R_1, R_2, \dots, R_N at time t_i to final positions R_1, R_2, \dots, R_N at time t_f . If the particles are distinguishable, then there are no topologically nontrivial trajectories, i.e., all trajectories can be continuously deformed into the trajectory in which the particles do not move at all (straight lines in the time direction). If the particles are indistinguishable, then the different trajectories fall into topological classes corresponding to the elements of the permutation group S_N , with each element of the group specifying how the initial positions are permuted to obtain the final positions. To define the quantum evolution of such a system, we must specify how the permutation group acts on the states of the system. Fermions and bosons correspond to the only two one-dimensional irreducible representations of the permutation group of N identical particles.¹

Two-dimensional systems are qualitatively different from those in three (and higher dimensions) in this respect. [For a pedagogical review, see [Stern \(2008\)](#).] A particle loop that encircles another particle in two di-

¹Higher-dimensional representations of the permutation group, known as “parastatistics,” can always be decomposed into fermions or bosons with an additional quantum number attached to each particle ([Doplicher *et al.*, 1971, 1974](#)).

mensions cannot be deformed to a point without cutting through the other particle. Consequently, the notion of a winding of one particle around another in two dimensions is well defined. Thus, when two particles are interchanged twice in a clockwise manner, their trajectory involves a nontrivial winding, and the system does not necessarily come back to the same state. This topological difference between two and three dimensions, first realized by [Leinaas and Myrheim \(1977\)](#) and [Wilczek \(1982a\)](#), leads to a difference in the possible quantum mechanical properties for quantum systems when particles are confined to (2+1)D (see also [Goldin *et al.*, 1981](#) and [Wu, 1984](#)). [As an aside, we mention that in (1+1)D quantum statistics is not well defined since particle interchange is impossible without one particle going through another, and bosons with hard-core repulsion are equivalent to fermions.]

Suppose that we have two identical particles in two dimensions. Then, when one particle is exchanged in a counterclockwise manner with the other, the wave function can change by an arbitrary phase,

$$\psi(\mathbf{r}_1, \mathbf{r}_2) \rightarrow e^{i\theta} \psi(\mathbf{r}_1, \mathbf{r}_2). \tag{1}$$

The phase need not be merely a \pm sign because a second counterclockwise exchange need not lead back to the initial state but can result in a nontrivial phase:

$$\psi(\mathbf{r}_1, \mathbf{r}_2) \rightarrow e^{2i\theta} \psi(\mathbf{r}_1, \mathbf{r}_2). \tag{2}$$

The special cases $\theta=0, \pi$ correspond to bosons and fermions, respectively. Particles with other values of the statistical angle θ are called *anyons* ([Wilczek, 1990](#)). We refer to such particles as anyons with statistics θ .

We now consider the general case of N particles, where a more complex structure arises. The topological classes of trajectories which take these particles from initial positions R_1, R_2, \dots, R_N at time t_i to final positions R_1, R_2, \dots, R_N at time t_f are in one-to-one correspondence with the elements of the braid group \mathcal{B}_N . An element of the braid group can be visualized by thinking of trajectories of particles as world lines (or strands) in (2+1)-dimensional space-time originating at initial positions and terminating at final positions, as shown in Fig. 1. The time direction will be represented vertically on the page, with the initial time at the bottom and the final time at the top. An element of the N -particle braid group is an equivalence class of such trajectories up to smooth deformations. To represent an element of a class, we draw the trajectories on paper with the initial and final points ordered along lines at the initial and final times. When drawing the trajectories, we must be careful to distinguish when one strand passes over or under another, corresponding to a clockwise or counterclockwise exchange. We also require that any intermediate time slice must intersect N strands. Strands cannot “double back,” which would amount to particle creation or annihilation at intermediate stages. We do not allow this because we assume that the particle number is known. (We consider particle creation and annihilation later when discussing field theories of anyons and, from

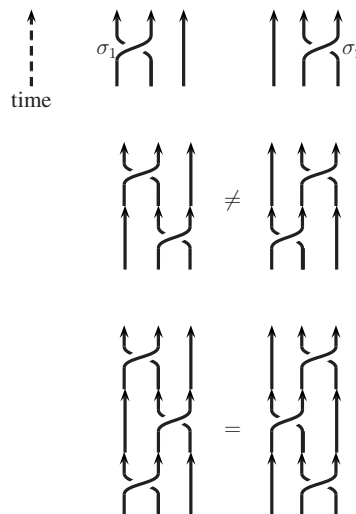


FIG. 1. Graphical representation of elements of the braid group. Top: The two elementary braid operations σ_1 and σ_2 on three particles. Middle: Shown here $\sigma_2 \sigma_1 \neq \sigma_1 \sigma_2$; hence the braid group is non-Abelian. Bottom: The braid relation [Eq. (3)] $\sigma_i \sigma_{i+1} \sigma_i = \sigma_{i+1} \sigma_i \sigma_{i+1}$.

a mathematical perspective, when discussing the idea of a “category” in Sec. IV.) Then, the multiplication of two elements of the braid group is the successive execution of the corresponding trajectories, i.e., the vertical stacking of the two drawings. (As may be seen from the figure, the order in which they are multiplied is important because the group is non-Abelian, meaning that multiplication is not commutative.)

The braid group can be represented algebraically in terms of generators σ_i , with $1 \leq i \leq N-1$. We choose an arbitrary ordering of the particles $1, 2, \dots, N$.² σ_i is a counterclockwise exchange of the i th and $(i+1)$ th particles. σ_i^{-1} is therefore a clockwise exchange of the i th and $(i+1)$ th particles. The σ_i 's satisfy the defining relations (see Fig. 1),

$$\sigma_i \sigma_j = \sigma_j \sigma_i \quad \text{for } |i - j| \geq 2,$$

$$\sigma_i \sigma_{i+1} \sigma_i = \sigma_{i+1} \sigma_i \sigma_{i+1} \quad \text{for } 1 \leq i \leq n - 1. \tag{3}$$

The only difference from the permutation group S_N is that $\sigma_i^2 \neq 1$, but this makes an enormous difference. While the permutation group is finite, the number of elements in the group $|S_N|=N!$, the braid group is infinite, even for just two particles. Furthermore, there are nontrivial topological classes of trajectories even when the particles are distinguishable, e.g., in the two-particle case those trajectories in which one particle winds around the other an integer number of times. These topological classes correspond to the elements of the “pure” braid group, which is the subgroup of the braid group containing only elements that bring each particle

²Choosing a different ordering would amount to relabeling elements of the braid group, as given by conjugation by the braid that transforms one ordering into the other.

back to its own initial position, not the initial position of other particles. The richness of the braid group is the key fact enabling quantum computation through quasi-particle braiding.

To define the quantum evolution of a system, we specify how the braid group acts on the states of the system. The simplest possibilities are one-dimensional representations of the braid group. In these cases, the wave function acquires a phase 2θ when one particle is taken around another, analogous to Eqs. (1) and (2). The special cases $\theta=0, \pi$ are bosons and fermions, respectively, while particles with other values of θ are anyons (Wilczek, 1990). These are straightforward many-particle generalizations of the two-particle case considered above. An arbitrary element of the braid group is represented by the factor $e^{im\theta}$, where m is the total number of times that one particle winds around another in a counterclockwise manner (minus the number of times that a particle winds around another in a clockwise manner). These representations are Abelian since the order of braiding operations is unimportant. However, they can still have quite rich structure since there can be n_s different particle species with parameters θ_{ab} , where $a, b = 1, 2, \dots, n_s$, specifying the phases resulting from braiding a particle of type a around a particle of type b . Since distinguishable particles can braid nontrivially, i.e., θ_{ab} can be nonzero for $a \neq b$ as well as for $a = b$, anyonic “statistics” is better understood as a kind of topological interaction between particles.

We now turn to non-Abelian braiding statistics, which are associated with higher-dimensional representations of the braid group. Higher-dimensional representations can occur when there is a degenerate set of g states with particles at fixed positions R_1, R_2, \dots, R_n . We define an orthonormal basis ψ_α , $\alpha = 1, 2, \dots, g$, of these degenerate states. Then an element of the braid group—say σ_1 , which exchanges particles 1 and 2—is represented by a $g \times g$ unitary matrix $\rho(\sigma_1)$ acting on these states,

$$\psi_\alpha \rightarrow [\rho(\sigma_1)]_{\alpha\beta} \psi_\beta. \quad (4)$$

On the other hand, exchanging particles 2 and 3 leads to

$$\psi_\alpha \rightarrow [\rho(\sigma_2)]_{\alpha\beta} \psi_\beta. \quad (5)$$

Both $\rho(\sigma_1)$ and $\rho(\sigma_2)$ are $(g \times g)$ -dimensional unitary matrices, which define unitary transformation within the subspace of degenerate ground states. If $\rho(\sigma_1)$ and $\rho(\sigma_2)$ do not commute, $[\rho(\sigma_1)]_{\alpha\beta} [\rho(\sigma_2)]_{\beta\gamma} \neq [\rho(\sigma_2)]_{\alpha\beta} [\rho(\sigma_1)]_{\beta\gamma}$, the particles obey *non-Abelian braiding statistics*. Unless they commute for any interchange of particles, in which case the particles’ braiding statistics is Abelian, braiding quasiparticles will cause nontrivial rotations within the degenerate many-quasiparticle Hilbert space. Furthermore, it will essentially be true at low energies that the only way to make nontrivial unitary operations on this degenerate space is by braiding quasiparticles around each other. This statement is equivalent to a statement that no local perturbation can have nonzero matrix elements within this degenerate space.

A system with anyonic particles will generally have multiple types of anyons. For instance, in a system with Abelian anyons with statistics θ , a bound state of two such particles has statistics 4θ . Even if no such stable bound state exists, we may wish to bring two anyons close together while all other particles are much further away. Then the two anyons can be approximated as a single particle whose quantum numbers are obtained by combining the quantum numbers, including the topological quantum numbers, of the two particles. As a result, a complete description of the system must also include these “higher” particle species. For instance, if there are $\theta = \pi/m$ anyons in the system, then there are also $\theta = 4\pi/m, 9\pi/m, \dots, (m-1)^2\pi/m$. Since the statistics parameter is well defined only up to 2π , $\theta = (m-1)^2\pi/m = +\pi/m$ for m even and $\pi + \pi/m$ for m odd. The formation of a different type of anyon by bringing together two anyons is called *fusion*. When a statistics- π/m particle is fused with a statistics- $(-\pi/m)$ particle, the result has statistics $\theta=0$. It is convenient to call this the “trivial” particle. As far as topological properties are concerned, such a boson is as good as the absence of any particle, so the trivial particle is also sometimes called the “vacuum.” We often denote the trivial particle by **1**.

With Abelian anyons that are made by forming successively larger composites of π/m particles, the fusion rule is $n^2\pi/m \times k^2\pi/m = (n+k)^2\pi/m$. (We use $a \times b$ to denote a fused with b .) However, for non-Abelian anyons, the situation is more complicated. As with ordinary quantum numbers, there might not be a unique way of combining topological quantum numbers (e.g., two spin-1/2 particles could combine to form either a spin-0 or a spin-1 particle). The different possibilities are called the different *fusion channels*. This is usually denoted by

$$\phi_a \times \phi_b = \sum_c N_{ab}^c \phi_c, \quad (6)$$

which represents the fact that, when a particle of species a fuses with one of species b , the result can be a particle of species c if $N_{ab}^c \neq 0$. For Abelian anyons, the fusion multiplicities $N_{ab}^c = 1$ for only one value of c and $N_{ab}^{c'} = 0$ for all $c' \neq c$. For particles of type k with statistics $\theta_k = \pi k^2/m$, i.e., $N_{kk'}^{k''} = \delta_{k+k', k''}$. For non-Abelian anyons, there is at least one a, b such that there are multiple fusion channels c with $N_{ab}^c \neq 0$. In the examples that we consider, $N_{ab}^c = 0$ or 1, but there are theories for which $N_{ab}^c > 1$ for some a, b, c . In this case, a and b can fuse to form c in $N_{ab}^c > 1$ different distinct ways. We use \bar{a} to denote the antiparticle of particle species a . When a and \bar{a} fuse, they can always fuse to **1** in precisely one way, i.e., $N_{a\bar{a}}^1 = 1$; in the non-Abelian case, they may or may not be able to fuse to other particle types as well.

The different fusion channels are one way of accounting for the different degenerate multiparticle states. We see how this works in one simple model of non-Abelian anyons, discussed in Sec. III. As discussed in Sec. III,

this model is associated with “Ising anyons” (which are so named for reasons that will clear in Secs. III.D and III.E), $SU(2)_2$, and chiral p superconductors. There are slight differences between these three theories, relating to Abelian phases, but these are unimportant for the present discussion. This model has three different types of anyon, which can be variously called $\mathbf{1}, \sigma, \psi$ or $0, \frac{1}{2}, \mathbf{1}$. (Unfortunately, the notation is confusing because the trivial particle is called “ $\mathbf{1}$ ” in the first model but “ 0 ” in the second; however, we avoid confusion by using bold-faced $\mathbf{1}$ to denote the trivial particle.) The fusion rules for such anyons are

$$\begin{aligned} \sigma \times \sigma &= \mathbf{1} + \psi, & \sigma \times \psi &= \sigma, & \psi \times \psi &= \mathbf{1}, \\ \mathbf{1} \times x &= x & \text{for } x &= \mathbf{1}, \sigma, \psi. \end{aligned} \quad (7)$$

[Translating these rules into the notation of $SU(2)_2$, we see that these fusion rules are similar to the decomposition rules for tensor products of irreducible $SU(2)$ representations, but differ in the important respect that $\mathbf{1}$ is the maximum spin so that $\frac{1}{2} \times \frac{1}{2} = 0 + 1$, as in the $SU(2)$ case, but $\frac{1}{2} \times 1 = \frac{1}{2}$ and $1 \times 1 = 0$.] Note that there are two different fusion channels for two σ 's. As a result, if there are four σ 's which fuse together to give $\mathbf{1}$, there is a two-dimensional space of such states. If we divided the four σ 's into two pairs, by grouping particles 1,2 and 3,4, then a basis for the two-dimensional space is given by the state in which 1,3 fuse to $\mathbf{1}$ or 1,3 fuse to ψ (2,4 must fuse to the same particle type as do 1,3 in order that all four particles fuse to $\mathbf{1}$). We call these states Ψ_1 and Ψ_ψ ; they are a basis for the four-quasiparticle Hilbert space with total topological charge $\mathbf{1}$. (Similarly, if they all fused to give ψ , there would be another two-dimensional degenerate space; one basis is given by the state in which the first pair fuses to $\mathbf{1}$ while the second fuses to ψ and the state in which the opposite occurs.)

Of course, our division of the four σ 's into two pairs was arbitrary. We could have divided them differently, say, into the pairs 1,3 and 2,4. We thereby obtain two different basis states $\tilde{\Psi}_1$ and $\tilde{\Psi}_\psi$ in which both pairs fuse to $\mathbf{1}$ or to ψ , respectively. This is a different basis in the same two-dimensional space. The matrix parametrizing this basis change (see also the Appendix) is called the F matrix: $\tilde{\Psi}_a = F_{ab} \Psi_b$, where $a, b = 1, \psi$. There should really be six indices on F if we include indices to specify the four particle types, $[F^{ijk}]_{ab}$, but we have dropped these other indices since $i=j=k=l=\sigma$ in our case. The F matrices are sometimes called $6j$ symbols since they are analogous to the corresponding quantities for $SU(2)$ representations. Recall that, in $SU(2)$, there are multiple states in which spins $\mathbf{j}_1, \mathbf{j}_2$, and \mathbf{j}_3 couple to form a total spin \mathbf{J} . For instance, \mathbf{j}_1 and \mathbf{j}_2 can add to form \mathbf{j}_{12} , which can then add with \mathbf{j}_3 to give \mathbf{J} . The eigenstates of $(\mathbf{j}_{12})^2$ form a basis of the different states with fixed $\mathbf{j}_1, \mathbf{j}_2, \mathbf{j}_3$, and \mathbf{J} . Alternatively, \mathbf{j}_2 and \mathbf{j}_3 can add to form \mathbf{j}_{23} , which can then add with \mathbf{j}_1 to give \mathbf{J} . The eigenstates of $(\mathbf{j}_{23})^2$ form a different basis. The $6j$ symbol gives the basis change between the two. The F matrix of a system of

anyons plays the same role when particles of topological charges i, j, k fuse to total topological charge l . If i and j fuse to a , which then fuses with k to give topological charge l , the different allowed a 's define a basis. If j and k fuse to b and then fuse with i to give topological charge l , this defines another basis, and the F matrix is the unitary transformation between the two bases. States with more than four quasiparticles can be understood by successively fusing additional particles, as described in Sec. III.A. The F matrix can be applied to any set of four consecutively fused particles.

The different states in this degenerate multianyon state space transform into each other under braiding. However, two particles cannot change their fusion channel simply by braiding with each other, since their total topological charge can be measured along a far distant loop enclosing the two particles. They must braid with a third particle in order to change their fusion channel. Consequently, when two particles fuse in a particular channel (rather than a linear superposition of channels), the effect of taking one particle around the other is multiplication by a phase. This phase resulting from a counterclockwise exchange of particles of types a and b which fuse to a particle of type c is called R_c^{ab} . In the Ising anyon case, as derived in Sec. III and the Appendix, $R_1^{\sigma\sigma} = e^{-\pi i/8}$, $R_\psi^{\sigma\sigma} = e^{3\pi i/8}$, $R_1^{\psi\psi} = -1$, $R_\sigma^{\sigma\psi} = i$. For an example of how this works, suppose that we create a pair of σ quasiparticles out of the vacuum. They will necessarily fuse to $\mathbf{1}$. If we take one around another, the state will change by a phase $e^{-\pi i/8}$. If we take a third σ quasiparticle and take it around one, but not both, of the first two, then the first two will now fuse to ψ , as shown in Sec. III. If we now take one of the first two around the other, the state will change by a phase $e^{3\pi i/8}$.

In order to fully specify the braiding statistics of a system of anyons, it is necessary to specify (i) the particle species, (ii) the fusion rules N_{ab}^c , (iii) the F matrices, and (iv) the R matrices. In Sec. IV, we introduce the other sets of parameters, namely, the topological spins Θ_a and the S matrix, which, together with the parameters i - iv above, fully characterize the topological properties of an anyon system. Some readers may be familiar with the incarnation of these mathematical structures in conformal field theory (CFT), where they occur for reasons explained in Sec. III.D; we review these properties in the CFT context in the Appendix.

Quasiparticles obeying non-Abelian braiding statistics, or simply non-Abelian anyons, were first considered in conformal field theory by Moore and Seiberg (1988, 1989) and in Chern-Simons theory by Witten (1989). They were discussed in discrete gauge theories and linked to the representation theory of *quantum groups* by Bais (1980) and Bais *et al.* (1992; Bais, van Driel, *et al.*, 1993; Bais, Morozov, *et al.*, 1993). They were discussed in a more general context by Fredenhagen *et al.* (1989) and Fröhlich and Gabbiani (1990). The properties of non-Abelian quasiparticles make them appealing for use in a quantum computer. But, before discussing this,

we review how they could occur in nature and then the basic ideas behind quantum computation.

2. Emergent anyons

The preceding considerations show that exotic braiding statistics is a theoretical possibility in (2+1)D, but they do not tell us when and where they might occur in nature. Electrons, protons, atoms, and photons are all either fermions or bosons even when they are confined to move in a two-dimensional plane. However, if a system of many electrons (or bosons, atoms, etc.) confined to a two-dimensional plane has excitations which are localized disturbances of its quantum mechanical ground state, known as *quasiparticles*, then these quasiparticles can be anyons. When a system has anyonic quasiparticle excitations above its ground state, it is in a *topological phase of matter*. (A more precise definition of a topological phase of matter is given in Sec. III.)

We now describe how anyons might arise as an emergent property of a many-particle system. Consider the ground state of a (2+1)-dimensional system of electrons, whose coordinates are (r_1, \dots, r_n) . We assume that the ground state is separated from the excited states by an energy gap (i.e., it is incompressible), as in fractional quantum Hall states in 2D electron systems. The lowest-energy electrically charged excitations are known as quasiparticles or quasiholes, depending on the sign of their electric charge. (The term quasiparticle is also used in a generic sense to mean both quasiparticle and quasihole as in the previous section.) These quasiparticles are local disturbances to the wave function of electrons corresponding to a quantized amount of total charge.

We now introduce into the system's Hamiltonian a scalar potential composed of many local "traps," each sufficient to capture exactly one quasiparticle. These traps may be created by impurities, by small gates, or by the potential created by tips of scanning microscopes. The quasiparticle's charge screens the potential introduced by the trap and the quasiparticle-tip combination cannot be observed by local measurements from far away. We denote the positions of these traps by (R_1, \dots, R_k) , and assume that these positions are well spaced from each other compared to the microscopic length scales. A state with quasiparticles at these positions can be viewed as an excited state of the Hamiltonian without the trap potential or, alternatively, as the ground state in the presence of the trap potential. When we refer to the ground state(s) of the system, we often refer to multi-quasiparticle states in the latter context. The quasiparticles' coordinates (R_1, \dots, R_k) are parameters both in the Hamiltonian and in the resulting ground state wave function for electrons.

We are concerned with the effect of taking these quasiparticles around each other. We imagine making the quasiparticles' coordinates $\mathbf{R}=(R_1, \dots, R_k)$ adiabatically time dependent. In particular, we consider a trajectory in which the final configuration of quasiparticles is a permutation of the initial configuration (i.e., at the end, the positions of quasiparticles are identical to the initial po-

sitions, but some quasiparticles may have interchanged positions with others). If the ground state wave function is single valued with respect to (R_1, \dots, R_k) , and if there is only one ground state for any given set of R_i 's, then the final ground state to which the system returns after the winding is identical to the initial one, up to a phase. Part of this phase is the dynamical phase, which depends on the energy of the quasiparticle state and the length of time for the process. In the adiabatic limit, it is $\int dt E[\mathbf{R}(t)]$. There is also a geometric phase which does not depend on how long the process takes. This Berry phase is (Berry, 1984)

$$\alpha = i \oint d\mathbf{R} \cdot \langle \psi(\mathbf{R}) | \nabla_{\mathbf{R}} | \psi(\mathbf{R}) \rangle, \quad (8)$$

where $|\psi(\mathbf{R})\rangle$ is the ground state with the quasiparticles at positions \mathbf{R} and the integral is taken along the trajectory $\mathbf{R}(t)$. It is manifestly dependent only on the trajectory taken by the particles and not on how long it takes to move along this trajectory.

The phase α has a piece that depends on the geometry of the path traversed (typically proportional to the area enclosed by all of the loops), and a piece θ that depends only on the topology of the loops created. If $\theta \neq 0$, then the quasiparticle excitations of the system are anyons. In particular, if we consider the case where only two quasiparticles are interchanged clockwise (without wrapping around any other quasiparticles), θ is the statistical angle of the quasiparticles.

There were two key conditions to our discussion above of the Berry phase. The single valuedness of the wave function is a technical issue. The nondegeneracy of the ground state, however, is an important physical condition. In fact, most of this paper deals with the situation in which this condition does not hold. We consider systems in which, once the positions (R_1, \dots, R_k) of the quasiparticles are fixed, there remain multiple degenerate ground states [i.e., ground states in the presence of a potential that captures quasiparticles at positions (R_1, \dots, R_k)], which are distinguished by a set of internal quantum numbers. For reasons that will become clear later, we refer to these quantum numbers as "topological."

When the ground state is degenerate, the effect of a closed trajectory of the R_i 's is not necessarily a phase factor. The system starts and ends in ground states, but the initial and final ground states may be different members of this degenerate space. The constraint imposed by adiabaticity in this case is that the adiabatic evolution of the system is confined to the subspace of ground states. Thus it may be expressed as a unitary transformation within this subspace. The inner product in Eq. (8) must be generalized to a matrix of such inner products:

$$\mathbf{m}_{ab} = \langle \psi_a(\mathbf{R}) | \nabla_{\mathbf{R}} | \psi_b(\mathbf{R}) \rangle, \quad (9)$$

where $|\psi_a(\mathbf{R})\rangle$, $a=1,2,\dots,g$, are the g degenerate ground states. Since these matrices at different points \mathbf{R} do not commute, we must path order the integral in

order to compute the transformation rule for the state $\psi_a \rightarrow M_{ab} \psi_b$, where

$$\begin{aligned}
 M_{ab} &= \mathcal{P} \exp \left(i \oint d\mathbf{R} \cdot \mathbf{m} \right) \\
 &= \sum_{n=0}^{\infty} i^n \int_0^{2\pi} ds_1 \int_0^{s_1} ds_2 \cdots \int_0^{s_{n-1}} ds_n \{ \dot{\mathbf{R}}(s_1) \\
 &\quad \cdot \mathbf{m}_{a a_1}[\mathbf{R}(s_1)] \cdots \dot{\mathbf{R}}(s_n) \cdot \mathbf{m}_{a_n b}[\mathbf{R}(s_n)] \}, \quad (10)
 \end{aligned}$$

with $\mathbf{R}(s)$, $s \in [0, 2\pi]$, the closed trajectory of the particles, and the path-ordering symbol \mathcal{P} is defined by the second equality. Again, the matrix M_{ab} may be the product of topological and nontopological parts. In a system in which quasiparticles obey non-Abelian braiding statistics, the nontopological part will be Abelian, that is, proportional to the unit matrix. Only the topological part will be non-Abelian.

The requirements for quasiparticles to follow non-Abelian statistics are then, first, that the N -quasiparticle ground state is degenerate. In general, the degeneracy will not be exact, but it should vanish exponentially as the quasiparticle separations are increased. Second, the adiabatic interchange of quasiparticles applies a unitary transformation on the ground state, whose non-Abelian part is determined only by the topology of the braid, while its nontopological part is Abelian. If the particles are not infinitely far apart, and the degeneracy is only approximate, then the adiabatic interchange must occur faster than the inverse of the energy splitting (Thouless and Gefen, 1991) between states in the nearly degenerate subspace (but still more slowly than the energy gap between this subspace and the excited states). Third, the only way to make unitary operations on the degenerate ground state space, so long as the particles are kept far apart, is by braiding. The simplest (albeit uninteresting) example of degenerate ground states may arise if each of the quasiparticles carried a spin $1/2$ with a vanishing g factor. If that were the case, the system would satisfy the first requirement. Spin-orbit coupling may conceivably lead to the second requirement being satisfied. Satisfying the third one, however, is much harder, and requires the subtle structure described below.

The degeneracy of N -quasiparticle ground states is conditioned on the quasiparticles being well separated from one another. When quasiparticles are allowed to approach one another too closely, the degeneracy is lifted. In other words, when non-Abelian anyonic quasiparticles are close together, their different fusion channels are split in energy. This dependence is analogous to the way the energy of a system of spins depends on their internal quantum numbers when the spins are close together and their coupling becomes significant. The splitting between different fusion channels is a means for a measurement of the internal quantum state, a measurement that is of importance in the context of quantum computation.

B. Topological quantum computation

1. Basics of quantum computation

As the components of computers become smaller and smaller, we are approaching the limit in which quantum effects become important. One might ask whether this is a problem or an opportunity. The founders of quantum computation (Manin, 1980; Feynman, 1982, 1986; Deutsch, 1985; and most dramatically, Shor, 1994) answered in favor of the latter. They showed that a computer which operates coherently on quantum states has potentially much greater power than a classical computer (Nielsen and Chuang, 2000).

The problem that Feynman had in mind for a quantum computer was the simulation of a quantum system (Feynman, 1982). He showed that certain many-body quantum Hamiltonians could be simulated exponentially faster on a quantum computer than on a classical computer. This is an important potential application of a quantum computer, since it would enable us to understand the properties of complex materials, e.g., to explain solve high-temperature superconductivity. Digital simulations of large-scale quantum many-body Hamiltonians are hopeless on classical computers because of the exponentially large Hilbert space. A quantum computer, using the physical resource of an exponentially large Hilbert space, may also enable progress in the solution of lattice gauge theory and quantum chromodynamics, thus shedding light on strongly interacting nuclear forces.

In 1994 Peter Shor found an application of a quantum computer which generated widespread interest not just inside but also outside the physics community (Shor, 1994). He invented an algorithm by which a quantum computer could find the prime factors of an m -digit number in a length of time $\sim m^2 \log m \log \log m$. This is much faster than the fastest known algorithm for a classical computer, which takes $\sim \exp(m^{1/3})$ time. Since many encryption schemes depend on the difficulty of finding the solution to problems similar to finding the prime factors of a large number, there is an obvious application of a quantum computer that is of great basic and applied interest.

The computation model set forth by these pioneers of quantum computing [and refined by DiVincenzo (2000)] is based on three steps: initialization, unitary evolution, and measurement. We assume that we have a system with Hilbert space \mathcal{H} . We further assume that we can initialize the system in some known state $|\psi_0\rangle$. We unitarily evolve the system until it is in some final state $U(t)|\psi_0\rangle$. This evolution will occur according to some Hamiltonian $H(t)$ such that $dU/dt = iH(t)U(t)/\hbar$. We require that we have enough control over this Hamiltonian so that $U(t)$ can be made to be any unitary transformation that we desire. Finally, we measure the state of the system at the end of this evolution. Such a process is called *quantum computation* (Nielsen and Chuang, 2000). The Hamiltonian $H(t)$ is the software program to

be run. The initial state is the input to the calculation, and the final measurement is the output.

The need for versatility, i.e., for one computer to efficiently solve many different problems, requires the construction of the computer out of smaller pieces that can be manipulated and reconfigured individually. Typically, the fundamental piece is taken to be a quantum two-state system known as a “qubit,” which is the quantum analog of a bit. (Of course, one could equally well take general “dits,” for which the fundamental unit is some d -state system with d not too large.) While a classical bit, i.e., a classical two-state system, can be either 0 or 1 at any given time, a qubit can be in one of the infinitely many superpositions $a|0\rangle + b|1\rangle$. For n qubits, the state becomes a vector in a 2^n -dimensional Hilbert space, in which the different qubits are generally entangled with one another.

The quantum phenomenon of superposition allows a system to traverse many trajectories in parallel, and determine its state by their coherent sum. In some sense this coherent sum amounts to a massive quantum parallelism. It should not, however, be confused with classical parallel computing, where many computers are run in parallel, and no coherent sum takes place.

The biggest obstacle to building a practical quantum computer is posed by errors, which invariably happen during any computation, quantum or classical. For any computation to be successful, one must devise practical schemes for error correction which can be effectively implemented (and which must be sufficiently fault tolerant). Errors are typically corrected in classical computers through redundancies, i.e., by keeping multiple copies of information and checking against these copies.

With a quantum computer, however, the situation is more complex. If we measure a quantum state during an intermediate stage of a calculation to see if an error has occurred, we collapse the wave function and thus destroy quantum superpositions and ruin the calculation. Furthermore, errors need not be merely a discrete flip of $|0\rangle$ to $|1\rangle$, but can be continuous: the state $a|0\rangle + b|1\rangle$ may drift, due to an error, to the state $\rightarrow a|0\rangle + be^{i\theta}|1\rangle$ with arbitrary θ .

In spite of these difficulties, error correction is possible for quantum computers (Shor, 1995; Calderbank and Shor, 1996; Steane, 1996a; Gottesman, 1998; Preskill, 2004). One can represent information redundantly so that errors can be identified without measuring the information. For instance, if we use three spins to represent each qubit, $|0\rangle \rightarrow |000\rangle$, $|1\rangle \rightarrow |111\rangle$, and the spin-flip rate is low, then we can identify errors by checking whether all three spins are the same (here we represent an up spin by 0 and a down spin by 1). Suppose that our spins are in the state $\alpha|000\rangle + \beta|111\rangle$. If the first spin has flipped erroneously, then our spins are in the state $\alpha|100\rangle + \beta|011\rangle$. We can detect this error by checking whether the first spin is the same as the other two; this does not require us to measure the state of the qubit [“We measure the errors, rather than the information.” (Preskill, 2004)]. If the first spin is different from the other two, then we just need to flip it. We repeat this

process with the second and third spins. So long as we can be sure that two spins have not erroneously flipped (i.e., so long as the basic spin-flip rate is low), this procedure will correct spin-flip errors. A more elaborate encoding is necessary in order to correct phase errors, but the key observation is that a phase error in the σ_z basis is a bit-flip error in the σ_x basis.

However, the error correction process may itself be a little noisy. More errors could then occur during error correction, and the whole procedure will fail unless the basic error rate is small. Estimates of the threshold error rate above which error correction is impossible depend on the particular error correction scheme, but fall in the range 10^{-4} – 10^{-6} (see, e.g., Aharonov and Ben-Or, 1997; Knill *et al.*, 1998). This means that we must be able to perform 10^4 – 10^6 operations perfectly before an error occurs. This is a stringent constraint, and it is presently unclear if local qubit-based quantum computation can ever be made fault tolerant through quantum error correction protocols.

Random errors are caused by the interaction between the quantum computer and the environment. As a result of this interaction, the quantum computer, which is initially in a pure superposition state, becomes entangled with its environment. This can cause errors as follows. Suppose that the quantum computer is in the state $|0\rangle$ and the environment is in the state $|E_0\rangle$ so that their combined state is $|0\rangle|E_0\rangle$. The interaction between the computer and the environment could cause this state to evolve to $\alpha|0\rangle|E_0\rangle + \beta|1\rangle|E_1\rangle$, where $|E_1\rangle$ is another state of the environment (not necessarily orthogonal to $|E_0\rangle$). The computer undergoes a transition to the state $|1\rangle$ with probability $|\beta|^2$. Furthermore, the computer and the environment are now entangled, so the reduced density matrix for the computer alone describes a mixed state, e.g., $\rho = \text{diag}(|\alpha|^2, |\beta|^2)$ if $\langle E_0|E_1\rangle = 0$. Since we cannot measure the state of the environment accurately, information is lost, as reflected in the evolution of the density matrix of the computer from a pure state to a mixed one. In other words, the environment has caused *decoherence*. Decoherence can destroy quantum information even if the state of the computer does not undergo a transition. Although whether or not a transition occurs is basis dependent (a bit flip in the σ_z basis is a phase flip in the σ_x basis), it is a useful distinction because many systems have a preferred basis, for instance, the ground state $|0\rangle$ and excited state $|1\rangle$ of an ion in a trap. Suppose the state $|0\rangle$ evolves as above, but with $\alpha=1$, $\beta=0$ so that no transition occurs, while the state $|1\rangle|E_0\rangle$ evolves to $|1\rangle|E'_1\rangle$ with $\langle E'_1|E_1\rangle = 0$. Then an initial pure state $(a|0\rangle + b|1\rangle)|E_0\rangle$ evolves to a mixed state with density matrix $\rho = \text{diag}(|a|^2, |b|^2)$. The correlations in which our quantum information resides is now transferred to correlation between the quantum computer and the environment. The quantum state of a system invariably loses coherence in this way over a characteristic time scale T_{coh} . It was universally assumed until the advent of quantum error correction (Shor, 1995; Steane, 1996a) that quantum computation is intrinsically impossible since decoherence-

induced quantum errors cannot be corrected in any real physical system. However, when error-correcting codes are used, the entanglement is transferred from the quantum computer to ancillary qubits so that the quantum information remains pure while the entropy is in the ancillary qubits.

Of course, even if the coupling to the environment were completely eliminated, so that there were no random errors, there could still be systematic errors. These are unitary errors which occur while we process quantum information. For instance, we may wish to rotate a qubit by 90° but might inadvertently rotate it by 90.01° .

From a practical standpoint, it is often useful to divide errors into two categories: (i) errors that occur when a qubit is processed (i.e., when computations are performed on that qubit), and (ii) errors that occur when a qubit is simply storing quantum information and is not being processed (i.e., when it is acting as a quantum memory). From a fundamental standpoint, this is a bit of a false dichotomy, since one can think of quantum information storage (or quantum memory) as a computer that applies the identity operation over and over to the qubit (i.e., leaves it unchanged). Nonetheless, the problems faced in the two categories might be quite different. For quantum information processing, unitary errors, such as rotating a qubit by 90.01° instead of 90° , are an issue of how precisely one can manipulate the system. On the other hand, when a qubit is storing information, one is more concerned about errors caused by interactions with the environment. This is instead an issue of how well isolated one can make the system. As shown below, a topological quantum computer is protected from problems in both of these categories.

2. Fault tolerance from non-Abelian anyons

Topological quantum computation is a scheme for using a system whose excitations satisfy non-Abelian braiding statistics to perform quantum computation in a way that is naturally immune to errors. The Hilbert space \mathcal{H} used for quantum computation is the subspace of the total Hilbert space of the system comprised of the degenerate ground states with a fixed number of quasiparticles at fixed positions. Operations within this subspace are carried out by braiding quasiparticles. As discussed above, the subspace of degenerate ground states is separated from the rest of the spectrum by an energy gap. Hence, if the temperature is much lower than the gap and the system is weakly perturbed using frequencies much smaller than the gap, the system evolves only within the ground state subspace. Furthermore, that evolution is severely constrained, since it is essentially the case (with exceptions that we discuss) that the only way the system can undergo a nontrivial unitary evolution—that is, an evolution that takes it from one ground state to another—is by having its quasiparticles braided. The reason for this stability is that any local perturbation [such as the electron-phonon interaction and the hyperfine electron-nuclear interaction, two major causes for decoherence in nontopological solid state

spin-based quantum computers (Witzel and Das Sarma, 2006) has no nontrivial matrix elements within the ground state subspace. Thus the system is rather immune from decoherence (Kitaev, 2003). Unitary errors are also unlikely since unitary transformations associated with braiding quasiparticles are sensitive only to the topology of the quasiparticle trajectories, and not to their geometry or dynamics.

A model in which non-Abelian quasiparticles are utilized for quantum computation starts with the construction of qubits. In sharp contrast to most realizations of a quantum computer, a qubit here is a nonlocal entity, comprised of several well-separated quasiparticles, with the two states of the qubit being two different values for the internal quantum numbers of this set of quasiparticles. In the simplest non-Abelian quantum Hall state, which has Landau-level filling factor $\nu=5/2$, two quasiparticles can be put together to form a qubit (see Secs. II.C.4 and IV.A). Unfortunately, as discussed in Secs. IV.A and IV.C, this system turns out to be incapable of universal topological quantum computation using only braiding operations; some unprotected operations are necessary in order to perform universal quantum computation. The simplest system that is capable of universal topological quantum computation is discussed in Sec. IV.B; it utilizes three quasiparticles to form one qubit.

As mentioned above, to perform a quantum computation one must be able to initialize the state of qubits at the beginning, perform arbitrary controlled unitary operations on the state, and then measure the state of qubits at the end. We now address each of these in turn.

Initialization may be performed by preparing the quasiparticles in a specific way. For example, if a quasiparticle-antiquasiparticle pair is created by “pulling” it apart from the vacuum (e.g., pair creation from the vacuum by an electric field), it will begin in an initial state with the pair necessarily having conjugate quantum numbers (i.e., the “total” quantum number of the pair remains the same as that of the vacuum). This gives us a known initial state to start with. It is also possible to use measurement and unitary evolution (both discussed below) as an initialization scheme—if one can measure the quantum numbers of some quasiparticles, one can then perform a controlled unitary operation to put them into any desired initial state.

Once the system is initialized, controlled unitary operations are performed by physically dragging quasiparticles around one another in some specified way. When quasiparticles belonging to different qubits braid, the state of the qubits changes. Since the resulting unitary evolution depends only on the topology of the braid that is formed and not on the details of how it is done, it is insensitive to wiggles in the path, resulting, e.g., from scattering of the quasiparticles by phonons or photons. Determining which braid corresponds to which computation is a complicated but eminently solvable task, discussed in Sec. IV.B.3.

Once the unitary evolution is completed, there are two ways to measure the state of the qubits. The first relies on the fact that the degeneracy of multiqubit

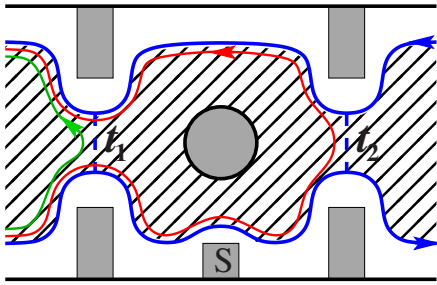


FIG. 2. (Color online) A quantum Hall analog of a Fabry-Perot interferometer. Quasiparticles can tunnel from one edge to the other at either of two point contacts. To lowest order in the tunneling amplitudes, the backscattering probability, and hence the conductance, is determined by the interference between these two processes. The area in the cell can be varied by means of a side gate S in order to observe an interference pattern.

ticle states is split when quasiparticles are brought close together (within some microscopic length scale). When two quasiparticles are brought close together, for instance, a measurement of this energy (or a measurement of the force between two quasiparticles) measures the topological charge of the pair. A second way to measure the topological charge of a group of quasiparticles is by carrying out an Aharonov-Bohm-type interference experiment. We take a “beam” of test quasiparticles, send it through a beam splitter, send one partial wave to the right of the group to be measured and another partial wave to the left of the group, and then reinterfere the two waves (see Fig. 2). Since the two different beams make different braids around the test group, they will experience different unitary evolution depending on the topological quantum numbers of the test group. Thus the reinterference of these two beams will reflect the topological quantum number of the group of quasiparticles enclosed.

This concludes a rough description of the way a topological quantum computation is to be performed. While the unitary transformation associated with a braid depends only on the topology of the braid, one may be concerned that errors could occur if one does not return the quasiparticles to precisely the correct position at the end of the braiding. This apparent problem, however, is evaded by the computations, which correspond to closed world lines that have no loose ends: when the computation involves creation and annihilation of a quasiparticle-quasihole pair, the world line is a closed curve in space-time. If the measurement occurs by bringing two particles together to measure their quantum charge, it does not matter precisely where they are brought together. Alternatively, when the measurement involves an interference experiment, the interfering particle must close a loop. In other words, a computation corresponds to a set of *links* rather than open braids, and the initialization and measurement techniques necessarily involve bringing quasiparticles together in some way, closing up the trajectories and making the full pro-

cess from initialization to measurement completely topological.

Due to its special characteristics topological quantum computation intrinsically guarantees fault tolerance, at the level of “hardware,” without “software”-based error correction schemes that are essential for nontopological quantum computers. This immunity to errors results from the stability with respect to local perturbations. In nontopological quantum computers, qubits are local, and operations on them are local, leading to a sensitivity to errors induced by local perturbations. In a topological quantum computer qubits are nonlocal and operations—quasiparticle braiding—are nonlocal, leading to an immunity to local perturbations.

Such immunity to local perturbation gives topological quantum memories protection from errors due to the interaction with the environment. However, note that topological quantum computers are also immune to unitary errors due to imprecise gate operation. Unlike other types of quantum computers, operations that can be performed on a topological quantum computer (braids) naturally take a discrete set of values. As discussed above, when one makes a 90° rotation of a spin-based qubit, for example, it is possible that one will mistakenly rotate by 90.01° , thus introducing a small error. In contrast, braids are discrete: a particle either is taken around another or it is not. There is no way to make a small error by having slight imprecision in the way quasiparticles are moved. (Taking a particle only part of the way around another particle rather than all of the way does not introduce errors so long as the topological class of the link formed by the particle trajectories, as described above, is unchanged.)

Given the stability of ground states, and their insensitivity to local perturbations that do not involve excitations to excited states, one may ask then which physical processes do cause errors in such a topological quantum computer. Due to the topological stability of the unitary transformations associated with braids, the only error processes that we are concerned with are processes that might cause us to form the wrong link, and hence the wrong computation. Certainly, one must keep track of the positions of all quasiparticles in the system during the computation and assure that one makes the correct braid to do the correct computation. This includes not just the “intended” quasiparticles that we need to manipulate for our quantum computation, but also any “unintended” quasiparticle that might be lurking in our system without our knowledge. Two possible sources of these unintended quasiparticles are thermally excited quasiparticle-quasihole pairs and randomly localized quasiparticles trapped by disorder (e.g., impurities, surface roughness, etc.). In a typical thermal fluctuation, for example, a quasiparticle-quasihole pair is thermally created from the vacuum, braids with existing intended quasiparticles, and then gets annihilated. Typically, such a pair has opposite electrical charges, so its constituents will be attracted back to each other and annihilate. However, entropy or temperature may lead the quasiparticle and quasihole to split fully apart and wander

freely through part of the system before coming back together and annihilating. This type of process may change the state of qubits encoded in intended quasiparticles, and hence disrupt the computation. Fortunately, as shown in Sec. IV.B, there is a whole class of such processes that do not in fact cause error. This class includes all of the most likely such thermal processes to occur: including when a pair is created, encircles a single already existing quasiparticle, and then reannihilates, or when a pair is created and one of the pair annihilates an already existing quasiparticle. For errors to be caused, the excited pair must braid at least two intended quasiparticles. Nonetheless, the possibility of thermally excited quasiparticles wandering through the system creating unintended braids and thereby causing error is a serious one. For this reason, topological quantum computation must be performed at temperatures well below the energy gap for quasiparticle-quasihole creation so that these errors will be exponentially suppressed.

Similarly, localized quasiparticles that are induced by disorder (e.g., randomly distributed impurities, surface roughness, etc.) are another serious obstacle to overcome, since they enlarge the dimension of the subspace of degenerate ground states in a way that is hard to control. In particular, these unaccounted-for quasiparticles may couple by tunneling to their intended counterparts, thereby introducing dynamics to what is supposed to be a topology-controlled system, and possibly ruining the quantum computation. We further note that, in quantum Hall systems (as discussed in the next section), slight deviations in density or magnetic field will also create unintended quasiparticles that must be avoided.

Finally, note that while non-Abelian quasiparticles are natural candidates for the realization of topological qubits, not every system where quasiparticles satisfy non-Abelian statistics is suitable for quantum computation. For this suitability it is essential that the set of unitary transformations induced by braiding quasiparticles is rich enough to allow for all operations needed for computation. The necessary and sufficient conditions for universal topological quantum computation are discussed in Sec. IV.C.

C. Non-Abelian quantum Hall states

A necessary condition for topological quantum computation using non-Abelian anyons is the existence of a physical system where non-Abelian anyons can be found, manipulated (e.g., braided), and conveniently read out. Several theoretical models and proposals for systems having these properties have been introduced (Fendley and Fradkin, 2005; Freedman *et al.*, 2005a; Levin and Wen, 2005b; Kitaev, 2006), and in Sec. II.D we mention some of these possibilities. Despite the theoretical work in these directions, the only real physical systems where there is even indirect experimental evidence that non-Abelian anyons exist are quantum Hall systems in two-dimensional electron gases (2DEGs) in high magnetic fields. Consequently, we devote a considerable part of our discussion to putative non-Abelian quantum Hall

systems which are also of great interest in their own right.

1. Rapid review of quantum Hall physics

A comprehensive review of the quantum Hall effect is well beyond the scope of this article and can be found in the literature (Prange and Girvin, 1990; Das Sarma and Pinczuk, 1997). This effect, realized for two-dimensional electronic systems in a strong magnetic field, is characterized by a gap between the ground and excited states (incompressibility); a vanishing longitudinal resistivity $\rho_{xx}=0$, which implies a dissipationless flow of current; and the quantization of the Hall resistivity to $\rho_{xy}=(1/\nu)h/e^2$, with ν an integer (the integer quantum Hall effect) or a fraction (the fractional quantum Hall effect). These values of the two resistivities imply a vanishing longitudinal conductivity $\sigma_{xx}=0$ and a quantized Hall conductivity $\sigma_{xy}=\nu e^2/h$.

To understand the quantized Hall effect, we begin by ignoring electron-electron Coulomb interactions; then the energy eigenstates of the single-electron Hamiltonian in a magnetic field $H_0=(1/2m)[\mathbf{p}_i-e/c\mathbf{A}(\mathbf{x}_i)]^2$ break up into an equally spaced set of degenerate levels called Landau levels. In symmetric gauge, $\mathbf{A}(\mathbf{x})=\frac{1}{2}\mathbf{B}\times\mathbf{x}$, a basis of single particle wave functions in the lowest Landau level (LLL) is $\varphi_m(z)=z^m \exp(-|z|^2/4\ell_0^2)$, where $z=x+iy$. If electrons are confined to a disk of area A pierced by magnetic flux BA , then there are $N_\Phi=BA/\Phi_0=BAe/hc$ states in the lowest Landau level (and in each higher Landau level), where B is the magnetic field; h , c , and e are, respectively, Planck's constant, the speed of light, and the electron charge; and $\Phi_0=h/e$ is the flux quantum. In the absence of disorder, these single-particle states are degenerate. When the chemical potential lies between the ν th and $(\nu+1)$ th Landau levels, the Hall conductance takes the quantized value $\sigma_{xy}=\nu e^2/h$ while $\sigma_{xx}=0$. The two-dimensional electron density n is related to ν via $n=\nu eB/hc$. In the presence of a periodic potential and/or disorder (e.g., impurities), the Landau levels broaden into bands. However, except at the center of a band, all states are localized when disorder is present (see Das Sarma and Pinczuk, 1997; Prange and Girvin, 1990, and references therein). When the chemical potential lies in the region of localized states between the centers of the ν th and $(\nu+1)$ th Landau bands, the Hall conductance again takes the quantized value $\sigma_{xy}=\nu e^2/h$ while $\sigma_{xx}=0$. The density will be near but not necessarily equal to $\nu eB/hc$. This is known as the integer quantum Hall effect (since ν is an integer).

The neglect of Coulomb interactions is justified when an integer number of Landau levels is filled, so long as the energy splitting between Landau levels, $\hbar\omega_c=\hbar eB/mc$, is much larger than the scale of the Coulomb energy, e^2/ℓ_0 , where $\ell_0=\sqrt{hc/eB}$ is the magnetic length. When the electron density is such that a Landau level is only partially filled, Coulomb interactions may be important.

In the absence of disorder, a partially filled Landau level has a highly degenerate set of multiparticle states. This degeneracy is broken by electron-electron interactions. For instance, when the number of electrons is $N = N_\Phi/3$, i.e., $\nu=1/3$, the ground state is nondegenerate and there is a gap to all excitations. When electrons interact through Coulomb repulsion, the Laughlin state

$$\Psi = \prod_{i>j} (z_i - z_j)^3 \exp\left(-\sum_i |z_i|^2/4\ell_0^2\right) \quad (11)$$

is an approximation to the ground state (and is the exact ground state for a repulsive ultra-short-ranged model interaction; see, e.g., Haldane in [Prange and Girvin, 1990](#)). Such ground states survive even in the presence of disorder if it is sufficiently weak compared to the gap to excited states. More delicate states with smaller excitation gaps are therefore seen only in extremely clean devices, as described in Sec. II.C.5. However, some disorder is necessary to pin the charged quasiparticle excitations which are created if the density or magnetic field is slightly varied. When these excitations are localized, they do not contribute to the Hall conductance, and a plateau is observed.

Quasiparticle excitations above fractional quantum Hall ground states, such as the $\nu=1/3$ Laughlin state (11), are emergent anyons as described in Sec. II.A.2. An explicit calculation of the Berry phase, along the lines of Eq. (8), shows that quasiparticle excitations above the $\nu=1/k$ Laughlin states have charge e/k and statistical angle $\theta=\pi/k$ ([Arovas *et al.*, 1984](#)). The charge is obtained from the nontopological part of the Berry phase, which is proportional to the flux enclosed by a particle's trajectory times the quasiparticle charge. This is in agreement with a general argument that such quasiparticles must have fractional charge ([Laughlin, 1983](#)). The result for the statistics of the quasiparticles follows from the topological part of the Berry phase; it is in agreement with strong theoretical arguments which suggest that fractionally charged excitations are necessarily Abelian anyons (see [Wilczek, 1990](#), and references therein). Definitive experimental evidence for the existence of fractionally charged excitations at $\nu=1/3$ has accumulated. ([Goldman and Su, 1995](#); [De Picciotto *et al.*, 1997](#); [Saminadayar *et al.*, 1997](#)). The observation of fractional statistics is much more subtle. First steps in that direction have been reported ([Camino *et al.*, 2005](#)) but are still debated ([Godfrey *et al.*, 2007](#); [Rosenow and Halperin, 2007](#)).

The Laughlin states, with $\nu=1/k$, are the best understood fractional quantum Hall states, both theoretically and experimentally. To explain more complicated observed fractions, with ν not of the form $\nu=1/k$, Haldane and Halperin ([Haldane, 1983](#); [Halperin 1984](#); [Prange and Girvin, 1990](#)) used a hierarchical construction in which quasiparticles of a principal $\nu=1/k$ state can then themselves condense into a quantized state. In this way, quantized Hall states can be constructed for any odd-denominator fraction ν —but only for odd-denominator fractions. These states all have quasiparticles with frac-

tional charge and Abelian fractional statistics. Later, it was noticed by Jain ([Jain, 1989](#); [Heinonen, 1998](#)) that the most prominent fractional quantum Hall states are $\nu = p/(2p+1)$, which can be explained by noting that a system of electrons in a high magnetic field can be approximated by a system of auxiliary fermions, called “composite fermions,” in a lower magnetic field. If the electrons are at $\nu=p/(2p+1)$, then the lower magnetic field seen by composite fermions is such that they fill an integer number of Landau levels $\nu'=p$. [See [López and Fradkin \(1991\)](#) and [Halperin *et al.* \(1993\)](#) for field-theoretic implementations.] Since the latter state has a gap, one can hope that the approximation is valid. The composite fermion picture of fractional quantum Hall states has proven to be qualitatively and semi-quantitatively correct in the LLL ([Murthy and Shankar, 2003](#)).

Systems with filling fraction $\nu>1$ can be mapped to $\nu'\leq 1$ by keeping the fractional part of ν and using an appropriately modified Coulomb interaction to account for the difference between cyclotron orbits in the LLL and those in higher Landau levels ([Prange and Girvin, 1990](#)). This involves the assumption that the inter-Landau-level coupling is negligibly small. We note that this may not be a particularly good assumption for higher Landau levels, where the composite fermion picture is less successful.

Our confidence in the picture described above for the $\nu=1/k$ Laughlin states and the hierarchy of odd-denominator states that descend from them derives largely from numerical studies. Experimentally most of what is known about quantum Hall states comes from transport experiments—measurements of the conductance (or resistance) tensor. While such measurements make it reasonably clear when a quantum Hall plateau exists at a given filling fraction, the nature of the plateau (i.e., the details of the low-energy theory) is extremely hard to discern. Because of this difficulty, numerical studies of small systems (exact diagonalizations and Monte Carlo) have played a prominent role in providing further insight. Indeed, even Laughlin's original work ([Laughlin, 1983](#)) on the $\nu=1/3$ state relied heavily on accompanying numerical work. The approach taken was the following. One assumed that the splitting between Landau levels is the largest energy in the problem. The Hamiltonian is projected into the lowest Landau level, where, for a finite number of electrons and a fixed magnetic flux, the Hilbert space is finite dimensional. Typically, the system is given periodic boundary conditions (i.e., is on a torus) or else is placed on a sphere; occasionally, one works on a disk, e.g., to study edge excitations. The Hamiltonian is then a finite-sized matrix which can be diagonalized by a computer so long as the number of electrons is not too large. Originally, Laughlin examined only three electrons, but modern computers can handle sometimes as many as 18 electrons. The resulting ground state wave function can be compared to a proposed trial wave function. Throughout the history of the field, this approach has proven to be powerful in identifying the nature of experimentally observed quan-

tum Hall states when the system in question is deep within a quantum Hall phase, so that the associated correlation length is short and the basic physics is already apparent in small systems.

There are several challenges in using such numerical work to interpret experiments. First, there is always the challenge of extrapolating finite-size results to the thermodynamic limit. Second, simple overlaps between a proposed trial state and an exact ground state may not be sufficiently informative. For example, it is possible that an exact ground state will be adiabatically connected to a particular trial state, i.e., the two wave functions represent the same phase of matter, but the overlaps may not be very high. For this reason it is necessary to also examine quantum numbers and symmetries of the ground state, as well as the response of the ground state to various perturbations, particularly the response to changes in boundary conditions and in the flux.

Another difficulty is the choice of Hamiltonian to diagonalize. One may think that the Hamiltonian for a quantum Hall system is just that of 2D electrons in a magnetic field interacting via Coulomb forces. However, the small but finite width (perpendicular to the plane of the system) of the quantum well slightly alters the effective interaction between electrons. Similarly, screening (from any nearby conductors, or from inter-Landau-level virtual excitations), in-plane magnetic fields, and even various types of disorder may alter the Hamiltonian in subtle ways. To make matters worse, one may not even know all the physical parameters (dimensions, doping levels, detailed chemical composition, etc.) of any particular experimental system accurately. Finally, Landau-level mixing is not small because the energy splitting between Landau levels is not much larger than the other energies in the problem. Thus it is not even clear that it is correct to truncate the Hilbert space to the finite-dimensional Hilbert space of a single Landau level.

In the case of robust states, such as the $\nu=1/3$ state, these subtle effects are unimportant; the ground state is essentially the same irrespective of these small deviations from the idealized Hamiltonian. However, in the case of weaker states, such as those observed between $\nu=2$ and 4 (some discussed below), it appears that small changes in the Hamiltonian can indeed affect the resulting ground state. Therefore a valuable approach is to guess a likely Hamiltonian, and search a space of “nearby” Hamiltonians, slightly varying the parameters of the Hamiltonian, to map out the phase diagram of the system. These phase diagrams suggest the technological possibility that detailed numerics will allow us to engineer samples with just the right small perturbations so as display certain quantum Hall states more clearly (Manfra *et al.*, 2008; Peterson and Das Sarma, 2008).

2. Possible non-Abelian states

The observation of a quantum Hall state with an even-denominator filling fraction (Willett *et al.*, 1987), the $\nu=5/2$ state, was the first indication that not all frac-

tional quantum Hall states fit the above hierarchy (or equivalently composite fermion) picture. Independently, it was recognized (Fubini, 1991; Fubini and Lutken, 1991; Moore and Read, 1991) that conformal field theory gives a way to write a variety of trial wave functions for quantum Hall states, as described in Sec. III.D. Using this approach, the so-called Moore-Read Pfaffian wave function was constructed (Moore and Read, 1991):

$$\Psi_{\text{Pf}} = \text{Pf} \left(\frac{1}{z_i - z_j} \right)_{i < j} \prod (z_i - z_j)^m \exp \left(- \sum_i |z_i|^2 / 4\ell_0^2 \right). \quad (12)$$

The Pfaffian is the square root of the determinant of an antisymmetric matrix or, equivalently, the antisymmetrized sum over pairs:

$$\text{Pf} \left(\frac{1}{z_j - z_k} \right) = \mathcal{A} \left(\frac{1}{z_1 - z_2} \frac{1}{z_3 - z_4} \dots \right). \quad (13)$$

For m even, this is an even-denominator quantum Hall state in the lowest Landau level. Moore and Read (1991) suggested that its quasiparticle excitations would exhibit non-Abelian statistics (Moore and Read, 1991). This wave function is the exact ground state of a three-body repulsive interaction; as discussed below, it is also an approximate ground state for more realistic interactions. This wave function is a representative of a universality class which has properties that are discussed in detail in this paper. In particular, the quasiparticle excitations above this state realize the second scenario discussed in Eqs. (9) and (10) in Sec. II.A.2. There are 2^{n-1} states with $2n$ quasiholes at fixed positions, thereby establishing the degeneracy of multi-quasiparticle states which is required for non-Abelian statistics (Nayak and Wilczek, 1996). Furthermore, these quasihole wave functions can also be related to conformal field theory (as discussed in Sec. III.D), from which it can be deduced that the 2^{n-1} -dimensional vector space of states can be understood as the spinor representation of $\text{SO}(2n)$; braiding particles i and j has the action of a $\pi/2$ rotation in the i - j plane in \mathbb{R}^{2n} (Nayak and Wilczek, 1996). In short, these quasiparticles are essentially Ising anyons (with the difference an additional Abelian component to their statistics). Although these properties were uncovered using specific wave functions which are eigenstates of the three-body interaction for which the Pfaffian wave function is the exact ground state, they are representative of an entire universality class. The effective field theory for this universality class is $\text{SU}(2)$ Chern-Simons theory at level $k=2$ together with an additional Abelian Chern-Simons term (Fradkin *et al.*, 1998, 2001). Chern-Simons theory is the archetypal topological quantum field theory (TQFT), and is discussed in Sec. III. As described, Chern-Simons theory is related to the Jones polynomial of knot theory (Witten, 1989); consequently, the current through an interferometer in such a non-Abelian quantum Hall state gives a direct measure of the Jones polynomial for the link produced by the quasiparticle trajectories (Fradkin *et al.*, 1998)!

One interesting feature of the Pfaffian wave function is that it is the quantum Hall analog of a $p+ip$ superconductor: the antisymmetrized product over pairs is the real-space form of the BCS wave function (Greiter *et al.*, 1992). Read and Green (2000) showed that the same topological properties mentioned above are realized by a $(p+ip)$ -wave superconductor, thereby cementing the identification between such a paired state and the Moore-Read state. Ivanov (2001) computed the braiding matrices by this approach (see also Stern *et al.*, 2004; Stone and Chung, 2006). Consequently, we are able to discuss $(p+ip)$ -wave superconductors and superfluids in parallel with the $\nu=5/2$ quantum Hall state, although the experimental probes are significantly different.

As discussed below, these theoretical developments garnered greater interest when numerical work (Morf, 1998; Rezayi and Haldane, 2000) showed that the ground state of systems of up to 18 electrons in the $N=1$ Landau level at filling fraction $1/2$ is in the universality class of the Moore-Read state. These results revived the conjecture that the lowest Landau level ($N=0$) of both spins is filled and inert, and electrons in the $N=1$ Landau level form the analog of the Pfaffian state (Greiter *et al.*, 1992). Consequently, it is the leading candidate for the experimentally observed $\nu=5/2$ state.

Read and Rezayi (1999) constructed a series of non-Abelian quantum Hall states at filling fraction $\nu=N+k/(Mk+2)$ with M odd, which generalize the Moore-Read state in a way discussed in Sec. III. These states are referred to as the Read-Rezayi \mathbb{Z}_k parafermion states as discussed in Sec. III.D. Recently, a quantum Hall state was observed experimentally with $\nu=12/5$ (Xia *et al.*, 2004). It is suspected (see below) that the $\nu=12/5$ state may be (the particle-hole conjugate of) the \mathbb{Z}_3 Read-Rezayi state, although it is also possible that $12/5$ belongs to the conventional Abelian hierarchy as the $2/5$ state does. Such an option is not possible at $\nu=5/2$ as a result of the even denominator.

In summary, it is well established that, if the observed $\nu=5/2$ state is in the same universality class as the Moore-Read Pfaffian state, then its quasiparticle excitations are non-Abelian anyons. Similarly, if the $\nu=12/5$ state is in the universality class of the \mathbb{Z}_3 Read-Rezayi state, its quasiparticles are non-Abelian anyons. There is no direct experimental evidence that the $\nu=5/2$ state is in this particular universality class, but there is evidence from numerics, as discussed below. There is even less evidence in the case of the $\nu=12/5$ state. In Secs. II.C.3 and II.C.4, we discuss proposed experiments that could directly verify the non-Abelian character of the $\nu=5/2$ state and mention their extension to the $\nu=12/5$ case. Both of these states, as well as others (e.g., Ardonne and Schoutens, 1999; Simon, Reyazi, Cooper, *et al.*, 2007), were constructed on the basis of deep connections between conformal field theory, knot theory, and low-dimensional topology (Witten, 1989). Using methods from these different branches of theoretical physics and mathematics, we explain the structure of the non-Abelian statistics of the $\nu=5/2$ and $12/5$ states within

the context of a large class of non-Abelian topological states. We show in Sec. III.C that this circle of ideas enables us to use the theory of knots to understand experiments on non-Abelian anyons.

Below we discuss numerical results for $\nu=5/2, 12/5$, and other candidates.

a. $5/2$ state

The $\nu=5/2$ fractional quantum Hall (FQH) state is a useful case history for how numerics can elucidate experiments. This incompressible state is easily destroyed by the application of an in-plane magnetic field (Eisenstein *et al.*, 1990). At first it was assumed that this implied that the $5/2$ state is spin unpolarized or partially polarized, since the in-plane magnetic field presumably couples only to the electron spin. Careful finite-size numerical work changed this perception, leading to our current belief that the $5/2$ FQH state is in the universality class of the spin-polarized Moore-Read Pfaffian state.

In rather pivotal work (Morf, 1998), it was shown that spin-polarized states at $\nu=5/2$ have lower energy than spin-unpolarized states. Furthermore, it was shown that varying the Hamiltonian slightly caused a phase transition between a gapped phase that has high overlap with the Moore-Read wave function and a compressible phase. The proposal put forth was that the most important effect of the in-plane field is not on electron spins. Instead, it is the slight alteration of the shape of the electron wave function perpendicular to the sample which, in turn, slightly alters the effective electron-electron interaction, pushing the system over a phase boundary and destroying the gapped state. Further experimental work showed that the effect of the in-plane magnetic field is to drive the system across a phase transition from a gapped quantum Hall phase into an anisotropic compressible phase (Lilly *et al.*, 1999a; Pan, Du, *et al.*, 1999). Further numerical work (Rezayi and Haldane, 2000) then mapped out a full phase diagram showing the transition between gapped and compressible phases and showing that the experimental systems lie exceedingly close to the phase boundary. The correspondence between numerics and experiment has been made more quantitative by comparisons between the energy gap obtained from numerics and the one measured in experiments (Morf *et al.*, 2002; Morf and d'Ambrumenil, 2003). This case has been further strengthened by the application of the density-matrix renormalization group (DMRG) method to this problem (Feiguin, Rezayi, *et al.*, 2008).

One issue worth considering is possible competitors to the Moore-Read Pfaffian state. Experiments have already told us that there is a fractional quantum Hall state at $\nu=5/2$. Therefore our job is to determine which of the possible states is realized there. Serious alternatives to the Moore-Read Pfaffian state fall into two categories. On the one hand, there is the possibility that the ground state at $\nu=5/2$ is not fully spin polarized. If it were completely unpolarized, the so-called $(3, 3, 1)$ state

(Halperin, 1983; Das Sarma and Pinczuk, 1997) would be a possibility. However, Morf's numerics (Morf, 1998) and a variational Monte Carlo study (Dimov *et al.*, 2008) indicate that an unpolarized state is higher in energy than a fully polarized state. This can be understood as a consequence of a tendency toward spontaneous ferromagnetism; however, a partially polarized alternative (which may be either Abelian or non-Abelian) to the Pfaffian is not ruled out (Dimov *et al.*, 2008). Second, even if the ground state at $\nu=5/2$ is fully spin polarized, the Pfaffian is not the only possibility. It was noticed that the Pfaffian state is not symmetric under a particle-hole transformation of a single Landau level (which in this case is the $N=1$ Landau level, with the $N=0$ Landau level filled and assumed inert), even though this is an exact symmetry of the Hamiltonian in the limit that the energy splitting between Landau levels is infinity. Therefore there is a distinct state, the anti-Pfaffian (Lee, Ryu, *et al.*, 2007; Levin *et al.*, 2007), which is an equally good state in this limit. Quasiparticles in this state are also essentially Ising anyons, but they differ from Pfaffian quasiparticles by Abelian statistical phases. In experiments, Landau-level mixing is not small, so one or the other state is lower in energy. On a finite torus, the symmetric combination of the Pfaffian and the anti-Pfaffian will be lower in energy, but as the thermodynamic limit is approached, the antisymmetric combination will become equal in energy. This is a possible factor that complicates the extrapolation of numerics to the thermodynamic limit. On a finite sphere, particle-hole symmetry is not exact; it relates a system with $2N-3$ flux quanta to a system with $2N+1$ flux quanta. Thus the anti-Pfaffian would not be apparent unless one looked at a different value of the flux. To summarize, the only known alternatives to the Pfaffian state—partially polarized states and the anti-Pfaffian—have not really been tested by numerics, either because the spin polarization was assumed to be 0% or 100% (Morf, 1998) or because Landau-level mixing was neglected.

With this caveat in mind, it is instructive to compare the evidence placing the $\nu=5/2$ FQH state in the Moore-Read Pfaffian universality class with the evidence placing the $\nu=1/3$ FQH state in the corresponding Laughlin universality class. In the latter case, there have been several experiments (Goldman and Su, 1995; De Picciotto *et al.*, 1997; Saminadayar *et al.*, 1997) which have observed quasiparticles with electrical charge $e/3$, in agreement with the prediction of the Laughlin universality class. In the case of the $\nu=5/2$ FQH state, we do not yet have the corresponding measurements of the quasiparticle charge, which should be $e/4$. However, the observation of charge $e/3$, while consistent with the Laughlin universality class, does not uniquely fix the observed state in this class (see, e.g., Wójs, 2001; Simon, Rezayi, Cooper, *et al.*, 2007). Thus much of our confidence derives from the (99% or better) overlap between the ground state obtained from exact diagonalization for a finite-size 2D system with up to 14 electrons and the Laughlin wave function. In the case of the $\nu=5/2$ FQH

state, the corresponding overlap (for 18 electrons on the sphere) between the $\nu=5/2$ ground state and the Moore-Read Pfaffian state is impressive ($\sim 80\%$). This can be improved by modifying the wave function at short distances without leaving the Pfaffian phase (Moller and Simon, 2008). However, on the torus, as mentioned above, the symmetric combination of the Pfaffian and the anti-Pfaffian is a better candidate wave function in a finite-size system than the Pfaffian itself (or the anti-Pfaffian). Indeed, the symmetric combination of the Pfaffian and the anti-Pfaffian has an overlap of 97% for 14 electrons (Rezayi and Haldane, 2000).

To summarize, the overlap is somewhat smaller in the $5/2$ case than in the $1/3$ case when particle-hole symmetry is not accounted for, but only slightly smaller when it is. This is an indication that Landau-level mixing—which will favor either the Pfaffian or the anti-Pfaffian—is an important effect at $\nu=5/2$, unlike at $\nu=1/3$. Moreover, Landau-level mixing is likely to be large because the $5/2$ FQH state is typically realized at relatively low magnetic fields, making the Landau level separation energy relatively small.

Given that potentially large effects have been neglected, it is not too surprising that the gap obtained by extrapolating numerical results for finite-size systems (Morf *et al.*, 2002; Morf and d'Ambrumenil, 2003) is larger than the experimentally measured activation gap. Also, the corresponding excitation gap obtained from numerics for the $\nu=1/3$ state is much larger than the measured activation gap. The discrepancy between the theoretical excitation gap and the measured activation gap is a generic problem of all FQH states, and may be related to poorly understood disorder effects and Landau-level mixing.

Finally, it is important to mention that several numerical works in the literature have raised some questions about the identification of the observed $5/2$ FQH state with the Moore-Read Pfaffian (Toke and Jain, 2006; Wojs and Quinn, 2006; Toke *et al.*, 2007). Considering the absence of a viable alternative (apart from the anti-Pfaffian and partially polarized states, which were not considered by these authors), it seems unlikely that these doubts will continue to persist, as more thorough numerical work indicates (Moller and Simon, 2008; Peterson and Das Sarma, 2008).

b. $12/5$ state

While our current understanding of the $5/2$ state is good, the situation for the experimentally observed $12/5$ state is more murky, although the possibilities are even more exciting, at least from the perspective of topological quantum computation. One (relatively dull) possibility is that the $12/5$ state is essentially the same as the observed $\nu=2/5$ state, which is Abelian. However, Read and Rezayi proposed in their work on non-Abelian generalizations of the Moore-Read state (Read and Rezayi, 1999) that the $12/5$ state might be (the particle-hole conjugate of) their \mathbb{Z}_3 parafermion [or $SU(2)$ level 3] state. This is an exciting possibility because, unlike the non-

Abelian Moore-Read state at $5/2$, the \mathbb{Z}_3 parafermion state would have braiding statistics that allow universal topological quantum computation.

The initial numerics by [Read and Rezayi \(1999\)](#) indicated that the $12/5$ state is close to a phase transition between the Abelian hierarchy state and the non-Abelian parafermion state. Recent work by the same authors ([Rezayi and Read, 2006](#)) has mapped out a detailed phase diagram showing for what range of parameters a system should be in the non-Abelian phase. It was found that the non-Abelian phase is not “far” from the results that would be expected from most real experimental systems. This again suggests that (if the system is not already in the non-Abelian phase), we may be able to engineer slight changes in an experimental sample that would push the system over the phase boundary into the non-Abelian phase.

Experimentally, little is known about the $12/5$ state. Indeed, a well-quantized plateau has only ever been seen in a single published ([Xia *et al.*, 2004](#)) experiment. Furthermore, there is no experimental information about spin polarization (the non-Abelian phase should be polarized whereas the Abelian phase could be either polarized or unpolarized), and it is not at all clear why the $12/5$ state has been seen, but its particle-hole conjugate, the $13/5$ state, has not (in the limit of infinite Landau level separation, these two states will be identical in energy). Nonetheless, despite the substantial uncertainties, there is a great deal of excitement about the possibility that this state will provide a route to topological quantum computation.

c. Other quantum Hall states

The most strongly observed fractional quantum Hall states are the composite fermion states $\nu = p/(2p+1)$, or are simple generalizations of them. There is little debate that these states are likely to be Abelian. However, there are a number of observed exotic states whose origin is not currently agreed upon. An optimist may look at any state of unknown origin and suggest that it is a non-Abelian state. Indeed, non-Abelian proposals have been made for a variety of states of uncertain origin including $3/8$, $4/11$, $8/3$, and $7/3$ ([Scarola *et al.*, 2002](#); [Wojs *et al.*, 2006](#); [Jolicœur, 2007](#); [Simon, Rezayi, Cooper, *et al.*, 2007](#); [Simon *et al.*, 2007a](#)). Of course, other more conventional Abelian proposals have been made for each of these states too ([Wojs and Quinn, 2002](#); [Chang and Jain, 2004](#); [Goerbig *et al.*, 2004](#); [López and Fradkin, 2004](#); [Wojs *et al.*, 2004](#)). For each of these states, there is a great deal of research left to be done, both theoretical and experimental, before any sort of definitive conclusion is reached.

In this context, it is worthwhile to mention another class of quantum Hall systems where non-Abelian anyons could exist, namely, bilayer or multilayer 2D systems ([Greiter *et al.*, 1991](#); [He *et al.*, 1991, 1993](#); [Das Sarma and Pinczuk, 1997](#)). More work is necessary in investigating the possibility of non-Abelian multilayer quantum Hall states.

3. Interference experiments

While numerics give useful insight about the topological nature of observed quantum Hall states, experimental measurements will ultimately play the decisive role. So far, little has been directly measured experimentally about the topological nature of the $\nu=5/2$ state, and even less is known about other putative non-Abelian quantum Hall states such as $\nu=12/5$. In particular, there is no direct experimental evidence for the non-Abelian nature of the quasiparticles. The existence of a degenerate, or almost degenerate, subspace of ground states leads to a zero-temperature entropy and heat capacity, but those are hard to measure experimentally. Furthermore, this degeneracy is just one requirement for non-Abelian statistics to occur. How then does one demonstrate experimentally that fractional quantum Hall states, particularly the $\nu=5/2$ state, are indeed non-Abelian?

The fundamental quasiparticles (i.e., the ones with the smallest electrical charge) of the Moore-Read Pfaffian state have charge $e/4$ ([Moore and Read, 1991](#); [Greiter *et al.*, 1992](#)). The fractional charge does not uniquely identify the state—the Abelian $(3, 3, 1)$ state has the same quasiparticle charge—but a different value of the minimal quasiparticle charge at $\nu=5/2$ would rule out the Pfaffian state. Hence the first important measurement is the quasiparticle charge, which was done more than ten years ago in the case of the $\nu=1/3$ state ([Goldman and Su, 1995](#); [De Picciotto *et al.*, 1997](#); [Saminadayar *et al.*, 1997](#)).

If the quasiparticle charge is shown to be $e/4$, then further experiments which probe the braiding statistics of the charge $e/4$ quasiparticles will be necessary to pin down the topological structure of the state. One way to do this is to use a mesoscopic interference device. Consider a Fabry-Perot interferometer, as depicted in Fig. 2. A Hall bar lying parallel to the x axis is put in a field such that it is at filling fraction $\nu=5/2$. It is perturbed by two constrictions, as shown in the figure. The two constrictions introduce two amplitudes for interedge tunneling $t_{1,2}$. To lowest order in $t_{1,2}$, the four-terminal longitudinal conductance of the Hall bar is

$$G_L \propto |t_1|^2 + |t_2|^2 + 2 \operatorname{Re}\{t_1^* t_2 e^{i\phi}\}. \quad (14)$$

For an integer Landau filling, the relative phase ϕ may be varied either by a variation of the magnetic field or by a variation of the area of the “cell” defined by the two edges and the two constrictions, since that phase is $2\pi\Phi/\Phi_0$, with $\Phi=BA$ the flux enclosed in the cell, A the area of the cell, and Φ_0 the flux quantum. Thus, when the area of the cell is varied by means of a side gate (labeled S in the figure), the backscattered current should oscillate.

For fractional quantum Hall states, the situation is different ([de C. Chamon *et al.*, 1997](#)). In an approximation in which the electronic density is determined by the requirement of charge neutrality, a variation of the cell area varies the flux it encloses and keeps its bulk Landau filling unaltered. In contrast, a variation of the magnetic

field changes the filling fraction in the bulk, and consequently introduces quasiparticles in the bulk. Since the statistics of the quasiparticles is fractional, they contribute to the phase ϕ . The backscattering probability is then determined not only by the two constrictions and the area of the cell they define, but also by the number of localized quasiparticles that the cell encloses. By varying the voltage applied to an antidot in the cell (the gray circle in Fig. 2), we can independently vary the number of quasiparticles in the cell. Again, however, as the area of the cell is varied, the backscattered current oscillates.

For non-Abelian quantum Hall states, the situation is more interesting (Fradkin *et al.*, 1998; Das Sarma *et al.*, 2005; Bonderson, Kitaev, *et al.*, 2006; Bonderson, Shtengel, *et al.*, 2006; Chung and Stone, 2006; Stern and Halperin, 2006). Consider the case of the Moore-Read Pfaffian state. For clarity, we assume that there are localized $e/4$ quasiparticles only within the cell (either at the antidot or elsewhere in the cell). If the current in Fig. 2 comes from the left, the portion of the current that is backreflected from the left constriction does not encircle any of these quasiparticles, and thus does not interact with them. The part of the current that is backscattered from the right constriction, on the other hand, does encircle the cell, and therefore applies a unitary transformation on the subspace of degenerate ground states. The final state of the ground state subspace that is coupled to the left backscattered wave $|\xi_0\rangle$ is then different from the state coupled to the right partial wave $\hat{U}|\xi_0\rangle$. Here \hat{U} is the unitary transformation that results from the encircling of the cell by the wave scattered from the right constriction. The interference term in the four-terminal longitudinal conductance, the final term in Eq. (14), is then multiplied by the matrix element $\langle\xi_0|\hat{U}|\xi_0\rangle$:

$$G_L \propto |t_1|^2 + |t_2|^2 + 2 \operatorname{Re}\{t_1^* t_2 e^{i\phi} \langle\xi_0|\hat{U}|\xi_0\rangle\}. \quad (15)$$

In Sec. III, we explain how $\langle\xi_0|\hat{U}|\xi_0\rangle$ can be calculated by several different methods. Here we give a brief description of the result.

For the Moore-Read Pfaffian state, which is believed to be realized at $\nu=5/2$, the expectation value $\langle\xi_0|\hat{U}|\xi_0\rangle$ depends first and foremost on the parity of the number of $e/4$ quasiparticles localized in the cell. When that number is odd, the resulting expectation value is zero. When that number is even, the expectation value is non-zero and may assume one of two possible values that differ by a minus sign. As a consequence, when the number of localized quasiparticles is odd, *no interference pattern is seen*, and the backscattered current does not oscillate with small variations of the area of the cell. When that number is even, the backscattered current oscillates as a function of the area of the cell.

A way to understand this result is to observe that localized quasiparticles in the cell can be viewed as being created in pairs from the vacuum. Suppose that we want to have N quasiparticles in the cell. If N is odd, then we can create $(N+1)/2$ pairs and take one of the resulting

quasiparticles outside the cell, where it is localized. Fusing all $N+1$ of these particles gives the trivial particle, since they were created from the vacuum. Now consider what happens when a current-carrying quasiparticle tunnels at one of the two point contacts. If it tunnels at the second one, it braids around the N quasiparticles in the cell [but not the $(N+1)$ th, which is outside the cell]. This changes the fusion channel of the $N+1$ localized quasiparticles. In the language introduced in Sec. II.A.1 each $e/4$ quasiparticle is a σ particle. An odd number N of them can only fuse to σ ; fused now with the $(N+1)$ th, they can give either $\mathbf{1}$ or ψ . Current-carrying quasiparticles, when they braid with the N in the cell, toggle the system between these two possibilities. Since the state of the localized quasiparticles has been changed, such a process cannot interfere with a process in which the current-carrying quasiparticle tunnels at the first junction and does not encircle any of the localized quasiparticles. Therefore localized quasiparticles “measure” which trajectory is taken by current-carrying quasiparticles (Overbosch and Bais, 2001; Bonderson *et al.*, 2007). If N is even, then we can create $(N+2)/2$ pairs and take two of the resulting quasiparticles outside of the cell. If the N quasiparticles in the cell all fuse to the trivial particle, then this is not necessary; we can just create $N/2$ pairs. However, if they fuse to a neutral fermion ψ , then we need a pair outside the cell which also fuses to ψ so that the total fuses to $\mathbf{1}$, as it must for pair creation from the vacuum. A current-carrying quasiparticle picks up a phase depending on whether the N quasiparticles in the cell fuse to $\mathbf{1}$ or ψ .

The Fabry-Perot interferometer depicted in Fig. 2 allows also for the interference of waves that are backreflected several times. For an integer filling factor, in the limit of strong backscattering at the constrictions, the sinusoidal dependence of the Hall bar’s conductance on the area of the cell gives way to a resonancelike dependence: the conductance is zero unless a Coulomb peak develops. For the $\nu=5/2$ state, again, the parity of the number of localized quasiparticles matters: when it is odd, the Coulomb blockade peaks are equally spaced; when it is even, the spacing between the peaks alternates between two values (Stern and Halperin, 2006).

The Moore-Read Pfaffian state, which is possibly realized at $\nu=5/2$, is the simplest of the non-Abelian states. The other states are more complex, but also richer. The geometry of the Fabry-Perot interferometer may be analyzed for these states as well. In general, for all non-Abelian states, the conductance of the Hall bar depends on the internal state of the quasiparticles localized between constrictions—i.e., the quasiparticle to which they fuse. However, only for the Moore-Read Pfaffian state is the effect quite so dramatic. For example, for the the \mathbb{Z}_3 parafermion state, which is possibly realized at $\nu=12/5$, when the number of localized quasiparticles is larger than 3, the fusion channel of quasiparticles determines whether the interference is fully visible or suppressed by a factor of $-\varphi^{-2}$ [with φ the golden ratio $(\sqrt{5}+1)/2$] (Bonderson, Shtengel, *et al.*, 2006;

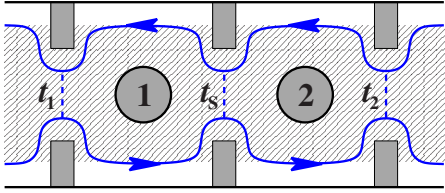


FIG. 3. (Color online) If a third constriction is added between the other two, the cell is broken into two halves. We suppose that there is one quasiparticle (or any odd number) in each half. These two quasiparticles (labeled 1 and 2) form a qubit which can be read by measuring the conductance of the interferometer if there is no backscattering at the middle constriction. When a single quasiparticle tunnels from one edge to the other at the middle constriction, a σ_x or NOT gate is applied to the qubit.

Chung and Stone, 2006). The number of quasiparticles, on the other hand, affects only the phase of the interference pattern. Similar to the case of $\nu=5/2$, here too the positions of Coulomb blockade peaks on the two-parameter plane of area and magnetic field reflect the non-Abelian nature of quasiparticles (Ilan *et al.*, 2008).

4. A fractional quantum Hall quantum computer

We now describe how the constricted Hall bar may be utilized as a quantum bit (Das Sarma *et al.*, 2005). To that end, an even number of $e/4$ quasiparticles should be trapped in the cell between constrictions, and a new, tunable, constriction should be added between the other two so that the cell is broken into two cells with an odd number of quasiparticles in each (see Fig. 3). One way to tune the number of quasiparticles in each half is to have two antidots in the Hall bar. By tuning the voltage on the antidots, we can change the number of quasiholes on each. Assume that we thereby fix the number of quasiparticles in each half of the cell to be odd. For concreteness, take this odd number to be 1 (i.e., assume that we are in the idealized situation in which there are no quasiparticles in the bulk, and one quasihole on each antidot). These two quasiholes then form a two-level system, i.e., a qubit. This two-level system can be understood in several ways, discussed in Sec. III. In brief, the two states correspond to whether the two σ 's fuse to $\mathbf{1}$ or ψ or, in the language of chiral p -wave superconductivity, the presence or absence of a neutral (“Majorana”) fermion; or, equivalently, to the fusion of two quasiparticles carrying the spin-1/2 representation of an SU(2) gauge symmetry in the spin-0 or spin-1 channels.

The interference between the t_1 and t_2 processes depends on the state of the two-level system, so the qubit can be read by a measurement of the four-terminal longitudinal conductance

$$G_L \propto |t_1|^2 + |t_2|^2 \pm 2 \operatorname{Re}\{t_1^* t_2 e^{i\phi}\}, \quad (16)$$

where the \pm comes from the dependence of $\langle \xi_0 | \hat{U} | \xi_0 \rangle$ on the state of the qubit, as discussed in Sec. III.

The purpose of the middle constriction is to allow us to manipulate the qubit. The state may be flipped, i.e., a

σ_x or NOT gate can be applied, by the passage of a single quasiparticle from one edge to the other, provided that its trajectory passes between the two localized quasiparticles. This is a simple example of how braiding causes nontrivial transformations of multi-quasiparticle states of non-Abelian quasiparticles, discussed in Sec. III. If we measure the four-terminal longitudinal conductance G_L before and after applying this NOT gate, we observe different values according to Eq. (16).

For this operation to be a NOT gate, it is important that a single quasiparticle (or any odd number) tunnels from one edge to the other across the middle constriction. In order to regulate the number of quasiparticles that pass across the constriction, it may be useful to have a small antidot in the middle of the constriction with a large charging energy so that only a single quasiparticle can pass through at a time. If we do not have good control over how many quasiparticles tunnel, then it will be random whether an even or odd number of quasiparticles tunnel across; half of the time, a NOT gate will be applied and the backscattering probability (hence the conductance) will change, while the other half of the time, the backscattering probability is unchanged. If the constriction is pinched down to such an extreme that the 5/2 state is disrupted between quasiparticles, then when it is restored there will be an equal probability for the qubit to be in either state.

This qubit is topologically protected because its state can be affected only by a charge- $e/4$ quasiparticle braiding with it. If a charge- $e/4$ quasiparticle winds around one of the antidots, it effects a NOT gate on the qubit. The probability for such an event can be small because the density of thermally excited charge- $e/4$ quasiparticles is exponentially suppressed at low temperatures, $n_{\text{qp}} \sim \exp[-\Delta/(2T)]$. The simplest estimate of the error rate Γ (in units of the gap) is then of activated form:

$$\Gamma/\Delta \sim (T/\Delta)e^{-\Delta/(2T)}. \quad (17)$$

The most favorable experimental situation (Xia *et al.*, 2004) considered by Das Sarma *et al.* (2005) has $\Delta \approx 500$ mK and $T \sim 5$ mK, producing a low error rate $\sim 10^{-15}$. This should be taken as an overly optimistic estimate. A more definitive answer is more complicated since there are multiple gaps which can be relevant in a disordered system. Furthermore, at low temperatures, we expect quasiparticle transport to be dominated by variable-range hopping of localized quasiparticles rather than thermal activation. Indeed, the crossover to this behavior may already be apparent (Pan, Xia, *et al.*, 1999), in which case the error suppression will be considerably weaker at the lowest temperatures. Although the error rate, which is determined by the probability for a quasiparticle to wind around the antidot, is not the same as the longitudinal resistance, which is the probability for it to go from one edge of the system to the other, the two are controlled by similar physical processes. A more sophisticated estimate would require a detailed analysis of the quasiparticle transport properties that contribute to the error rate. In addition, this

error estimate assumes that all trapped (unintended) quasiparticles are kept far from the quasiparticles which we use for our qubit, so that they cannot exchange topological quantum numbers with our qubit via tunneling. We comment on the issues involved in more detailed error estimates in Sec. IV.D.

The device envisioned above can be generalized to one with many antidots and therefore many qubits. More complicated gates, such as a controlled-NOT (CNOT) gate, can be applied by braiding quasiparticles. It is not clear how to braid quasiparticles localized in the bulk—perhaps by transferring them from one antidot to another in a kind of “bucket brigade.” This is an important problem for any realization of topological quantum computing. However, as discussed in Sec. IV, even if this were solved, there would still be the problem that braiding alone is not sufficient for universal quantum computation in the $\nu=5/2$ state (assuming that it is the Moore-Read Pfaffian state). One must either use some unprotected operations (just two, in fact) or else use the $\nu=12/5$ state if it turns out to be the Z_3 parafermion non-Abelian state.

5. Physical systems and materials considerations

As seen in the device described in the previous section, topological protection in non-Abelian fractional quantum Hall states hinges on the energy gap (Δ) separating the many-body degenerate ground states from the low-lying excited states. This excitation gap also leads to the incompressibility of the quantum Hall state and the quantization of the Hall resistance. Generally speaking, the larger the size of this excitation gap compared to the temperature, the more robust the topological protection, since thermal excitation of stray quasiparticles, which varies as $\exp[-\Delta/(2T)]$, could lead to errors.

It must be emphasized that the relevant T here is the temperature of electrons (or more precisely, quasiparticles) and not that of the GaAs-AlGaAs lattice surrounding the 2D electron layer. Although the surrounding bath temperature could be lowered to 1 mK or below using adiabatic demagnetization in dilution refrigerators, the 2D electrons themselves thermally decouple from the bath at low temperatures, and it is difficult to cool the 2D electrons below $T \approx 20$ mK. It will be a great boost to hopes for topological quantum computation using non-Abelian fractional quantum Hall states if the electron temperature can be lowered to 1 mK or even below, and serious efforts are currently under way in several laboratories with this goal.

Unfortunately, the excitation gaps for the expected non-Abelian fractional quantum Hall states are typically small (compared, for example, with the $\nu=1/3$ fractional quantum Hall state). The early measured gap for the $5/2$ state was around $\Delta \sim 25$ mK (Willett *et al.*, 1987), but steady improvement in materials quality, as measured by the sample mobility, has considerably enhanced this gap. In the highest-mobility samples currently available, $\Delta \approx 600$ mK (Choi *et al.*, 2008). Indeed, there appears to be a close connection between the excitation gap Δ and the

mobility (or the sample quality). Although the details of this connection are not well understood, it is empirically well established that enhancing the 2D mobility invariably leads to larger measured excitation gaps. In particular, an empirical relation $\Delta = \Delta_0 - \Gamma$, where Δ is the measured activation gap and Δ_0 is the ideal excitation gap with Γ the level broadening arising from impurity and disorder scattering, has often been discussed (see, e.g., Du *et al.*, 1993). Setting the mobility $\mu = e\tau/m$, with τ the zero-field Drude scattering time, we can write (an approximation of) the level broadening as $\Gamma = \hbar/(2\tau)$, indicating $\Gamma \sim \mu^{-1}$ in this simple picture, and therefore increasing the mobility should steadily enhance the operational excitation gap, as is found experimentally. It has been pointed out (Morf *et al.*, 2002) that, if Γ is reduced, a FQH gap of 2–3 K may be achievable in the $5/2$ FQH state. Much less is currently known about the $12/5$ state, but recent numerics (Rezayi and Read, 2006) suggest that the maximal gap in typical samples will be quite a bit lower than for $5/2$.

It is also possible to consider designing samples that would inherently have particularly large gaps. First, the interaction energy (which sets the overall scale of the gap) is roughly of the $1/r$ Coulomb form, so it scales as the inverse of the interparticle spacing. Doubling the density should therefore increase the gaps by roughly 40%. Although there are efforts under way to increase the density of samples (Willett *et al.*, 2007), there are practical limitations to how high a density one can obtain since, if one tries to overfill a quantum well with electrons, the electrons will no longer remain strictly two dimensional (i.e., they will start filling higher subbands, or they will not remain in the well at all). Second, as discussed in Sec. II.C.2, since the non-Abelian states appear generally to be sensitive to the precise parameters of the Hamiltonian, another possible route to increased excitation gap would be to design the precise form of the interelectron interaction [which can be modified by well width, screening layers, and particularly spin-orbit coupling (Manfra *et al.*, 2007)] so that the Hamiltonian is at a point in the phase diagram with maximal gap. With all approaches for redesigning samples, however, it is crucial to keep the disorder level low, which is a difficult challenge.

Note that a large excitation gap (and correspondingly low temperature) suppresses thermally excited quasiparticles but does not preclude stray localized quasiparticles which could be present even at $T=0$. As long as their positions are known and fixed, and as long as they are few enough in number to be sufficiently well separated, these quasiparticles would not present a problem, as one could avoid moving other quasiparticles near their positions, and one could then tailor algorithms to account for their presence. If the density of stray localized quasiparticles is sufficiently high, however, this would no longer be possible. Fortunately, these stray particles can be minimized by one of the methods discussed above to keep the energy gap large—by improving the mobility of the 2D electron sample on which the measurements (i.e.,

the computation operations) are carried out. Improvement in the mobility leads to both the enhancement of the excitation gap and the suppression of unwanted quasiparticle localization by disorder.

We emphasize, however, the extremely high quality of the current samples. Current “good” sample mobilities are in the range $(10\text{--}30) \times 10^6 \text{ cm}^2/\text{Vs}$. To give the reader an idea of how impressive this is, we note that under such conditions, at low temperatures, the mean free path for an electron may be a macroscopic length of 0.1 mm or more. (Compare this to, say, copper at room temperature, which has a mean free path of tens of nanometers or less.)

Nonetheless, further technique and design improvement fit molecular-beam epitaxy (MBE) may be needed to push low-temperature 2D electron mobilities to $100 \times 10^6 \text{ cm}^2/\text{Vs}$ or above for topological quantum computation to be feasible. At lower temperatures, $T < 100 \text{ mK}$, phonon scattering is strongly suppressed (Stormer *et al.*, 1990; Kawamura and Das Sarma, 1992), and therefore there is essentially no intrinsic limit to the 2D electron mobility, since extrinsic scattering associated with impurities and disorder can, in principle, be eliminated through materials improvement. In fact, steady materials improvement in modulation-doped 2D GaAs-AlGaAs heterostructures grown by the MBE technique has enhanced the 2D electron mobility from $10^4 \text{ cm}^2/\text{Vs}$ in the early 1980s to $30 \times 10^6 \text{ cm}^2/\text{Vs}$ in 2004, a three orders of magnitude improvement in materials quality in roughly 20 years. Indeed, the vitality of the entire field of quantum Hall physics is a result of these amazing advances. Another factor of 2–3 improvement in the mobility seems possible (Pfeiffer, 2007), and may be needed for the successful experimental observation of non-Abelian anyonic statistics and topological quantum computation.

D. Other proposed non-Abelian systems

This review focuses on the non-Abelian anyonic properties of certain fractional quantum Hall states (e.g., $\nu = 5/2, 12/5$, etc. states) in two-dimensional semiconductor structures, mainly because theoretical and experimental study of such (possibly) non-Abelian fractional quantized Hall states is a mature subject, dating back to 1986, with many concrete results and ideas, including a proposal (Das Sarma *et al.*, 2005) for the construction of qubits and a NOT gate for topological quantum computation (described in Sec. II.C.4 and in Sec. IV). But there are several other systems that are potential candidates for topological quantum computation, and we briefly discuss these systems in this section. Indeed, the earliest proposals for fault-tolerant quantum computation with anyons were based on spin systems, not the quantum Hall effect (Kitaev, 2003).

First, we emphasize that the most crucial necessary condition for carrying out topological quantum computation is the existence of appropriate “topological matter,” i.e., a physical system in a topological phase. Such a

phase of matter has suitable ground state properties and quasiparticle excitations manifesting non-Abelian statistics. Unfortunately, the necessary and sufficient conditions for the existence of topological ground states are not known even in theoretical models. We note that the topological symmetry of the ground state is an emergent symmetry at low energy, which is not present in the microscopic Hamiltonian of the system. Consequently, given a Hamiltonian, it is difficult to determine if its ground state is in a topological phase. It is certainly no easier than showing that any other low-energy emergent phenomenon occurs in a particular model. Except for exactly solvable models (see, e.g., Levin and Wen 2005b; Kitaev, 2006), described in Sec. III.G, topological ground states are inferred on the basis of approximations and guesswork. On the other hand, if topological states exist at all, they will be robust (i.e., their topological nature should be fairly insensitive to local perturbations, e.g., electron-phonon interaction or charge fluctuations between traps). For this reason, we believe that, if it can be shown that some model Hamiltonian has a topological ground state, then a real material which is described approximately by that model is likely to have a topological ground state as well.

One theoretical model that is known to have a non-Abelian topological ground state is a $(p+ip)$ -wave superconductor (i.e., a superconductor where the order parameter is of p_x+ip_y symmetry). As described in Sec. III.B, vortices in a superconductor of $p+ip$ pairing symmetry exhibit non-Abelian braiding statistics. This is a reincarnation of the physics of the Pfaffian state (believed to be realized at the $\nu=5/2$ quantum Hall plateau) in zero magnetic field. Chiral p -wave superconductivity or superfluidity is currently the most transparent route to non-Abelian anyons. As discussed below, there are multiple physical systems that may host such a reincarnation. The Kitaev honeycomb model (see also Sec. III.G) (Kitaev, 2006) is a different model which gives rise to the same physics. In it, spins interact anisotropically such that their Hilbert space can be mapped onto that of a system of Majorana fermions. In various parameter ranges, the ground state is in either an Abelian topological phase or a non-Abelian one in the same universality class as a $p+ip$ superconductor.

Chiral p -wave superconductors, like quantum Hall states, break parity and time-reversal symmetries, although they do so spontaneously, rather than as a result of a large magnetic field. However, it is also possible to have a topological phase that does not break these symmetries. Soluble theoretical models of spins on a lattice have been constructed that have P, T -invariant topological ground states. A simple model of this type with an Abelian topological ground state, called the “toric code,” was proposed by Kitaev (2003). Even though it is not sufficient for topological quantum computation because it is Abelian, it is instructive to consider this model because non-Abelian models can be viewed as more complex versions of it. It describes $s=1/2$ spins on a lattice interacting through the following Hamiltonian (Kitaev, 2003):

$$H = -J_1 \sum_i A_i - J_2 \sum_p F_p. \quad (18)$$

This model can be defined on an arbitrary lattice. The spins are assumed to be on the links of the lattice: $A_i \equiv \prod_{\alpha \in \mathcal{N}(i)} \sigma_z^\alpha$, where $\mathcal{N}(i)$ is the set of spins on links α which touch the vertex i , and $F_p \equiv \prod_{\alpha \in p} \sigma_x^\alpha$, where p is a plaquette and $\alpha \in p$ are the spins on the links comprising the plaquette. This model is exactly soluble because the A_i 's and F_p 's all commute with each other. For any $J_1, J_2 > 0$, the ground state $|0\rangle$ is given by $A_i|0\rangle = F_p|0\rangle = |0\rangle$ for all i, p . Quasiparticle excitations are sites $A_i|0\rangle = -|0\rangle$ or plaquettes p at which $F_p|0\rangle = -|0\rangle$. A pair of excited sites can be created at i and i' by acting on the ground state with $\prod_{\alpha \in \mathcal{C}} \sigma_x^\alpha$, where the product is over the links in a chain \mathcal{C} on the lattice connecting i and i' . Similarly, a pair of excited plaquettes can be created by acting on the ground state with connected $\prod_{\alpha \in \tilde{\mathcal{C}}} \sigma_z^\alpha$ where the product is over the links crossed by a chain $\tilde{\mathcal{C}}$ on the dual lattice connecting the centers of plaquettes p and p' . Both types of excitation are bosons, but when an excited site is taken around an excited plaquette, the wave function acquires a minus sign. Thus these two types of bosons are *relative semions*.

The toric code model is not realistic, but it is closely related to more realistic models, such as the quantum dimer model (Klein, 1982; Rokhsar and Kivelson, 1988; Chayes *et al.*, 1989; Moessner and Sondhi, 2001; Nayak and Shtengel, 2001). The degrees of freedom in this model are dimers on the links of a lattice, which represent a spin singlet bond between the two spins on either end of a link. The quantum dimer model was proposed as an effective model for frustrated antiferromagnets, in which the spins do not order, but instead form singlet bonds that resonate among the links of the lattice—the resonating valence bond (RVB) state (Anderson, 1973; 1987; Baskaran *et al.*, 1987; Kivelson *et al.*, 1987) which, in modern language, we would describe as a specific realization of a simple Abelian topological state (Balents *et al.*, 1999, 2000; Senthil and Fisher, 2000, 2001a; Moessner and Sondhi, 2001). While the quantum dimer model on the square lattice does not have a topological phase for any range of parameter values (the RVB state is the ground state only at a critical point), the model on a triangular lattice does have a topological phase (Moessner and Sondhi, 2001).

Levin and Wen (2005a, 2005b) constructed a model which is a non-Abelian generalization of Kitaev's toric code model. It is an exactly soluble model of spins on the links (two on each link) of the honeycomb lattice with three-spin interactions at each vertex and twelve-spin interactions around each plaquette, described in Sec. III.G. This model realizes a non-Abelian phase that supports Fibonacci anyons, which permits universal topological quantum computation (and generalizes to other non-Abelian topological phases). Other models have been constructed (Fendley and Fradkin, 2005; Freedman *et al.*, 2005a), which are not exactly soluble but have only two-body interactions and can be argued

to support topological phases in some parameter regime. However, there is still a considerable gap between models that are soluble or quasisoluble and models that might be considered realistic for some material.

Models such as the Kitaev and Levin-Wen models are deep within topological phases; there are no other competing states nearby in their phase diagram. However, simple models such as the Heisenberg model or extensions of the Hubbard model are not of this form. The implication is that such models are not deep within a topological phase, and topological phases must compete with other phases, such as broken symmetry phases. In the quantum dimer model (Rokhsar and Kivelson, 1988; Moessner and Sondhi, 2001), for instance, an Abelian topological phase must compete with various crystalline phases which occupy most of the phase diagram. This is presumably one obstacle to finding topological phases in more realistic models, i.e., models that give an approximate description of some concrete physical system.

There are several physical systems—apart from fractional quantum Hall states—that might be promising hunting grounds for topological phases, including transition metal oxides and ultracold atoms in optical traps. The transition metal oxides have an advantage: we already know that they give rise to collective phenomena such as high- T_c superconductivity, colossal magnetoresistance, stripes, and thermoelectricity. Unfortunately, their physics is difficult to unravel both theoretically and experimentally for this very reason: there are often many different competing phenomena in these materials. This is reflected in the models that describe transition metal oxides. They tend to have many closely competing phases, so that different approximate treatments find rather different phase diagrams. There is a second advantage to the transition metal oxides, namely, that many experimental techniques have been developed to study them, including transport, thermodynamic measurements, photoemission, neutron scattering, x-ray scattering, and NMR. Unfortunately, however, these methods are tailored for detecting broken-symmetry states or for giving a detailed understanding of metallic behavior, not for uncovering a topological phase. Nevertheless, this is such a rich family of materials that it would be surprising if there were not a topological phase hiding there (whether we find it is another matter). There is one particular material in this family, Sr_2RuO_4 , for which there is evidence that it is a chiral p -wave superconductor at low temperatures, $T_c \approx 1.5$ K (Kidwingira *et al.*, 2006; Xia *et al.*, 2006). Half quantum vortices in a thin film of such a superconductor would exhibit non-Abelian braiding statistics (since Sr_2RuO_4 is not spin polarized, one must use half quantum vortices, not ordinary vortices). However, half quantum vortices are usually not the lowest-energy vortices in a chiral p -wave superconductor, and a direct experimental observation of the half vortices themselves would be a milestone on the way to topological quantum computation (Das Sarma Nayak, *et al.*, 2006).

The current status of research is as follows. Three-dimensional single crystals and thin films of Sr_2RuO_4

have been fabricated and studied. The superconductivity of these samples has been studied by many experimental probes, with the goal of identifying the symmetry of the Cooper pair. There are many indications that support the identification of Sr_2RuO_4 as a p_x+ip_y superconductor. First, experiments that probe the spins of the Cooper pair indicate triplet pairing (Mackenzie and Maeno, 2003). Such experiments probe the spin susceptibility through measurements of the NMR Knight shift and of neutron scattering. For singlet spin pairing, the susceptibility vanishes at zero temperature, since the spins retain a zero polarization state in order to form Cooper pairs. In contrast, the susceptibility remains finite for triplet pairing, and this is indeed the observed behavior. Second, several experiments that probe time-reversal symmetry have indicated that it is broken, as expected from a $p\pm ip$ superconductor. These experiments include muon spin relaxation (Mackenzie and Maeno, 2003) and the polar Kerr effect (Xia *et al.*, 2006). In contrast, magnetic imaging experiments designed to probe the edge currents that are associated with a superconductor that breaks time reversal symmetry did not find the expected signal (Kirtley *et al.*, 2007). The absence of this signal may be attributed to the existence of domains of $p+ip$ interleaved with those of $p-ip$. In summary, Sr_2RuO_4 is likely to be a three dimensional $p+ip$ superconductor, which may open the way for realization of a two-dimensional superconductor that breaks time-reversal symmetry.

The other promising direction to look for topological phases, ultracold atoms in traps, also has several advantages. The Hamiltonian can often be tuned by, for instance, tuning the lasers which define an optical lattice or by tuning through a Feshbach resonance. For instance, there is a specific scheme for realizing the Hubbard model (Jaksch and Zoller, 2005) in this way. At present there are relatively few experimental probes of these systems, as compared with transition metal oxides or even semiconductor devices. However, some available probes give information that cannot be measured in electronic systems. Furthermore, new probes for cold atom systems are being developed at a remarkable rate.

There are two different schemes for generating topological phases in ultracold atomic gases that seem promising at the current time. The first is the approach of using fast-rotating dilute Bose gases (Wilkin *et al.*, 1998) to make quantum Hall systems of bosons (Cooper *et al.*, 2001). Here the rotation plays the role of an effective magnetic field, and the filling fraction is given by the ratio of the number of bosons to the number of vortices caused by rotation. Experimental techniques (Aboshaeer *et al.*, 2001; Bretin *et al.*, 2004; Schweikhard *et al.*, 2004) have been developed that can give large rotation rates, and filling fractions can be generated which are as low as $\nu=500$ (Schweikhard *et al.*, 2004). While this is sufficiently low that all of the bosons are in a single Landau level (since there is no Pauli exclusion, $\nu>1$ can still be a lowest-Landau-level state), it is still predicted to be several orders of magnitude too high for interesting topological states to be realized. Theoretically, the inter-

esting topological states occur for $\nu<10$ (Cooper *et al.*, 2001). In particular, evidence is strong that $\nu=1$, should it be achieved, would be the bosonic analog of the Moore-Read state, and slightly less strong evidence suggests that $\nu=3/2$ and 2 would be the Read-Rezayi states, if the interboson interactions were appropriately adjusted (Rezayi *et al.*, 2005; Cooper and Rezayi, 2007). In order to access this regime, either rotation rates will need to be increased substantially or densities will have to be decreased substantially. While the latter sounds easier, it then results in all interaction scales being correspondingly lower, and hence implies that the temperature would have to be lower also, which again becomes a challenge. Several other works have proposed using atomic lattice systems where manipulation of parameters of the Hamiltonian induces effective magnetic fields and should also result in quantum Hall physics (Mueller, 2004; Popp *et al.*, 2004; Sørensen *et al.*, 2005).

The second route to generating topological phases in cold atoms is the idea of using a gas of ultracold fermions with a p -wave Feshbach resonance, which could form a spin-polarized chiral p -wave superfluid (Gurarie *et al.*, 2005). Preliminary studies of such p -wave systems have been made experimentally (Gaebler *et al.*, 2007) and, unfortunately, it appears that the decay time of the Feshbach bound states may be so short that thermalization is impossible. Indeed, recent theoretical work (Levinson *et al.*, 2007) suggests that this may be a generic problem and additional tricks may be necessary if a p -wave superfluid is to be produced in this way.

We note that both the $\nu=1$ rotating boson system and the chiral p -wave superfluid would be quite closely related to the putative non-Abelian quantum Hall state at $\nu=5/2$ (as is Sr_2RuO_4). However, there is an important difference between a p -wave superfluid of cold fermions and the $\nu=5/2$ state. Two-dimensional superconductors, as well as superfluids in any dimension, have a gapless Goldstone mode. Therefore there is the danger that the motion of vortices may cause the excitation of low-energy modes. Superfluids of cold atoms may, however, be good test grounds for the detection of localized Majorana modes associated with localized vortices, as those are expected to have a clear signature in the absorption spectrum of rf radiation (Tewari, Das Sarma, Nayak, *et al.*, 2007), in the form of a discrete absorption peak whose density and weight are determined by the density of vortices (Grosfeld *et al.*, 2007). One can also realize, using suitable laser configurations, Kitaev's honeycomb lattice model [Eq. (58)] with cold atoms on an optical lattice (Duan *et al.*, 2003). Zhang *et al.* (2007) showed how to braid anyons in such a model.

A major difficulty in finding a topological phase in either a transition metal oxide or an ultracold atomic system is that topological phases are hard to detect directly. If the phase breaks parity and time-reversal symmetries, either spontaneously or as a result of an external magnetic field, then there is usually an experimental handle through transport, as in the fractional quantum Hall states or chiral p -wave superconductors. If the state

does not break parity and time-reversal symmetry, however, there is no “smoking gun” experiment, short of creating quasiparticles, braiding them, and measuring the outcome.

Any detailed discussion of the physics of these “alternative” topological systems is beyond the scope of the current review. We refer the readers to the existing literature on these systems for details. In Sec. III (especially Sec. III.G), however, we discuss soluble models that support topological phases because many of their mathematical features elucidate the underlying structure of topological phases.

III. TOPOLOGICAL PHASES OF MATTER AND NON-ABELIAN ANYONS

Topological quantum computation is predicated on the existence in nature of topological phases of matter. In this section, we discuss the physics of topological phases from several different perspectives, using a variety of theoretical tools. The reader interested primarily in the application of topological phases to quantum computation can skim this section and still understand Sec. IV. However, a reader with a background in condensed matter physics and quantum field theory may find it enlightening to read a more detailed account of the theory of topological phases and the emergence of anyons from such phases, with explicit derivations of some of the results mentioned in Sec. II and used in Sec. IV. These readers may find topological phases interesting in and of themselves, apart from possible applications.

Topological phases, the states of matter which support anyons, occur in many-particle physical systems. Therefore we use field theory techniques to study these states. A canonical example of a field theory for a topological phase is Chern-Simons theory. We use this theory to illustrate the general points we make about topological phases. In Sec. V, we make a few comments about the problem of classifying topological phases, and how this example, Chern-Simons theory, fits in the general classification. In Sec. III.A, we give a more precise definition of a topological phase and connect this definition with the existence of anyons. We also introduce Chern-Simons theory, discussed throughout Sec. III as an example of the general structure discussed in Sec. III.A. In Sec. III.B, we discuss a topological phase that is superficially rather different but, in fact, will prove to be a special case of Chern-Simons theory. This phase can be analyzed using the formalism of BCS theory. In Sec. III.C, we further analyze Chern-Simons theory, giving an account of its topological properties, especially the braiding of anyons. We describe Witten’s work (Witten, 1989) connecting Chern-Simons theory with the knot and link invariants of Jones and Kauffman (Jones, 1985; Kauffman, 1987). We show how the latter can be used to derive the properties of anyons in these topological phases. In Sec. III.D, we describe a complementary approach by which Chern-Simons theory can be understood: through its connection to conformal field theory.

We explain how this approach can be fruitful in connection with fractional quantum Hall states. In Sec. III.E, we discuss the gapless excitations which must be present at the edge of any chiral topological phase. Their physics is intimately connected with the topological properties of the bulk and, at the same time, is directly probed by transport experiments in quantum Hall devices. In Sec. III.F, we apply knowledge gained about the properties of Chern-Simons theory to the interferometry experiments that we discussed in Sec. II.C.3. Finally, in Sec. III.G we discuss a related but different class of topological phases which can arise in lattice models and may be relevant to transition metal oxides or “artificial” solids such as ultracold atoms in optical lattices.

Interesting work which is only partially reviewed here may be found in Jackiw and Rebbi (1976); Schwarz (1978); Fradkin and Kadanoff (1980); Su *et al.* (1980); Goldstone and Wilczek (1981); Jackiw and Schrieffer (1981); Laughlin (1981, 1988a, 1988b); Su and Schrieffer (1981); Tsui *et al.* (1982); Wilczek (1982b); Tao and Wu (1984); Fateev and Zamolodchikov (1985); Niu *et al.* (1985); Cardy (1986); Zhang and Das Sarma (1986); Boebinger *et al.* (1987); Girvin and MacDonald (1987); Kalmeyer and Laughlin (1987); Fröhlich and Marchetti (1988, 1989, 1991); Sutherland (1988); Willett *et al.* (1988); Aneziris *et al.* (1989); Bonesteel (1989, 2000); Chen *et al.* (1989); Fetter *et al.* (1989); Kivelson (1989); Read (1989, 2003); Read and Chakraborty (1989); Alford *et al.* (1990); Dijkgraaf and Witten (1990); Kivelson and Rokhsar (1990); Imbo and March-Russell (1990); Imbo *et al.* (1990); Rokhsar (1990); Verlinde (1990); Wen (1990, 1991a); Wen and Niu (1990); Balatsky and Fradkin (1991); Lo and Preskill (1993); Kauffman and Lins (1994); Lee and Oh (1994); Mudry and Fradkin (1994a, 1994b); Blanchet *et al.* (1995); Morf and d’Ambrumenil (1995); Bonesteel *et al.* (1996); Koulakov *et al.* (1996); Milovanović and Read (1996); Steane (1996b, 1996c); Henley (1997); Ortalan *et al.* (1997); Balents *et al.* (1998, 2002); Bouwknegt and Schoutens (1999); Cappelli *et al.* (1999); Kitaev *et al.* (1999); Lilly *et al.* (1999b); Misguich *et al.* (1999); Moessner *et al.* (1999); Pan *et al.* (1999); Jacob and Mathieu (2000, 2002); Ardonne *et al.* (2001); Freedman (2001, 2003); Harrow (2001); Senthil and Fisher (2001b); Ardonne (2002); Eisenstein *et al.* (2002); Fendley *et al.* (2002, 2007b); Ioffe *et al.* (2002); Motrunich and Senthil (2002); Senthil and Motrunich (2002); Freedman, Kitaev, *et al.* (2003); Freedman, Nayak, *et al.* (2003); Mochon (2003, 2004); Motrunich (2003); Douçot *et al.* (2004, 2005); Stern *et al.* (2004); Freedman *et al.* (2005b); Marzuoli and Rasetti (2005); Bergholtz *et al.* (2006); Feldman and Kitaev (2006); Georgiev and Geller (2006); Hou and Chamon (2006); Pachos (2006, 2007); Seidel and Lee (2006); Semenov and Sodano (2006, 2007); Wan *et al.* (2006, 2007); Ardonne and Schoutens (2007); Brennen and Pachos (2007); Chen and Hu (2007); Chung and Stone (2007); Dyakonov (2007); Lee *et al.* (2007); Miller *et al.* (2007); Oshikawa *et al.* (2007); Pfeiffer (2007); Simon *et al.* (2007b); Tewari *et al.* (2007, 2008); Bishara and Nayak (2008); Bishara *et al.* (2008); Dean *et al.* (2008); Fiete *et al.* (2008); Zhang *et al.* (2008).

A. Topological phases of matter

In Sec. II of this paper, we used the term topological phase as being essentially synonymous with any system whose quasiparticle excitations are anyons. However, a precise definition is the following. A system is in a topological phase if, at low temperatures and energies and long wavelengths, all observable properties (e.g., correlation functions) are invariant under smooth deformations (diffeomorphisms) of the space-time manifold in which the system lives. Equivalently, all observable properties are independent of the choice of space-time coordinates, which need not be inertial or rectilinear. (This is the “passive” sense of a diffeomorphism, while the first statement uses the active sense of a transformation.) By “at low temperatures and energies and long wavelengths,” we mean that diffeomorphism invariance is violated only by terms that vanish as $\sim \max(e^{-\Delta/T}, e^{-|\xi|/\xi})$ for some nonzero energy gap Δ and finite correlation length ξ . Thus topological phases have, in general, an energy gap separating the ground state(s) from the lowest excited states. Note that an excitation gap, while necessary, is not sufficient to ensure that a system is in a topological phase.

The invariance of all correlation functions under diffeomorphisms means that the only local operator that has nonvanishing correlation functions is the identity. For instance, under an arbitrary change of space-time coordinates $x \rightarrow x' = f(x)$, the correlations of a scalar operator $\phi(x)$ must satisfy $\langle 0_i | \phi(x_1) \phi(x_2) \cdots \phi(x_n) | 0_j \rangle = \langle 0_i | \phi(x'_1) \phi(x'_2) \cdots \phi(x'_n) | 0_j \rangle$, which implies that $\langle 0_i | \phi(x_1) \phi(x_2) \cdots \phi(x_n) | 0_j \rangle = 0$ unless $\phi(x) \equiv c$ for some constant c . Here $|0_i\rangle$ and $|0_j\rangle$ are ground states of the system (which may or may not be different). This property is important because any local perturbation, such as the environment, couples to a local operator. Hence these local perturbations are proportional to the identity. Consequently, they cannot have nontrivial matrix elements between different ground states. The only way in which they can affect the system is by exciting the system to high energies, at which diffeomorphism invariance is violated. At low temperatures, the probability for this is exponentially suppressed.

The preceding definition of a topological phase may be stated more compactly by simply saying that a system is in a topological phase if its low energy effective field theory is a topological quantum field theory (TQFT), i.e., a field theory whose correlation functions are invariant under diffeomorphisms. Remarkably, topological invariance does not imply trivial low-energy physics.

1. Chern-Simons theory

Consider the simplest example of a TQFT, Abelian Chern-Simons theory, which is relevant to the Laughlin states at filling fractions $\nu = 1/k$, with k an odd integer. Although there are many ways to understand the Laughlin states, it is useful for us to take the viewpoint of a low-energy effective theory. Since quantum Hall

systems are gapped, we can describe the system by a field theory with few degrees of freedom. To this end, we consider the action

$$S_{\text{CS}} = \frac{k}{4\pi} \int d^2\mathbf{r} dt \epsilon^{\mu\nu\rho} a_\mu \partial_\nu a_\rho, \quad (19)$$

where k is an integer and ϵ is the antisymmetric tensor. Here a is a U(1) gauge field and the indices μ, ν , and ρ take the values 0 (for the time direction), 1 and 2 (space directions). This action represents the low-energy degrees of freedom of the system, which are purely topological.

The Chern-Simons gauge field a in Eq. (19) is an emergent degree of freedom which encodes the low-energy physics of a quantum Hall system. Although, in this particular case, it is related to the electronic charge density, we will also consider systems in which emergent Chern-Simons gauge fields cannot be related in a simple way to the underlying electronic degrees of freedom.

In the presence of an external electromagnetic field and quasiparticles, the action takes the form

$$S = S_{\text{CS}} - \int d^2\mathbf{r} dt \left(\frac{1}{2\pi} \epsilon^{\mu\nu\rho} A_\mu \partial_\nu a_\rho + j_\mu^{\text{qp}} a_\mu \right), \quad (20)$$

where j_μ^{qp} is the quasiparticle current, $j_0^{\text{qp}} = \rho^{\text{qp}}$ is the quasiparticle density, $\mathbf{j}^{\text{qp}} = (j_1^{\text{qp}}, j_2^{\text{qp}})$ is the quasiparticle spatial current, and A_μ is the external electromagnetic field. We assume that quasiparticles are not dynamical, but instead move along some fixed classically prescribed trajectories which determine j_μ^{qp} . The electrical current is

$$\mathbf{j}_\mu = \partial \mathcal{L} / \partial A_\mu = (1/2\pi) \epsilon^{\mu\nu\rho} \partial_\nu a_\rho. \quad (21)$$

Since the action is quadratic, it is completely solvable, and one can integrate out the field a_μ to obtain the response of the current to the external electromagnetic field. The result of such a calculation is the quantized Hall conductivity $\sigma_{xx} = 0$ and $\sigma_{xy} = (1/k)e^2/h$.

The equation of motion obtained by varying a_0 is the Chern-Simons constraint:

$$(k/2\pi) \nabla \times \mathbf{a} = j_0^{\text{qp}} + (1/2\pi) B. \quad (22)$$

According to this equation, each quasiparticle has Chern-Simons flux $2\pi/k$ attached to it (the magnetic field is assumed fixed). Consequently, it has electrical charge $1/k$, according to Eq. (21). As a result of the Chern-Simons flux, another quasiparticle moving in this Chern-Simons field picks up an Aharonov-Bohm phase. The action associated with taking one quasiparticle around another is, according to Eq. (20), of the form

$$\frac{1}{2} k \int d\mathbf{r} dt \mathbf{j} \cdot \mathbf{a} = kQ \int_c d\mathbf{r} \cdot \mathbf{a}, \quad (23)$$

where Q is the charge of the quasiparticle and the final integral is the Chern-Simons flux enclosed in the path. [The factor of $1/2$ on the left-hand side is due to the action of the Chern-Simons term itself which, according to the constraint Eq. (22), is $-1/2$ times the Aharonov-Bohm phase. This is canceled by a factor of 2 coming

from the fact that each particle sees the other's flux.] Thus the contribution to a path integral $e^{iS_{CS}}$ gives an Aharonov-Bohm phase associated with moving a charge around the Chern-Simons flux attached to the other charges. The phases generated in this way give the quasiparticles of this Chern-Simons theory $\theta = \pi/k$ Abelian braiding statistics.³

Therefore an Abelian Chern-Simons term implements Abelian anyonic statistics. In fact, it does nothing else. An Abelian gauge field in 2+1 dimensions has only one transverse component; the other two components can be eliminated by fixing the gauge. This degree of freedom is fixed by the Chern-Simons constraint (22). Therefore a Chern-Simons gauge field has no local degrees of freedom and no dynamics.

We now turn to non-Abelian Chern-Simons theory. This TQFT describes non-Abelian anyons. It is analogous to the Abelian Chern-Simons described above, but different methods are needed for its solution, as described in this section. The action can be written on an arbitrary manifold \mathcal{M} in the form

$$\begin{aligned} S_{CS}[a] &= \frac{k}{4\pi} \int_{\mathcal{M}} \text{tr} \left(a \wedge da + \frac{2}{3} a \wedge a \wedge a \right) \\ &= \frac{k}{4\pi} \int_{\mathcal{M}} \epsilon^{\mu\nu\rho} \left(a_{\mu}^a \partial_{\nu} a_{\rho}^a + \frac{2}{3} f_{abc} a_{\mu}^a a_{\nu}^b a_{\rho}^c \right). \end{aligned} \quad (24)$$

In this expression, the gauge field takes values in the Lie algebra of the group G . f_{abc} are the structure constants of the Lie algebra which are ϵ_{abc} for the case of $SU(2)$. For the case of $SU(2)$, we thus have a gauge field a_{μ}^a , where the underlined indices run from 1 to 3. A matter field transforming in the spin- j representation of the $SU(2)$ gauge group will couple to the combination $a_{\mu}^a x_a$, where x_a are the three generator matrices of $\mathfrak{su}(2)$ in the spin- j representation. For gauge group G and coupling constant k (called the “level”), we denote such a theory by G_k . In this paper, we are primarily concerned with $SU(2)_k$ Chern-Simons theory.

To see that Chern-Simons theory is a TQFT, note that the Chern-Simons action (24) is invariant under all diffeomorphisms of \mathcal{M} to itself, $f: \mathcal{M} \rightarrow \mathcal{M}$. The differential form notation in Eq. (24) makes this manifest, but it can be checked in coordinate form for $x^{\mu} \rightarrow f^{\mu}(x)$. Diffeomorphism invariance stems from the absence of the metric tensor in the Chern-Simons action. Written out in component form, as in Eq. (24), indices are, instead, contracted with $\epsilon^{\mu\nu\lambda}$.

³The Chern-Simons effective action for a hierarchical state is equivalent to the action for the composite fermion state at the same filling fraction (Blok and Wen, 1990; Read, 1990; Wen and Zee, 1992). It is a simple generalization of Eq. (19) which contains several internal gauge fields a_{μ}^n (with $n=1,2,\dots$), corresponding to in essence the action for the different species of particles (either the different levels of the hierarchy or the different composite fermion Landau levels).

Before analyzing the physics of this action (24), we make two observations. First, as a result of the presence of $\epsilon^{\mu\nu\lambda}$, the action changes sign under parity or time-reversal transformations. In this paper, we concentrate on topological phases that are chiral, i.e., that break parity and time-reversal symmetries. These are phases that can appear in the fractional quantum Hall effect, where the large magnetic field breaks P and T symmetries. However, we also discuss nonchiral topological phases in Sec. III.G, especially in connection with topological phases emerging from lattice models.

Second, the Chern-Simons action is not quite fully invariant under gauge transformations $a_{\mu} \rightarrow ga_{\mu}g^{-1} + g\partial_{\mu}g^{-1}$, where $g: \mathcal{M} \rightarrow G$ is any function on the manifold taking values in the group G . On a closed manifold, it is invariant only under “small” gauge transformations. Suppose that the manifold \mathcal{M} is the three-sphere S^3 . Then, gauge transformations are maps $S^3 \rightarrow G$, which can be classified topologically according to its homotopy $\pi_3(G)$. For any simple compact group G , $\pi_3(G) = \mathbb{Z}$, so gauge transformations can be classified according to their “winding number.” Under a gauge transformation with winding m ,

$$S_{CS}[a] \rightarrow S_{CS}[a] + 2\pi km \quad (25)$$

(Deser *et al.*, 1982). While the action is invariant under “small” gauge transformations, which are continuously connected to the identity and have $m=0$, it is not invariant under “large” gauge transformations ($m \neq 0$). However, it is sufficient for $\exp(iS)$ to be gauge invariant, which will be the case as long as we require that the level k be an integer. The requirement that the level k be an integer is an example of the highly rigid structure of TQFTs. A small perturbation of the microscopic Hamiltonian cannot continuously change the value of k in the effective low-energy theory; only a perturbation that is large enough to change k by an integer can do this.

The failure of gauge invariance under large gauge transformations is also reflected in the properties of Chern-Simons theory on a surface with boundary, where the Chern-Simons action is gauge invariant only up to a surface term. Consequently, there must be gapless degrees of freedom at the edge of the system whose dynamics is dictated by the requirement of gauge invariance of the combined bulk and edge (Wen, 1992), as discussed in Sec. III.E.

To unravel the physics of Chern-Simons theory, it is useful to specialize to the case in which the space-time manifold \mathcal{M} can be decomposed into a product of a spatial surface and time, $\mathcal{M} = \Sigma \times \mathbb{R}$. On such a manifold, Chern-Simons theory is a theory of the ground states of a topologically ordered system on Σ . There are no excited states in Chern-Simons theory because the Hamiltonian vanishes. This is seen in $a_0=0$ gauge, where the momentum canonically conjugate to a_1 is $-(k/4\pi)a_2$,

and the momentum canonically conjugate to a_2 is $(k/4\pi)a_1$ so that

$$\mathcal{H} = (k/4\pi)\text{tr}(a_2\partial_0a_1 - a_1\partial_0a_2) - \mathcal{L} = 0. \tag{26}$$

Note that this is a special feature of an action with a Chern-Simons term alone. If the action had both a Chern-Simons and a Yang-Mills term, then the Hamiltonian would not vanish, and the theory would have both ground and excited states with a finite gap. Since the Yang-Mills term is subleading compared to the Chern-Simons term [i.e., irrelevant in a renormalization group (RG) sense], we can forget about it at energies smaller than the gap and consider the Chern-Simons term alone.

Therefore when Chern-Simons theory is viewed as an effective field theory, it can only be valid at energies much smaller than the energy gap. As a result, it is presently unclear whether Chern-Simons theory has anything to say about the properties of quasiparticles—which are excitations above the gap—or whether those properties are part of the universal low-energy physics of the system (i.e., are controlled by the infrared RG fixed point). Nevertheless, as we see in a moment, it does and they are.

Although the Hamiltonian vanishes, the theory is still not trivial because one must solve the constraint which follows by varying a_0 . For the sake of concreteness, we specialize to the case $G=\text{SU}(2)$. Then the constraint reads

$$\epsilon_{ij}\partial_t a_j^a + f^{abc}a_1^b a_2^c = 0, \tag{27}$$

where $i, j=1, 2$. The left-hand side of this equation is the field strength of the gauge field a_i^a , where $a=1, 2, 3$ is an $\text{su}(2)$ index. Since the field strength must vanish, we can always perform a gauge transformation so that $a_i^a=0$ locally. Therefore this theory has no local degrees of freedom. However, for some field configurations satisfying the constraint, there may be a global topological obstruction which prevents us from making the gauge field zero everywhere. Clearly, this can happen only if Σ is topologically nontrivial.

The simplest nontrivial manifold is the annulus, which is topologically equivalent to a sphere with two punctures. Following [Elitzur *et al.* \(1989\)](#) [see also [Wen and Zee \(1998\)](#) for a similar construction on the torus], we take coordinates (r, ϕ) on the annulus, with $r_1 < r < r_2$, and let t be time. Then we can write $a_\mu = g\partial_\mu g^{-1}$, where

$$g(r, \phi, t) = e^{i\omega(r, \phi, t)} e^{i(\phi/k)\lambda(t)}, \tag{28}$$

where $\omega(r, \phi, t)$ and $\lambda(t)$ take values in the Lie algebra $\text{su}(2)$ and $\omega(r, \phi, t)$ is a single-valued function of ϕ . The functions ω and λ are the dynamical variables of Chern-Simons theory on the annulus. Substituting Eq. (28) into the Chern-Simons action, we see that it now takes the form

$$S = \frac{1}{2\pi} \int dt \text{tr}(\lambda\partial_t\Omega), \tag{29}$$

where $\Omega(r, t) = \int_0^{2\pi} d\phi [\omega(r_1, \phi, t) - \omega(r_2, \phi, t)]$. Therefore Ω is canonically conjugate to λ . By a gauge transformation, we can always rotate λ and Ω so that they are along the 3 direction in $\text{su}(2)$, i.e., $\lambda = \lambda_3 T^3$, $\Omega = \Omega_3 T^3$. Since it is defined through the exponential in Eq. (28), Ω_3 takes values in $[0, 2\pi]$. Therefore its canonical conjugate λ_3 is quantized to be an integer. From the definition of λ in Eq. (28), we see that $\lambda_3 \equiv \lambda_3 + 2k$. However, by a gauge transformation given by a rotation around the 1 axis, we can transform $\lambda \rightarrow -\lambda$. Hence the independent allowed values of λ are $0, 1, \dots, k$.

On the two-punctured sphere, if one puncture is of type a , the other puncture must be of type \bar{a} . (If the topological charge at one puncture is measured along a loop around the puncture—e.g., by a Wilson loop, see Sec. III.C—then the loop can be deformed so that it goes around the other puncture, but in the opposite direction. Therefore the two punctures necessarily have conjugate topological charges.) For $\text{SU}(2)$, $a = \bar{a}$, so both punctures have the same topological charge. Therefore the restriction to only $k+1$ different possible allowed boundary conditions λ for the two-punctured sphere implies that there are $k+1$ different quasiparticle types in $\text{SU}(2)_k$ Chern-Simons theory. As described in later sections, these allowed quasiparticle types can be identified with the $j=0, 1/2, \dots, k/2$ representations of the $\text{SU}(2)_2$ Kac-Moody algebra.

2. TQFTs and quasiparticle properties

We continue with our analysis of Chern-Simons theory in Secs. III.C and III.D. Here we make some general observations about TQFTs and the topological properties of quasiparticles. We turn to the n -punctured sphere, $\Sigma = S^2 \setminus P_1 \cup P_2 \cup \dots \cup P_n$, i.e., the sphere S^2 with the points P_1, P_2, \dots, P_n deleted, which is equivalent to $n-1$ quasiparticles in the plane (the n th puncture becomes the point at ∞). This allows us to study the topological properties of quasiparticle excitations purely from ground state properties. To see how braiding emerges in this approach, it is useful to note that diffeomorphisms should have a unitary representation on the ground state Hilbert space (i.e., they should commute with the Hamiltonian). Diffeomorphisms that can be smoothly deformed to the identity should have a trivial action on the Hilbert space of the theory since there are no local degrees of freedom. However, “large” diffeomorphisms could have a nontrivial unitary representation on the theory’s Hilbert space. If we take the quotient of the diffeomorphism group by the set of diffeomorphisms which can be smoothly deformed to the identity, then we obtain the mapping class group. On the n -punctured sphere, the braid group \mathcal{B}_{n-1} is a subgroup

of the mapping class group.⁴ Therefore if we study Chern-Simons theory on the n -punctured sphere as we did for the two-punctured sphere above, and determine how the mapping class group acts, we can learn all information about quasiparticle braiding. We do this by two different methods in Secs. III.C and III.D.

One extra transformation in the mapping class group, compared to the braid group, is a 2π rotation of a puncture or particle relative to the rest of the system (a Dehn twist). If we consider particles with a finite extent, rather than point particles, then we must consider the possibility of such rotations. For instance, if the particles are small dipoles, then we can represent their world lines as ribbons. A Dehn twist then corresponds to a twist of the ribbon. Thickening a world line into a ribbon is called a *framing*. A given world line has multiple choices of framing, corresponding to how many times the ribbon twists. A framing is essential in Chern-Simons theory because flux is attached to charge through the constraint (22) and (27). By putting the flux and charge at opposite edges of the ribbon, which is a short-distance regularization of the theory, we associate a well-defined phase to a particle trajectory. Otherwise, we would not know how many times the charge went around the flux.

Any transformation acting on a single particle can only result in a phase; the corresponding phase is called the twist parameter Θ_a . Often, one writes $\Theta_a \equiv e^{2\pi i h_a}$, where h_a is called the *spin* of the particle.⁵ (One must, however, be careful to distinguish this from the actual spin of the particle, which determines its transformation properties under the three-dimensional rotation group and must be half integral.) However, h_a is well defined even if the system is not rotationally invariant, so it is usually called the *topological spin* of the particle. For Abelian anyons, it is just the statistics parameter, $\theta = 2\pi i h_a$.

The ground state properties on arbitrary surfaces, including the n -punctured sphere and the torus, can be

built up from more primitive vector spaces in the following way. An arbitrary closed surface can be divided into a collection of three-punctured spheres which are glued together at their boundaries. This is called a “pants decomposition” because of the topological equivalence of a three-punctured sphere to a pair of pants. Therefore the three-punctured sphere plays a fundamental role in the description of a topological phase. Its Hilbert space is denoted by V_{ab}^c , if a , b , and c are the particle types at the three punctures. If the a and b punctures are fused, a two-punctured sphere will result. From the above analysis, it has a one-dimensional vector space if both punctures have topological charge c and a zero-dimensional vector space otherwise. The dimension of the Hilbert space of the three-punctured sphere is given by the fusion multiplicity $N_{ab}^c = \dim(V_{ab}^c)$ which appears in the fusion rule $\phi_a \times \phi_b = \sum_c N_{ab}^c \phi_c$. The Hilbert space on a surface obtained by gluing together three-punctured spheres is obtained by tensoring together V 's and summing over the particle types at the punctures where gluing occurs. For instance, the Hilbert space on the four-punctured sphere is given by $V_{abd}^e = \oplus_c V_{ab}^c V_{cd}^e$; the Hilbert space on the torus is $V_{T^2} = \oplus_a V_{1a}^a V_{a1}^a$. (If one of the particle types is the vacuum, then the corresponding puncture can be removed; the three-punctured sphere is then actually only two-punctured. Gluing two of them together end to end gives a torus. This is one way of seeing that the degeneracy on the torus is the number of particle types.)

The Hilbert space of the n -punctured sphere with topological charge a at each puncture can be constructed by sewing together a chain of $(n-2)$ three-punctured spheres. The resulting Hilbert space is $V_{a \dots a}^1 = \oplus_{b_1} V_{aa}^{b_1} V_{ab_1}^{b_2} \dots V_{ab_{n-3}}^a$. A simple graphical notation for a set of basis states of this Hilbert space is given by a *fusion chain* (similar to the fusion tree discussed in the Appendix):

$$\begin{array}{cccccccc}
 & a & & a & & a & & a & & a & & a & & a \\
 a & | & b_1 & | & b_2 & | & b_3 & | & b_4 & \dots & b_{n-4} & | & b_{n-3} & | & a
 \end{array}$$

The first two a 's on the far left fuse to b_1 . The next a fuses with b_1 to give b_2 . The next a fuses with b_2 to give b_3 , and so on. The different basis vectors in this Hilbert space correspond to the different possible allowed b_i 's. The dimension of this Hilbert space is $N_{aa}^{b_1} N_{ab_1}^{b_2} \dots N_{ab_{n-3}}^a = (N_a)_{a1}^{b_1} (N_a)_{b_1}^{b_2} \dots (N_a)_{b_{n-3}}^a$. On the right-hand side of this equation, we suggested that the fusion multiplicity N_{ab}^c can be viewed as a matrix $(N_a)_b^c$ associated with quasiparticle species a . We denote the largest eigenvalue of the matrix N_a by d_a . Then the Hilbert space of M quasiparticles of type a has dimension $\sim d_a^{M-2}$ for large M . For this reason, d_a is called the *quantum dimension* of an a quasiparticle. It is the asymptotic degeneracy per particle of a collection of a quasiparticles. For Abelian particles, $d_a=1$ since the multiparticle Hilbert space is one dimensional (for fixed particle positions). Non-Abelian particles have $d_a > 1$. Note that d_a is

⁴The mapping class group is nontrivial solely as a result of the punctures. In particular, any diffeomorphism that moves one or more puncture around other punctures cannot be deformed to the identity; conversely, if two diffeomorphisms move the same punctures along trajectories that can be deformed into each other, then the diffeomorphisms themselves can also be deformed into each other. These classes of diffeomorphisms correspond to the braid group which is, in fact, a normal subgroup. If we took the quotient of the mapping class group by the Dehn twists of $n-1$ of the punctures—all except the point at infinity—we would be left with the braid group \mathcal{B}_{n-1} .

⁵If a is its own antiparticle, so that two a 's can fuse to $\mathbf{1}$, then $R_1^{aa} = \pm \Theta_a^*$, where the minus sign is acquired for some particle types a which are not quite their own antiparticles but only up to some transformation that squares to -1 . This is analogous to the fact that the fundamental representation of $SU(2)$ is not real but pseudoreal. Consequently, a spin-1/2 particle ψ_μ and antiparticle $\psi^{\mu\dagger}$ can form a singlet $\psi^{\mu\dagger} \psi_\mu$, but two spin-1/2 particles can as well, $\psi_\mu \psi_\nu (\sigma_y)^{\mu\nu}$, where σ_y is the antisymmetric Pauli matrix. When some quantities are computed, an extra factor of $(i\sigma_y)^2 = -1$ results. This \pm sign is called the Froebenius-Schur indicator. (See, for instance, Bantay, 1997.)

not, in general, an integer, which is symptomatic of the nonlocality of the Hilbert space: it is not the tensor product of d_a -dimensional Hilbert spaces associated locally with each particle.

This nonlocality is responsible for the stability of this degenerate ground state Hilbert space. Not only the Yang-Mills term, but all possible gauge-invariant terms that we can add to the action (24), are irrelevant. This means that adding such a term to the action might split the $\sim d_a^{M-2}$ -dimensional space of degenerate states in a finite-size system, but the splitting must vanish as the system size and particle separations go to infinity. In fact, we can make an even stronger statement than that. All ground state matrix elements of gauge-invariant local operators such as the field strength squared $F_{\mu\nu}^a F^{\mu\nu a}$ vanish identically because of the Chern-Simons constraint. Therefore the degeneracy is not lifted at all in perturbation theory. It can only be lifted by nonperturbative effects (e.g., instantons or quantum tunneling), which could cause a splitting $\sim e^{-g^L}$, where g is inversely proportional to the coefficient of the Yang-Mills term. Therefore the multi-quasiparticle states are degenerate to within exponential accuracy. At finite temperatures, one must also consider transitions to excited states, but the contributions of these will be $\sim e^{-\Delta/T}$. Furthermore, if we add a time-dependent (source) term to the action, these properties would remain preserved so long as the frequency of this term remains small compared with the gap.

Aside from the n -punctured spheres, the torus is the most important manifold for considering topological phases. Although not directly relevant to experiments, the torus is important for numerical simulations since periodic boundary conditions are often the simplest choice. As noted above, the ground state degeneracy on the torus is equal to the number of quasiparticle species. Suppose one can numerically solve a Hamiltonian on the torus. If it has a gap between its ground state(s) and lowest energy excited states, then its ground state degeneracy is an important topological property of the state—namely, the number of quasiparticle species. A simple physical understanding of this degeneracy can be obtained in the following way. Suppose that we have a system of electrons in a topological phase. If we consider the system on the torus, then the electrons must have periodic boundary conditions around either generator of the torus (i.e., around either handle), but the quasiparticles need not. In the Abelian $\nu=1/m$ fractional quantum Hall state, for instance, it is possible for a quasiparticle to pick up a phase $e^{2\pi i n/m}$ in going around the meridian of the torus, where n can take any of the values $n=0, 1, \dots, m-1$; electrons would still have periodic boundary conditions since they are made up of m quasiparticles. Indeed, all m of these possibilities occur, so the ground state is m -fold degenerate.

To make this a little more precise, we introduce operators T_1 and T_2 which create a quasiparticle-quasihole pair, take the quasiparticle around the meridian or lon-

gitude, respectively, of the torus and annihilate them again. Then T_1 and T_2 must satisfy

$$T_2^{-1} T_1^{-1} T_2 T_1 = e^{2\pi i/m}, \quad (30)$$

because $T_1^{-1} T_1$ amounts to a contractible quasiparticle-quasihole loop, as does $T_2^{-1} T_2$; by alternating these processes, we cause these loops to be linked. The quasiparticle trajectories in space-time (which can be visualized as a thickened torus) are equivalent to a link between two circles (the Hopf link): the first quasiparticle-quasihole pair is pulled apart along the meridian (T_1); but before they can be brought back together (T_1^{-1}), the second pair is pulled apart along the longitude (T_2). After the first pair is brought back together and annihilated (T_1^{-1}), the second one is too (T_2^{-1}). In other words, the phase on the right-hand side of Eq. (30) is the phase obtained when one quasiparticle winds around another. This algebra can be represented on a vector space of minimum dimension m . We call the states in this vector space $|n\rangle$, $n=0, 1, \dots, m-1$. Then

$$\begin{aligned} T_1 |n\rangle &= e^{2\pi i n/m} |n\rangle, \\ T_2 |n\rangle &= |(n+1) \bmod m\rangle. \end{aligned} \quad (31)$$

These m states correspond to $n=0, 1, \dots, m-1$ quanta of flux threaded through the torus. If we cut along a meridian and open the torus into an annulus, then these states would have flux n threaded through the hole in the annulus and charge n/m at the inner boundary of the annulus (and a compensating charge at the outer boundary). We can instead switch to a basis in which T_2 is diagonal by a discrete Fourier transform. If we write $|\tilde{n}\rangle = (1/\sqrt{m}) \sum_{n=0}^{m-1} e^{2\pi i n \tilde{n}/m} |n\rangle$, then $|\tilde{n}\rangle$ is an eigenstate of T_2 with eigenvalue $e^{2\pi i \tilde{n}/m}$. In this basis, T_1 is an off-diagonal operator that changes the boundary conditions of quasiparticles around the longitude of the torus. In non-Abelian states, a more complicated version of the same thing occurs, as discussed for the case of Ising anyons in Sec. III.B. Different boundary conditions around the meridian correspond to different possible quasiparticle types which could thread the torus (or, equivalently, could be present at the inner boundary of the annulus if the torus were cut open along a meridian). One can switch to a basis in which the boundary conditions around the longitude are fixed. The desired basis change is analogous to the discrete Fourier transform given above and is given by the S matrix or modular S matrix of the theory. Switching the longitude and meridian is one generator of the mapping class group of the torus; the S matrix expresses how it acts on the ground state Hilbert space. The elements of the S matrix are closely related to quasiparticle braiding. By following a similar construction to the one with T_1 and T_2 above, one can see that S_{ab} is equal to the amplitude for creating $a\bar{a}$ and $b\bar{b}$ pairs, braiding a and b , and annihilating again in pairs. This is why, in an Abelian state, the elements of the S matrix are all phases (up to an overall normalization which ensures unitarity), e.g., $S_{nn'}$

$= (1/\sqrt{m})e^{2\pi i n m' / m}$ in the example above. In a non-Abelian state, the different entries in the matrix can have different magnitudes, so the basis change is a little more complicated than a Fourier transform. Entries can even vanish in the non-Abelian case since, after a and b have been braided, a and \bar{a} may no longer fuse to $\mathbf{1}$.

In the case of Ising anyons on the torus $[\text{SU}(2)_2]$, there are three ground states. One basis is $|\mathbf{1}_m\rangle$, $|\sigma_m\rangle$, $|\psi_m\rangle$, corresponding to the different allowed topological charges which would be measured at the inner boundary of the resulting annulus if the torus were cut open along its meridian. An equally good basis is given by eigenstates of topological charge around the longitude: $|\mathbf{1}_l\rangle$, $|\sigma_l\rangle$, $|\psi_l\rangle$. As we see at the end of the next section, the basis change between them is given by

$$S = \begin{pmatrix} \frac{1}{2} & \frac{1}{\sqrt{2}} & \frac{1}{2} \\ \frac{1}{\sqrt{2}} & 0 & -\frac{1}{\sqrt{2}} \\ \frac{1}{2} & -\frac{1}{\sqrt{2}} & \frac{1}{2} \end{pmatrix}. \quad (32)$$

The S matrix not only contains information about braiding, but also about fusion, according to Verlinde's formula (Verlinde, 1988) (for proof, see Moore and Seiberg, 1988, 1989):

$$N_{ab}^c = \sum_x \frac{S_{ax} S_{bx} S_{cx}}{S_{1x}}. \quad (33)$$

Consequently, the quantum dimension of a particle of species a is

$$d_a = S_{1a} / S_{11}. \quad (34)$$

The mathematical structure encapsulating these braiding and fusion rules is a modular tensor category (Walker, 1991; Turaev, 1994; Kassel, 1995; Bakalov and Kirillov, 2001; Kitaev, 2006). A category is composed of objects and morphisms, which are maps between the objects that preserve their defining structure. The idea is that one can learn more about the objects by understanding the morphisms between them. In our case, the objects are particles with labels (which specify their species) as well as fixed configurations of several particles. The morphisms are particle trajectories, which map a set of labeled particles at some initial time to a set of labeled particles at some final time. A tensor category has a tensor product structure for multiplying objects; here this is simply the fact that one can take two well-separated (and historically well-separated) collections of particles and consider their union to be a new "tensor-product" collection. Since we consider particles in two dimensions, the trajectories are essentially the elements of the braid group, but they include the additional possibility of twisting. (Allowing twists in the strands of a braid yields a braided ribbon category.) We further allow the trajectories to include the fusion of two particles (so that

we now have a fusion category). Morphisms can therefore be defined by specifying Θ_a , V_{ab}^c , R , and F .

Why is it necessary to invoke category theory simply to specify the topological properties of non-Abelian anyons? Could the braid group not be the highest level of abstraction that we need? The answer is that, for a fixed number of particles n , the braid group \mathcal{B}_n completely specifies their topological properties (perhaps with the addition of twists Θ_a to account for the finite size of the particles). However, we need representations of \mathcal{B}_n for all values of n that are compatible with each other and with fusion (of which pair creation and annihilation is the special case of fusion to the vacuum). So we really need a more complex—and much more tightly constrained—structure. This is provided by the concept of a modular tensor category. The F and R matrices play important roles. The F matrix can essentially be viewed as an associativity relation for fusion: we could first fuse i with j , and then fuse the result with k ; or we could fuse i with the result of fusing j with k . The consistency of this property leads to a constraint on the F matrices called the pentagon equation. (An explicit example of the pentagon equation is worked out in Sec. IV.B.) Consistency between F and R leads to a constraint called the hexagon equation. Modularity is the condition that the S matrix be invertible. These self-consistency conditions are sufficiently strong that a solution to them completely defines a topological phase.⁶

An equivalent alternative to studying punctured surfaces is to add nondynamical charges that are coupled to the Chern-Simons gauge field. Then the right-hand side of the constraint (27) is modified and a nontrivial gauge field configuration is again obtained which is equivalent to that obtained around a puncture. In the following sections, we discuss the Hilbert spaces of $\text{SU}(2)_k$ Chern-Simons theory, either on the n -punctured sphere or in the presence of nondynamical sources. These discussions enable us to compute the braiding and fusion matrices. The nontrivial quasiparticle of $\text{SU}(2)_1$ is actually Abelian so we do not discuss this "trivial" case. The next case, $\text{SU}(2)_2$, is non-Abelian and may be relevant to the $\nu=5/2$ fractional quantum Hall state. It can be understood in several different ways, which express its underlying free Majorana fermion structure. Quantum computation with Majorana fermions is described in Sec. IV.A. In the next section, we explain this structure from the perspective of a superconductor with $p+ip$ pairing symmetry. Although this description is elegant, it cannot be generalized to higher k . Therefore in the two sections after that, we describe two different approaches to solving $\text{SU}(2)_k$ Chern-Simons theory for general k . We recapitulate the case of $\text{SU}(2)_2$ in these other languages and also describe the case of $\text{SU}(2)_3$. The latter has quasiparticles in its spectrum which are Fibonacci anyons, a par-

⁶Modulo details regarding the central charge c at the edge. $e^{2\pi i c/8}$ can be obtained from the topological spins, but not c itself.

ticularly beautiful non-Abelian anyonic structure which allows for universal topological quantum computation. It may also underlie the observed $\nu=12/5$ fractional quantum Hall state. More details of the Fibonacci theory are given in Sec. IV.B.

B. Superconductors with $p+ip$ pairing symmetry

In this section, we discuss the topological properties of a superconductor with $p+ip$ pairing symmetry following [Read and Green \(2000\)](#). This method is the most elementary way in which a non-Abelian topological state can emerge as the ground state of a many-body system. This non-Abelian topological state has several possible realizations in various two-dimensional systems: $p+ip$ superconductors, such as Sr_2RuO_4 [although the non-Abelian quasiparticles are half quantum vortices in this case ([Das Sarma, Nayak, et al., 2006](#))]; $p+ip$ superfluids of cold atoms in optical traps ([Gurarie et al., 2005](#); [Tewari, Das Sharma, Nayak, et al., 2007](#)); the A phase [especially the A_1 phase ([Leggett, 1975](#); [Volovik, 1994](#))] of ^3He films; and the Moore-Read Pfaffian quantum Hall state ([Moore and Read, 1991](#)). The last of these is a quantum Hall incarnation of this state: electrons at filling fraction $\nu=1/2$ are equivalent to fermions in zero field interacting with an Abelian Chern-Simons gauge field. When the fermions pair and condense in a $p+ip$ superconducting state, the Pfaffian quantum Hall state forms ([Greiter et al., 1992](#)). Such a state can occur at $\frac{5}{2}=2+\frac{1}{2}$ if the lowest Landau level (of both spins) is filled and inert, and the first excited Landau level is half filled.

Ordinarily, one makes a distinction between the fermionic quasiparticles (or Bogoliubov–de Gennes quasiparticles) of a superconductor and vortices in a superconductor. This is because, in terms of electron variables, the former are relatively simple while the latter are rather complicated. Furthermore, the energy and length scales associated with the two are different in the weak-coupling limit. However, fermionic quasiparticles and vortices are different types of quasiparticle excitations in a superconductor—i.e., different types of localized disturbances above the ground state. Therefore we refer to them both as simply quasiparticles and use the terms Bogoliubov–de Gennes or fermionic when referring to the former. In a $p+ip$ superconductor, the quasiparticles which exhibit non-Abelian statistics are flux $hc/2e$ vortices.

1. Vortices and fermion zero modes

Suppose that we have a system of fully spin-polarized electrons in a superconducting state of p_x+ip_y pairing symmetry. The mean field Hamiltonian for such a superconductor is

$$H = \int d\mathbf{r} \psi^\dagger(\mathbf{r}) h_0 \psi(\mathbf{r}) + \frac{1}{2} \int d\mathbf{r} d\mathbf{r}' [D^*(\mathbf{r}, \mathbf{r}') \psi(\mathbf{r}') \psi(\mathbf{r}) + D(\mathbf{r}, \mathbf{r}') \psi^\dagger(\mathbf{r}) \psi^\dagger(\mathbf{r}')] \quad (35)$$

with the single-particle term $h_0 = -(1/2m)\nabla^2 - \mu$ and complex p -wave pairing function

$$D(\mathbf{r}, \mathbf{r}') = \Delta((\mathbf{r} + \mathbf{r}')/2)(i\partial_{x'} - \partial_{y'})\delta(\mathbf{r} - \mathbf{r}'). \quad (36)$$

The dynamics of Δ is governed by a Landau-Ginzburg-type Hamiltonian and will be discussed later. The quadratic Hamiltonian (36) may be diagonalized by solving the corresponding Bogoliubov–de Gennes equations (BdG) equations,

$$E \begin{pmatrix} u(\mathbf{r}) \\ v(\mathbf{r}) \end{pmatrix} = \begin{pmatrix} h_0 & \frac{i}{2}\{\Delta(\mathbf{r}), \partial_x + i\partial_y\} \\ \frac{i}{2}\{\Delta^*(\mathbf{r}), \partial_x - i\partial_y\} & -h_0 \end{pmatrix} \times \begin{pmatrix} u(\mathbf{r}) \\ v(\mathbf{r}) \end{pmatrix}. \quad (37)$$

The Hamiltonian then takes the form

$$H = E_0 + \sum_E E \Gamma_E^\dagger \Gamma_E, \quad (38)$$

where $\Gamma_E^\dagger \equiv \int d\mathbf{r} [u_E(\mathbf{r}) \psi(\mathbf{r}) + v_E(\mathbf{r}) \psi^\dagger(\mathbf{r})]$ is the creation operator formed by the positive-energy solutions of the Bogoliubov–de Gennes equations and E_0 is the ground state energy. For the ground state of the Hamiltonian (36) to be degenerate in the presence of several vortices (which are the most interesting quasiparticles in this theory) it is essential that the BdG equations have solutions with eigenvalue zero in this situation.

Before searching for zero eigenvalues of Eq. (38) in the presence of vortices, however, we focus on a uniform superconductor, where Δ is a constant. [Read and Green \(2000\)](#) retained only the potential part of h_0 , which for a uniform superconductor is a constant $-\mu$. With this simplification, a BdG eigenstate with momentum k has energy

$$E_k = \sqrt{\mu^2 + \Delta^2 |k|^2}. \quad (39)$$

The ground state of Eq. (36) is the celebrated BCS wave function, written here in an unnormalized form,

$$|\text{gs}\rangle = \prod_{\mathbf{k}} \left(1 + \frac{v_{\mathbf{k}}}{u_{\mathbf{k}}} c_{\mathbf{k}}^\dagger c_{-\mathbf{k}}^\dagger \right) |\text{vac}\rangle = \exp \left(\sum_{\mathbf{k}} \frac{v_{\mathbf{k}}}{u_{\mathbf{k}}} c_{\mathbf{k}}^\dagger c_{-\mathbf{k}}^\dagger \right) |\text{vac}\rangle, \quad (40)$$

where

$$\begin{pmatrix} |u_{\mathbf{k}}|^2 \\ |v_{\mathbf{k}}|^2 \end{pmatrix} = \frac{1}{2} \begin{pmatrix} 1 \\ 1 \mp \frac{\mu}{\sqrt{\mu^2 + |\Delta k|^2}} \end{pmatrix} \quad (41)$$

are the BCS coherence factors. The wave function (40) describes a coherent state of an undetermined number of Cooper pairs, each in an internal state of angular momentum $\ell = -1$. Its projection onto a fixed even number of particles N is carried out by expanding the exponent

in Eq. (40) to the $(N/2)$ th order. When written in first-quantized language, this wave function describes a properly antisymmetrized wave function of $N/2$ Cooper pairs, each in an internal state

$$g(\mathbf{r}) = \sum_{\mathbf{k}} \frac{v_{\mathbf{k}}}{u_{\mathbf{k}}} e^{i\mathbf{k}\cdot\mathbf{r}}. \quad (42)$$

In first-quantized form the multiparticle BCS wave function is then of the Pfaffian form of an antisymmetric matrix whose $i-j$ element is $g(\mathbf{r}_i - \mathbf{r}_j)$, an antisymmetrized product of pair wave functions

$$\begin{aligned} \Psi_{\text{BCS}} &= \text{Pf}[g(\mathbf{r}_i - \mathbf{r}_j)] \\ &= \mathcal{A}[g(\mathbf{r}_1 - \mathbf{r}_2)g(\mathbf{r}_3 - \mathbf{r}_4) \cdots g(\mathbf{r}_{N-1} - \mathbf{r}_N)] \end{aligned} \quad (43)$$

with \mathcal{A} an antisymmetrization operator.

The function $g(\mathbf{r})$ depends on the sign of μ , since the small- k behavior of $v_{\mathbf{k}}/u_{\mathbf{k}}$ depends on that sign. When $\mu > 0$, we have $g(r) = 1/(x+iy)$ in the long-distance limit (Read and Green, 2000). If we assume that this form holds for all distances, the Pfaffian wave function obtained is identical to the Moore-Read form discussed below in connection with the Ising model and the $\nu = 5/2$ quantum Hall state in Sec. III.D [see Eqs. (12) and (92)]. The slow decay of $g(r)$ implies a weak Cooper pairing. (But it does not imply that the state is gapless. One can verify that electron Green's functions all decay exponentially for any nonzero μ .) When $\mu < 0$ the function $g(r)$ decays much more rapidly with r , generically in an exponential way, such that the Cooper pairs are strongly bound. Furthermore, there is a topological distinction between the $\mu > 0$ and $\mu < 0$ phases. The distinction, discussed by Read and Green (2000), implies that, despite the fact that both states are superconducting, the $\mu > 0$ and $\mu < 0$ states must be separated by a phase transition. [In the analogous quantum Hall state, both states are characterized by the same Hall conductivity but are separated by a phase transition, and are distinguished by their thermal Hall conductivities (Read and Green, 2000).] Indeed, from Eq. (39) we see that the gap vanishes for a uniform $p+ip$ superconductor with $\mu=0$. The low-energy BdG eigenstates at this second-order phase transition point form a Dirac cone.

For every solution (u, v) of the BdG equations with energy E , there is a solution (v^*, u^*) of energy $-E$. A solution with $u=v^*$ therefore has energy zero. We soon consider situations in which there are multiple zero-energy solutions (u_i, u_i^*) , $i=1, 2, \dots$. If we denote the corresponding operators by γ_i [see Eq. (47) below], then they satisfy

$$\gamma_i^\dagger = \gamma_i. \quad (44)$$

Equation (44) is the definition of a Majorana fermion operator.

We now consider the BdG equations in the presence of vortices when the bulk of the superconductor is in the $\mu > 0$ phase. As usual, a vortex is characterized by a point of vanishing Δ , and a 2π winding of the phase of Δ around that point. In principle we should, then, solve the

BdG equations in the presence of such a nonuniform Δ . However, we can, instead, solve them in the presence of a nonuniform μ , which is much simpler. All we need is to make the core of the superconductor topologically distinct from the bulk, i.e., a puncture in the superconductivity. Making $\mu < 0$ in the core is just as good as taking Δ to zero, as far as topological properties are concerned. Therefore we associate the core of the vortex with a region of $\mu < 0$, whereas the bulk is at $\mu > 0$. Thus there is a $\mu=0$ line encircling the vortex core. This line is an internal edge of the system. We consider the dynamics of edge excitations in Sec. III.E, but here we simply show that a zero-energy mode is among them.

The simplest situation to consider is that of azimuthal symmetry, with the polar coordinates denoted by r and θ . Imagine the vortex core to be at the origin, so that $\Delta(r, \theta) = |\Delta(r)|e^{i\theta+i\Omega}$. Here Ω is the phase of the order parameter along the $\theta=0$ line, a phase which will play an important role later in our discussion. Assume that the $\mu=0$ line is the circle $r=r_0$, and write

$$\mu(r) = \Delta h(r), \quad (45)$$

with $h(r)$ large and positive for large r , and $h(r) < 0$ for $r < r_0$; therefore the electron density will vanish for $r \ll r_0$. Such a potential defines an edge at $r=r_0$. There are low-energy eigenstates of the BdG Hamiltonian that are spatially localized near $r=0$ and are exponentially decaying for $r \rightarrow \infty$:

$$\phi_E^{\text{edge}}(r, \theta) = e^{i\ell\theta} \exp\left(-\int_0^r h(r')dr'\right) \begin{pmatrix} e^{-i\theta/2} \\ e^{i\theta/2} \end{pmatrix}. \quad (46)$$

The spinor on the right-hand side points in a direction in pseudospin space that is tangent to the $r=r_0$ circle at θ . This wave function describes a chiral wave propagating around the edge, with angular momentum ℓ and energy $E = \Delta\ell/r_0$. Since the flux is an odd multiple of $hc/2e$, the Bogoliubov quasiparticle (46) must be antiperiodic as it goes around the vortex. However, the spinor on the right-hand side of Eq. (46) is also antiperiodic. Therefore the angular momentum ℓ must be an integer, $\ell \in \mathbb{Z}$. Consequently, a flux $hc/2e$ vortex has an $\ell=0$ solution, with energy $E=0$. (Conversely, if the flux through the vortex were an even multiple of $hc/2e$, ℓ would be a half integer, $\ell \in \mathbb{Z} + \frac{1}{2}$, and there would be no zero mode.) The operator corresponding to this zero mode, which we call γ , can be written in the form

$$\gamma = \frac{1}{\sqrt{2}} \int dr [F(\mathbf{r})e^{-(i/2)\Omega} \psi(\mathbf{r}) + F^*(\mathbf{r})e^{(i/2)\Omega} \psi^\dagger(\mathbf{r})]. \quad (47)$$

Here $F(\mathbf{r}) = \exp[\int_0^r h(r')dr']e^{-i\theta/2}$. Since each γ is an equal superposition of electron and hole, it is overall a chargeless, neutral fermion operator.

When there are several well separated vortices at positions \mathbf{R}_i , the gap function near the i th vortex takes the form $\Delta(\mathbf{r}) = |\Delta(\mathbf{r})|\exp(i\theta_i + i\Omega_i)$, with $\theta_i = \arg(\mathbf{r} - \mathbf{R}_i)$ and $\Omega_i = \sum_{j \neq i} \arg(\mathbf{R}_j - \mathbf{R}_i)$. There is then one zero-energy solution per vortex. Each zero-energy solution γ_i is localized near the core of its vortex at \mathbf{R}_i , but the phase Ω_i

that replaces Ω in Eq. (47) depends on the position of all vortices. Moreover, the dependence of the Majorana operators γ_i on the positions \mathbf{R}_i is not single valued.

While for any $E \neq 0$ the operators Γ_E^\dagger and Γ_E are conventional fermionic creation and annihilation operators, the γ_i 's are not. In particular, for $E \neq 0$ we have $(\Gamma_E^\dagger)^2 = \Gamma_E^2 = 0$, but the zero-energy operators follow (with a convenient choice of normalization) $\gamma_i^2 = 1$. The two types of fermion operator share the property of mutual anticommutation, i.e., the γ 's satisfy $\{\gamma_i, \gamma_j\} = 2\delta_{ij}$.

2. Topological properties of $p + ip$ superconductors

The existence of the γ_i 's implies a degeneracy of the ground state. Counting the number of degenerate ground states should be done with care. A pair of conventional fermionic creation and annihilation operators span a two-dimensional Hilbert space, since their square vanishes. This is not true for a Majorana operator. Thus, to count the degeneracy of the ground state when $2N_0$ vortices are present, we construct ‘‘conventional’’ complex (Dirac) fermionic creation and annihilation operators,

$$\psi_i = (\gamma_i + i\gamma_{N_0+i})/2, \quad (48)$$

$$\psi_i^\dagger = (\gamma_i - i\gamma_{N_0+i})/2. \quad (49)$$

These operators satisfy $\psi_i^2 = (\psi_i^\dagger)^2 = 0$ and thus span a two-dimensional subspace of degenerate ground states associated with these operators. Overall, the system has 2^{N_0} degenerate ground states. If the fermion number is fixed to be even or odd, then the degeneracy is 2^{N_0-1} . Therefore the quantum dimension of a vortex is $d_{\text{vort}} = \sqrt{2}$ or, in the notation introduced in Sec. II.A.1 for Ising anyons, $d_\sigma = \sqrt{2}$.

For any two vortices i and j , we can associate a two-state system. If we work in the basis of $i\gamma_i\gamma_j$ eigenstates, then $i\gamma_i\gamma_j$ acts as σ_z with eigenvalues ± 1 , while γ_i and γ_j act as σ_x and σ_y . (However, it is important to keep in mind that Majorana fermions γ_k and γ_l anticommute with γ_i and γ_j , unlike operators associated with different spins, which commute.) The two eigenvalues $i\gamma_i\gamma_j = \mp 1$ are the two fusion channels of two fermions. If we form the Dirac fermion $\psi = (\gamma_i + i\gamma_j)/2$, then the two $i\gamma_i\gamma_j$ eigenstates have $\psi^\dagger\psi = 0, 1$. Therefore we call these fusion channels **1** and ψ . (One is then tempted to refer to the state for which $\psi^\dagger\psi = 1$ as a filled fermion, and to the $\psi^\dagger\psi = 0$ state as an empty fermion. Note, however, that the eigenvalue of $\psi^\dagger\psi$ has no bearing on the occupation of single-particle states.)

Of course, the pairing of vortices to form Dirac fermions is arbitrary. A given pairing defines a basis, but one can transform to a basis associated with another pairing. Consider four vortices with corresponding zero modes $\gamma_1, \gamma_2, \gamma_3, \gamma_4$. The F matrix transforms states from the basis in which $i\gamma_1\gamma_2$ and $i\gamma_3\gamma_4$ are diagonal to the basis in

which $i\gamma_1\gamma_4$ and $i\gamma_2\gamma_3$ are diagonal. Since $i\gamma_1\gamma_4$ acts as σ_x on an $i\gamma_1\gamma_2$ eigenstate, the F matrix is just the basis change from the σ_z basis to the σ_x basis:

$$[F_\sigma^{\sigma\sigma}] = \frac{1}{\sqrt{2}} \begin{pmatrix} 1 & 1 \\ 1 & -1 \end{pmatrix}. \quad (50)$$

We refer to this type of non-Abelian anyon by the name ‘‘Ising anyons’’; this is the model introduced in Sec. II.A.1. The reason for the name will be explained in Sec. III.E.

In a compact geometry, there must be an even number of vortices (since a vortex carries half a flux quantum, and the number of flux quanta penetrating a compact surface must be an integer). In a noncompact geometry, if the number of vortices is odd, the edge has a zero-energy state of its own, as shown in Sec. III.E.

Now, we examine what happens to the Majorana operators and to the ground states as vortices move. The positions of the vortices are parameters in the Hamiltonian (36). When they vary adiabatically in time, the operators γ_i vary adiabatically in time. In principle, there are two sources for this variation—the explicit dependence of γ_i on the positions and the Berry phase associated with the motion. The choice of phases taken at Eq. (47) is such that the Berry phase vanishes, and the entire time dependence is explicit. The non-single-valuedness of the phases in Eq. (47) implies then that a change of 2π in Ω , which takes place when one vortex encircles another, does not leave the state unchanged.

As vortices adiabatically traverse trajectories that start and end in the same set of positions (Ivanov, 2001; Stern *et al.*, 2004), there is a unitary transformation U within the subspace of ground states that takes the initial state $|\psi(t=0)\rangle$ to the final one $|\psi(t=T)\rangle$,

$$|\psi(t=T)\rangle = U|\psi(t=0)\rangle. \quad (51)$$

Correspondingly, the time evolution of the operators γ_i is

$$\gamma_i(t=T) = U\gamma_i(t=0)U^\dagger. \quad (52)$$

By reading the time evolution of γ_i from their explicit form (47), we can determine U up to a phase. Indeed, one expects this Abelian phase to depend not only on the topology of the trajectory but also on its geometry, especially in the analogous quantum Hall case, where there is an Aharonov-Bohm phase accumulated as a result of the charge carried by the quasiparticle.

When vortex i encircles vortex $i+1$, the unitary transformation is simple: both γ_i and γ_{i+1} are multiplied by -1 , with all other operators unchanged. This is a consequence of the fact that when the order parameter changes by a phase factor 2π , fermionic operators change by a phase π . Exchange trajectories, in which some of the vortices trade places, are more complicated, since the phase changes of Ω_k associated with a particular trajectory do not only depend on the winding numbers, but also on the details of the trajectory and on the precise definition of the cut of the function $\arg(\mathbf{r})$ where its value jumps by 2π .

The simplest example is the interchange of two vortices. Inevitably, one of the vortices crosses the branch cut line of the other vortex. We can place the branch cuts so that a counterclockwise exchange of vortices 1 and 2 transforms $c_1 \rightarrow c_2$ and $c_2 \rightarrow -c_1$ while a clockwise exchange transforms $c_1 \rightarrow -c_2$ and $c_2 \rightarrow c_1$ (Ivanov, 2001).

This may be summarized by writing the representation matrices for the braid group generators (Nayak and Wilczek, 1996; Ivanov, 2001):

$$\rho(\sigma_i) = e^{i\theta} e^{-(\pi/4)\gamma_i\gamma_{i+1}}, \quad (53)$$

where θ is the Abelian part of the transformation. The two eigenvalues $i\gamma_i\gamma_{i+1} = \mp 1$ are the two fusion channels $\mathbf{1}$ and ψ of a pair of vortices. From Eq. (53), we see that the R matrices satisfy $R_{\psi}^{\sigma\sigma} = iR_{\mathbf{1}}^{\sigma\sigma}$ (i.e., the phases of taking two σ particles around each other differ by i depending on whether they fuse to ψ or $\mathbf{1}$). It is difficult to obtain the Abelian part of the phase using the methods of this section, but we derive it by other methods in Secs. III.C and III.D. The non-Abelian part of Eq. (53), i.e., the second factor on the right-hand side, is the same as a $\pi/2$ rotation in the spinor representation of $SO(2n)$ [see Nayak and Wilczek (1996), for details]. The fact that braiding enacts only $\pi/2$ rotations is the reason why this type of non-Abelian anyon does not enable universal topological quantum computation, as discussed in Sec. IV.

According to Eq. (53), if a system starts in a ground state $|gs_\alpha\rangle$ and vortex j winds around vortex $j+1$, the system's final state is $\gamma_j\gamma_{j+1}|gs_\alpha\rangle$. Writing this out in terms of the original electron operators, we have

$$(c_j e^{(i/2)\Omega_j} + c_j^\dagger e^{-(i/2)\Omega_j})(c_{j+1} e^{(i/2)\Omega_{j+1}} + c_{j+1}^\dagger e^{-(i/2)\Omega_{j+1}})|gs_\alpha\rangle, \quad (54)$$

where $c_j^{(\dagger)}$ annihilates a particle in the state $F(r-R_j)$ and $c_{j+1}^{(\dagger)}$ creates a particle in the state $F(r-R_{j+1})$ localized close to the cores of the j th and $(j+1)$ th vortices, respectively. Equation (54) seemingly implies that the motion of the j th vortex around the $(j+1)$ th vortex affects the occupations of states close to the cores of the two vortices. This is in contrast, however, to the derivation leading to Eq. (54), which explicitly assumes that vortices are kept far enough from one another so that tunneling between vortex cores may be disregarded.

This seeming contradiction is analyzed in Stern *et al.* (2004), where it is shown that the unitary transformation (54) does not affect the occupation of the core states of the $j, j+1$ vortices, because all ground states are composed of superpositions in which the core states have a probability of one-half to be occupied and one-half to be empty. The unitary transformation within the ground state subspace does not change that probability. Rather, they affect phases in the superpositions. Using this point of view it is then possible to show that two ingredients are essential for the non-Abelian statistics of the vortices. The first is the *quantum entanglement* of the occupation of states near the cores of distant vortices. The second ingredient is familiar from (Abelian) fractional

statistics: the *geometric phase* accumulated by a vortex traversing a closed loop.

Therefore we conclude that, for p -wave superconductors, the existence of zero-energy intravortex modes leads, first, to a multitude of ground states, and, second, to a particle-hole symmetric occupation of the vortex cores in all ground states. When represented in an occupation-number basis, a ground state is a superposition that has equal probability for the vortex core to be empty or occupied by one fermion. When a vortex traverses a trajectory that encircles another vortex, the phase it accumulates depends again on the number of fluid particles it encircles. Since a fluid particle is, in this case, a Cooper pair, the occupation of a vortex core by a fermion, half a pair, leads to an accumulation of a phase of π relative to the case when the core is empty. And since the ground state is a superposition with equal weights for the two possibilities, the relative phase of π introduced by the encircling might in this case transform the system from one ground state to another.

Now consider the ground state degeneracy of a $p+ip$ superconductor on the torus. We define, following Oshikawa *et al.* (2007) (see also Chung and Stone, 2007), the operators A_1 and A_2 that create a pair of Bogoliubov-de Gennes quasiparticles, take one around the meridian or longitude of the torus, respectively, and annihilate them again. We then define B_1 and B_2 as operators that create a vortex-antivortex pair, take the vortex around the meridian or longitude of the torus, respectively, and annihilate them. B_1 increases the flux through the hole encircled by the longitude of the torus by one-half of a flux quantum while B_2 does the same for the other hole. These operators satisfy the commutation relations $[A_1, A_2] = 0$ and $A_1 B_2 = -B_2 A_1$, $A_2 B_1 = -B_1 A_2$. We can construct a multiplet of ground states as follows. Since A_1 and A_2 commute and square to 1, we can label states by their A_1 and A_2 eigenvalues ± 1 . Let $|1, 1\rangle$ be the state with both eigenvalues equal to 1, i.e., $A_1|1, 1\rangle = A_2|1, 1\rangle = |1, 1\rangle$. Then $B_1|1, 1\rangle = |1, -1\rangle$ and $B_2|1, 1\rangle = |-1, 1\rangle$. Suppose we now try to apply B_2 to $B_1|1, 1\rangle = |1, -1\rangle$. This will create a vortex-antivortex pair; the Majorana zero modes γ_a and γ_b associated with the vortex and antivortex will be in the state $|0\rangle$ defined by $(\gamma_a + i\gamma_b)|0\rangle = 0$. When the vortex is taken around the longitude of the torus, its Majorana mode will be multiplied by -1 : $\gamma_a \rightarrow -\gamma_a$. Now, the vortex-antivortex pair will no longer be in the state $|0\rangle$, but will instead be in the state $|1\rangle$ defined by $(\gamma_a - i\gamma_b)|1\rangle = 0$. Consequently, the vortex-antivortex pair can no longer annihilate to the vacuum. When they fuse, a fermion is left over. Therefore $B_2 B_1|1, 1\rangle$ does not give a new ground state (and, by a similar argument, neither does $B_1 B_2|1, 1\rangle$). Consequently, a $p+ip$ superconductor has only three ground states on the torus. A basis in which B_1 is diagonal is given by $(|1, 1\rangle \pm |1, -1\rangle)/\sqrt{2}$, with eigenvalue ± 1 , and $|-1, 1\rangle$, with eigenvalue 0 (since there is zero amplitude for $B_1|-1, 1\rangle$ in the ground state subspace). They can be identified with the states $|1_m\rangle$, $|\psi_m\rangle$, and $|\sigma_m\rangle$ in Ising anyon language. Meanwhile, B_2 is diagonal in the basis

$(|1,1\rangle \pm |-1,1\rangle)/\sqrt{2}$, $|1,-1\rangle$. By changing from one basis to the other, we find that the S matrix given in the previous section follows.

The essential feature of chiral p -wave superconductors is that they have Majorana fermion excitations which have zero-energy modes at vortices (and gapless excitations at the edge of the system; see Sec. III.E). The Majorana character is a result of the superconductivity, which mixes particle and hole states; the zero modes and gapless edge excitations result from the chirality. Majorana fermions arise in a different way in the Kitaev honeycomb lattice model (Kitaev, 2006):

$$H = -J_x \sum_{x \text{ links}} \sigma_j^x \sigma_j^x - J_y \sum_{y \text{ links}} \sigma_j^y \sigma_j^y - J_z \sum_{z \text{ links}} \sigma_j^z \sigma_j^z, \quad (55)$$

where the z links are the vertical links on the honeycomb lattice, and the x and y links are at angles $\pm\pi/3$ from the vertical. The spins can be represented by Majorana fermions b^x , b^y , b^z , and c according to $\sigma_j^x = ib_j^x c_j$, $\sigma_j^y = ib_j^y c_j$, $\sigma_j^z = ib_j^z c_j$ so long as the constraint $b_j^x b_j^y b_j^z c_j = 1$ is satisfied. Then, the Hamiltonian is quartic in Majorana fermion operators, but the operators $b_j^x b_k^x$, $b_j^y b_k^y$, $b_j^z b_k^z$ commute with the Hamiltonian. Therefore we take their eigenvalues as parameters $u_{jk} = b_j^\alpha b_k^\alpha$, with $\alpha = x, y$, or z appropriate to the jk link. These parameters can be varied to minimize the Hamiltonian, which describes Majorana fermions hopping on the honeycomb lattice:

$$H = \frac{i}{4} \sum_{jk} t_{jk} c_j c_k, \quad (56)$$

where $t_{jk} = 2J_\alpha u_{jk}$ for nearest-neighbor j, k and zero otherwise. For different values of J_α 's, the t_{jk} 's take different values. The topological properties of the corresponding c_j bands are encapsulated by their Chern number (Kitaev, 2006). For a certain range of J_α 's, a P, T -violating perturbation gives the Majorana fermions a gap in such a way as to support zero modes on vortexlike excitations (plaquettes on which one u_{jk} is reversed in sign). These excitations are identical in topological character to the vortices of a $p+ip$ superconductor discussed above.

C. Chern-Simons effective field theories, the Jones polynomial, and non-Abelian topological phases

1. Chern-Simons theory and link invariants

In the previous section, we saw a extremely simple and transparent formulation of quasiparticle braiding properties for a particular non-Abelian topological state which, as we see later in this section, is equivalent to $SU(2)_2$ Chern-Simons theory. It describes the multi-quasiparticle Hilbert space and the action of braiding operations in terms of free fermions. Most non-Abelian topological states are not so simple, however. In particular, $SU(2)_k$ Chern-Simons theory for $k > 2$ does not have a

free fermion or boson description.⁷ Therefore in the next two sections, we discuss these field theories using more general methods.

Even though its Hamiltonian vanishes and it has no local degrees of freedom, solving Chern-Simons theory is still a nontrivial matter. The reason is that it is difficult in a non-Abelian gauge theory to disentangle the physical topological degrees of freedom from the unphysical local gauge degrees of freedom. There are essentially two approaches. Each has its advantages, and we describe them both. One is to work entirely with gauge-invariant quantities and derive rules governing them; this is the route pursued in this section. The second is to pick a gauge and simply calculate within this gauge, which we do in the next section (Sec. III.D).

Consider $SU(2)_k$ non-Abelian Chern-Simons theory:

$$S_{\text{CS}}[a] = \frac{k}{4\pi} \int_{\mathcal{M}} \text{tr} \left(a \wedge da + \frac{2}{3} a \wedge a \wedge a \right). \quad (57)$$

We modify the action by the addition of sources $j^{\mu a}$ according to $\mathcal{L} \rightarrow \mathcal{L} + \text{tr}(j \cdot a)$. We take the sources to be a set of particles on prescribed classical trajectories. The i th particle carries the spin- j_i representation of $SU(2)$. As shown in Sec. III.A, there are only $k+1$ allowed representations; later in this section, we see that, if we give a particle a higher-spin representation than $j = k/2$, then the amplitude will vanish identically. Therefore j_i must be in an allowed set of $k+1$ possibilities: $0, 1/2, \dots, k/2$. The functional integral in the presence of these sources can be written in terms of Wilson loops $W_{\gamma, j_i}[a]$, which are defined as follows. The holonomy $U_{\gamma, j}[a]$ is an $SU(2)$ matrix associated with a curve γ . It is defined as the path-ordered exponential integral of the gauge field along the path γ :

$$\begin{aligned} U_{\gamma, j}[a] &\equiv \mathcal{P} \exp \left(i \oint_{\gamma} \mathbf{a}^\epsilon T^{\epsilon} \cdot d\mathbf{l} \right) \\ &= \sum_{n=0}^{\infty} i^n \int_0^{2\pi} ds_1 \int_0^{s_1} ds_2 \cdots \\ &\quad \times \int_0^{s_{n-1}} ds_n [\dot{\gamma}(s_1) \cdot \mathbf{a}^{a_1}(\gamma(s_1)) T^{a_1} \cdots \\ &\quad \times \dot{\gamma}(s_n) \cdot \mathbf{a}^{a_n}(\gamma(s_n)) T^{a_n}], \end{aligned} \quad (58)$$

where \mathcal{P} is the path-ordering symbol. The Lie algebra generators T^a are taken in the spin- j representation. $\tilde{\gamma}(s)$, $s \in [0, 2\pi]$, is a parametrization of γ ; the holonomy is independent of the parametrization. The Wilson loop is the trace of the holonomy:

⁷It is an open question whether there is an alternative description of an $SU(2)_k$ topological phase with $k > 2$ in terms of fermions or bosons which is similar to the $p+ip$ chiral superconductor formulation of $SU(2)_2$.

$$W_{\gamma_j}[a] = \text{tr}(U_{\gamma_j}[a]). \tag{59}$$

We consider the simplest case, in which the source is a quasiparticle-quasihole pair of type j which is created out of the ground state, propagated for a period of time, and then annihilated, returning the system to the ground state. The amplitude for such a process is given by

$$\langle 0|0\rangle_{\gamma_j} = \int \mathcal{D}a e^{iS_{CS}[a]} W_{\gamma_j}[a]. \tag{60}$$

Here γ is the space-time loop formed by the trajectory of the quasiparticle-quasihole pair. The Wilson loop was introduced as an order parameter for confinement in a gauge theory because this amplitude measures the force between the quasiparticle and the quasihole. If they were to interact with a confining force $V(r) \sim r$, then the logarithm of this amplitude would be proportional to the area of the loop; if they were to have a short-ranged interaction, it would be proportional to the perimeter of the loop. However, Chern-Simons theory is independent of a metric, so the amplitude cannot depend on any length scales. It must simply be a constant. For $j=1/2$, we call this constant d . As the notation implies, it is, in fact, the quantum dimension of a $j=1/2$ particle. As shown below, d can be determined in terms of the level k , and the quantum dimensions of higher-spin particles can be expressed in terms of d .

We also consider the amplitude for two pairs of quasiparticles to be created out of the ground state, propagated for some time, and then annihilated, returning the system to the ground state:

$$\langle 0|0\rangle_{\gamma_j; \gamma'_j} = \int \mathcal{D}a e^{iS_{CS}[a]} W_{\gamma_j}[a] W_{\gamma'_j}[a]. \tag{61}$$

This amplitude can take different values depending on how γ and γ' are linked, as in Fig. 4(a) vs Fig. 4(b). If the curves are unlinked the integral must give d^2 , but when they are linked the value can be nontrivial. In a similar way, we formulate the amplitudes for an arbitrary number of sources.

It is useful to think about the history in Fig. 4(a) as a two-step process: from $t=-\infty$ to $t=0$ and from $t=0$ to $t=\infty$. (The two pairs are created at some time $t < 0$ and annihilated at some time $t > 0$.) At $t=0^-$, the system is in a four-quasiparticle state. [Quasiparticles and quasiholes are topologically equivalent if $G=\text{SU}(2)$, so we use “quasiparticle” to refer to both.] We use call this state ψ :

$$\begin{aligned} \psi[A] &= \int_{a(\mathbf{x},0)=A(\mathbf{x})} \mathcal{D}a(\mathbf{x},t) W_{\gamma_-}[a] W_{\gamma'_-}[a] \\ &\times \exp\left(\int_{-\infty}^0 dt \int d^2x \mathcal{L}_{CS}\right), \end{aligned} \tag{62}$$

where γ_- and γ'_- are the arcs given by $\gamma(t)$ and $\gamma'(t)$ for $t < 0$. $A(\mathbf{x})$ is the value of the gauge field on the $t=0$ spatial slice; the wave functional $\psi[A]$ assigns an amplitude to every spatial gauge field configuration. For $G=\text{SU}(2)$ and $k > 1$, there are actually two different four-

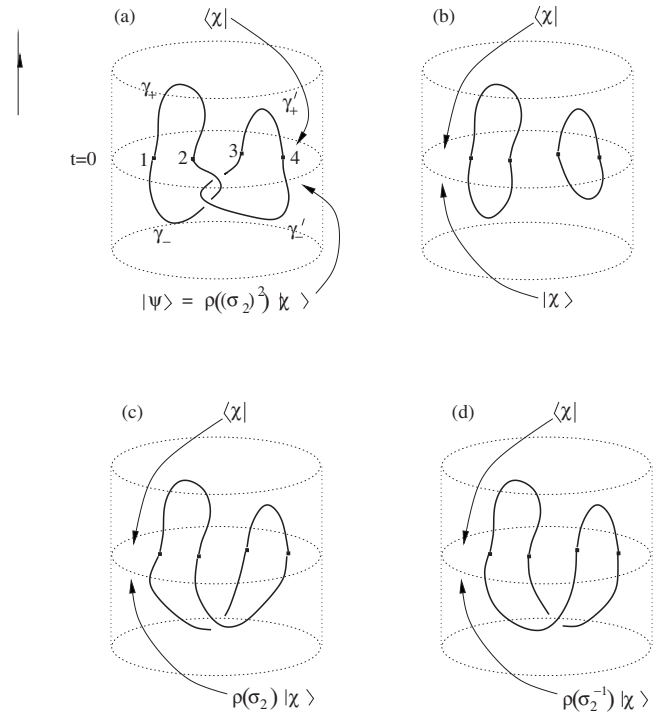


FIG. 4. The functional integrals that give (a) $\langle \chi | \rho(\sigma_2^2) | \chi \rangle$, (b) $\langle \chi | \chi \rangle$, (c) $\langle \chi | \rho(\sigma_2) | \chi \rangle$, and (d) $\langle \chi | \rho(\sigma_2^{-1}) | \chi \rangle$.

quasiparticle states: if particles 1 and 2 fuse to the identity field $j=0$, then particles 3 and 4 must as well; if particles 1 and 2 fuse to $j=1$, then particles 3 and 4 must as well. These are the only possibilities. (For $k=1$, fusion to $j=1$ is not possible.) Which one the system is in depends on how the trajectories of the four quasiparticles are intertwined. Although quasiparticles 1 and 2 were created as a pair from the vacuum, quasiparticle 2 braided with quasiparticle 3, so 1 and 2 may no longer fuse to the vacuum. Shortly, we show an example of a different four-quasiparticle state.

We now interpret the $t=0$ to $t=\infty$ history as the conjugate of a $t=-\infty$ to $t=0$ history. In other words, it gives us a four-quasiparticle bra rather than a four-quasiparticle ket:

$$\begin{aligned} \chi^*[A] &= \int_{a(\mathbf{x},0)=A(\mathbf{x})} \mathcal{D}a(\mathbf{x},t) W_{\gamma_+}[a] W_{\gamma'_+}[a] \\ &\times \exp\left(\int_0^{\infty} dt \int d^2x \mathcal{L}_{CS}\right). \end{aligned} \tag{63}$$

In the state $|\chi\rangle$, quasiparticles 1 and 2 fuse to form the trivial quasiparticle, as do quasiparticles 3 and 4. Then we interpret the functional integral from $t=-\infty$ to $t=\infty$ as the matrix element between the bra and the ket:

$$\langle \chi | \psi \rangle = \int \mathcal{D}a e^{iS_{CS}[a]} W_{\gamma_1 j_1}[a] W_{\gamma_2 j_2}[a]. \tag{64}$$

Now, observe that $|\psi\rangle$ is obtained from $|\chi\rangle$ by taking quasiparticle 2 around quasiparticle 3, i.e., by exchanging quasiparticles 2 and 3 twice, $|\psi\rangle = \rho(\sigma_2^2) |\chi\rangle$. Hence

$$\langle \chi | \rho(\sigma_2^2) | \chi \rangle = \int Da e^{iS_{CS}[a]} W_{\gamma_1 j_1}[a] W_{\gamma_2 j_2}[a]. \quad (65)$$

In this way, we compute the entries of the braiding matrices $\rho(\sigma_i)$ by computing functional integrals such as the one on the right-hand side of Eq. (65). Note that we normalize the state $|\chi\rangle$ by computing Fig. 4(b), which gives its matrix element with itself.

Consider now the state $\rho(\sigma_2)|\chi\rangle$, in which particles 2 and 3 are exchanged just once. It is depicted in Fig. 4(c). Similarly, the state $\rho(\sigma_2^{-1})|\psi\rangle$ is depicted in Fig. 4(d). From the figure, we see that

$$\langle \chi | \rho(\sigma_2) | \chi \rangle = d, \quad (66)$$

$$\langle \chi | \rho(\sigma_2^{-1}) | \chi \rangle = d, \quad (67)$$

since both histories contain a single unknotted loop. Meanwhile,

$$\langle \chi | \chi \rangle = d^2. \quad (68)$$

Since the four-quasiparticle Hilbert space is two dimensional, $\rho(\sigma_2)$ has two eigenvalues λ_1 and λ_2 , so that

$$\rho(\sigma) - (\lambda_1 + \lambda_2) + \lambda_1 \lambda_2 \rho(\sigma^{-1}) = 0. \quad (69)$$

Taking the expectation value in the state $|\chi\rangle$, we find

$$d - (\lambda_1 + \lambda_2)d^2 + \lambda_1 \lambda_2 d = 0, \quad (70)$$

so that

$$d = (1 + \lambda_1 \lambda_2) / (\lambda_1 + \lambda_2). \quad (71)$$

Since the braiding matrix is unitary, λ_1 and λ_2 are phases. The overall phase is unimportant for quantum computation, so we need only a single number. In fact, this number can be obtained from self-consistency conditions (Freedman *et al.*, 2004). However, the details of the computation of λ_1 and λ_2 are technical and require a careful discussion of framing; the result is (Witten, 1989) that $\lambda_1 = -e^{-3\pi i/2(k+2)}$, $\lambda_2 = e^{\pi i/2(k+2)}$. These eigenvalues are simply $R_0^{1/2,1/2} = \lambda_1$, $R_1^{1/2,1/2} = \lambda_2$. Consequently,

$$d = 2 \cos(\pi/(k+2)) \quad (72)$$

and

$$q^{-1/2} \rho(\sigma_i) - q^{1/2} \rho(\sigma_i^{-1}) = q - q^{-1}, \quad (73)$$

where $q = -e^{\pi i/(k+2)}$ (see Fig. 18). Since this operator equation applies regardless of the state to which it is applied, we can apply it locally to any given part of a knot diagram to relate the amplitude to the amplitude for topologically simpler processes, as shown below (Kauffman, 2001). This is an example of a *skein relation*; in this case, it is the skein relation which defines the Jones polynomial. In arriving at this skein relation, we retrace the connection between Wilson loops in Chern-Simons theory and knot invariants made by Witten (1989). In this paper, Witten showed that correlation functions of Wilson loop operators in $SU(2)_k$ Chern-Simons theory are equal to corresponding evaluations of the Jones polynomial, which is a topological invariant of knot theory (Jones, 1985):

$$\int Da W_{\gamma_1, (1/2)}[a] \cdots W_{\gamma_n, (1/2)}[a] e^{iS_{CS}[a]} = V_L(q). \quad (74)$$

$V_L(q)$ is the Jones polynomial associated with the link $L = \gamma_1 \cup \cdots \cup \gamma_n$, evaluated at $q = -e^{\pi i/(k+2)}$ using the skein relation (73). Note that we assume here that all quasiparticles transform under the $j = \frac{1}{2}$ representation of $SU(2)$. The other quasiparticle types can be obtained through the fusion of several $j = 1/2$ quasiparticles, as discussed in Sec. III.C.2.

2. Combinatorial evaluation of link invariants and quasiparticle properties

The Jones polynomial (Jones, 1985) $V_L(q)$ is a formal Laurent series in a variable q which is associated with a link $L = \gamma_1 \cup \cdots \cup \gamma_n$. It can be computed recursively using Eq. (73). We illustrate how this is done by showing how to use a skein relation to compute a related quantity called the Kauffman bracket $K_L(q)$ (Kauffman, 1987), which differs from the Jones polynomial by a normalization:

$$V_L(q) = (1/d)(-q^{3/2})^{w(L)} K_L(q), \quad (75)$$

where $w(L)$ is the writhe of the link. (The Jones polynomial is defined for an oriented link. Given an orientation, each crossing can be assigned a sign ± 1 ; the writhe is the sum over all crossings of these signs.) The link L embedded in three-dimensional space (or, rather, three-dimensional space-time in our case) is projected onto the plane. This can be done faithfully if we are careful to mark overcrossings and undercrossings. Such a projection is not unique, but the same Kauffman bracket is obtained for all possible 2D projections of a knot (we will see an example of this below). An unknotted loop \bigcirc is given the value $K_{\bigcirc}(q) = d \equiv -q - q^{-1} = 2 \cos \pi/(k+2)$. For notational simplicity, when we draw a knot, we actually mean the Kauffman bracket associated to this knot. Hence we write

$$\bigcirc = d. \quad (76)$$

The disjoint union of n unknotted loops is assigned the value d^n .

The Kauffman bracket for any given knot can be obtained recursively by repeated application of the following skein relation which relates it with the Kauffman brackets for two knots, both of which have one fewer crossing according to the rule:

$$\begin{array}{c} \diagup \\ \diagdown \end{array} = q^{1/2} \left| \begin{array}{c} | \\ | \end{array} \right| + q^{-1/2} \begin{array}{c} \cup \\ \cap \end{array}. \quad (77)$$

With this rule, we can eliminate all crossings. At this point, we are left with a linear combination of the Kauffman brackets for various disjoint unions of unknotted loops. Adding up these contributions of the form d^m with their appropriate coefficients coming from the recursion relation (77), we obtain the Kauffman bracket for the knot with which we started.

$$\begin{aligned}
 \text{Diagram 1} &= q^{1/2} \text{Diagram 2} + q^{-1/2} \text{Diagram 3} \\
 &= q \text{Diagram 4} + \text{Diagram 5} \\
 &\quad + q^{-1} \text{Diagram 6} + \text{Diagram 7} \\
 &= \text{Diagram 8} + (q + q^{-1} + d) \text{Diagram 9} \\
 &= \text{Diagram 10}
 \end{aligned}$$

FIG. 5. The Kauffman bracket is invariant under continuous motions of the arcs and therefore independent of the particular projection of a link to the plane.

We see how this works with a simple example. First, consider the two arcs that cross twice in Fig. 5. We assume that these arcs continue in some arbitrary way and form closed loops. By applying the Kauffman bracket recursion relation in Fig. 5, we see that these arcs can be replaced by two arcs which do not cross.

In Sec. II.C.3, we use these methods to evaluate some matrix elements relevant to interference experiments.

Now, we consider the two fusion channels of a pair of quasiparticles in detail. When the two quasiparticles fuse to the trivial particle, as 1 and 2 did above, we depict such a state, which we call $|0\rangle$, as $1/\sqrt{d}$ times the state yielded by the functional integral (62) with a Wilson line that looks like \cup because two quasiparticles which are created as a pair out of the ground state must necessarily fuse to spin 0 if they do not braid with any other particles. (The factor $1/\sqrt{d}$ normalizes the state.) Hence we project any two quasiparticles onto the $j=0$ state by evolving them with a history which looks like

$$\Pi_0 = \frac{1}{d} \begin{array}{c} \cup \\ \cap \end{array}. \tag{78}$$

On the right-hand side of this equation, we mean a functional integral between two times t_1 and t_2 . The functional integral has two Wilson lines in the manner indicated pictorially. On the left-hand side, we suggest that evolving a state through this history can be viewed as acting on it with the projection operator $\Pi_0 = |0\rangle\langle 0|$.

However, the two quasiparticles could instead be in the state $|1\rangle$, in which they fuse to form the $j=1$ particle. Since these states must be orthogonal, $\langle 0|1\rangle=0$, we must get identically zero if we follow the history (78) with a history that defines a projection operator Π_1 onto the $j=1$ state:

$$\Pi_1 = \left| \left| - \frac{1}{d} \begin{array}{c} \cup \\ \cap \end{array} \right. \right. \tag{79}$$

It is easy to see that, if this operator acts on a state which is given by a functional integral that looks like \cup , the result is zero.

The projection operators Π_0 , Π_1 , which are called Jones-Wenzl projection operators, project a pair of a

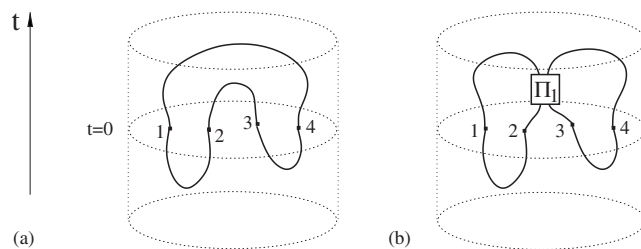


FIG. 6. The elements of the F matrix obtained by computing matrix elements between kets in which 1 and 2 have a definite fusion channel and bras in which 1 and 4 have a definite fusion channel.

quasiparticles onto the two natural basis states of their qubit. In other words, we do not need to introduce new types of lines in order to compute the expectation values of Wilson loops carrying $j=0$ or 1. We can denote them with pairs of lines projected onto either of these states. Recall that a $j=1/2$ loop had amplitude d , which was the quantum dimension of a $j=1/2$ particle. Using the projection operator (79), we see that a $j=1$ loop has amplitude $d^2 - 1$ (by connecting the top of the line segments to the bottom and evaluating the Kauffman bracket). One can continue in this way to construct projection operators which project m lines onto $j=m/2$. This projection operator must be orthogonal to the $j=0, 1, 3/2, 2, \dots, (m-1)/2$ projection operators acting on subsets of the m lines, and this condition is sufficient to construct all Jones-Wenzl projection operators recursively. Similarly, the quantum dimensions can be computed through a recursion relation. At level k , we find that quasiparticles with $j > k/2$ have quantum dimensions which vanish identically (e.g., for $k=1$, $d=1$ so the quantum dimension of a $j=1$ particle is $d^2 - 1 = 0$). Consequently, these quasiparticle types do not occur. Only $j=0, 1/2, \dots, k/2$ occur.

The entries in the F matrix can be obtained by graphically computing the matrix element between a state in which, for instance, 1 and 2 fuse to the vacuum and 3 and 4 fuse to the vacuum and a state in which 1 and 4 fuse to the vacuum and 2 and 3 fuse to the vacuum, which is depicted in Fig. 6(a). (The matrix element in this figure must be normalized by the norms of the top and bottom states to obtain the F -matrix elements.) To compute the matrix element between a state in which 1 and 2 fuse to the vacuum and 3 and 4 fuse to the vacuum and a state in which 1 and 4 fuse to $j=1$ and 2 and 3 fuse to $j=1$, we compute the diagram in Fig. 6(b). For $k=2$, we find the same F matrix as for Ising anyons in Sec. III.B.

We now consider the ground state properties of the $SU(2)_k$ theory on the torus. As above, we integrate the Chern-Simons Lagrangian over a three-manifold \mathcal{M} with boundary Σ , i.e., $\mathcal{M} = \Sigma \times (-\infty, 0]$, in order to obtain a $t=0$ state. The boundary Σ is the spatial slice at $t=0$. For the torus, $\Sigma = T^2$, we take \mathcal{M} to be the solid torus, $\mathcal{M} = S^1 \times D^2$, where D^2 is the disk. By foliating the solid torus, we obtain earlier spatial slices. If there are no

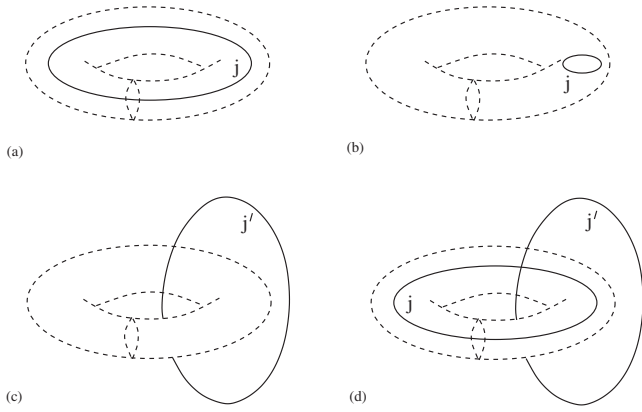


FIG. 7. Chern-Simons theory on the torus. (a) Different degenerate ground states on the torus are given by performing the functional integral with longitudinal Wilson loops carrying spin $j=0, 1/2, \dots, k/2$. (b) Meridional Wilson loops are contractible; they do not give new ground states. (c) The corresponding bras have Wilson lines in the exterior solid torus. (d) S -matrix elements are given by evaluating the history obtained by combining a bra and ket with their linked Wilson lines.

quasiparticles, then there are no Wilson lines terminating at Σ . However, the functional integral can have Wilson loops in the body of the solid torus as in Fig. 7(a). These correspond to processes in the past, $t < 0$, in which a quasiparticle-quashole pair was created, taken around the meridian of the torus and annihilated. The Wilson loop can be in any of the $k+1$ allowed representations $j=0, 1/2, \dots, k/2$; in this way, we obtain $k+1$ ground state kets on the torus (we show shortly that they are all linearly independent). Wilson loops around the meridian are contractible [Fig. 7(b)], so they can be evaluated by taking their Kauffman bracket; they multiply the state by d_j . Evidently, these Wilson loop operators are diagonal in this basis. Bras can be obtained by integrating the Chern-Simons Lagrangian over the three-manifold $\mathcal{M}' = \Sigma \times [0, \infty) = S^3 \setminus S^1 \times D^2$, i.e., the exterior of the torus. Wilson loops in the exterior torus are now contractible if they are parallel to a longitude but nontrivial if they are around the meridian, as shown in Fig. 7(c). Again, we obtain $k+1$ ground state bras in this way. The matrix elements between these bras and kets (appropriately normalized such that the matrix product of a bra with its conjugate ket is unity) are the entries in the S matrix, which is precisely the basis change between the longitudinal and meridional bases. A matrix element can be computed by evaluating the corresponding picture. The ab entry in the S matrix is given by evaluating the Kauffman bracket of the picture in Fig. 7(d) (and dividing by the normalization of the states). This figure makes the relationship between the S matrix and braiding clear.

Finally, we comment on the difference between $SU(2)_2$ and Ising anyons, which we have previously described as differing only slightly from each other (see also the end of Sec. III.E). The effective field theory for Ising anyons contains an additional $U(1)$ Chern-Simons gauge field, in addition to an $SU(2)_2$ gauge field (Fradkin

et al., 1998, 2001). The consequences of this difference are that $\Theta_\sigma = e^{-\pi i/8}$ while $\Theta_{1/2} = e^{-3\pi i/8}$; $R_1^{\sigma\sigma} = e^{-\pi i/8}$ while $R_0^{1/2,1/2} = -e^{-3\pi i/8}$; $R_\psi^{\sigma\sigma} = e^{3\pi i/8}$ while $R_1^{1/2,1/2} = e^{\pi i/8}$; $[F_\sigma^{\sigma\sigma}]_{ab} = -[F_{1/2}^{1/2,1/2,1/2}]_{ab}$. The rest of the F matrices are the same, as are the fusion multiplicities N_{ab}^c and the S matrix. In other words, the basic structure of the non-Abelian statistics is the same in the two theories, but there are some minor differences in the $U(1)$ phases which result from braiding. Both theories have threefold ground state degeneracy on the torus; the Moore-Read Pfaffian state has ground state degeneracy 6 because of an extra $U(1)$ factor corresponding to the electrical charge degrees of freedom.

Of course, in the $k=2$ case we already obtained these results by the method of the previous section. However, this approach has two advantages: (i) once Witten's result (74) and Kauffman's recursion relation (77) are accepted, braiding matrix elements can be obtained by straightforward high-school algebra; (ii) the method applies to all levels k , unlike free Majorana fermion methods, which apply only to the $k=2$ case. There is an added bonus, which is that this formalism is closely related to the techniques used to analyze lattice models of topological phases, discussed in a later section.

D. Chern-Simons theory, conformal field theory, and fractional quantum Hall states

1. The relation between Chern-Simons theory and conformal field theory

Now, we consider Chern-Simons theory in a particular gauge, namely, the holomorphic gauge (to be defined below). The ground state wave function(s) of Chern-Simons theory can be obtained by performing the functional integral from the distant past, $t = -\infty$, to time $t = 0$ as in the previous section:

$$\psi[A(\mathbf{x})] = \int_{a(\mathbf{x},0)=A(\mathbf{x})} \mathcal{D}a(\mathbf{x},t) \exp\left(\int_{-\infty}^0 dt \int_{\Sigma} d^2x \mathcal{L}_{CS}\right). \tag{80}$$

For the sake of concreteness, we consider the torus $\Sigma = T^2$ for which the space-time manifold is $\mathcal{M} = (-\infty, 0] \times T^2 = S^1 \times D^2$. We assume that there are no Wilson loops (either contained within the solid torus or terminating at the boundary). If x and y are coordinates on the torus (the fields will be subject to periodicity requirements), we write $z = x + iy$. We can then change to coordinates z and \bar{z} and, as usual, treat a_z^a and $a_{\bar{z}}^a$ as independent variables. Then we take the holomorphic gauge $a_{\bar{z}}^a = 0$. The field a_z^a only appears in the action linearly, so the functional integral over a_z^a may be performed, yielding a δ function:

$$\int Da \exp \left[\frac{k}{4\pi} \int_{D^2 \times S^1} \epsilon^{\mu\nu\lambda} \left(a_\mu^a \partial_\nu a_\lambda^a + \frac{2}{3} f_{abc} a_\mu^a a_\nu^b a_\lambda^c \right) \right] \\ = \int Da_i \delta(f_{ij}^a) \exp \left((k/4\pi) \int_{D^2 \times S^1} \epsilon^{ij} a_i^a \partial_z a_j^a \right), \quad (81)$$

where $i, j = t, z$. Here $f_{ij}^a = \partial_i a_j^a - \partial_j a_i^a + i \epsilon_{abc} a_i^a a_j^b$ are the spatial components of the field strength. There are no other cubic terms in the action once $a_{\bar{z}}$ has been eliminated (as is the case in any such gauge in which one of the components of the gauge field vanishes). The constraint imposed by the δ function can be solved by taking

$$a_i^a = \partial_i U U^{-1}, \quad (82)$$

where U is a single-valued function taking values in the Lie group. Substituting this into the right-hand side of Eq. (81), we find that the action which appears in the exponent in the functional integral takes the form

$$S = \frac{k}{4\pi} \int_{D^2 \times S^1} \epsilon^{ij} \text{tr} [\partial_i U U^{-1} \partial_z (\partial_j U U^{-1})] \\ = \frac{k}{4\pi} \int_{D^2 \times S^1} \epsilon^{ij} [\text{tr} (\partial_i U U^{-1} \partial_z \partial_j U U^{-1}) \\ + \text{tr} (\partial_i U U^{-1} \partial_j U \partial_z U^{-1})] \\ = \frac{k}{4\pi} \int_{D^2 \times S^1} \epsilon^{ij} [\partial_j \text{tr} (\partial_i U^{-1} \partial_z U) \\ + \text{tr} (\partial_i U U^{-1} \partial_j U \partial_z U^{-1})] \\ = \frac{k}{4\pi} \int_{T^2} \text{tr} (\partial_z U^{-1} \partial_z U) \\ + \frac{k}{12\pi} \int_{D^2 \times S^1} \epsilon^{\mu\nu\lambda} \text{tr} (\partial_\mu U U^{-1} \partial_\nu U U^{-1} \partial_\lambda U U^{-1}). \quad (83)$$

The Jacobian which comes from the δ function $\delta(f_{ij}^a)$ is canceled by that associated with the change of integration variable from Da to DU . In the final line, the first term has been integrated by parts while the second term, although it appears to be an integral over the 3D manifold, depends only on the boundary values of U (Wess and Zumino, 1971; Witten, 1983). This is the Wess-Zumino-Witten (WZW) action. What we learn from Eq. (83), then, is that, in a particular gauge, the ground state wave function of $(2+1)D$ Chern-Simons theory can be viewed as the partition function of a $(2+0)$ -dimensional WZW model.

For positive integer k , the WZW model is a 2D conformal field theory which, in the $SU(2)$ case, has Virasoro central charge $c = \bar{c} = 3k/(k+2)$. (For a review of some of the basics of conformal field theory, see the Appendix and references therein.) However, in computing properties of the Chern-Simons theory from which we have derived it, we couple only to $a_z = \partial_z U \cdot U^{-1}$; i.e., only to the holomorphic or right-moving sector of the theory.

Thus it is the chiral WZW model which controls the ground state wave function(s) of Chern-Simons theory.

If we follow the same strategy to calculate the Chern-Simons ground state wave function with Wilson lines or punctures present, then we end up with a correlation function of operators in the chiral WZW model transforming under the corresponding representations of $SU(2)$. (Strictly speaking, it is not a correlation function, but a *conformal block*, which is a chiral building block for a correlation function. While correlation functions are single valued, conformal blocks have the nontrivial monodromy properties that we need, as discussed in the Appendix.) Therefore following Elitzur *et al.* (1989) and Witten (1989), we have mapped the problem of computing the ground state wave function (in $2+0$ dimensions) of Chern-Simons theory, which is a topological theory with a gap, to the problem of computing a correlation function in the chiral WZW model (in $1+1$ dimensions), which is a critical theory. This is a bit peculiar since one theory is gapped while the other is gapless. However, the gapless degrees of freedom of the WZW model for the $t=0$ spatial slice are pure gauge degrees of freedom for the corresponding Chern-Simons theory. [In the similar situation of a surface Σ with boundary, however, the corresponding conformally invariant $(1+1)D$ theory describes the actual dynamical excitations of the edge of the system, as discussed in Sec. III.E.] Only the topological properties of the chiral WZW conformal blocks are physically meaningful for us.

More complicated topological states with multiple Chern-Simons fields and, possibly, Higgs fields (Fradkin *et al.*, 1998, 1999, 2001) correspond in a similar way to other chiral rational conformal field theories (RCFTs) which are obtained by tensoring or cosetting WZW models. (RCFTs are those CFTs that have a finite number of primary fields—see the Appendix for the definition of a primary field—under some extended chiral algebra which envelopes the Virasoro algebra; a Kac-Moody algebra in the WZW case; and, possibly, other symmetry generators.) Consequently, it is possible using algebraic techniques of rational conformal field theory to compute the ground state wave functions for a large class of topological states of matter. The quasiparticles of the topological state correspond to the primary fields of the chiral RCFT. (It is a matter of convenience whether one computes correlation functions with a primary field or one of its descendants since their topological properties are the same. This is a freedom which can be exploited, as described below.)

The conformal blocks of an RCFT have one property that is particularly useful for us, namely, they are holomorphic functions of the coordinates. This makes them excellent candidate wave functions for quantum Hall states. We identify primary fields with quasiparticles of the quantum Hall state, and compute the corresponding conformal block. However, there is one important issue that must be resolved: a quantum Hall wave function is normally viewed as a wave function for electrons (quasiparticle positions, by contrast, are usually viewed as collective coordinates specifying a given excited state).

Where are electrons in our RCFT? Electrons have trivial braiding properties. When one electron is taken around another, the wave function is unchanged, except for a phase change which is an odd integral multiple of 2π . More importantly, when any quasiparticle is taken around an electron, the wave function is unchanged apart from a phase change that is an integral multiple of 2π . Therefore the electron must be a descendant of the identity. In other words, the RCFT must contain a fermionic operator by which we can extend the chiral algebra. This new symmetry generator is essentially the electron creation operator—which is therefore a descendant of the identity under its own action. Not all RCFTs have such an operator in their spectrum, so this is a strong constraint on RCFTs which can describe quantum Hall states. If we are interested, instead, in a quantum Hall state of bosons, as could occur with ultracold bosonic atoms in a rotating optical trap (Cooper *et al.*, 2001), then the RCFT must contain a bosonic field by which we can extend the chiral algebra.

A RCFT correlation function of N_e electron operators therefore corresponds to the Chern-Simons ground state wave function with N_e topologically trivial Wilson lines. From a purely topological perspective, such a wave function is as good as a wave function with no Wilson lines, so the Wilson lines would seem superfluous. However, if the descendant field which represents the electron operator is chosen cleverly, then the wave function with N_e Wilson lines may be a “good” trial wave function for electrons in the quantum Hall regime. Indeed, in some cases, one finds that these trial wave functions are the exact quantum Hall ground states of simple model Hamiltonians (Greiter *et al.*, 1991; Moore and Read, 1991; Blok and Wen, 1992; Wen and Wu, 1994; Ardonne and Schoutens, 1999; Read and Rezayi, 1999). In the study of the quantum Hall effect, however, a wave function is good if it is energetically favorable for a realistic Hamiltonian, which is beyond the scope of the underlying Chern-Simons theory, which itself knows only about braiding properties. It is unexpected that the trial wave functions obtained from Chern-Simons theory are often found to be good from this energetic perspective, which is a reflection of how highly constrained quantum Hall wave functions are, and how central these braiding properties are to their physics. We emphasize, however, that a wave function obtained in this way will not be the exact ground state wave function for electrons with Coulomb interactions. In some cases it might not even have particularly high overlap with the ground state wave function, or have good energetics. The one thing that it does capture is the topological structure of a particular universality class.

2. Quantum Hall wave functions from conformal field theory

Ideally, the logic that would lead us to a particular RCFT would be as follows, as displayed in Fig. 8. One begins with the experimental observation of the quantized Hall effect at some filling fraction ν (shown at the top). We know that the Hamiltonian for the system is

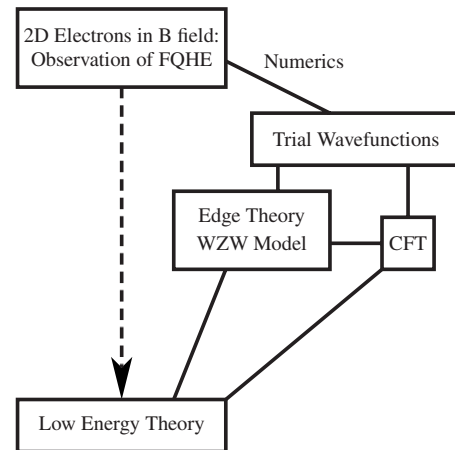


FIG. 8. How one arrives at a low-energy theory of the quantum Hall effect. At the top, one begins with the experimental observation of the quantized Hall effect. At the bottom, we know the low-energy theory should be of Chern-Simons form. One would like to be able to “integrate out” high-energy degrees of freedom directly to obtain the low-energy theory, as shown by the dotted line, but must instead take a more circuitous route.

simply that of 2D electrons in a magnetic field, and at the bottom we know the form of the low-energy theory should be of Chern-Simons form. One would like to be able to “integrate out” high-energy degrees of freedom directly to obtain the low-energy theory. Given the low-energy Chern-Simons effective field theory, one can pass to the associated RCFT, as described above. With the RCFT in hand, one can construct wave functions, as described below. Indeed, such a procedure has been achieved for Abelian quantum Hall states (Zhang *et al.*, 1989; López and Fradkin, 1991). In some special non-Abelian cases, progress in this direction has been made (Wen, 1991b, 1999).

For most non-Abelian theories, however, the situation is not so simple. The RCFT is obtained through inspired guesswork (Moore and Read, 1991; Blok and Wen, 1992; Ardonne and Schoutens, 1999; Read and Rezayi, 1999; Cappelli *et al.*, 2001; Simon, Rezayi, Cooper, *et al.*, 2007). One may try to justify it *ex post facto* by solving for the properties of quasiholes of a system with some unrealistic (e.g., involving three-body or higher interactions) but soluble Hamiltonian. The degeneracy can be established by counting (Nayak and Wilczek, 1996; Read and Rezayi, 1996; Read, 2006). The braiding matrices can be obtained by numerically computing the Berry integrals for the given wave functions (Tserkovnyak and Simon, 2003) or by using their connection to conformal field theory to deduce them (Moore and Read, 1991; Nayak and Wilczek, 1996; Gurarie and Nayak, 1997; Slingerland and Bais, 2001). One can then deduce the Chern-Simons effective field theory of the state either from the quasiparticle properties or from the associated conformal field theory with which both it and the wave functions are connected.

We now show how such wave functions can be constructed through some examples. In the Appendix, we review some rudiments of conformal field theory.

a. Wave functions from CFTs

Our goal is to construct a LLL FQH wave function $\Psi(z_1, \dots, z_N)$ which describes an electron fluid in a circular droplet centered at the origin. Ψ must be a homogeneous antisymmetric analytic function of z_i 's, independent of \bar{z}_i 's apart from the Gaussian factor, which we frequently ignore (see Sec. II.C.1). If we consider the FQHE of bosons, we need Ψ to instead be symmetric. The filling fraction ν of a FQH wave function Ψ is given by $\nu = N/N_\Phi$, where N is the number of electrons and N_Φ is the number of flux quanta penetrating the droplet (Prange and Girvin, 1990). In the LLL, N_Φ is given by the highest power of z occurring in Ψ .

We also frequently need the fact that in an incompressible state of filling fraction ν , multiplying a wave function by a factor $\prod_i (z_i - w)^m$ pushes a charge νm away from the point w . This can be understood (Laughlin, 1983) as insertion of m flux quanta at the point w , which via Faraday's law creates an azimuthal electric field, which then via the Hall conductivity transfers charge νm away from the point w .

Our strategy will be to choose a particular chiral RCFT, pick an "electron" field ψ_e in this theory (which, by the reasoning given above, must be a fermionic generator of the extended chiral algebra of the theory), and write a ground state trial wave function Ψ_{gs} for N electrons as

$$\Psi_{\text{gs}} = \langle \psi_e(z_1) \cdots \psi_e(z_N) \rangle. \quad (84)$$

The field ψ_e must be fermionic since the quantum Hall wave function on the left-hand side must be suitable for electrons. Not all RCFTs have such a field in their spectrum, so this requirement constrains our choice. This requirement also ensures that we obtain a wave function which has no branch cuts; in particular, there will only be one conformal block on the right-hand side of Eq. (84). We must do a little more work in choosing ψ_e so that there are no poles either on the right-hand side of Eq. (84). As discussed above, the correlation function on the right-hand side of Eq. (84) is a ground state wave function of Chern-Simons theory with N_e trivial topological charges at fixed positions z_1, z_2, \dots, z_{N_e} .

Of course, there is not a unique choice of RCFT, even at a given filling fraction. Therefore there are different fractional quantum Hall states that can be constructed in this way. Which fractional quantum Hall state is observed at a particular ν is determined by comparing the energies of the various possible competing ground states. Having a good wave function is, by itself, no guarantee that this wave function describes the physical system. Only a calculation of its energy gives real evidence that it is better than other possible states.

The reason for introducing this complex machinery simply to construct a wave function becomes clearer when we consider quasihole wave functions, which are

Chern-Simons ground state wave functions with N_e trivial topological charges and N_{qh} nontrivial topological charges. In general, there are many possible quasihole operators, corresponding to the different primary fields of the theory, so we must consider $N_{\text{qh}1}, N_{\text{qh}2}, \dots, N_{\text{qh}m}$ numbers of quasiholes if there are m primary fields. Each different primary field corresponds to a different topologically distinct type of "defect" in the ground state. (As in the case of electrons, we are free to choose a descendant field in place of the corresponding primary field since the two have identical topological properties although the wave function generated by a descendant will be different from that generated by its primary.) Suppose that we focus attention on a particular type of quasiparticle which, in most cases, will be the quasiparticle of minimal electrical charge. Then we can write a wave function with quasiholes at positions w_1, \dots, w_M as

$$\Psi(w_1 \cdots w_M) = \langle \psi_{\text{qh}}(w_1) \cdots \psi_{\text{qh}}(w_M) \psi_e(z_1) \cdots \psi_e(z_N) \rangle, \quad (85)$$

where ψ_{qh} is the corresponding primary field. Since ψ_{qh} is a primary field and ψ_e is a descendant of the identity, we are guaranteed that ψ_{qh} and ψ_e are local with respect to each other, i.e., taking one field around another can only produce a phase that is a multiple of 2π . Consequently, the wave function Ψ remains analytic in the electron coordinates z_i even after the fields $\psi_{\text{qh}}(w_1) \cdots \psi_{\text{qh}}(w_M)$ have been inserted into the correlation function.

One important feature of the conformal block on the right-hand side of Eq. (85) is that $\psi_{\text{qh}}(w_a)$ and $\psi_e(z_i)$ are on roughly the same footing—they are both fields in some conformal field theory (or, equivalently, they are both fixed sources coupled to the Chern-Simons gauge field). However, when interpreted as a wave function on the left-hand side of Eq. (85), the electron coordinates z_i are the variables for which the wave function gives a probability amplitude while the quasihole coordinates w_a are merely some parameters in this wave function. If we normalize the wave function differently, we multiply by an arbitrary function of the w_a 's. However, the particular normalization that is given by the right-hand side of Eq. (85) is particularly convenient, as shown shortly. Note that since the quasihole positions w_j are merely parameters in the wave function, the wave function need not be analytic in these coordinates.

b. Quasiparticle braiding

The branch cuts in quasihole positions w_a are due to the fact that there may be a vector space of conformal blocks corresponding to the right-hand side of Eq. (85). In such a case, even when the quasihole positions are fixed, there are several possible linearly independent wave functions. These multiple degenerate states are necessary for non-Abelian statistics, and they will generically mix when the quasiholes are dragged around each other.

However, there is still a logical gap in the above reasoning. The wave functions produced by a RCFT have the correct braiding properties for the corresponding

Chern-Simons ground state wave function built into them through their explicit monodromy properties. As a result of the branch cuts in the conformal blocks as a function of w_a 's, when one quasihole is taken around another, the wave function Ψ^α transforms into $M^{\alpha\beta}\Psi^\beta$, where the index $\alpha=1,2,\dots,g$ runs over the g different degenerate n -quasihole states. However, when viewed as quantum Hall wave functions, their quasiparticle braiding properties are a combination of their explicit monodromy and the Berry matrix which is obtained from

$$e^{i\gamma_{\alpha\beta}} = \mathcal{P} \exp\left(\oint d\vec{w} \langle \Psi^\alpha | \nabla_{\vec{w}} | \Psi^\beta \rangle\right), \quad (86)$$

where Ψ^α , $\alpha=1,2,\dots,g$, are the g different degenerate n -quasihole states and \mathcal{P} is the path-ordering symbol. In this equation, z_i 's are integrated over in order to compute the inner product, but w_a 's are held fixed, except for the one that is taken around some loop.

Strictly speaking, the effect of braiding is to transform a state according to $\Psi^\alpha \rightarrow e^{i\gamma_{\alpha\beta}} M^{\beta\gamma} \Psi^\gamma$. By changing the normalization of the wave function, we can alter $e^{i\gamma_{\alpha\beta}}$ and $M^{\beta\gamma}$. Only the product of the two matrices on the right-hand side of this equation is gauge invariant and physically meaningful. When we presume that the braiding properties of this wave function are given by those of the corresponding CFT and Chern-Simons theory, we take it to be equal to $M^{\beta\gamma}$ and ignore $e^{i\gamma_{\alpha\beta}}$. This can be correct only if $\gamma_{\alpha\beta}$ vanishes up to a geometric phase proportional to the area for a wave function given by a CFT conformal block. In the case of the Laughlin states, it can be verified that this is indeed correct by repeating the Arovas-Schrieffer-Wilczek, calculation (Arovas *et al.*, 1984) with the Laughlin state normalized according to the quasihole position dependence given by the corresponding CFT (see below) (Blok and Wen, 1992). This calculation rests upon Laughlin's plasma analogy (1983). For other, more complex states, it is more difficult to compute the Berry matrix. A version of a plasma analogy for the Moore-Read (MR) Pfaffian state was constructed in Gurarie and Nayak (1997); one could thereby verify the vanishing of the Berry matrix for a two-quasihole state and, with some further assumptions, for four and higher multi-quasihole states. A direct evaluation of the integral in Eq. (86) by the Monte Carlo method (Tserkovnyak and Simon, 2003) established that it vanishes for MR Pfaffian quasiholes. The effect of Landau level mixing on statistics has also been studied (Simon, 2008). Although there has not been a complete proof that the CFT Chern-Simons braiding rules are identical to those of the wave function, when it is interpreted as an electron wave function [i.e., there has not been a complete proof that Eq. (86) vanishes when the wave function is a CFT conformal block], there is evidence for the MR Pfaffian state, and it is almost certainly true for many other states as well. We therefore take it as a given that we can simply read off the braiding properties of the wave functions constructed below.

c. The Laughlin state

We now consider wave functions generated by the simplest CFT, the chiral boson. Suppose that the chiral boson has compactification radius \sqrt{m} , so that $\phi \equiv \phi + 2\pi\sqrt{m}$. The U(1) Kac-Moody algebra and enveloping Virasoro algebra can be extended by the symmetry generator $e^{i\phi/\sqrt{m}}$. Since the dimension of this operator is $m/2$, it is fermionic for odd m and bosonic for even m . The primary fields of this extended chiral algebra are of the form $e^{in\phi/\sqrt{m}}$, with $n=0,1,\dots,m-1$. They are all of the fields that are not descendants and are local with respect to $e^{i\phi/\sqrt{m}}$ (and to the Kac-Moody and Virasoro generators), as may be seen from the operator product expansion (OPE) (see the Appendix):

$$e^{i\phi(z)/\sqrt{m}} e^{in\phi(0)/\sqrt{m}} \sim z^n e^{i(n+m)\phi(0)/\sqrt{m}} + \dots \quad (87)$$

When z is taken around the origin, the right-hand side is unchanged. It is convenient to normalize the U(1) current as $j=(1/\sqrt{m})\partial\phi$; then the primary field $e^{in\phi/\sqrt{m}}$ has charge n/m . We take $\psi_e=e^{i\phi/\sqrt{m}}$ as our electron field (which has charge 1) and consider the resulting ground state wave function according to Eq. (84). Using Eq. (A7) we find

$$\Psi_{\text{gs}} = \langle \psi_e(z_1) \cdots \psi_e(z_N) \rangle = \prod_{i<j} (z_i - z_j)^m. \quad (88)$$

It is now clear why we have chosen this CFT. To have Ψ_{gs} given by correlators of a vertex operator of the form $e^{i\alpha\phi}$ analytic (no branch cuts or poles) we must have $\alpha^2 = m$ a nonnegative integer, and m must be odd to obtain an antisymmetric wave function (or even for symmetric). We recognize Ψ_{gs} as the $\nu=1/m$ Laughlin wave function. The astute reader will notice that the correlator in Eq. (88) violates the neutrality condition discussed in the Appendix and so it should actually have zero value. One fix for this problem is to insert (by hand) into the correlator a neutralizing vertex operator at infinity, $e^{-iN\phi(z=\infty)/\sqrt{m}}$, which then makes Eq. (88) valid (up to a constant factor). Another approach is to insert an operator that smears the neutralizing background over the entire system (Moore and Read, 1991). This approach also results in the neglected Gaussian factors reappearing. We ignore these neutralizing factors for simplicity. From now on, we drop the Gaussian factors from quantum Hall wave functions, with the understanding that they result from including a smeared neutralizing background.

The quasihole operator must be a primary field; the primary field of minimum charge is $e^{i\phi/\sqrt{m}}$. Using Eq. (A7), Eq. (85) yields

$$\Psi(w_1, \dots, w_M) = \prod_{i<j}^M (w_i - w_j)^{1/m} \prod_{i=1}^N \prod_{j=1}^M (z_i - w_j) \Psi_{\text{gs}}. \quad (89)$$

As mentioned above, the factor $\prod_j (z_j - w)$ "pushes" charge away from the position w , leaving a hole of charge precisely $Q = +e/m$. The first term on the right of

Eq. (89) results from the fusion of quasihole operators with each other, and shows the fractional statistics of the quasiholes. Adiabatically taking two quasiholes around each other results in a fractional phase of $2\pi/m$. This statistical term appears automatically in the wave function given by this CFT.

d. Moore-Read Pfaffian state

In the Ising CFT (see the Appendix), we use $\psi(z)$ as the electron field (Moore and Read, 1991). The ψ fields can fuse together in pairs to give the identity (since $\psi \times \psi = \mathbf{1}$) so long as there are an even number of fields. However, when we take two ψ fields close to each other, the OPE tells us that

$$\lim_{z_i \rightarrow z_j} \psi(z_i) \psi(z_j) \sim \mathbf{1}/(z_i - z_j) \quad (90)$$

which diverges as $z_i \rightarrow z_j$ and is therefore unacceptable as a wave function. To remedy this problem, we tensor the Ising CFT with the chiral boson CFT. There is now an operator $\psi e^{i\phi/\sqrt{m}}$ by which we can extend the chiral algebra. (If m is even, this symmetry generator is fermionic; if m is odd, it is bosonic.) As before, we take this symmetry generator to be our electron field. The corresponding primary fields are of the form $e^{in\phi/\sqrt{m}}$, $\sigma e^{i(2n+1)\phi/2\sqrt{m}}$, and $\psi e^{in\phi/\sqrt{m}}$, where $n=0,1,\dots,m-1$. Again, these are determined by the requirement of locality with respect to the generators of the chiral algebra, i.e., that they are single valued when taken around a symmetry generator, in particular the electron field $\psi e^{i\phi/\sqrt{m}}$. For instance,

$$\begin{aligned} \psi(z) e^{i\phi(z)/\sqrt{m}} \sigma(0) e^{i(2n+1)\phi(0)/2\sqrt{m}} \\ \sim z^{-1/2} \sigma(0) z^{n+1/2} e^{i[2(n+m)+1]\phi(0)/\sqrt{m}} + \dots \\ = z^n \sigma(0) e^{i[2(n+m)+1]\phi(0)/\sqrt{m}}, \end{aligned} \quad (91)$$

and similarly for the other primary fields.

Using our new symmetry generator as the electron field, we obtain the ground state wave function according to Eq. (84):

$$\begin{aligned} \Psi_{\text{gs}} &= \langle \psi(z_1) \cdots \psi(z_N) \rangle \prod_{i<j} (z_i - z_j)^m \\ &= \text{Pf} \left(\frac{1}{z_i - z_j} \right) \prod_{i<j} (z_i - z_j)^m \end{aligned} \quad (92)$$

[see, e.g., Di Francesco *et al.* (1997) for calculation of this correlation function]. Here, m even gives an antisymmetric wave function and m odd gives a symmetric wave function. For $m=2$ (and even N), Eq. (92) gives the Moore-Read Pfaffian wave function [Eq. (43) with $g=1/z$ and two Jastrow factors attached].

To determine the filling fraction of our newly constructed wave function, we need only look at the exponent of the Jastrow factor in Eq. (92). Recall that the filling fraction is determined by the highest power of any z (see Sec. III.D.1). There are $m(N-1)$ factors of z_1 in the Jastrow factor. The Pfaffian has a factor of z_1 in the

denominator, so the highest power of z_1 is $m(N-1)-1$. However, in the thermodynamic limit, the number of factors scales as mN . Thus the filling fraction is $\nu=1/m$.

We now consider quasihole operators. As in the Laughlin case we consider the primary fields $\psi_{\text{qh}} = e^{in\phi/\sqrt{m}}$. Similar arguments as in the Laughlin case show that the $n=1$ case generates the Laughlin quasihole of charge $Q=+e/m$. However, we have other options for our quasihole, which have smaller electrical charge. The primary field $\sigma e^{i\phi/2\sqrt{m}}$ has charge $Q=+e/2m$. We then obtain the wave function according to Eq. (85),

$$\begin{aligned} \Psi(w_1, \dots, w_M) &= \langle \sigma(w_1) \cdots \sigma(w_m) \psi(z_1) \cdots \psi(z_N) \rangle \\ &\times \prod_{i<j}^M (w_i - w_j)^{1/2m} \\ &\times \prod_{i=1}^N \prod_{j=1}^M (z_i - w_j)^{1/2} \prod_{i<j}^N (z_i - z_j)^m. \end{aligned} \quad (93)$$

Using the fusion rules of the σ fields [see Eq. (7), as well as Fig. 22 and Table II in the Appendix], we see that it is impossible to obtain $\mathbf{1}$ from an odd number of σ fields. We conclude that quasiholes ψ_{qh} can only occur in pairs. Then consider the simplest case of two quasiholes. If there is an even number of electrons, the ψ fields fuse in pairs to form $\mathbf{1}$, and the remaining two quasiholes must fuse to form $\mathbf{1}$ also. As discussed in Eq. (A3) the OPE of the two σ fields will then have a factor of $(w_1 - w_2)^{-1/8}$. In addition, the fusion of the two vertex operators $e^{i\phi/2\sqrt{m}}$ results in the first term in the second line of Eq. (93), $(w_1 - w_2)^{1/(4m)}$. Thus the phase accumulated by taking the two quasiholes around each other is $-2\pi/8 + 2\pi/4m$.

On the other hand, with an odd number of electrons in the system, ψ 's fuse in pairs, but leave one unpaired ψ . The two σ 's must then fuse to form a ψ which can then fuse with the unpaired ψ to give the identity [see Eq. (A3)]. In this case, the OPE of the two σ fields will give a factor of $(w_1 - w_2)^{3/8}$. Thus the phase accumulated by taking the two quasiholes around each other is $6\pi/8 + 2\pi/4m$.

In the language of Sec. III.B, when there is an even number of electrons in the system, all of these are paired and the fermion orbital shared by the quasiholes is unoccupied. When an odd electron is added, it ‘‘occupies’’ this orbital, although the fermion orbital is neutral and the electron is charged (we can think of the electron's charge as screened by the superfluid).

When there are many quasiholes, they may fuse together in many different ways. Thus even when the quasihole positions are fixed there are many degenerate ground states, each corresponding to a different conformal block (see the Appendix). This degeneracy is precisely what is required for non-Abelian statistics. Braiding the quasiholes around each other produces a rotation within this degenerate space.

Fusing $2m$ σ fields results in 2^{m-1} conformal blocks, as seen by examining the Bratteli diagram of Fig. 22 in the

Appendix. When two quasiholes come together, they may fuse to form either $\mathbf{1}$ or ψ . As above, if they come together to form $\mathbf{1}$ then taking the two quasiholes around each other gives a phase of $-2\pi/8+2\pi/4m$. On the other hand, if they fuse to form ψ then taking them around each other gives a phase of $2\pi 3/8+2\pi/4m$.

These conclusions can be illustrated in the cases of two and four quasiholes. For the case of two quasiholes, the correlation function (93) can be evaluated to give (Moore and Read, 1991; Nayak and Wilczek, 1996) (for an even number of electrons)

$$\Psi(w_1, w_2) = \prod_{j < k} (z_j - z_k)^2 \times \text{Pf} \left(\frac{(z_j - w_1)(z_k - w_2) + z_j \leftrightarrow z_k}{z_j - z_k} \right), \quad (94)$$

where $w_{12}=w_1-w_2$. For simplicity, we specialize to the case $m=2$; in general, there would be a prefactor $(w_{12})^{1/4m-1/8}$. When the two quasiholes at w_1 and w_2 are brought together at the point w , a single-flux-quantum Laughlin quasiparticle results, since two σ 's can only

fuse to the identity in this case, as expected from the above arguments:

$$\Psi_{\text{qh}}(w) = \prod_{j < k} (z_j - z_k)^2 \prod_i (z_i - w) \text{Pf} \left(\frac{1}{z_j - z_k} \right). \quad (95)$$

The situation becomes more interesting when we consider states with four quasiholes. The ground state is twofold degenerate (see the Appendix). If there is an even number of electrons (which fuse to form the identity), we are then concerned with the $\langle \sigma\sigma\sigma\sigma \rangle$ correlator. As discussed in the Appendix, two orthogonal conformal blocks can be specified by whether 1 and 2 fuse to form either $\mathbf{1}$ or ψ . The corresponding wave functions obtained by evaluating these conformal blocks are (Nayak and Wilczek, 1996)

$$\Psi^{(1, \psi)} = \frac{(w_{13}w_{24})^{1/4}}{(1 \pm \sqrt{x})^{1/2}} (\Psi_{(13)(24)} \pm \sqrt{x} \Psi_{(14)(23)}), \quad (96)$$

where $x=w_{14}w_{23}/w_{13}w_{24}$. [Note that we have taken a slightly different anharmonic ratio x than in Nayak and Wilczek, (1996) in order to make Eq. (96) more compact than Eqs. (7.17) and (7.18) of Nayak and Wilczek, (1996).] In this expression,

$$\Psi_{(13)(24)} = \prod_{j < k} (z_j - z_k)^2 \text{Pf} \left(\frac{(z_j - w_1)(z_j - w_3)(z_k - w_2)(z_k - w_4) + (j \leftrightarrow k)}{z_j - z_k} \right) \quad (97)$$

and

$$\Psi_{(14)(23)} = \prod_{j < k} (z_j - z_k)^2 \text{Pf} \left(\frac{(z_j - w_1)(z_j - w_4)(z_k - w_2)(z_k - w_3) + (j \leftrightarrow k)}{z_j - z_k} \right). \quad (98)$$

Suppose now that the system is in the state $\Psi^{(1)}$. Braiding 1 around 2 or 3 around 4 simply gives a phase (which is $R_1^{\sigma\sigma}$ multiplied by a contribution from the Abelian part of the theory). However, if we take w_2 around w_3 , then after the braiding, the system will be in the state $\Psi^{(\psi)}$ as a result of the branch cuts in Eq. (96). Now, 1 and 2 will instead fuse together to form ψ , as expected from

TABLE I. Summary of CFT wave-function correspondences discussed here. In all cases $M \geq 0$. Odd (even) M represents a Fermi (Bose) wave function.

State	CFT	ν	ψ_e	ψ_{qh}
Laughlin	Boson	$\frac{1}{M}$	$e^{i\phi\sqrt{M}}$	$e^{i\phi/\sqrt{M}}$
Moore-Read	Ising	$\frac{1}{M+1}$	$\psi_e e^{i\phi\sqrt{M+1}}$	$\sigma e^{i\phi/(2\sqrt{M+1})}$
\mathbb{Z}_3 RR	\mathbb{Z}_3 parafermion	$\frac{1}{M+2/3}$	$\psi_1 e^{i\phi\sqrt{M+2/3}}$	$\sigma_1 e^{i\phi/(3\sqrt{M+2/3})}$

the general argument in Eq. (A6). Thus the braiding yields a rotation in the degenerate space. The resulting prediction for the behavior under braiding for the Moore-Read Pfaffian state is in agreement with the results obtained in Secs. III.B and III.C.

e. \mathbb{Z}_3 Read-Rezayi state (briefly)

We follow a completely analogous procedure with a CFT which is the tensor product of the \mathbb{Z}_3 parafermion CFT with a chiral boson (see Tables I and II). As before, the electron operator is a product of a chiral vertex operator from the bosonic theory with an operator from the parafermion theory. The simplest choice is $\psi_e = \psi_1 e^{i\alpha\phi}$. We would like this field to be fermionic so that it can be an electron creation operator by which we can extend the chiral algebra (i.e., so that the electron wave function has no branch cuts or singularities). (See the Appendix for the notation for parafermion fields.) The fusion rules for ψ_1 in the \mathbb{Z}_3 parafermion CFT are $\psi_1 \times \psi_1 \sim \psi_2$ but $\psi_1 \times \psi_1 \times \psi_1 \sim \mathbf{1}$ so that the correlator in Eq. (84) is

TABLE II. Conformal data for three CFTs. The primary fields of each CFT are listed with their conformal dimension as well as the fusion table and central charge. In addition, every CFT has an identity field $\mathbf{1}$ with dimension $\Delta=0$ which fuses trivially with any field ($\mathbf{1} \times \phi_i = \phi_i$ for any ϕ_i). Note that fusion tables are symmetric so only the lower part is given. In the Ising CFT the field ψ is frequently denoted as ϵ . This fusion table indicates the nonzero elements of the fusion matrix N_{ab}^c . For example, in the \mathbb{Z}_3 CFT, since $\sigma_1 \times \sigma_2 = \mathbf{1} + \epsilon$, $N_{\sigma_1 \sigma_2}^{\mathbf{1}} = N_{\sigma_1 \sigma_2}^{\epsilon} = 1$, and $N_{\sigma_1 \sigma_2}^c = 0$ for all c not equal to $\mathbf{1}$ or ϵ .

Chiral Bose Vertex:		Ising CFT: ($c = 1/2$)															
$(c = 1)$	<table border="1" style="display: inline-table; border-collapse: collapse;"> <tr><td></td><td style="text-align: center;">Δ</td></tr> <tr><td style="text-align: center;">$e^{i\alpha\phi}$</td><td style="text-align: center;">$\alpha^2/2$</td></tr> </table>		Δ	$e^{i\alpha\phi}$	$\alpha^2/2$	<table border="1" style="display: inline-table; border-collapse: collapse;"> <tr><td style="text-align: center;">\times</td><td style="text-align: center;">$e^{i\alpha\phi}$</td></tr> <tr><td style="text-align: center;">$e^{i\beta\phi}$</td><td style="text-align: center;">$e^{i(\alpha+\beta)\phi}$</td></tr> </table>	\times	$e^{i\alpha\phi}$	$e^{i\beta\phi}$	$e^{i(\alpha+\beta)\phi}$	<table border="1" style="display: inline-table; border-collapse: collapse;"> <tr><td></td><td style="text-align: center;">Δ</td></tr> <tr><td style="text-align: center;">ψ</td><td style="text-align: center;">$1/2$</td></tr> <tr><td style="text-align: center;">σ</td><td style="text-align: center;">$1/16$</td></tr> </table>		Δ	ψ	$1/2$	σ	$1/16$
	Δ																
$e^{i\alpha\phi}$	$\alpha^2/2$																
\times	$e^{i\alpha\phi}$																
$e^{i\beta\phi}$	$e^{i(\alpha+\beta)\phi}$																
	Δ																
ψ	$1/2$																
σ	$1/16$																
\mathbb{Z}_3 Parafermion CFT: ($c = 4/5$)																	
	Δ	\times	$\psi_1 \quad \psi_2 \quad \sigma_1 \quad \sigma_2 \quad \epsilon$														
ψ_1	$2/3$	ψ_1	ψ_2														
ψ_2	$2/3$	ψ_2	$\mathbf{1} \quad \psi_1$														
σ_1	$1/15$	σ_1	$\epsilon \quad \sigma_2 \quad \sigma_2 + \psi_1$														
σ_2	$1/15$	σ_2	$\sigma_1 \quad \epsilon \quad \mathbf{1} + \epsilon \quad \sigma_1 + \psi_2$														
ϵ	$2/5$	ϵ	$\sigma_2 \quad \sigma_1 \quad \sigma_1 + \psi_2 \quad \sigma_2 + \psi_1 \quad \mathbf{1} + \epsilon$														

only nonzero if N is divisible by 3. From the OPE, we obtain $\psi_1(z_1)\psi_1(z_2) \sim (z_1 - z_2)^{-2/3}\psi_2$ so in order to have the wave function analytic, we must choose $\alpha = \sqrt{m+2/3}$ with $m \geq 0$ an integer (m odd results in an antisymmetric wave function and even results in symmetric). The filling fraction in the thermodynamic limit is determined entirely by the vertex operator $e^{i\alpha\phi}$, resulting in $\nu = 1/\alpha^2 = 1/(m+2/3)$.

The ground state wave function for $N=3n$ electrons takes the form

$$\Psi_{\text{gs}}(z_1, \dots, z_{3n}) = \prod_{i < j} (z_i - z_j)^m \times \mathcal{S} \left\{ \prod_{0 \leq r < s < n} \chi_{r,s}(z_{3r+1}, \dots, z_{3r+k}, z_{3k+1}, \dots, z_{3s+3}) \right\}, \tag{99}$$

where m must be odd for electrons, \mathcal{S} means the symmetrization over all permutations, and

$$\chi_{r,s} = (z_{3r+1} - z_{3s+1})(z_{3r+1} - z_{3s+2})(z_{3r+2} - z_{3s+2}) \times (z_{3r+2} - z_{3s+3}) \cdots (z_{3r+3} - z_{3s+3})(z_{3r+3} - z_{3s+1}). \tag{100}$$

With the electron operator in hand, we can determine the primary fields of the theory. The primary field of minimum electrical charge is $\psi_{qh} = \sigma_1 e^{i\phi/3\alpha}$. To see that

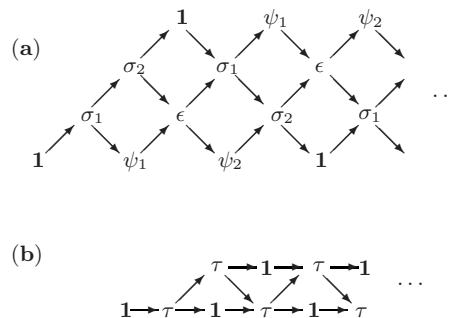


FIG. 9. Examples of the Brattelli diagrams. (a) Brattelli diagram for fusion of multiple σ_1 fields in the \mathbb{Z}_3 parafermion CFT. (b) Brattelli diagram for Fibonacci anyons.

this field is local with respect to ψ_e (i.e., there should be no branch cuts for the electron coordinates z_i), observe that $\sigma_1(w)\psi_1(z) \sim (z-w)^{-1/3}\psi$ and $e^{i\phi/3\alpha(w)}e^{i\alpha\phi(z)} \sim (z-w)^{1/3}$. Constructing the full wave function [as in Eq. (85) and analogous to Eq. (93)] the fusion of $e^{i\phi/3\alpha}$ (from ψ_{qh}) with $e^{i\alpha\phi}$ (from ψ_e) generates a factor of $\prod_i (z_i - w)^{1/3}$. We conclude that the elementary quasihole has charge $Q = +e\nu/3$.

The general braiding behavior for the \mathbb{Z}_3 parafermions has been worked out by Slingerland and Bais (2001). It is trivial, however, to work out the dimension of the degenerate space by examining the Brattelli diagram Fig. 9(a) (see the Appendix for explanation of this diagram). For example, if the number of electrons is a multiple of 3 then they fuse together to form the identity. Then, for example, with six quasiholes one has five paths of length 5 ending at $\mathbf{1}$ (hence a five-dimensional degenerate space). However, if, for example, the number of electrons is $1 \pmod 3$, then electrons fuse in threes to form $\mathbf{1}$ but there is one ψ_1 left over. Thus the quasiholes must fuse together to form ψ_2 which can fuse with the leftover ψ_1 to form $\mathbf{1}$. In this case, for example, with four quasiholes there is a two-dimensional space. It is easy to see that (if the number of electrons is divisible by 3) the number of blocks with n quasiparticles is given by the $n-1$ st Fibonacci number, denoted $\text{Fib}(n-1)$ defined by $\text{Fib}(1)=\text{Fib}(2)=1$ and $\text{Fib}(n)=\text{Fib}(n-1)+\text{Fib}(n-2)$ for $n > 2$.

E. Edge excitations

When a system in a chiral topological phase has a boundary (as it must in any experiment), there must be gapless excitations at the boundary (Halperin, 1982; Wen, 1992). To see this, consider the Chern-Simons action on a manifold \mathcal{M} with boundary $\partial\mathcal{M}$ (Elitzur *et al.*, 1989; Witten, 1989), Eq. (24). The change in the action under a gauge transformation, $a_\mu \rightarrow ga_\mu g^{-1} + g\partial_\mu g^{-1}$, is

$$S_{\text{CS}}[a] \rightarrow S_{\text{CS}}[a] + \frac{k}{4\pi} \int_{\partial\mathcal{M}} \text{tr}(g^{-1}dg \wedge a). \tag{101}$$

In order for the action to be invariant, we fix the boundary condition so that the second term on the right-hand

side vanishes. For instance, take the boundary condition $(a_0^g)|_{\partial\mathcal{M}}=0$, where x_0 and x_1 are coordinates on the boundary of \mathcal{M} and x_2 is the coordinate perpendicular to the boundary of \mathcal{M} . Then the action is invariant under all transformations that respect this boundary condition, i.e., that satisfy $\partial_0 g=0$ on the boundary. We separate these into gauge and global symmetries. Functions $g:\mathcal{M}\rightarrow G$ satisfying $g|_{\partial\mathcal{M}}=1$ are the gauge symmetries of the theory. (They necessarily satisfy $\partial_0 g=0$ since x_0 is a coordinate along the boundary.) Meanwhile, functions $f:\mathcal{M}\rightarrow G$ which are independent of x_0 are global symmetries of the theory. Representations of this global symmetry form the spectrum of edge excitations of the theory. The distinction between gauge and global transformations is that a gauge transformation can leave the $t=0$ state unchanged while changing the state of the system at a later time t . Since it is therefore not possible for a given initial condition to uniquely define the state of the system at a later time, all physically observable quantities must be invariant under the gauge transformation. By contrast, a global symmetry, even if it acts differently at different spatial points, cannot leave the $t=0$ state unchanged while changing the state of the system at a later time t . A global symmetry does not prevent the dynamics from uniquely defining the state of the system at a later time for a given initial condition. Therefore physically observable quantities need not be invariant under global transformations. Instead, the spectrum of the theory can be divided into representations of the symmetry.

With this boundary condition, the natural gauge choice for the bulk is $a_0^g=0$. We then transform the Chern-Simons functional integral into the chiral WZW functional integral following the steps in Eqs. (81)–(83) (Elitzur *et al.*, 1989):

$$S = \frac{k}{4\pi} \int_{\partial\mathcal{M}} \text{tr}(\partial_0 U^{-1} \partial_1 U) + \frac{k}{12\pi} \int_{\mathcal{M}} \epsilon^{\mu\nu\lambda} \text{tr}(\partial_\mu U U^{-1} \partial_\nu U U^{-1} \partial_\lambda U U^{-1}). \quad (102)$$

Note the off-diagonal form of the quadratic term [analogous to the $z-\bar{z}$ form in Eq. (83)], which follows from our choice of boundary condition. This boundary condition is not unique, however. The topological order of the bulk state does not determine the boundary condition. It is determined by the physical properties of the edge. Consider, for instance, the alternative boundary condition $(a_0^g + v a_1^g)|_{\partial\mathcal{M}}=0$ for some constant v with dimensions of velocity. With this boundary condition, the quadratic term in the Lagrangian will now be $\text{tr}[(\partial_0 + v \partial_1) U^{-1} \partial_1 U]$ and the edge theory is the chiral WZW model with non-zero velocity.

It is beyond the scope of this paper to discuss the chiral WZW model in any detail (for more details, see Knizhnik and Zamolodchikov, 1984; Gepner and Witten, 1986; Gepner and Qiu, 1987). However, there are a few key properties that we list now. The chiral WZW model is a conformal field theory. Therefore, although there is

a gap to all excitations in the bulk, there are gapless excitations at the edge of the system. The spectrum of the WZW model is organized into representations of the Virasoro algebra and is further organized into representations of the G_k Kac-Moody algebra. For the sake of concreteness, we consider the case of $SU(2)_k$. The $SU(2)_k$ WZW model contains primary fields ϕ_j , transforming in the $j=0, 1/2, 1, \dots, k/2$ representations. These correspond to the allowed quasiparticle species: when the total topological charge of all quasiparticles in the bulk is j , the edge must be in the sector created by acting with the spin- j primary field on the vacuum.

The G_k case is a generalization of the $U(1)_m$ case, where $g=e^{i\phi}$ and the WZW model reduces to a free chiral bosonic theory:

$$S = \frac{m}{4\pi} \int d^2x (\partial_t + v \partial_x) \phi \partial_x \phi. \quad (103)$$

[In Sec. III.A, we used k for the coefficient of an Abelian Chern-Simons term; here we use m to avoid confusion with the corresponding coupling of the $SU(2)$ Chern-Simons term in situations in which both gauge fields are present.] The primary fields are $e^{im\phi}$, with $n=0, 1, \dots, m-1$. (The field $e^{im\phi}$ is either fermionic or bosonic for m odd or even, respectively, so it is not a primary field, but is rather included as a generator of an extended algebra.) A quantum Hall state will always have such a term in its edge effective field theory; the $U(1)$ is the symmetry responsible for charge conservation and gapless chiral excitations (103) carry the quantized Hall current.

Therefore we see that chiral topological phases, such as fractional quantum Hall states, must have gapless chiral edge excitations. Furthermore, the conformal field theory that models the low-energy properties of the edge is the *same* conformal field theory that generates ground state wave functions of the corresponding Chern-Simons action. This is clear from the fact that the two derivations [Eqs. (83) and (102)] are virtually identical. The underlying reason is that Chern-Simons theory is a topological field theory. When it is solved on a manifold with boundary, it is unimportant whether the manifold is a fixed-time spatial slice or the world sheet of the system's edge. In either case, Chern-Simons theory reduces to the same conformal field theory (which is an example of “holography”). One important difference, however, is that, in the latter case, a physical boundary condition is imposed and there are real gapless degrees of freedom. (In the former case, the CFT associated with a wave function for a fixed-time spatial slice may have apparent gapless degrees of freedom which are an artifact of a gauge choice, as discussed in Sec. III.D.)

The WZW models do not, in general, have free field representations. One well-known exception is the equivalence between the $SU(N)_1 \times U(1)_N$ chiral WZW model and N free chiral Dirac fermions. A somewhat less well-known exception is the $SU(2)_2$ chiral WZW model, which has a representation in terms of three free chiral Majorana fermions. Before discussing this repre-

sensation, we first consider the edge excitations of a $p + ip$ superconductor, which supports Ising anyons, which in turn differ from $SU(2)_2$ only by a $U(1)$ factor.

We solve the Bogoliubov–de Gennes Hamiltonian (38) with a spatially varying chemical potential, as done in Sec. III.B. However, instead of a circular vortex, we consider an edge at $y=0$:

$$\mu(y) = \Delta h(y), \quad (104)$$

with $h(y)$ large and positive for large y , and $h(y) < 0$ for $y < 0$; therefore the electron density will vanish for y large and positive. Such a potential defines an edge at $y=0$. There are low-energy eigenstates of the BdG Hamiltonian which are spatially localized near $y=0$:

$$\phi_E^{\text{edge}}(\mathbf{x}) \approx e^{ikx} \exp\left(-\int_0^y h(y') dy'\right) \phi_0, \quad (105)$$

with $\phi_0 = \begin{pmatrix} 1 \\ 1 \end{pmatrix}$ an eigenstate of σ^x . This wave function describes a chiral wave propagating in the x direction localized on the edge, with wave vector $k = E/\Delta$. A more complete solution of the superconducting Hamiltonian in this situation would involve self-consistently solving the BdG equations, so that both the density and the gap $\Delta(y)$ would vanish for large positive y . The velocity of the chiral edge mode would then depend on how sharply $h(y)$ varies. However, the solutions given above with fixed constant Δ are sufficient to show the existence of the edge mode.

If we define an edge fermion operator $\psi(\mathbf{x})$,

$$\begin{aligned} \psi(\mathbf{x}) &= \exp\left(-\int_0^y h(y') dy'\right) \\ &\times \sum_{k>0} (\psi_k e^{ikx} \phi_0 + \psi_{-k} e^{-ikx} \phi_0). \end{aligned}$$

The fermion operators ψ_k satisfy $\psi_{-k} = \psi_k^\dagger$, so $\psi(x) = \sum_k \psi_k e^{ikx}$ is a real Majorana field, $\psi(x) = \psi^\dagger(x)$. The edge Hamiltonian is

$$\hat{\mathcal{H}}_{\text{edge}} = \sum_{k>0} v_n k \psi_k^\dagger \psi_k = \int dx \psi(x) (-iv_n \partial_x) \psi(x), \quad (106)$$

where the edge velocity $v = \Delta$. The Lagrangian density takes the form

$$\mathcal{L}_{\text{fermion}} = i\psi(x)(\partial_t + v_n \partial_x) \psi(x). \quad (107)$$

The 2D Ising model can be mapped onto the problem of (nonchiral) Majorana fermions on a lattice. At the critical point, the Majorana fermions become massless. Therefore the edge excitations are the right-moving chiral part of the critical Ising model. (This is why the vortices of a $p + ip$ superconductor are called Ising anyons.) However, the edge excitations have nontrivial topological structure for the same reason that correlation functions of the spin field are nontrivial in the Ising model: while fermions are free, the Ising spin field is nonlocal in terms of fermions, so its correlations are nontrivial. The Ising spin field $\sigma(z)$ inserts a branch cut running from

$z = v_n x + it$ to infinity for the fermion ψ . This is precisely what happens when a flux- $(hc/2e)$ vortex is created in a $p + ip$ superconductor.

The primary fields of the free Majorana fermion are $\mathbf{1}$, σ , and ψ with respective scaling dimensions 0, $1/16$, and $1/2$, as discussed in Sec. III.D. When there is an odd number of flux- $(hc/2e)$ vortices in the bulk, the edge is in the $\sigma(0)|0\rangle$ sector. When there is an even number, the edge is in either the $|0\rangle$ or $\psi(0)|0\rangle$ sector, depending on whether there is an even or odd number of fermions in the system. So long as quasiparticles do not go from the edge to the bulk, or vice versa, however, the system remains in one of these sectors and all excitations are free fermion excitations built on top of the ground state in the relevant sector.

However, when a quasiparticle tunnels from the edge to the bulk (or through the bulk), the edge goes from one sector to another—i.e., it is acted on by a primary field. Hence, in the presence of a constriction at which vortices of fermions can tunnel from one edge to another, the edge Lagrangian of a $p + ip$ superconductor is (Fendley *et al.*, 2007a)

$$\begin{aligned} S &= \int d\tau dx [\mathcal{L}_{\text{fermion}}(\psi_a) + \mathcal{L}_{\text{fermion}}(\psi_b)] \\ &+ \int d\tau \lambda_{\psi} i \psi_a \psi_b + \int d\tau \lambda_{\sigma} \sigma_a \sigma_b, \end{aligned} \quad (108)$$

where a and b denote the two edges (we have dropped all irrelevant terms, e.g., descendant fields). In other words, although the edge theory is a free theory in the absence of coupling to the bulk or to another edge through the bulk, it is perturbed by primary fields when quasiparticles can tunnel to or from the edge through the bulk. The topological structure of the bulk constrains the edge through the spectrum of primary fields.

As discussed in Sec. III.D, the edge of the Moore-Read Pfaffian quantum Hall state is a chiral Majorana fermion together with a free chiral boson ϕ for the charge sector of the theory. As in the case of a $p + ip$ superconductor, the primary fields of this theory determine how the edge is perturbed by the tunneling of quasiparticles between two edges through the bulk (Fendley *et al.*, 2006, 2007a):

$$\begin{aligned} S &= \int d\tau \left(\int dx [\mathcal{L}_{\text{edge}}(\psi_a, \phi_a) + \mathcal{L}_{\text{edge}}(\psi_b, \phi_b)] \right. \\ &+ \lambda_{1/2} \cos\{[\phi_a(0) - \phi_b(0)]/\sqrt{2}\} + \lambda_{\psi,0} i \psi_a \psi_b \\ &\left. + \lambda_{1/4} \sigma_a(0) \sigma_b(0) \cos\{[\phi_a(0) - \phi_b(0)]/2\sqrt{2}\} \right). \end{aligned} \quad (109)$$

The most relevant coupling is $\lambda_{1/4}$, so the tunneling of charge- $(e/4)$ quasiparticles dominates the transport of charge from one edge to the other at the point contact. [The tunneling of charge- $(e/2)$ quasiparticles makes a subleading contribution while the tunneling of neutral fermions contributes only to thermal transport.] At low enough temperatures, this relevant tunneling process

causes the point contact to be pinched off (Fendley *et al.*, 2006, 2007a; Feiguin, Fendley, *et al.*, 2008), but, at temperatures that are not too low, we can treat the tunneling of $e/4$ quasiparticles perturbatively and neglect other tunneling operators. Of course, the structure of the edge may be more complex than the minimal structure dictated by the bulk analyzed here. This depends on the details of the confining potential defining the system boundary, but, at low enough temperatures, the picture described here should still apply. Interesting information about the non-Abelian character of the Moore-Read Pfaffian state can be obtained from the temperature dependence of the tunneling conductance (Fendley *et al.*, 2006, 2007a) and from current noise (Bena and Nayak, 2006).

Finally, we return to $SU(2)_2$. The $SU(2)_2$ WZW model is a triplet of chiral Majorana fermions, ψ_1, ψ_2, ψ_3 —i.e., three identical copies of the chiral Ising model. This triplet is the spin-1 primary field (with scaling dimension $1/2$). The spin-1/2 primary field is roughly $\sim \sigma_1 \sigma_2 \sigma_3$ with dimension $3/16$ (a more precise expression involves the sum of products such as $\sigma_1 \sigma_2 \mu_3$, where μ is the Ising disorder operator dual to σ). This is one of the primary differences between the Ising model and $SU(2)_2$: σ is a dimension $1/16$ field, while the spin-1/2 primary field of $SU(2)_2$ has dimension $3/16$. Another way to understand the difference between the two models is that the $SU(2)_2$ WZW model has two extra Majorana fermions. The pair of Majorana fermions can be viewed equally well as a Dirac fermion or, through bosonization, as a free chiral boson, which has $U(1)$ symmetry. Thus the Ising model is often written as $SU(2)_2/U(1)$ to signify that the $U(1)$ chiral boson has been removed. [This notion can be made precise with the notion of a *coset* conformal field theory (Di Francesco *et al.*, 1997) or by adding a $U(1)$ gauge field to the 2D action and coupling it to a $U(1)$ subgroup of the $SU(2)$ WZW field g (Gawędzki and Kupiainen, 1988; Karabali *et al.*, 1989). The gauge field has no Maxwell term, so it serves only to eliminate some of the degrees of freedom, namely, the $U(1)$ piece.] As discussed in Sec. III.C, these differences are also manifested in the bulk, where they lead to differences in the Abelian phases which result from braiding but do not change the basic non-Abelian structure of the state.

On the other hand, the edge of the Moore-Read Pfaffian quantum Hall state is a chiral Majorana fermion together with a free chiral boson ϕ which carries the charged degrees of freedom. So we restore the chiral boson that we eliminated in passing from $SU(2)_2$ to the Ising model, with one important difference. The compactification radius R (i.e., the theory is invariant under $\phi \rightarrow \phi + 2\pi R$) of the charged boson need not be the same as that of the boson that was removed by cosetting. For the special case of bosons at $\nu=1$, the boson is, in fact, at the right radius. Therefore the charge boson can be fermionized so that there is a triplet of Majorana fermions. In this case, the edge theory is the $SU(2)_2$ WZW model (Fradkin *et al.*, 1998). In the case of electrons at $\nu=2+1/2$, the chiral boson is not at this radius, so the edge

theory is $U(1)_2 \times$ Ising, which is not quite the $SU(2)_2$ WZW model.

F. Interferometry with anyons

In Sec. II we described an interference experiment that is designed to demonstrate the non-Abelian statistics of quasiparticles in the $\nu=5/2$ state. We start by returning to this experiment, and using it as an exercise for the application of the calculational methods reviewed above. We then generalize our analysis to arbitrary $SU(2)_k$ non-Abelian states and describe other experiments that share the same goal.

In the experiment described in Sec. II, a Fabry-Perot interference device is made of a Hall bar perturbed by two constrictions (see Fig. 2). The backscattered current is measured as a function of the cell area enclosed by the two constrictions and of the magnetic field. We assume that the system is at $\nu=5/2$ and consider interference experiments which can determine if electrons are in the Moore-Read Pfaffian quantum Hall state.

Generally speaking, the amplitude for backscattering is a sum over trajectories that wind the cell ℓ times, with $\ell=0,1,2,\dots$ an integer. The partial wave that winds the cell ℓ times winds the n quasiparticles localized inside the cell ℓ times. From the analysis in Sec. III.B, if electrons are in the Pfaffian state, the unitary transformation that the tunneling quasiparticle applies on the wave function of the zero-energy modes is

$$(\hat{U}_n)^\ell = \left[e^{i\alpha_n} \gamma_a^n \prod_{i=1}^n \gamma_i \right]^\ell, \quad (110)$$

where γ_i 's are the Majorana modes of the localized bulk quasiparticles, γ_a is the Majorana mode of the quasiparticle that flows around the cell, and α_n is an Abelian phase calculated below.

The difference between the even and odd values of n , which we described in Sec. II, is evident from Eq. (110) when we look at the lowest order, $\ell=1$. For even n , \hat{U}_n is independent of γ_a . Thus each tunneling quasiparticle applies the same unitary transformation on the ground state. The flowing current then *measures* the operator \hat{U}_n (more precisely, it measures the interference term, which is a Hermitian operator; from that term the value of \hat{U}_n may be extracted). In contrast, when n is odd the operator \hat{U}_n depends on γ_a . Thus a different unitary operation is applied by every incoming quasiparticle. Moreover, the different unitary operators do not commute, and share no eigenvectors. Thus their expectation values average to zero, and no interference is observed. This analysis holds in fact for all odd values of ℓ .

The phase α_n is composed of two parts. First, the quasiparticle accumulates an Aharonov-Bohm phase of $2\pi e^* \Phi / hc$, where $e^*=e/4$ is the quasiparticle charge for $\nu=5/2$ and Φ is the flux enclosed. And, second, the tunneling quasiparticle accumulates a phase as a consequence of its interaction with the n localized quasiparti-

cles. When a charge- $(e/4)$ object goes around n flux tubes of half a flux quantum each, the phase it accumulates is $n\pi/4$.

Altogether the unitary transformation (120) has two eigenvalues. For even n , they are $(\pm i)^{n/2}$. For odd n , they are $(\pm i)^{(n-1)/2}$. The backscattered current assumes the following form (Stern and Halperin, 2006):

$$I_{\text{bs}} = \sum_{m=0}^{\infty} I_m \cos^2 mn \frac{\pi}{2} \cos m \left(\phi + \frac{\tilde{n}\pi}{4} + \frac{\pi\alpha}{2} \right), \quad (111)$$

where $\tilde{n}=n$ for n even, and $\tilde{n}=n+1$ for n odd. The m th term of this sum is the contribution from a process that loops around m times, which vanishes if n and m are both odd.

We can restate this analysis using the CFT description of the Moore-Read Pfaffian state. Charge- $(e/4)$ quasiparticles are associated with the operator $\sigma e^{i\phi/\sqrt{8}}$. The fusion of n such quasiparticles is

$$e^{in\phi/\sqrt{8}} \times \begin{cases} 1, \\ \psi, \\ \sigma, \end{cases} \quad (112)$$

where either of the first two is possible for even n , and the last is the outcome of the fusion for odd n . In order to determine the effect of braiding an incoming quasiparticle around the n bulk ones, we consider the possible fusion channels of one quasiparticle with Eq. (122). The fusion of the bosonic factors (i.e., the electrical charge) is

$$e^{in\phi(z_1)/\sqrt{8}} e^{i\phi(z_2)/\sqrt{8}} \rightarrow e^{i(n+1)\phi(z_1)/\sqrt{8}} (z_1 - z_2)^{-n/8}. \quad (113)$$

Thus, when the incoming quasiparticle, at coordinate z_2 , encircles the bulk ℓ times, it accumulates a phase of $2\pi \times (n/8) \times \ell = n\ell\pi/4$ purely as a result of the U(1) part of the theory. Now consider the neutral sector. The fusion of the σ operator depends on the state of the bulk. When the bulk has total topological charge $\mathbf{1}$, the fusion is trivial, and does not involve any accumulation of phases. When the bulk has total topological charge ψ , the fusion is

$$\sigma(z_2) \times \psi(z_1) \rightarrow \sigma(z_1) \times (z_1 - z_2)^{-1/2}, \quad (114)$$

and an extra phase of $\pi\ell$ is accumulated when the incoming quasiparticle winds the bulk quasiparticles ℓ times. When the bulk has total topological charge σ , i.e., when n is odd, the non-Abelian fusion rule applies [see Eq. (A3)], and

$$\sigma(z_1) \times \sigma(z_2) \rightarrow (z_1 - z_2)^{-1/8} [1 + (z_1 - z_2)^{1/2} \psi(z_1)]. \quad (115)$$

Since the probability for the two fusion outcomes is equal,⁸ for any odd ℓ we get two interference patterns that are mutually shifted by π , and hence mutually cancel one another, while for even ℓ we get an extra phase

$$\begin{aligned} \text{Figure-eight} &= q \text{ (two loops)} + \text{Figure-eight} \\ &+ \text{Figure-eight with dot} + q^{-1} \text{ (loop with dot)} \\ &= (q + q^{-1})d^2 + 2d \end{aligned}$$

FIG. 10. Using the recursion relation (77), we can evaluate $\langle \chi | \rho(\sigma_2^2) | \chi \rangle$.

of $\ell\pi/4$. Altogether, this reproduces the expression (111).

Now consider the same calculation using the relation between Chern-Simons theory and the Jones polynomial. For simplicity, just compute the current due to a single backscattering and neglect multiple-tunneling processes, which can be computed in a similar way. The elementary quasiparticles have $j=1/2$. These are the quasiparticles that will tunnel at the point contacts, either encircling the bulk quasiparticles or not. (Other quasiparticles will give a subleading contribution to the current because their tunneling amplitudes are smaller and less relevant in the RG sense.) First, consider the case in which there is a single $j=1/2$ quasiparticle in the bulk. The backscattered current is

$$I_{\text{bs}} = I_0 + I_1 \text{Re}[e^{i\phi} \langle \chi | \rho(\sigma_2^2) | \chi \rangle]. \quad (116)$$

The matrix element on the right-hand side is given by evaluation of the link in Fig. 4(a) (Fradkin *et al.*, 1998; Bonderson, Kitaev, *et al.*, 2006) (up to a normalization of the bra and ket; see Sec. III.C). The matrix element is between a state $|\chi\rangle$, the state in which 1 and 2 fuse to the trivial particle as do 3 and 4 and the state $\rho(\sigma_2^2)|\chi\rangle$. The former is the state in which the tunneling quasiparticle (qp 3) does not encircle the bulk quasiparticle (qp 2); the latter is the state in which it does. The matrix element between these two states determines the interference.

Using the recursion relation (77) as shown in Fig. 10, we obtain

$$\langle \chi | \rho(\sigma_2^2) | \chi \rangle = (q + q^{-1})d^2 + 2d = -d^3 + 2d. \quad (117)$$

For $k=2$, $d=\sqrt{2}$, and so this vanishes. Consequently, the interference term in Eq. (116) also vanishes, as found above by other methods. The case of an arbitrary odd number of quasiparticles in the island is similar.

Now consider the case in which there are an even number of quasiparticles in the island. For the sake of simplicity, we consider the case in which there are two quasiparticles in the bulk, i.e., a qubit. The pair can fuse to either $j=0$ or $j=1$. In the former case, it is clear that no phase is acquired [see Fig. 11(a)]. In the latter case, the recursion rule (77) gives us a -1 , as depicted in Fig. 11. This difference allows us to read out the value of a topologically protected qubit (Das Sarma *et al.*, 2005).

What happens if the qubit is in a superposition of $j=0$ and $j=1$? The interference measurement causes the tunneling quasiparticles to become entangled with the bulk quasiparticle (Overbosch and Bais, 2001; Freedman *et al.*, 2006; Bonderson *et al.*, 2007). When the integrated

⁸This follows from $N_{\sigma\sigma}^1 = N_{\sigma\sigma}^\psi = 1$.

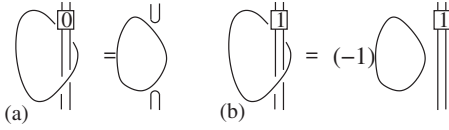


FIG. 11. We can obtain the result of taking a $j=1/2$ quasiparticle around a qubit from the two diagrams. In (a) The qubit is in the state 0, while in (b) it is in state 1. These diagrams are similar to the left-hand side of Fig. 10, but with the loop on the right replaced by a loop with (a) $j=0$ or (b) $j=1$.

current is large enough that many quasiparticles have tunneled and equilibrated at the current leads, the $j=0$ and $j=1$ possibilities will have decohered. The measurement will see one of the two possibilities with corresponding probabilities.

The experiment that we analyzed above for $\nu=5/2$ may also be analyzed for other non-Abelian states. The computation using knot invariants can be immediately adapted to other $SU(2)_k$ states by replacing $d=\sqrt{2}$ with $d=2 \cos \pi/(k+2)$. We calculate the value of the Hopf link as in Figs. 10 and 11, with one of the loops corresponding to the tunneling quasiparticle and the other loop corresponding to the total topological charge of the bulk quasiparticles. The result can be written in the more general form (Bonderson, Shtengel, *et al.*, 2006):

$$I_{bs}(a) = I_0 + I_1 |M_{ab}| \cos(\beta + \theta_{ab}), \quad (118)$$

where M_{ab} is defined in terms of the S matrix:

$$M_{ab} = S_{ab} S_{11} / S_{1a} S_{1b}, \quad (119)$$

and $M_{ab} = |M_{ab}| e^{i\theta_{ab}}$. Equation (118) gives the current due to a quasiparticles if the quasiparticles in the bulk fuse to b . If the contribution of $j=1/2$ quasiparticles dominates, as in the $\nu=5/2$ case, then we should set $a=\frac{1}{2}$ in this equation. For the level $k=3$ case, taking $a=\frac{1}{2}$, $|M_{ab}|=1$ for $b=0, \frac{3}{2}$ while $|M_{ab}|=\phi^{-2}$ for $b=\frac{1}{2}, 1$, where ϕ is the golden mean, $\phi=(1+\sqrt{5})/2$. (In \mathbb{Z}_3 parafermion language, $b=0, \frac{3}{2}$ corresponds to the fields $\mathbf{1}, \psi_{1,2}$ while $b=\frac{1}{2}, 1$ corresponds to the fields $\sigma_{1,2}, \varepsilon$.)

Finally, we analyze the operation of an interferometer using the edge theory (109). The preceding discussion assumed that the current is carried by noninteracting anyonic quasiparticles. However, the edge is gapless and, in general, does not even have well-defined quasiparticles. Therefore a computation using the edge theory is more complete. The expected results are recovered since they are determined by the topological structure of the state, which is shared by both the bulk and the edge. However, the edge theory also enables one to determine the temperature and voltage dependences of I_0, I_1, \dots in Eqs. (111) and (116) (Bishara and Nayak, 2007; Fidkowski, 2007; Ardonne and Kim, 2008). As is discussed in these papers, at finite temperature, interference will not be visible if the two point contacts are further apart than the thermal length scale L_ϕ , where $L_\phi^{-1} = k_B T (\frac{1/8}{v_c} + \frac{1/8}{v_n})$, if the charged and neutral mode velocities are v_c , and v_n . Another important feature is that the interfer-

ence term (when it is nonvanishing) is oscillatory in the source-drain voltage while the I_0 term has a power-law dependence.

The assumption that the edge and the bulk are well separated is crucial to the above calculations of interference, but in practice this may not be the case. When there is bulk-edge tunneling one might imagine that a quasiparticle moving along the edge may tunnel into the bulk for a moment and thereby evade encircling some localized quasiparticles, thus smearing out any interference pattern. The first theoretical steps toward analyzing this situation have been taken by Overbosch and Wen (2007) and Rosenow *et al.* (2008), where tunneling to a single impurity is considered. Surprisingly, it is found that the interference pattern is full strength in both the strong- as well as the weak-tunneling limits.

While the experiment described for the $\nu=5/2$ state does not require precise determination of n , as it is only its parity that determines the amplitude of the interference pattern, it does require that the number n does not fluctuate within the duration of the experiment. Generally, fluctuations in n would be suppressed by low temperature, large charging energy, and diminished tunnel coupling between the bulk and the edge. However, when their suppression is not strong enough, and n fluctuates over a range much larger than 1 within the time of the measurement, two signatures of the non-Abelian statistics of quasiparticles survive, at least as long as the characteristic time scale of these fluctuations is much longer than the time between backscattering events. First, any change in n would translate to a change in the backscattered current, or the two-terminal conductance of the device. Hence fluctuations in n would introduce current noise of the telegraph type, with a unique frequency dependence (Grosfeld *et al.*, 2006). Second, fluctuations in n would suppress all terms in Eq. (111) other than those where $m=4k$ with k an integer. Thus the backscattered current will have a periodicity of one flux quantum Φ_0 , and the visibility of flux oscillations, for weak backscattering, will be $I_4/I_0 \propto I_0^3$.

A similar relation holds also for another type of interference experiment, in which the interferometer is of the Mach-Zehnder type, rather than the Fabry-Perot type. [A Mach-Zehnder interferometer has already been constructed in the integer quantum Hall regime (Ji *et al.*, 2003).] If we are to describe the Mach-Zehnder interferometer in a language close to that we used for the Fabry-Perot one, we should note the following important differences. First, no multiple-backscattering events are allowed; and, second, since the area enclosed by the interfering partial waves now encompasses the inner edge, the quantum state of the encircled area changes with each tunneling quasiparticle. Thus it is not surprising that the outcome of an interference experiment in a Mach-Zehnder geometry will be very close to that of a Fabry-Perot experiment with strong fluctuations in n . The telegraph noise in the Fabry-Perot case (Grosfeld *et al.*, 2006) becomes shot noise in the Mach-Zehnder case. Remarkably (Feldman *et al.*, 2007), the effective charge

extracted from that noise carries a signature of the non-Abelian statistics: as the flux is varied, the charge changes from $e/4$ to about $3e$.

Other than interference experiments, there are several proposals for experiments that probe certain aspects of the physics of non-Abelian states. The degeneracy of the ground state in the presence of vortices may be probed (Grosfeld and Stern, 2006) by the consequences of its removal: when the filling factor is $\nu=5/2+\epsilon$ with $\epsilon\ll 1$, quasiparticles are introduced into the bulk of the system, with a density proportional to ϵ . For a clean enough sample and a low enough density, quasiparticles form a lattice. In that lattice, the Majorana zero modes of different quasiparticles couple by tunneling, and the degeneracy of the ground states is removed. The subspace of multiply degenerate ground states is then replaced by a band of excitations. The neutrality of the Majorana modes is removed too, and the excitations carry a charge that is proportional to their energy. This charge causes these modes to weakly couple to an externally applied electric field, and provides a mechanism for a dissipation of energy, with a characteristic dependence on the wave vector and frequency of the electric field. Since the tunnel coupling between neighboring quasiparticles depends exponentially on their separation, this mechanism will be exponentially sensitive to the distance of the filling factor from $5/2$ (Grosfeld and Stern, 2006).

G. Lattice models with P, T -invariant topological phases

Our discussion of topological phases has revolved around fractional quantum Hall states because these are the only ones known to occur in nature [although two-dimensional $^3\text{He-A}$ (Leggett, 1975; Volovik, 1994) and Sr_2RuO_4 may join this list (Kidwingira *et al.*, 2006; Xia *et al.*, 2006)]. However, there is nothing inherent in the definition of a topological phase that consigns it to the regime of high magnetic fields and low temperatures. Indeed, highly idealized models of frustrated magnets also show such phases, as discussed in Sec. II.D. Of course, it is an open question whether these models have anything to do with any real electronic materials or their analogs with cold atoms in optical lattices, i.e., whether the idealized models can be adiabatically connected to more realistic models. In this section, we do not attempt to answer this question but focus, instead, on understanding how these models of topological phases can be solved. As we show, their solubility lies in their incorporation of the basic topological structure of the corresponding phases.

One way in which a topological phase can emerge from some microscopic model of interacting electrons, spins, or cold atoms is if the low-lying degrees of freedom of the microscopic model can be mapped to the degrees of freedom of the topological phase in question. As we show in Sec. III.C, these degrees of freedom are Wilson loops (59). Loops are the natural degrees of freedom in a topological phase because the topological

charge of a particle or collection of particles can only be determined, in general, by taking a test particle around the particle or collection in question. Therefore the most direct way in which a system can settle into a topological phase is if the microscopic degrees of freedom organize themselves so that the low-energy degrees of freedom are loops or, as we show below, string nets (in which we allow vertices into which three lines can run). As described below, the Hilbert space of a non-chiral topological phase can be described roughly as a Fock space for loops Freedman *et al.* (2004). Wilson loop operators are essentially creation or annihilation operators for loops. The Hilbert space is spanned by basis states, which can be built up by acting with Wilson loop operators on the state with no loops, i.e., $|\gamma_1 \cup \dots \cup \gamma_n\rangle = W[\gamma_n] \dots W[\gamma_1] |\emptyset\rangle$ is analogous to $|k_1, \dots, k_2\rangle \equiv a_{k_n}^\dagger \dots a_{k_1}^\dagger |0\rangle$. An important difference is that states in the topological theory must satisfy extra constraints in order to correctly represent the algebra of the operators $W[\gamma]$. If we write an arbitrary state $|\Psi\rangle$ in the basis given above, $\Psi[\gamma_1 \cup \dots \cup \gamma_n] = \langle \Psi | \gamma_1 \cup \dots \cup \gamma_n \rangle$, then the ground state(s) of the theory are linearly independent, $\Psi[\gamma_1 \cup \dots \cup \gamma_n]$ satisfying some constraints.

In fact, we have seen an example of this in Sec. II.D: Kitaev's toric code model (18). We now represent the solution in a way which makes the emergence of loops clear. We color every link of the lattice on which the spin points up. Then, the first term in Eq. (18) requires that there be an even number of colored links emerging from each site on the lattice. In other words, the colored links form loops which never terminate. On the square lattice, loops can cross, but they cannot cross on the honeycomb lattice; for this reason, we find it more convenient to work on the honeycomb lattice. The second term in the Hamiltonian requires that the ground state satisfy three further properties: the amplitude for two configurations is the same if one configuration can be transformed into another by (i) deforming some loop without cutting it, (ii) removing a loop that runs around a single plaquette of the lattice, or (iii) cutting open two loops that approach each other within a lattice spacing and rejoining them into a single loop (or vice versa), which is called *surgery*. A vertex at which the first term in the Hamiltonian is not satisfied is an excitation, as is a plaquette at which the second term is not satisfied. The first type of excitation acquires a -1 when it is taken around the second.

The toric code is associated with the low-energy physics of the deconfined phase of \mathbb{Z}_2 gauge theory (Fradkin and Shenker, 1975; Kogut, 1979; see also Senthil and Fisher, 2000) for strongly correlated electron systems. This low-energy physics can be described by an Abelian BF theory (Hansson *et al.*, 2004):

$$\mathcal{S} = \frac{1}{\pi} \int e_\mu \epsilon^{\mu\nu\lambda} \partial_\nu a_\lambda = \mathcal{S}_{\text{CS}} \left(a + \frac{1}{2} e \right) - \mathcal{S}_{\text{CS}} \left(a - \frac{1}{2} e \right). \quad (120)$$

e_μ is usually denoted b_μ and $\epsilon^{\mu\nu\lambda} \partial_\nu a_\lambda = 1/2 \epsilon^{\mu\nu\lambda} f_{\nu\lambda}$, hence the name ‘‘BF.’’ Note that this theory is nonchiral. Un-

der a combined parity and time-reversal transformation, e_μ must change sign, and the action is invariant. This is important since it enables the fluctuating loops described above to represent the Wilson loops of the gauge field a_μ . In a chiral theory, it is not clear how to do this since a_1 and a_2 do not commute with each other. They cannot both be diagonalized; we must arbitrarily choose one direction in which Wilson loops are diagonal operators. It is not clear how this will emerge from some microscopic model, where we would expect that loops would not have a preferred direction, as shown above in the toric code. Therefore we focus on nonchiral phases, in particular, the $SU(2)_k$ analog of Eq. (120) (Cattaneo *et al.*, 1995):

$$\begin{aligned} \mathcal{S} &= S_{CS}^k(a+e) - S_{CS}^k(a-e) \\ &= \frac{k}{4\pi} \int \text{tr} \left(e \wedge f + \frac{1}{3} e \wedge e \wedge e \right). \end{aligned} \quad (121)$$

We call this theory *doubled* $SU(2)_k$ Chern-Simons theory (Freedman *et al.*, 2004).

We want a microscopic lattice model whose low-energy Hilbert space is composed of wave functions $\Psi[\gamma_1 \cup \dots \cup \gamma_n]$ which assign a complex amplitude to a given configuration of loops. The model must differ from the toric code in the constraints that it imposes on these wave functions. The corresponding constraints for Eq. (121) are essentially the rules for Wilson loops that we discussed in Sec. III.C (Freedman *et al.*, 2004). For instance, ground state wave functions should not give the same amplitude for two configurations if one configuration can be transformed into another by removing a loop which runs around a single plaquette of the lattice. Instead, the amplitude for the former configuration should be larger by a factor of $d=2 \cos \pi/(k+2)$, which is the value of a single unknotted Wilson loop. Meanwhile, the appropriate surgery relation is not the joining of two nearby loops into a single one, but instead the condition that, when $k+1$ lines come close together, the amplitudes for configurations in which they are cut open and rejoined in different ways satisfy some linear relation. This relation is essentially the requirement that the $j=(k+1)/2$ Jones-Wenzl projector should vanish within any loop configuration, as expected since a Wilson loop carrying the corresponding $SU(2)$ representation should vanish.

The basic operators in the theory are Wilson loops $W[\gamma]$ of the gauge field a_μ^a in Eq. (121) in the fundamental ($j=1/2$) representation of $SU(2)$. A Wilson loop in a higher- j representation can be constructed by taking $2j$ copies of a $j=1/2$ Wilson loop and using the appropriate Jones-Wenzl projector to eliminate the other representations which result in the fusion of $2j$ copies of $j=1/2$. If the wave function satisfies the constraint mentioned above, then it will vanish identically if acted on by a $j > k/2$ Wilson loop.

These conditions are of a topological nature, so they are most natural in the continuum. In constructing a lattice model from which they emerge, we have a certain

amount of freedom in deciding how these conditions are realized at the lattice scale. Depending on our choice of short-distance regularization, the model may be more or less easily solved. In some cases, an inconvenient choice of short-distance regularization may actually drive the system out of the desired topological phase. Loops on the lattice prove not to be the most convenient regularization of loops in the continuum, essentially because, when d is large, the lattice fills up with loops which then have no freedom to fluctuate (Freedman *et al.*, 2004). Instead, trivalent graphs on the lattice prove to be a better way of proceeding [and, in the case of $SU(3)_k$ and other gauge groups, trivalent graphs are essential (Turaev and Viro, 1992; Kuperberg, 1996)]. The most convenient lattice is the honeycomb lattice, since each vertex is trivalent. A trivalent graph is a subset of links on the honeycomb lattice such that no vertex has only a single link from the subset emanating from it. Zero, two, or three links can emanate from a vertex, corresponding to vertices which are not visited by the trivalent graph, vertices through which a curve passes, and vertices at which three curves meet. We penalize energetically vertices from which a single colored link emanates. The ground state will not contain such vertices which will be quasiparticle excitations. Therefore, the ground state $\Psi[\Gamma]$ assigns a complex amplitude to a trivalent graph Γ .

Such a structure arises in a manner analogous to the loop structure of the toric code: if we have spins on links of the honeycomb lattice, then an appropriate choice of interaction at each vertex requires that colored links (on which the spin points up) form a trivalent graph. We note that links can be given a further labeling, although we will not discuss this more complicated situation in detail. Each colored link can be assigned a j in the set $1/2, 1, \dots, k/2$. Uncolored links are assigned $j=0$. Rather than spin-1/2 spins on each link, we take spin $k/2$ on each link, with $S_z = -k/2$ corresponding to $j=0$, $S_z = -k/2 + 1$ corresponding to $j=1/2$, etc. (or, perhaps, we consider models with rather different microscopic degrees of freedom). In this case, we require that links around each vertex should satisfy the branching rules of $SU(2)_k$: $|j_1 - j_2| \geq j_3 \leq \min(j_1 + j_2, k/2 - j_1 - j_2)$. The case described in the previous paragraph, without the additional j label, could be applied to the level $k=1$ case, with colored links carrying $j=1/2$, or to level $k=3$, with colored links carrying $j=1$, as discussed further below. A trivalent graph represents a loop configuration in the manner depicted in Fig. 12(a). One nice feature is that the Jones-Wenzl projections are enforced on every link from the start, so no corresponding surgery constraint is needed.

If we want a lattice model to be in the doubled $SU(2)_3$ universality class, which has quasiparticle excitations that are Fibonacci anyons, then its Hamiltonian should impose the following: all low-energy states should have vanishing amplitude on configurations that are not trivalent graphs, as defined above; and the amplitude for a configuration with a contractible loop should be larger than the amplitude for a configuration without this loop

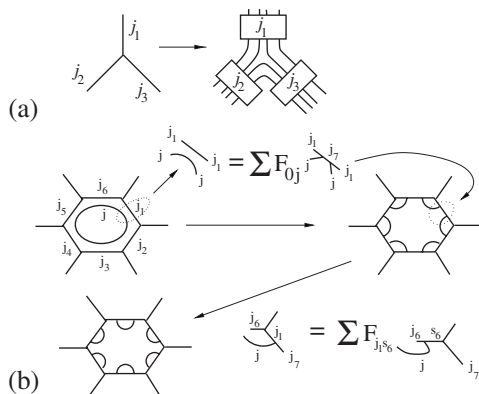


FIG. 12. Pictorial representation of the terms in the Hamiltonian of Levin and Wen. (a) $j/2$ parallel lines projected onto representation j are represented by j on a link. (b) The plaquette terms add a representation j loop. This can be transformed back into a trivalent graph on the lattice using the F matrix.

by $d=2\cos(\pi/5)=\phi=(1+\sqrt{5})/2$ for a closed, contractible loop. These conditions can be imposed by terms in the Hamiltonian which are more complicated versions of the vertex and plaquette terms of Eq. (18). It is furthermore necessary for the ground state wave function(s) to assign the same amplitude to any two trivalent graphs which can be continuously deformed into each other. However, as mentioned above, surgery is not necessary. The Hamiltonian takes the form (Levin and Wen, 2005b; see also Turaev and Viro, 1992)

$$H = -J_1 \sum A_i - J_2 \sum_p \sum_{j=0}^{k/2} F_p^{(j)}. \quad (122)$$

Here and below, we specialize to $k=3$. The degrees of freedom on each link are $s=1/2$ spins; $s_z=+\frac{1}{2}$ is interpreted as a $j=1$ colored link, while $s_z=-\frac{1}{2}$ is interpreted as a $j=0$ uncolored link. The vertex terms impose the triangle inequality $|j_1-j_2| \geq j_3 \leq \min(j_1+j_2, \frac{3}{2}-j_1-j_2)$ on the three j 's on links neighboring each vertex. For Fibonacci anyons (see Sec. 4.2), which can only have $j=0,1$, this means that if links with $j=1$ are colored, then the colored links must form a trivalent graph, i.e., no vertex can have only a single up spin adjacent to it. (There is no further requirement, unlike in the general case, in which there are additional labels on the trivalent graph.)

The plaquette terms in the Hamiltonian are complicated in form but their action can be understood in the following way. We imagine adding to a plaquette a loop γ carrying representation j and require that the amplitude for the new configuration $\Psi[\Gamma \cup \gamma]$ be larger than the amplitude for the old configuration by a factor of d_j . For Fibonacci anyons, the only nontrivial representation is $j=1$; we require that the wave function change by a factor of $d=\phi$ when such a loop is added. If the plaquette is empty, then “adding a loop” is simple. We have a new trivalent graph with one extra loop. If the plaquette is not empty, however, then we need to specify

how to add the additional loop to the occupied links. We draw the new loop in the interior of the plaquette so that it runs alongside the links of the plaquette, some of which are occupied. Then we use the F matrix, as depicted in Fig. 12(b), to recouple links of the plaquette (Levin and Wen, 2005b; see also Turaev and Viro, 1992). This transforms the plaquette so that it is now in a superposition of states with different j 's, as depicted in Fig. 12(b); the coefficients in the superposition are sums of products of elements of the F matrix. The plaquette term commutes with the vertex terms since adding a loop to a plaquette cannot violate the triangle inequality [see Fig. 12(a)]. Clearly, vertex terms commute with each other, as do distant plaquette terms. Plaquette terms on adjacent plaquettes also commute because they add loops to the link which they share. (This is related to the pentagon identity, which expresses the associativity of fusion.) Therefore the model is exactly soluble since all terms can be simultaneously diagonalized. Vertices with a single adjacent colored link (i.e., monovalent vertices) are non-Abelian anyonic excitations carrying $j=1$ under the $SU(2)$ gauge group of a_μ^a in Eq. (121). A state at which the plaquette term in Eq. (122) is not satisfied is a non-Abelian anyonic excitation carrying $j=1$ under the $SU(2)$ gauge group of e_μ^a (or, equivalently, a_μ^a flux).

One interesting feature of the ground state wave function $\Psi[\Gamma]$ of Eq. (122), and of related models with loop representations (Freedman *et al.*, 2004; Fendley and Fradkin, 2005; Fidkowski *et al.*, 2006), is their relation to the Boltzmann weights of statistical mechanical models. For instance, the norm squared of the ground state of (122), satisfies $|\Psi[\Gamma]|^2 = e^{-\beta H}$, where βH is the Hamiltonian of the $(q=\phi+2)$ -state Potts model. More precisely, it is the low-temperature expansion of the $(q=\phi+2)$ -state Potts model extrapolated to infinite temperature $\beta=0$. The square of the ground state of the toric code (18) is the low-temperature expansion of the Boltzmann weight of the $(q=2)$ -state Potts model extrapolated to infinite temperature $\beta=0$. On the other hand, the squares of the ground states $|\Psi[\gamma_1 \cup \dots \cup \gamma_n]|^2$ of loop models (Freedman *et al.*, 2004) are equal to the partition functions of $O(n)$ loop gas models of statistical mechanics, with $n=d^2$. These relations allow one to use known results from statistical mechanics to compute equal-time ground state correlation functions in a topological ground state, although the interesting ones are usually of operators which are nonlocal in the original quantum-mechanical degrees of freedom of the model.

It is also worth noting that a quasi-one-dimensional analog has been studied (Bonesteel and Yang, 2007; Feiguin, Trebst, *et al.*, 2007). It is gapless for a single chain and has an interesting phase diagram for ladders.

Finally, we note that the model of Levin and Wen is artificial looking. However, a model in the same universality class might emerge from simpler models (Fidkowski *et al.*, 2006). Since Eq. (122) has a gap, it will be stable against small perturbations. In the case of the toric code, it is known that even fairly large perturbations do not destabilize the state (Trebst *et al.*, 2007).

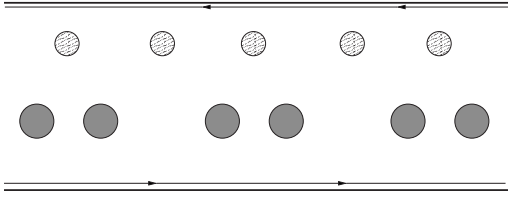


FIG. 13. A system with n quasihole pairs (held at pairs of antidots, depicted as shaded circles) supports n qubits. Additional antidots (hatched) can be used to move quasiparticles.

This brings to a close our survey of the physics of topological phases. In Sec. IV, we consider their application to quantum computing.

IV. QUANTUM COMPUTING WITH ANYONS

A. $\nu=5/2$ qubits and gates

A topological quantum computer is constructed using a system in a non-Abelian topological phase. A computation is performed by creating quasiparticles, braiding them, and measuring their final state. In Sec. II.C.4, we saw how a qubit could be constructed with the $\nu=5/2$ state and a NOT gate applied. In this section, we discuss some ideas about how a quantum computer could be built by extending these ideas.

The basic feature of the Ising TQFT and its close relative $SU(2)_2$, which we exploit for storing quantum information, is the existence of two fusion channels for a pair of σ quasiparticles, $\sigma \times \sigma \sim \mathbf{1} + \psi$. When the fusion outcome is $\mathbf{1}$, we say that the qubit is in the state $|0\rangle$; when it is ψ , the state is $|1\rangle$. When there are $2n$ quasiparticles, there is a 2^{n-1} -dimensional space of states. (This is how many states there are with total topological charge $\mathbf{1}$; there is an equal number with total topological charge ψ .) We use this 2^{n-1} -dimensional space to store quantum information; the most straightforward way to do so is to view it as $n-1$ qubits.

Generalizing the construction of Sec. II.C.4 to many pairs of antidots, we envision (Freedman *et al.*, 2006) an $(n-1)$ -qubit system which is a Hall bar with $2n$ antidots at which quasiholes are pinned, as in Fig. 13.

The NOT gate discussed in Sec. II.C.4 did not require us to move the quasiparticles comprising the qubit, only additional quasiparticles brought in from the edge. However, to implement other gates, we need to move the quasiparticles on the antidots. In this figure, we have also depicted additional antidots which can be used to move quasiparticles from one antidot to another (e.g., as a “bucket brigade”); see, for instance, Simon (2000). If we exchange two quasiparticles from the same qubit, then we apply the phase gate $U = e^{\pi i/8} \text{diag}(R_1^{\sigma\sigma}, R_\psi^{\sigma\sigma})$ [the phase in front of the matrix comes from the $U(1)$ part of the theory]. However, if the two quasiparticles are from different qubits, then we apply the transformation

$$U = \frac{1}{\sqrt{2}} \begin{pmatrix} 1 & 0 & 0 & -i \\ 0 & 1 & -i & 0 \\ 0 & -i & 1 & 0 \\ -i & 0 & 0 & 1 \end{pmatrix} \quad (123)$$

to the two-qubit Hilbert space.

By coupling two qubits in this way, a CNOT gate can be constructed. Suppose that we have four quasiparticles. Then, the first pair can fuse to either $\mathbf{1}$ or ψ , as can the second pair. Naively, this is four states but, in fact, it is really two states with total topological charge $\mathbf{1}$ and two states with total topological charge ψ . These two subspaces cannot mix by braiding the four quasiparticles. However, by braiding our qubits with additional quasiparticles, we can mix these four states. (In our single-qubit NOT gate, we did this using quasiparticles from the edge.) Therefore, following Georgiev (2006), we consider a system with six quasiparticles. Quasiparticles 1 and 2 will be qubit 1; when they fuse to $\mathbf{1}$ or ψ , qubit 1 is in state $|0\rangle$ or $|1\rangle$. Quasiparticles 5 and 6 will be qubit 2; when they fuse to $\mathbf{1}$ or ψ , qubit 2 is in state $|0\rangle$ or $|1\rangle$. Quasiparticles 3 and 4 soak up the extra ψ , if necessary to maintain total topological charge $\mathbf{1}$ for the entire six-quasiparticle system. In the four states $|0, 0\rangle$, $|1, 0\rangle$, $|0, 1\rangle$, and $|1, 1\rangle$, the quasiparticle pairs fuse to $\mathbf{1}, \mathbf{1}, \mathbf{1}$, to $\psi, \psi, \mathbf{1}$, to $\mathbf{1}, \psi, \psi$, and to $\psi, 1, \psi$, respectively.

In this basis, $\rho(\sigma_1)$, $\rho(\sigma_3)$, $\rho(\sigma_5)$ are diagonal, while $\rho(\sigma_2)$ and $\rho(\sigma_4)$ are off diagonal [e.g., $\rho(\sigma_2)$ is Eq. (123) rewritten in the two-qubit–six-quasiparticle basis]. By direct calculation [e.g., by using $\rho(\sigma_i) = e^{(\pi/4)\gamma_i\gamma_{i+1}}$], it can be shown (Georgiev, 2006) that

$$\rho(\sigma_3^{-1} \sigma_4 \sigma_3 \sigma_1 \sigma_5 \sigma_4 \sigma_3^{-1}) = \begin{pmatrix} 1 & 0 & 0 & 0 \\ 0 & 1 & 0 & 0 \\ 0 & 0 & 0 & 1 \\ 0 & 0 & 1 & 0 \end{pmatrix} \quad (124)$$

which is simply a controlled-NOT (CNOT) operation.

One can presumably continue in this way, with one extra pair of quasiparticles, which is used to soak up an extra ψ if necessary. However, this is not a particularly convenient way of proceeding since various gates will be different for different numbers of particles: the CNOT gate above exploited the extra quasiparticle pair which is shared equally between the two qubits acted on by the gate, but this will not work in the same way for more than two qubits. Instead, it would be easier to encode each qubit in four quasiparticles. If each quartet of quasiparticles has total topological charge $\mathbf{1}$, then it can be in either of two states since a given pair within a quartet can fuse to either $\mathbf{1}$ or ψ . In other words, each quasiparticle pair comes with its own spare pair of quasiparticles to soak up its ψ if necessary.

Unfortunately, the $SU(2)_2$ phase of matter is not capable of universal quantum computation, i.e., the transformations generated by braiding operations are not sufficient to implement all possible unitary transformations (Freedman *et al.*, 2002a, 2002b). The reason for this shortcoming is that, in this theory, braiding of two par-

ticles has the effect of a 90° rotation (Nayak and Wilczek, 1996) in the multi-quasiparticle Hilbert space. Composing such 90° rotations will clearly not allow one to construct arbitrary unitary operations (the set of 90° rotations form a finite closed set).

However, we do not need to supplement braiding with much in order to obtain a universal gate set. All that is needed is a single-qubit $\pi/8$ phase gate and a two-qubit measurement. One way to implement these extra gates is to use some nontopological operations (Bravyi, 2006). First, consider the single-qubit phase gate. Suppose quasiparticles 1, 2, 3, 4 comprise the qubit. The states $|0\rangle$ and $|1\rangle$ correspond to 1 and 2 fusing to $\mathbf{1}$ or ψ (3 and 4 must fuse to the same as 1 and 2, since the total topological charge is required to be $\mathbf{1}$). If we bring quasiparticles 1 and 2 close together, then their splitting will become appreciable. We expect it to depend on the separation r as $\Delta E(r) \sim e^{-r\Delta/c}$, where r is the distance between quasiparticles and c is some constant with dimensions of velocity. If we wait a time T_p before pulling the quasiparticles apart again, then we apply the phase gate (Freedman *et al.*, 2006) $U_p = \text{diag}(1, e^{i\Delta E(r)T_p})$. If the time T and distance r are chosen so that $\Delta E(r)T_p = \pi/4$, then, up to an overall phase, we apply the phase gate

$$U_{\pi/8} = \begin{pmatrix} e^{-\pi i/8} & 0 \\ 0 & e^{\pi i/8} \end{pmatrix}. \quad (125)$$

We note that, in principle, by measuring the energy when the two quasiparticles are brought together, the state of the qubit can be measured.

The other gate that we need for universal quantum computation is the nondestructive measurement of the total topological charge of any four quasiparticles. This can be done with an interference measurement. Suppose we have two qubits which are associated with quasiparticles 1, 2, 3, 4 and quasiparticles 5, 6, 7, 8, and we measure the total topological charge of 3, 4, 5, 6. The interference measurement is of the type described in Sec. II.C.3: edge currents tunnel across the bulk at two points on either side of the set of four quasiparticles. Depending on whether the four quasiparticles have total topological charge $\mathbf{1}$ or ψ , the two possible trajectories interfere with a phase ± 1 . We can thereby measure the total parity of two qubits. (For more details, see Freedman *et al.*, 2006.)

Neither of these gates can be applied exactly, which means surrendering some of the protection we have worked so hard to obtain and we need some software error correction. However, it is not necessary for the $\pi/8$ phase gate or the two-qubit measurement to be extremely accurate in order for error correction to work. The former needs to be accurate to within 14% and the latter to within 38% (Bravyi, 2006). Thus the requisite quantum error correction protocols are not particularly stringent.

An alternate solution, at least in principle, involves changing the topology of the manifold on which the quasiparticles live (Bravyi and Kitaev, 2001). This can be realized in a device by performing interference measure-

ments in the presence of moving quasiparticles (Freedman *et al.*, 2006).

However, a more elegant approach is to work with a non-Abelian topological state which supports universal topological quantum computation through quasiparticle braiding alone. In the next section, we give an example of such a state and how quantum computation can be performed with it. In Sec. IV.C, we sketch the proof that a large class of such states is universal.

B. Fibonacci anyons: A simple example that is universal for quantum computation

One of the simplest models of non-Abelian statistics is known as the Fibonacci anyon model, or golden theory (Freedman *et al.*, 2002a; Preskill, 2004; Bonesteel *et al.*, 2005; Hormozi *et al.*, 2007). In this model, there are only two fields: the identity ($\mathbf{1}$) as well as a single nontrivial field usually called τ which represents the non-Abelian quasiparticle. (Note that there is no field representing the underlying electron in this simplified theory.) There is a single nontrivial fusion rule in this model,

$$\tau \times \tau = \mathbf{1} + \tau, \quad (126)$$

which results in the Bratteli diagram given in Fig. 9(b). This model is particularly simple in that any cluster of quasiparticles can fuse to only $\mathbf{1}$ or τ .

The $j=0$ and 1 quasiparticles in $SU(2)_3$ satisfy the fusion rules of Fibonacci anyons. Therefore if we omit the $j=1/2$ and $3/2$ quasiparticles from $SU(2)_3$, we have Fibonacci anyons. This is perfectly consistent since half-integral j will never arise from the fusions of integral j 's; the model with only integer spins can be called $SO(3)_3$ or, sometimes the even part of $SU(2)_3$. As a result of the connection to $SU(2)_3$, sometimes $\mathbf{1}$ is called q -spin 0 and τ is called q -spin 1 (see Hormozi *et al.*, 2007). \mathbb{Z}_3 parafermions are equivalent to a coset theory $SU(2)_3/U(1)$. This can be realized with an $SU(2)_3$ WZW model in which the $U(1)$ subgroup is coupled to a gauge field (Gawędzki and Kupiainen, 1988; Karabali *et al.*, 1989). Consequently, \mathbb{Z}_3 parafermions have the same fusion rules as $SU(2)_3$; there are some phase differences between the two theories which show up in the R and F matrices. In the \mathbb{Z}_3 parafermion theory, the field ϵ that results from fusing σ_1 with ψ_1 satisfies the Fibonacci fusion rule Eq. (126), i.e., $\epsilon \times \epsilon = \mathbf{1} + \epsilon$.

As with the \mathbb{Z}_3 parafermion model described above, the dimension of the Hilbert space with n quasiparticles [i.e., the number of paths through the Bratteli diagram Fig. 9(b), terminating at $\mathbf{1}$] is given by the Fibonacci number $\text{Fib}(n-1)$; hence the name Fibonacci anyons. And similarly the number terminating at τ is $\text{Fib}(n)$. Therefore the quantum dimension of the τ particle is the golden mean $d_\tau = \phi \equiv (1 + \sqrt{5})/2$ (from which the theory receives the name “golden theory”). The Fibonacci model is the simplest known non-Abelian model that is capable of universal quantum computation (Freedman *et al.*, 2002a). [In the next section, the proof will be described for $SU(2)_3$, but the Fibonacci theory, which is its

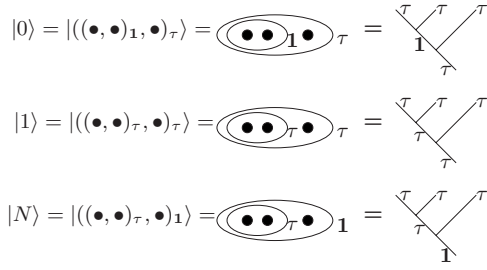


FIG. 14. The three possible states of three Fibonacci particles, shown in several common notations. The “quantum number” of an individual particle is τ . In the parentheses and ellipse notation (middle), each particle is shown as a black dot, and each pair of parentheses or ellipse around a group of particles is labeled at the lower right with the total quantum number associated with the fusion of that group. Analogously, in the fusion tree notation (right) we group particles as described by the branching of the tree, and each line is labeled with the quantum number corresponding to the fusion of all particles in the branches above it. For example, on the top line the two particles on the left fuse to form $\mathbf{1}$ which then fuses with the remaining particle on the right to form τ . As discussed in Sec. IV.B.3, three Fibonacci particles can be used to represent a qubit. The three possible states are labeled (far left) as the logical $|0\rangle$, $|1\rangle$, and $|N\rangle$ (noncomputational) of the qubit.

even part, is also universal.] It is thus useful to study this model in detail. Many principles described here will generalize to other non-Abelian models. We note that a detailed discussion of computing with the Fibonacci model has also been given by [Hormozi *et al.* \(2007\)](#).

1. Structure of the Hilbert space

An important feature of non-Abelian systems is the detailed structure of the Hilbert space. A given state in the space will be described by a “fusion path,” or “fusion tree” (see the Appendix). For example, using the fusion rule (126) or examining the Bratteli diagram we see that when two τ particles are present, they may fuse into two possible orthogonal degenerate states—one in which they fuse to form $\mathbf{1}$ and one in which they fuse to form τ . A convenient notation ([Bonesteel *et al.*, 2005](#)) for these two states is $|(\cdot, \cdot)_{\mathbf{1}}\rangle$ and $|(\cdot, \cdot)_{\tau}\rangle$. Here each \cdot represents a particle. From the fusion rule, when a third is added to two particles already in the $\mathbf{1}$ state [i.e., in $|(\cdot, \cdot)_{\mathbf{1}}\rangle$] it must fuse to form τ . We denote the resulting state as $|((\cdot, \cdot)_{\mathbf{1}}, \cdot)_{\tau}\rangle \equiv |0\rangle$. But if the third is added to two in the τ state, it may fuse to form either τ or $\mathbf{1}$, giving the two states $|((\cdot, \cdot)_{\tau}, \cdot)_{\tau}\rangle \equiv |1\rangle$ and $|((\cdot, \cdot)_{\tau}, \cdot)_{\mathbf{1}}\rangle \equiv |N\rangle$, respectively. (The notations $|0\rangle$, $|1\rangle$, and $|N\rangle$ will be discussed further below.) Thus we have a three-dimensional Hilbert space for three particles, shown using several notations in Fig. 14.

In the previous example, and in Fig. 14, we have chosen to fuse particles together starting at the left and going to the right. It is, of course, also possible to fuse particles in the opposite order, fusing the two particles on the right first, and then fusing with the particle furthest on the left last. We can correspondingly denote the

three resulting states as $|(\cdot, (\cdot, \cdot)_{\mathbf{1}})_{\tau}\rangle$, $|(\cdot, (\cdot, \cdot)_{\tau})_{\tau}\rangle$, and $|(\cdot, (\cdot, \cdot)_{\mathbf{1}})_{\mathbf{1}}\rangle$. The space of states that is spanned by fusion of non-Abelian particles is independent of the fusion order. However, different fusion orders result in a different basis set for that space. This change of basis is precisely that given by the F matrix. For Fibonacci anyons it is easy to see that

$$|(\cdot, (\cdot, \cdot)_{\tau})_{\mathbf{1}}\rangle = |((\cdot, \cdot)_{\tau}, \cdot)_{\mathbf{1}}\rangle, \quad (127)$$

since in either fusion order there is only a single state that has total topological charge $\mathbf{1}$ (the overall quantum number of a group of particles is independent of the basis). However, the other two states of the three-particle space transform nontrivially under change of fusion order. As described in the Appendix, we can write a change of basis using the F matrix as

$$|(\cdot, (\cdot, \cdot)_{i})_{k}\rangle = \sum_j [F_k^{\tau\tau\tau}]_{ij} |((\cdot, \cdot)_j, \cdot)_k\rangle, \quad (128)$$

where i, j, k take the values of the fields $\mathbf{1}$ or τ . (This is just a rewriting of a special case of Fig. 23.) Clearly from Eq. (127), $F_{\mathbf{1}}^{\tau\tau\tau}$ is trivially unity. However, the 2×2 matrix $F_{\tau}^{\tau\tau\tau}$ is nontrivial,

$$[F_{\tau}^{\tau\tau\tau}] = \begin{pmatrix} F_{\mathbf{1}\mathbf{1}} & F_{\mathbf{1}\tau} \\ F_{\tau\mathbf{1}} & F_{\tau\tau} \end{pmatrix} = \begin{pmatrix} \phi^{-1} & \sqrt{\phi^{-1}} \\ \sqrt{\phi^{-1}} & -\phi^{-1} \end{pmatrix}. \quad (129)$$

Using this F matrix, one can translate between bases that describe arbitrary fusion orders of many particles.

For the Fibonacci theory ([Preskill, 2004](#)), it turns out to be easy to calculate the F matrix using a consistency condition known as the pentagon equation ([Moore and Seiberg, 1988, 1989](#); [Fuchs, 1992](#); [Gómez *et al.*, 1996](#)). This condition says that one should be able to make changes of basis for four particles in several ways and get the same result in the end. As an example, consider

$$|(\cdot, (\cdot, (\cdot, \cdot)_{\tau})_{\mathbf{1}})_{\tau}\rangle_{\mathbf{1}} = |((\cdot, \cdot)_{\mathbf{1}}, (\cdot, \cdot)_{\mathbf{1}})_{\tau}\rangle_{\mathbf{1}} \\ = |(((\cdot, \cdot)_{\mathbf{1}}, \cdot)_{\tau}, \cdot)_{\mathbf{1}}\rangle_{\mathbf{1}}, \quad (130)$$

where both equalities, as in Eq. (127), can be deduced from the fusion rules alone. For example, in the first equality, given (on the left-hand side) that the overall quantum number is $\mathbf{1}$ and the rightmost two particles are in a state $\mathbf{1}$, then (on the right-hand side) when we fuse the leftmost two particles they must fuse to $\mathbf{1}$ such that the overall quantum number remains $\mathbf{1}$. On the other hand, we can also use the F matrix [Eq. (128)] to write

$$|(\cdot, (\cdot, (\cdot, \cdot)_{\tau})_{\tau})_{\mathbf{1}}\rangle_{\tau} \\ = F_{\mathbf{1}\mathbf{1}} |(\cdot, ((\cdot, \cdot)_{\mathbf{1}}, \cdot)_{\tau})_{\mathbf{1}}\rangle_{\tau} + F_{\mathbf{1}\tau} |(\cdot, ((\cdot, \cdot)_{\tau}, \cdot)_{\tau})_{\mathbf{1}}\rangle_{\tau} \\ = F_{\mathbf{1}\mathbf{1}} |((\cdot, (\cdot, \cdot)_{\mathbf{1}})_{\tau}, \cdot)_{\mathbf{1}}\rangle_{\tau} + F_{\mathbf{1}\tau} |((\cdot, (\cdot, \cdot)_{\tau})_{\tau}, \cdot)_{\mathbf{1}}\rangle_{\tau} \\ = \sum_j (F_{\mathbf{1}\mathbf{1}} F_{\mathbf{1}j} + F_{\mathbf{1}\tau} F_{\tau j}) |(((\cdot, \cdot)_j, \cdot)_{\tau}, \cdot)_{\mathbf{1}}\rangle_{\tau}. \quad (131)$$

Comparison to Eq. (130) yields $F_{\mathbf{1}\tau}(F_{\mathbf{1}\mathbf{1}} + F_{\tau\tau}) = 0$ and $F_{\mathbf{1}\mathbf{1}}F_{\mathbf{1}\mathbf{1}} + F_{\mathbf{1}\tau}F_{\tau\mathbf{1}} = 1$. This, and other similar consistency identities, along with the requirement that F be unitary completely fix the Fibonacci F matrix to be precisely

that given in Eq. (129) (up to a gauge freedom in the definition of the phase of the basis states).

2. Braiding Fibonacci anyons

As discussed in the Introduction, for non-Abelian systems, adiabatically braiding particles around each other results in a unitary operation on the degenerate Hilbert space. Here we determine which unitary operation results from which braid. We start by considering what happens to two Fibonacci particles when they are braided around each other. It is known (Fuchs, 1992) that the topological spin Θ_τ of a Fibonacci field τ is $\Theta_\tau \equiv e^{2\pi i \Delta_\tau} = e^{4\pi i/5}$. (Note that Δ_τ is also the dimension of the ϵ field of the Z_3 theory; see the Appendix.) With this information, we use the OPE (see the Appendix) as in Sec. III.D above to determine the phase accumulated when two particles wrap around each other. If the two τ fields fuse together to form $\mathbf{1}$, then taking the two fields around each other clockwise results in a phase $-8\pi/5 = 2\pi(-2\Delta_\tau)$ whereas, if the two fields fuse to form τ , taking the two fields around each other results in a phase $-4\pi/5 = 2\pi(-\Delta_\tau)$. Note that a Fibonacci theory with the opposite chirality can exist too (an “antiholomorphic theory”), in which case one accumulates the opposite phase. A particularly interesting nonchiral (or “achiral”) theory also exists, which is equivalent to a combination of two chiral Fibonacci theories with opposite chiralities. In Sec. III.G, we discussed lattice spin models (Levin and Wen, 2005b) which give rise to a nonchiral (or achiral) theory that is equivalent to a combination of two chiral Fibonacci theories with opposite chiralities. We will not discuss these theories further here.

Once we have determined the phase accumulated for a full wrapping of two particles, we then know that clockwise exchange of two particles (half of a full wrapping) gives a phase of $\pm 4\pi/5$ if the fields fuse to $\mathbf{1}$ or $\pm 2\pi/5$ if the fields fuse to τ . Once again we resort to consistency conditions to determine these signs. In this case, we invoke the so-called hexagon identities (Moore and Seiberg, 1988, 1989; Fuchs, 1992) which in essence assure that the rotation operations are consistent with the F matrix, i.e., that we can rotate before or after changing bases and get the same result. (Indeed, one way of proving that $\Delta_\tau=2/5$ is by using this consistency condition.) We thus determine that the R matrix is given by

$$\hat{R}|(\cdot, \cdot)_\mathbf{1}\rangle = e^{-4\pi i/5}|(\cdot, \cdot)_\mathbf{1}\rangle, \tag{132}$$

$$\hat{R}|(\cdot, \cdot)_\tau\rangle = -e^{-2\pi i/5}|(\cdot, \cdot)_\tau\rangle, \tag{133}$$

i.e., $R^1_{\tau\tau} = e^{-4\pi i/5}$ and $R^\tau_{\tau\tau} = -e^{-2\pi i/5}$. Using the R matrix, as well as the basis-changing F matrix, we determine the unitary operation that results from performing any braid on any number of particles. As an example, consider three particles. The braid group is generated by σ_1 and σ_2 (see Fig. 15). As discussed above, the Hilbert space of three particles is three dimensional as shown in Fig. 14.

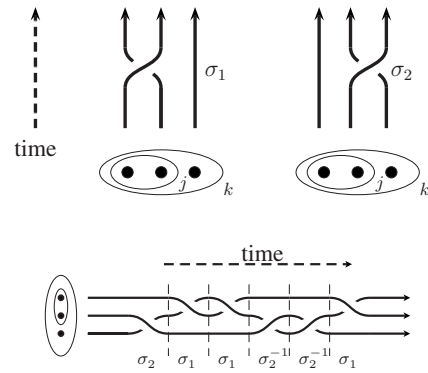


FIG. 15. Three-particle braids. Top: The two elementary braid operations σ_1 and σ_2 on three particles. Bottom: Using these two braid operations and their inverses, an arbitrary braid on three strands can be built. The braid shown is $\sigma_2\sigma_1\sigma_1\sigma_2^{-1}\sigma_2^{-1}\sigma_1$.

We use Eqs. (132) and (133) to determine that the unitary operation corresponding to the braid σ_1 is given by

$$\begin{pmatrix} |0\rangle \\ |1\rangle \\ |N\rangle \end{pmatrix} \rightarrow \underbrace{\begin{pmatrix} e^{-4\pi i/5} & 0 & 0 \\ 0 & -e^{-2\pi i/5} & 0 \\ 0 & 0 & -e^{-2\pi i/5} \end{pmatrix}}_{\rho(\sigma_1)} \begin{pmatrix} |0\rangle \\ |1\rangle \\ |N\rangle \end{pmatrix} \tag{134}$$

where we have used the shorthand notation (see Fig. 14) for the three-particle states. Evaluating the effect of σ_2 is less trivial. Here we first make a basis change (using F) in order to determine how the two right-most particles fuse. Then we make the rotation using \hat{R} and finally undo the basis change. Symbolically, we write $\rho(\sigma_2) = F^{-1} \hat{R} F$, where \hat{R} rotates the two right-most particles. To be more explicit, consider what happens to the state $|0\rangle$. First, we use Eq. (128) to write $|0\rangle = F_{\mathbf{11}}|(\cdot, (\cdot, \cdot))_\mathbf{1}\rangle_\tau + F_{\tau\mathbf{1}}|(\cdot, (\cdot, \cdot))_\tau\rangle$. Rotating the two right particles then gives $e^{-4\pi i/5} F_{\mathbf{11}}|(\cdot, (\cdot, \cdot))_\tau\rangle - e^{-2\pi i/5} F_{\tau\mathbf{1}}|(\cdot, (\cdot, \cdot))_\tau\rangle$, and then we transform back to the original basis using the inverse of Eq. (128) to yield $\rho(\sigma_2)|0\rangle = ([F^{-1}]_{\mathbf{11}} e^{-4\pi i/5} F_{\mathbf{11}} - [F^{-1}]_{\mathbf{1}\tau} e^{-2\pi i/5} F_{\tau\mathbf{1}})|0\rangle + ([F^{-1}]_{\tau\mathbf{1}} \times e^{-4\pi i/5} F_{\mathbf{11}} - [F^{-1}]_{\tau\tau} e^{-2\pi i/5} F_{\tau\mathbf{1}})|1\rangle = -e^{-\pi i/5}|\phi\rangle - ie^{-i\pi/10}/\sqrt{\phi}|1\rangle$. Similar results can be derived for the other two basis states to give

$$\rho(\sigma_2) = \begin{pmatrix} -e^{-\pi i/5}/\phi & -ie^{-i\pi/10}/\sqrt{\phi} & 0 \\ -ie^{-i\pi/10}/\sqrt{\phi} & -1/\phi & 0 \\ 0 & 0 & -e^{-2\pi i/5} \end{pmatrix}. \tag{135}$$

Since the braid operations σ_1 and σ_2 (and their inverses) generate all possible braids on three strands (see Fig. 15), we can use Eqs. (134) and (135) to determine the unitary operation resulting from any braid on three strands, with the unitary operations built from the elementary matrices $\rho(\sigma_1)$ and $\rho(\sigma_2)$ in the same way that the complicated braids are built from the braid generators σ_1 and σ_2 . For example, the braid $\sigma_2\sigma_1\sigma_1\sigma_2^{-1}\sigma_2^{-1}\sigma_1$ shown in Fig. 15 corresponds to the unitary matrix

$\rho(\sigma_1)\rho(\sigma_2^{-1})\rho(\sigma_2^{-1})\rho(\sigma_1)\rho(\sigma_1)\rho(\sigma_2)$ (note that the order is reversed since the operations that occur at earlier times are written to the left in conventional braid notation, but on the right when multiplying matrices together).

3. Computing with Fibonacci anyons

Now that we know many properties of Fibonacci anyons, we show how to compute with them. First, we need to construct our qubits. An obvious choice might be to use two particles for a qubit and declare the two states $|(\cdot, \cdot)_1\rangle$ and $|(\cdot, \cdot)_\tau\rangle$ to be the two orthogonal states of the qubit. While this is a reasonably natural looking qubit, it turns out not to be convenient for computations. The reason for this is that we want to do single-qubit operations (simple rotations) by braiding. However, it is not possible to change the overall quantum number of a group of particles by braiding within that group. Thus, by braiding the two particles around each other, we can never change $|(\cdot, \cdot)_1\rangle$ to $|(\cdot, \cdot)_\tau\rangle$. To remedy this problem, it is convenient to use three quasiparticles to represent a qubit as suggested by [Freedman *et al.* \(2002a\)](#) [many other schemes for encoding qubits are also possible ([Freedman *et al.*, 2002a](#); [Hormozi *et al.*, 2007](#))]. Thus we represent the two states of the qubit as the $|0\rangle$ and $|1\rangle$ states shown in Fig. 14. The additional state $|N\rangle$ is a “noncomputational” state. In other words, we arrange that at the beginning and end of our computations there is no amplitude in this state. Any amplitude that ends up in this state is known as “leakage error.” We note, however, that the braiding matrices $\rho(\sigma_1)$ and $\rho(\sigma_2)$ are block diagonal and therefore never mix the noncomputational state $|N\rangle$ with the computational space $|0\rangle$ and $|1\rangle$ (this is just another way to say that the overall quantum number of the three particles must remain unchanged under any amount of braiding). Therefore braiding the three particles gives us a way to do single-qubit operations with no leakage.

In Sec. IV.C, we describe a proof that the set of braids has a “dense image” in the set of unitary operations for the Fibonacci theory. This means that there exists a braid that corresponds to a unitary operation arbitrarily close to any desired operation. The closer one wants to approximate the desired unitary operation, the longer the braid typically needs to be, although only logarithmically so (i.e., the necessary braid length grows only as the logarithm of the allowed error distance to the target operation). The problem of finding braids that correspond to desired unitary operations, while apparently complicated, turns out to be straightforward ([Bonesteel *et al.*, 2005](#); [Hormozi *et al.*, 2007](#)). One simple approach is to implement a brute force search on a (classical) computer to examine all possible braids (on three strands) up to some certain length, looking for a braid that happens to generate a unitary operation close to some desired result. While this approach works well for searching short braids ([Bonesteel *et al.*, 2005](#); [Hormozi *et al.*, 2007](#)), the job of searching all braids grows exponentially in the length of the braid, making this scheme unfeasible if one requires high-accuracy long braids. Fortunately,

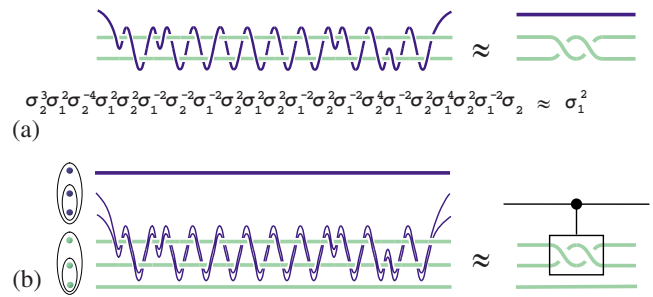


FIG. 16. (Color online) Construction of a two-qubit gate from a certain three-particle braid. Time flows from left to right in this picture. In the top we construct a braid on three strands by moving only the blue (dark) particle, which has the same effect as interchanging the two green (light) strands. Using this same braid (bottom) then constructs a controlled rotation gate. If the state of the upper (control) qubit is $|0\rangle$, i.e., the control pair is in state $\mathbf{1}$, then the braid has no effect on the Hilbert space (up to a phase). If the upper (control) qubit is in the state $|1\rangle$ then the braid has the same effect as winding two of the particles in the lower qubit. Figure from [Bonesteel *et al.*, 2005](#).

there is an iterative algorithm by Solovay and Kitaev (see [Nielsen and Chuang, 2000](#)) which allows one to put together many short braids to efficiently construct a long braid arbitrarily close to any desired target unitary operation. While this algorithm does not generally find the shortest braid for performing some operation (within some allowed error), it does find a braid that is only polylogarithmically long in the allowed error distance to the desired operation. Furthermore, the (classical) algorithm for finding such a braid is only algebraically hard in the length of the braid.

Having solved the single-qubit problem, now imagine we have multiple qubits, each encoded with three particles. To perform universal quantum computation, in addition to being able to perform single-qubit operations, we must also be able to perform two-qubit entangling gates ([Nielsen and Chuang, 2000](#); [Bremner *et al.*, 2002](#)). Such two-qubit gates will necessarily involve braiding together (physically “entangling”) the particles from two different qubits. The result of [Freedman *et al.* \(2002a\)](#) generally guarantees that braids exist corresponding to any desired unitary operation on a two-qubit Hilbert space. However, finding such braids is now a much more formidable task. The full Hilbert space for six Fibonacci particles (constituting two qubits) is now 13 dimensional, and searching for a desired result in such a high-dimensional space is hard even for a powerful classical computer. Therefore the problem needs to be tackled by divide-and-conquer approaches, building up two-qubit gates out of simple braids on three particles ([Bonesteel *et al.*, 2005](#); [Hormozi *et al.*, 2007](#)). A simple example of such a construction is sketched in Fig. 16. First, in Fig. 16(a), we consider braids on three strands that move [“weave” ([Simon *et al.*, 2006](#))] only a single particle, the blue or dark particle in the figure, through two stationary particles, the green or light particles in the figure. We search for such a braid whose

action on the Hilbert space is equivalent to exchanging the two stationary (green or light) particles twice. Since this is now just a three-particle problem, finding such a braid, to arbitrary accuracy, is computationally tractable. Next, for the two-qubit problem, we label one qubit the control [blue in Fig. 16(b)] and another qubit the target. We take a pair of particles from the control qubit (the control pair) and weave them as a group through two of the particles in the target, using the same braid we found for the three-particle problem. Now, if the quantum number of the control pair is $\mathbf{1}$ (i.e., control qubit is in state $|0\rangle$), then any amount of braiding of this pair will necessarily give just an Abelian phase (since moving $\mathbf{1}$ around is like moving nothing around). However, if the quantum number of the control pair is τ (i.e., the control qubit is in state $|1\rangle$), then we can think of this pair as equivalent to a single τ particle, and we will cause the same nontrivial rotation as in Fig. 16(a) above (crucially, this is designed to not allow any leakage error). Thus we have constructed a “controlled-rotation” gate, where the state of the target qubit is changed only if the control qubit is in state $|1\rangle$, where the rotation that occurs is equivalent to exchanging two particles of the target qubit as shown in Fig. 16(b). The resulting two-qubit controlled gate, along with single-qubit rotations, makes a universal set for quantum computation (Bremner *et al.*, 2002). More conventional two-qubit gates, such as the controlled-NOT (CNOT) gates, have also been designed using braids (Bonesteel *et al.*, 2005; Hormozi *et al.*, 2007).

4. Other theories

The Fibonacci theory is a particularly interesting theory to study, not only because of its simplicity, but also because of its close relationship (see the discussion at the beginning of Sec. IV.B) with the \mathbb{Z}_3 parafermion theory—a theory thought to describe (Rezayi and Read, 2006) the observed quantum Hall state at $\nu=12/5$ (Xia *et al.*, 2004). It is not hard to show that a given braid will perform the same quantum computation in either theory (Hormozi *et al.*, 2007), up to an irrelevant overall Abelian phase. Therefore the Fibonacci theory and the associated braiding may be physically relevant for fractional quantum Hall topological quantum computation in high-mobility 2D semiconductor structures.

However, there are many other non-Abelian theories which are not related to Fibonacci anyons. Nonetheless, for arbitrary non-Abelian theories, many themes discussed in this section continue to apply. In all cases, the Hilbert space can be understood via fusion rules and an F matrix; rotations of two particles can be understood as a rotation \hat{R} operator that produces a phase dependent on the quantum number of the two particles; and one can always encode qubits in the quantum number of some particles. If we want to do single-qubit operations by braiding particles within a qubit (in a theory that allows universal quantum computation), we always need to encode a qubit with at least three particles (sometimes more). To perform two-qubit operations, we always need to braid particles constituting one qubit with

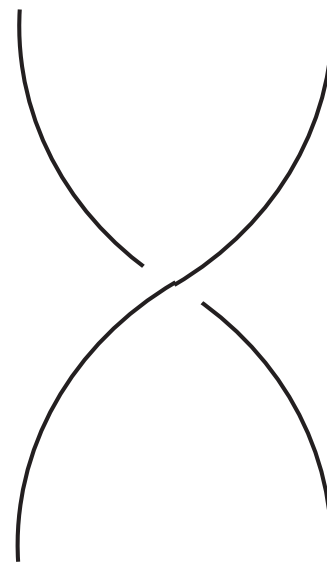


FIG. 17. The entire gate set needed in a state supporting universal quantum computation.

the particles constituting another qubit. It is always the case that any unitary operation that can be achieved by braiding n particles around each other with an arbitrary braid can also be achieved by weaving a single particle around $n-1$ others that remain stationary (Simon *et al.*, 2006) [note that we implicitly used this fact in constructing Fig. 15(a)]. So long as the state is among the ones known to have braid group representations with dense images in the unitary group, as described in Sec. IV.C, it will be able to support universal quantum computation. Finally, we note that it seems to always be true that the practical construction of complicated braids for multi-qubit operations needs to be subdivided into more manageable smaller problems for the problem to be tractable.

C. Universal topological quantum computation

As we saw in Sec. IV.A, even if the $\nu=5/2$ state is non-Abelian, it is not non-Abelian enough to function as a universal quantum computer by simply braiding anyons. However, in Sec. IV.B, we described Fibonacci anyons which we claimed were capable of supporting universal topological quantum computation. In this section, we sketch a proof of this claim within the context of the more general question: which topological states are universal for quantum computation or, in starker terms, for which topological states is the entire gate set required to simulate an arbitrary quantum circuit to arbitrary accuracy simply that depicted in Fig. 17 (see also Kauffman and Lomonaco, 2004, 2007). The discussion of this section is more mathematical than the rest of the paper and can be skipped on the first reading.

In other words, the general braid is composed of copies of a single operation (depicted in Fig. 17) and its inverse. (Actually, as we see “positive braids” will prove to be sufficient, so there is no necessity to ever use the

inverse operation.) Fibonacci anyons, discussed in Sec. IV.B, are an example that have this property. In this section, we see why.

For the sake of concreteness, assume that we use a single species of quasiparticle, called σ . When there are n σ 's at fixed positions z_1, \dots, z_n , there is an exponentially large [$\sim (d_\sigma)^n$ -dimensional] ground state subspace of Hilbert space. We call this vector space V_n . Braiding σ 's produces a representation ρ_n characteristic of the topological phase in question, $\rho_n: \mathcal{B}_n \rightarrow U(V_n)$ from the braid group on n strands into the unitary transformations of V_n . We do not care about the overall phase of the wave function, since only the projective reduction in $PU(V_n)$ has physical significance. [$PU(V_n)$ is the set of unitary transformations on V_n with two transformations identified if they differ only by a phase.] We want to enact an arbitrary unitary transformation, so $\rho(\mathcal{B}_n)$ should be dense in $PU(V_n)$, i.e., dense up to a phase. By "dense" in $PU(V_n)$, we mean that the intersection of all closed sets containing $\rho(\mathcal{B}_n)$ should be $PU(V_n)$. Equivalently, it means that an arbitrary unitary transformation can be approximated, up to a phase, by a transformation in $\rho(\mathcal{B}_n)$ to within any desired accuracy. This is the condition that our topological phase must satisfy.

For a modestly large number (≥ 7) of σ 's, it was shown (Freedman *et al.*, 2002a, 2002b) that the braid group representations associated with $SU(2)$ Chern-Simons theory at level $k \neq 1, 2, 4$ are dense in $SU(V_{n,k})$ [and hence in $PU(V_{n,k})$]. With only a small number of low-level and small-anyon-number exceptions, density was shown for almost all $SU(N)_k$.

These Jones-Witten (JW) representations satisfy a key "two-eigenvalue property" (TEVP), discussed below, derived in this $SU(N)$ setting from the Hecke relations, and corresponding to the HOMFLY polynomial [see, for instance, Kauffman (2001), and references therein]. The analysis was extended with similar conclusions by Larsen *et al.* (2005) to the case where the Lie group G is of type B , C , or D and braid generators have three eigenvalues, corresponding to the Birman-Murakami-Wenzl algebra and the two-variable Kauffman polynomial. For JW representations of the exceptional group at level k , the number of eigenvalues of braid generators can be composite integers (such as 4 for G_2) and this has so far blocked attempts to prove density for these JW representations.

In order to perform quantum computation with anyons, there are many details needed to align the topological picture with the usual quantum-circuit model from computer science. First, qubits must be located in the state space V_n . Since V_n has no natural tensor factoring (it can have prime dimension) this alignment (Freedman *et al.*, 2002a) is necessarily somewhat inefficient;⁹ some directions in V_n are discarded from the

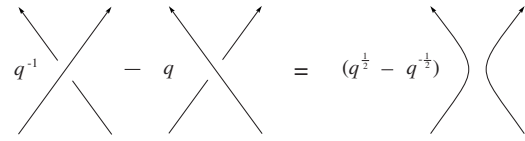


FIG. 18. Jones skein relation [see Eq. (73)].

computational space and so we must always guard against unintended leakage into the discarded directions. A possible research project is how to adapt computation to the Fibonacci space (see Sec. IV.B) rather than attempting to find binary structure within V_n . A somewhat forced binary structure was explained in Sec. IV.B in connection with encoding qubits into $SU(2)_3$, as done for level 2 in Sec. IV.A. (A puzzle for readers. Suppose we write integers out as Fibonacci numerals: 0 cannot follow 0, but 0 or 1 can follow 1. How do you do addition and multiplication?) However, we will not dwell on these issues but instead go directly to the essential mathematical point: How, in practice, does one tell which braid group representations are dense and which are not, i.e., which ones are sufficient for universal topological quantum computation and which ones need to be augmented by additional nontopological gate operations?

We begin by noting that the fundamental skein relation of Jones' theory is as in Fig. 18. [see Eq. (73) and the associated relation for the Kauffman bracket (77)]. This is a quadratic relation in each braid generator σ_i and by inspection any representation of σ_i will have only two distinct eigenvalues $q^{3/2}$ and $-q^{1/2}$. It turns out to be rare to have a representation of a compact Lie group H , where H is densely generated by elements σ_i with this eigenvalue restriction. This facilitates the identification of the compact closure $H = \overline{\text{image}(\rho)}$ among the various compact subgroups of $U(V_n)$.

Definition IV.1. Let G be a compact Lie group and V a faithful, irreducible, unitary representation. The pair (G, V) has the two eigenvalue property (TEVP) if there exists a conjugacy class $[g]$ of G such that (1) $[g]$ generates a dense set in G , and (2) for any $g \in [g]$ g acts on V with exactly two distinct eigenvalues whose ratio is not -1 .

Let H be the closed image of some Jones representation $\rho: \mathcal{B}_n \rightarrow U(V_n)$. We would like to use Fig. 18 to assert that the fundamental representation of $U(V_n)$ restricted to H , call it θ , has the TEVP. All braid generators σ_i are conjugate and, in nontrivial cases, the eigenvalue ratio is $-q \neq -1$. However, we do not yet know if the restriction is irreducible. This problem has been solved by a series of technical lemmas by Freedman *et al.* (2002a). Using the TEVP, it is shown first that the further restriction to the identity component H_0 is isotopic and then irreducible. This implies that H_0 is reductive, so its derived group $[H_0, H_0]$ is semisimple and, it is argued, still satisfies the TEVP. A final (and harmless) variation on H is to pass to the universal cover $H' := \widehat{[H_0, H_0]}$. The pulled back representation θ' still has the TEVP and we are

⁹Actually, current schemes use approximately half the theoretical number of qubits. One finds $\alpha \log_2(\dim V_n)$ computational qubits in V_n , for $\alpha = (\log_2 \tau^3)^{-1} \approx 0.48$, $\phi = (1 + \sqrt{5})/2$.

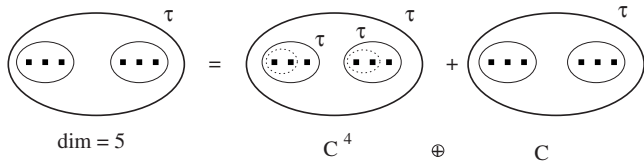


FIG. 19. The charge on the dotted circle can be 1 or τ , providing the qubit.

finally in a situation, namely, irreducible representations of semisimple Lie groups of bounded dimension, where we can hope to apply the classification of such representations (McKay and Patera, 1981) to show that our mysterious H' is none other than $SU(V_n)$. If this is so, then it will follow that the preceding transformations $H \rightarrow H_0 \rightarrow [H_0, H_0] \rightarrow \widehat{[H_0, H_0]}$ did nothing (beyond the first arrow, which may have eliminated some components of H on which the determinant is a nontrivial root of unity).

In general, getting the answer (to the question of which Jones representations are projectively dense) out of the classification requires some tricky combinatorics and rank-level (Freedman *et al.*, 2002b) duality. Here we are content with solving the easiest nontrivial case. Consider six Fibonacci anyons τ with total charge=1. The associated $V_6 \cong C^5 \cong 2$ qubits \oplus noncomputational C are shown in Fig. 19.

In coordinates, ρ takes the braid generators (projectively) to these operators:

$$\sigma_1 \mapsto \begin{bmatrix} -1 & & & & \\ & q & & & \\ & & -1 & & \\ & & & q & \\ & & & & q \end{bmatrix}, \quad q = e^{-2\pi i/5},$$

$$\sigma_2 \mapsto \begin{bmatrix} \frac{q^2}{q+1} & -\frac{q\sqrt{[3]}}{q+1} & & & \\ -\frac{q\sqrt{[3]}}{q+1} & -\frac{1}{q+1} & & & \\ & & \frac{q^2}{q+1} & -\frac{q\sqrt{[3]}}{q+1} & \\ & & -\frac{q\sqrt{[3]}}{q+1} & -\frac{1}{q+1} & \\ & & & & q \end{bmatrix},$$

where $[3]=q+q^{-1}+1$ and σ_i , for $i=3,4,5$, are similar. See Funar (1999) for details.

The closed image of ρ is $H \subset U(5)$, so our irreducible representation θ' of H' , coming from $U(5)$'s fundamental, is exactly five dimensional (we do not yet know the dimension of H'). From McKay and Patera (1981), there are four five-dimensional irreducible representations, which we list by rank: (1) rank=1: ($SU(2), 4\pi_1$); (2) rank=2: ($Sp(4), \pi_2$); (3) rank=4: ($SU(5), \pi_i$), $i=1,4$.

Suppose $x \in SU(2)$ has eigenvalues α and β in π_1 . Then under $4\pi_1$, it will have $\alpha^i \beta^j$, $i+j=4$ ($i, j \geq 0$) as eigenvalues, which are too many (unless $\alpha/\beta=-1$). In case 2, since 5 is odd, every element has at least one real eigenvalue, with the others coming in reciprocal pairs. Again, there is no solution. Thus the TEVP shows that

we are in case 3, i.e., that $H' \cong SU(5)$. It follows from degree theory that $[H_0, H_0] \cong SU(5)$ and from this we get the desired conclusion: $SU(5) \subset H \subset U(5)$.

We have not yet explained in what sense the topological implementations of quantum computations are efficient. Suffice it to say that there are (nearly) quadratic time algorithms due to Kitaev and Solovay (Nielsen and Chuang, 2000) for finding the braids that approximate a given quantum circuit. In practice, brute force, load-balanced searches for braids representing fundamental gates should yield accuracies on the order of 10^{-5} (within the “error threshold”). Note that these are systematic, unitary errors resulting from the fact that we are enacting a unitary transformation which is a little different from what an algorithm may ask for. Random errors, due to decoherence, are caused by uncontrolled physical processes, as discussed in the next section.

D. Errors

As discussed in Sec. II.B.2, small inaccuracies in the trajectories along which we move our quasiparticles are not a source of error. The topological class of quasiparticles' trajectories (including undesired quasiparticles) must change in order for an error to occur. Therefore, to avoid errors, one must keep careful track of all quasiparticles in the system and move them so that the intended braid is performed. As mentioned in Sec. II.B.2, stray thermally excited quasiparticles could form unintended braids with quasiparticles of our system and cause errors in the computation. Fortunately, as mentioned in Sec. II.B.2, there is a large class of such processes that actually do not result in errors. We discuss the two most important of these.

Perhaps the simplest such process that does not cause errors is when a quasiparticle-quasihole pair is thermally (or virtually) excited from the vacuum, one of the two excited particles wanders around a single quasiparticle in our system and then returns to reannihilate its partner [see Fig. 20(a)]. For the sake of argument, imagine that our initial computational system is a pair of quasiparticles in state j . At some time t_1 (marked by \times in the figure), we imagine that a quasiparticle-quasihole pair becomes excited from the vacuum. Since the pair comes from the vacuum, it necessarily has overall quantum number 1 (i.e., fusing these particles back together gives the vacuum 1). Thus the overall quantum number of all four particles is j . (In the above notation, we could draw a circle around all four particles and label it j). We then imagine that one of our newly created quasiparticle wanders around one quasiparticle of our computational system as shown in the figure. Using F matrices or braiding matrices $\hat{\sigma}$, we could compute the full state of the system after this braiding operation. Importantly, however, the overall quantum number j of all four particles is preserved.

Now at some later time t_2 the two created particles reannihilate each other and are returned to the vacuum as shown by the second \times in Fig. 20(a). It is crucial to

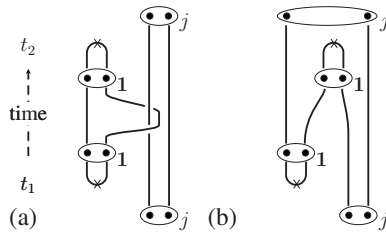


FIG. 20. Two processes involving excited quasiparticle-quasihole pairs that do not cause errors in a topological quantum computation. (a) In the process shown on the left, a quasiparticle-quasihole pair is excited at time t_1 (marked by an \times); one of these particles wraps around a quasiparticle of our computational system, and then comes back to its partner and reannihilates at a later time t_2 . When the pair is created it necessarily has the identity quantum number $\mathbf{1}$ of the vacuum, and when it annihilates, it also necessarily has this vacuum quantum number. As a result the quantum number of the computational system is not changed by this process. (b) In the process shown on the right, a quasiparticle-quasihole pair is excited at time t_1 (marked by \times); one of these particles annihilates an existing quasiparticle of our computational system at a later time t_2 , and leaves behind its partner to replace the annihilated quasiparticle of the computational system. Again, when the pair is created, it necessarily has the identity quantum number $\mathbf{1}$ of the vacuum. Similarly, the annihilating pair has the quantum number of the vacuum. As a result, the two particles remaining in the end have the same quantum numbers as the two initial quantum numbers of the computational system.

point out that, in order for two particles to annihilate, they must have the identity quantum number $\mathbf{1}$ (i.e., they must fuse to $\mathbf{1}$). The annihilation can therefore be thought of as a measurement of the quantum number of these two particles. The full state of the system then collapses to a state where the annihilating particles have quantum number $\mathbf{1}$. However, the overall quantum number of all four particles must remain in the state j . Further, in order for the overall state of the four particles to be j and the two annihilating particles to be $\mathbf{1}$, the two other (original) particles must have quantum number j . Thus, as shown in the figure, the two original quasiparticles must end up in their original state j once the created particles are reannihilated. Similarly, if the original particles had started in a superposition of states, that superposition would be preserved after the annihilation of the two excited particles. (Note that an arbitrary phase might occur, although this phase is independent of the quantum number j and therefore is irrelevant in the context of quantum computations.)

Another important process that does not cause errors is shown in Fig. 20(b). In this process, one member of a thermally excited quasiparticle-quasihole pair annihilates with one particle in our computational system, leaving behind its partner as a replacement. Again, since both the created pair and annihilating particles have the same quantum numbers as the vacuum, it is easy to see (using similar arguments as above) that the final state of the two remaining particles must be the same as that of

the original two particles; thus no errors are caused so long as the new particle is used as a replacement for the annihilated quasiparticle.

The fact that the two processes described above do not cause errors is essential to the notion of topological quantum computation. Since the created quasiparticles need not move very far in either process, these processes can occur very frequently, and can even occur virtually since they could have low total action. Thus it is crucial that these likely processes do not cause errors. The simplest processes that can actually cause error would require a thermally (or virtually) created quasiparticle-quasihole pair to braid nontrivially with at least two quasiparticles of our computational system. Since it is assumed that all quasiparticles that are part of our system are kept far from each other, the action for a process that wraps a (virtually) created quasiparticle around two different particles of our system can be arbitrarily large, and hence these virtual processes can be suppressed. Similarly, it can be made unlikely that thermally excited quasiparticles will wrap around two separate particles of our system before reannihilating. Indeed, since in two dimensions a random walk returns to its origin many times, a wandering quasiparticle may have many chances to reannihilate before it wraps around two particles of our computational system and causes errors. Nonetheless, in principle, this process is a serious consideration and has the potential to cause errors if too many quasiparticle-quasihole pairs are excited.

The probability for these error-causing processes is naively $\sim e^{-\Delta/(2T)}$ (thermally excited quasiparticles) or $\sim e^{-\Delta L/v}$ (virtual quasiparticles), where T is the temperature, Δ is the quasiparticle energy gap, L is the distance between the quasiparticles comprising a qubit, and v is a characteristic velocity. However, transport in real systems is, in fact, more complicated. Since there are different types of quasiparticles, the gap measured from the resistance may not be the smallest gap in the system. For instance, neutral fermionic excitations in the Pfaffian state $SU(2)_2$ may have a small gap, thereby leading to a splitting between the two states of a qubit if the two quasiparticles are too close together. Second, in the presence of disorder, the gap will vary throughout the system. Processes that take advantage of regions with small gaps may dominate the error rate. Furthermore, in a disordered system, variable-range hopping, rather than thermally activated transport, is the most important process. Localized quasiparticles are an additional complication. If they are truly fixed, then they can be corrected by software, but if they drift during the course of a calculation, they are a potential problem. In short, quasiparticle transport, even ordinary electrical transport, is complicated in semiconductor quantum Hall systems. A complete theory does not exist. Such a theory is essential for an accurate prediction of the error rate for topological quantum computation in non-Abelian quantum Hall states in semiconductor devices and is an important future challenge for solid state theory.

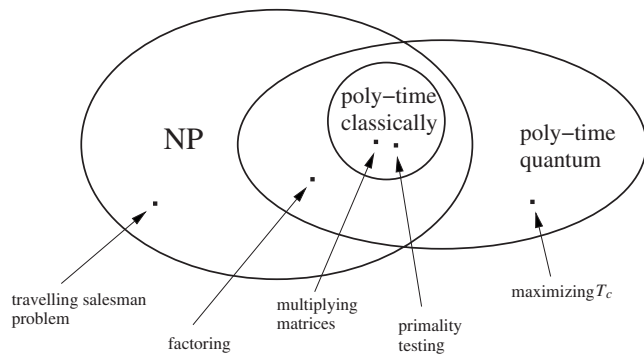


FIG. 21. A conjectural view of relative computational complexity

V. FUTURE CHALLENGES FOR THEORY AND EXPERIMENT

Quantum mechanics represented a huge revolution in thought. It was such a stretch of the imagination that many great minds and much experimental information were required to put it into place. Now, 80 years later, another collaborative effort is afoot to revolutionize computation by a particularly rich use of quantum mechanics. The preceding information revolution, which was based on the transistor, rested on the one-electron physics of semiconductors. The revolution that we advocate will require the understanding and manipulation of strongly interacting electron systems. Modern condensed matter physics has powerful tools to analyze such systems: renormalization group, conformal field theory, Bethe ansatz, dualities, and numerics. Even without the quantum computing connection, many of the most interesting problems in physics lie in this direction. Prominent here is the problem of creating, manipulating, and classifying topological states of matter.

There is a second “richness” in the connection between quantum mechanics and computation. The kind of computation that will emerge is altogether new. While the silicon revolution facilitated the same arithmetic as was done on the abacus, the quantum computer will compute in superposition. We have some knowledge about what this will allow us to do. Select mathematical problems (factoring, finding units in number fields, searching) have efficient solutions in the quantum model. Many others may succumb to quantum heuristics [e.g., adiabatic computation (Farhi *et al.*, 2000)], but we will not know until we can play with real quantum computers. Some physical problems, such as maximizing T_c within a class of superconductors, should be advanced by quantum computers, even though, viewed as math problems, they lie even outside class NP (i.e., they are very hard). A conjectural view of relative computational complexity is shown in Fig. 21.

But, before we can enter this quantum computing paradise, there are fundamental issues of physics to be tackled. The first problem is to find a non-Abelian topological phase in nature. The same resistance to local perturbation that makes topological phases astonishing (and, we hope, useful) also makes them somewhat co-

vert. An optimist might hope that they are abundant and that we are merely untutored and have trouble noticing them. At present, our search is guided primarily by a process of elimination: we have focused our attention on those systems in which the alternatives do not occur—either quantum Hall states for which there is no presumptive Abelian candidate or frustrated magnets which do not order into a conventional broken-symmetry state. What we need to do is observe some topological property of the system, e.g., create quasiparticle excitations above the ground state, braid them, and observe how the state of the system changes as a result. In order to do this, we need to be able to (i) create a specified number of quasiparticles at known positions, (ii) move them in a controlled way, and (iii) observe their state. All of these tasks are difficult, but not impossible.

It is instructive to see how these difficulties are manifested in the case of quantum Hall states and other possible topological states. The existence of a topological phase in the quantum Hall regime is signaled by the quantization of the Hall conductance. This is a special feature of those chiral topological phases in which there is a conserved current J_μ (e.g., an electrical charge or spin current). Topological invariance and P, T violation permit a nonvanishing correlation function of the form

$$\langle J_\mu(q) J_\nu(-q) \rangle = C \epsilon_{\mu\nu\lambda} q_\lambda, \quad (136)$$

where C is a topological invariant. If the topological phase does not break P and T or if there is no conserved current in the low-energy effective field theory, then there will not be such a dramatic signature. However, even in the quantum Hall context, in which we have an advantage thanks to the Hall conductance, it is still a subtle matter to determine which topological phase the system is in.

As described, we used theoretical input to focus our attention on the $\nu=5/2$ and $12/5$ states. Without such input, the available phase space is too large and signatures of a topological phase are too subtle. One benefit of having a particular theoretical model of a topological phase is that experiments can be done to verify other (i.e., nontopological) aspects of the model. By corroborating the model in this way, we gain indirect evidence about the nature of the topological phase. In the case of the $\nu=5/2$ state, the Pfaffian model wave function (Moore and Read, 1991; Greiter *et al.*, 1992) for this state is fully spin polarized. Therefore measuring the spin polarization at $\nu=5/2$ confirms this aspect of the model, thereby strengthening our belief in the model as a whole—including its topological features (see Tracy *et al.*, 2007, for such a measurement at $\nu=1/2$). In the case of Sr_2RuO_4 , the $p+ip$ BCS model predicts a nonzero Kerr rotation (Xia *et al.*, 2006). This is not a topological invariant, but when it is nonzero and the superconducting order parameter is known to be a spin triplet, we infer a nonzero spin quantum Hall effect (which is a topological invariant but is more difficult to measure). Thus nontopological measurements can teach us a great deal when we have a particular model in mind.

In frustrated magnets, one reduces the complex many-dimensional parameter space in the following way: one focuses on systems in which there is no conventional long-range order. Although it is possible for a system to be in a topological phase and simultaneously show conventional long-range order (quantum Hall ferromagnets are an example), the absence of conventional long-range order is often used as circumstantial evidence that the ground state is “exotic” (Coldea *et al.*, 2003; Shimizu *et al.*, 2003). This is a reasonable place to start, but in the absence of a theoretical model predicting a specific topological state it is unclear whether the ground state is expected to be topological or merely exotic in some other way (see below for a further discussion of this point).

While theoretical models and indirect probes can help to identify strong candidates, only the direct measurement of a topological property can demonstrate that a system is in a topological phase. If, as in the quantum Hall effect, a system has been shown to be in a topological phase through the measurement of one property (e.g., the Hall conductance), then there is still the problem of identifying which topological phase. This requires the complete determination of all of its topological properties (in principle, the quasiparticle species, their topological spins, fusion rules, and R and F matrices). Finding nontrivial quasiparticles is the first step. In the quantum Hall regime, quasiparticles carry electrical charge (generally fractional). Through capacitive measurements of quasiparticle electric charges (Goldman and Su, 1995) or from shot noise measurements (De Picciotto *et al.*, 1997; Saminadayar *et al.*, 1997), one can measure the minimal electric charges and infer the allowed quasiparticle electric charges. The observation of charge- $(e/4)$ quasiparticles by either of these methods would be an important step in characterizing the $\nu = 5/2$ state. Detecting charged quasiparticles capacitatively or through noise measurements necessitates gated samples: antidots and/or point contacts. In the case of delicate states such as $\nu = 5/2$, this is a challenge; we do not want the gates to reduce the quality of the device and excessively degrade the robustness of the states. Even if this proves not to be surmountable, it only solves the problem of measuring charged quasiparticles; it does not directly help us with nontrivial neutral quasiparticles (such as those that we believe exist at $\nu = 5/2$).

Again, a particular theoretical model of the state can be helpful. In the case of the toric code, an excited plaquette or \mathbb{Z}_2 vortex (see Secs. II.D and III.G) is a neutral spinless excitation and therefore difficult to probe. However, when such a phase arises in models of superconductor–Mott insulator transitions, \mathbb{Z}_2 vortices can be isolated by going back and forth through a direct second-order phase transition between a topological phase and a superconducting phase (Senthil and Fisher, 2001a). Consider a superconductor in an annular geometry with a single half-flux quantum vortex through the hole in the annulus. Now suppose that some parameter can be tuned so that the system undergoes a second-order phase transition into an insulating state which is a

topological phase of the toric code or \mathbb{Z}_2 variety. Then the single vortex ground state of the superconductor will evolve into a state with a \mathbb{Z}_2 vortex in the hole of the annulus. The magnetic flux will escape, but the \mathbb{Z}_2 vortex will remain. (Eventually, it will either quantum tunnel out of the system or, at finite temperature, be thermally excited out of the system. It is important to perform the experiment on shorter time scales.) If the system is then taken back into the superconducting state, the \mathbb{Z}_2 vortex will evolve back into a superconducting vortex; the flux must be regenerated, although its direction is arbitrary. Although Senthil and Fisher considered the case of a \mathbb{Z}_2 topological phase, other topological phases with direct second-order phase transitions into superconducting states will have a similar signature. On the other hand, in a nontopological phase, there will be nothing left in the insulating phase after the flux has escaped. Therefore, when the system is taken back into the superconducting phase, a vortex will not reappear. The effect described above is not a feature of the topological phase alone, but depends on the existence of a second-order quantum phase transition between this topological state and a superconducting state. However, in the circumstance that such a transition does exist between two such phases of some material, this experiment can definitively identify a topologically nontrivial neutral excitation. In practice, the system is not tuned through a quantum phase transition but instead through a finite-temperature one; however, so long as the temperature is much smaller than the energy gap for a \mathbb{Z}_2 vortex, this is an unimportant distinction. This experiment was performed on an underdoped cuprate superconductor by Wynn *et al.* (2001). The result was negative, implying that there is not a topological phase in the low-doping part of the phase diagram of that material, but the experimental technique may still prove to be a valuable way to test some other candidate material in the future. It would be interesting and useful to design analogous experiments which could exploit the possible proximity of topological phases to other long-range ordered states besides superconductors.

Even if nontrivial quasiparticles have been found, there is still the problem of determining their braiding properties. In the quantum Hall case, we described in Secs. II.C.3 and III.F how this can be done using quasiparticle tunneling and interferometry experiments. This requires even more intricate gating. However, even these difficult experiments are the most concrete that we have, and they work only because these states are chiral and have gapless edge excitations—and therefore have nontrivial dc transport properties—and because charged anyons contribute directly to these transport properties. Neutral quasiparticles are an even bigger challenge. Perhaps they can be probed through thermal transport or even, if they carry spin, through spin transport.

As shown in Sec. II.C.3, Abelian and non-Abelian interference effects are qualitatively different. Indeed, the latter may actually be easier to observe in practice. It is striking that quasiparticle interferometry, which sounds like an *application* of topological phases, is studied as a

basic probe of the state. The naive logical order is reversed: to see if a system is in a topological phase, we say (ironically) “shape the system into a simple computer and if it computes as expected, then it must have been in the suspected phase.” This is a charming inversion, but it should not close the door on the subject of probes. It is, however, important to pause and note that we now know the operational principles and methodology for carrying out quasiparticle braiding in a concrete physical system. It is therefore possible that non-Abelian anyons will be observed in the quantum Hall regime in the near future. This is truly remarkable. It would not close the book on non-Abelian anyons, but open a new chapter and encourage us to look for non-Abelian anyons elsewhere even while trying to build a quantum computer with a quantum Hall state.

One important feature of non-Abelian anyons is that they generally have multiple fusion channels. These different fusion channels can be distinguished interferometrically, as discussed in Secs. II.C.3 and III.F. This is not the only possibility. In ultracold neutral atom systems, they can be optically detected (Grosfeld *et al.*, 2007; Tewari, Das Sarma, Nayak, *et al.*, 2007), in the case of states with Ising anyons. Perhaps, in a solid, it will be possible to measure the force between two anyons. Since the two fusion channels have different energies when the anyons are close together, there will be different forces between them depending on how the anyons fuse. If an atomic force microscope can “grab” an anyon in order to measure this force, perhaps it can also be used to drag one around and perform a braid.

Thus we see that new ideas would be helpful in the search for non-Abelian topological phases. It may be the case that each physical system, e.g., FQHE, cold atoms, Sr_2RuO_4 films, etc., may be suited to its own types of measurements, such as the ones described above and in Secs. II.C.3 and III.F, but general considerations, such as topological entropy (Kitaev and Preskill, 2006; Levin and Wen, 2006), may inform and unify these investigations. Another difficulty is that, as mentioned above, we are currently searching for non-Abelian topological phases in those systems in which there is an absence of alternatives. It would be far better to have positive *a priori* reasons to look at particular systems.

This state of affairs points to the dire need for general principles, perhaps of a mathematical nature, which tell us when a system is likely to have a topological phase. Equivalently, can we define the necessary conditions for the existence of a topological phase with non-Abelian quasiparticle statistics? For contrast, consider the case of magnetism. Although there is a great deal which we do not know about magnetism, we do know that we need solids containing ions with partially filled d or f shells. Depending on the effective Coulomb interaction within these orbitals and their filling fractions, we understand how various mechanisms such as exchange and superexchange can lead to effective spin-spin interactions which, in turn, can lead to ferromagnetism, antiferromagnetism, spin-density waves, etc. We need a comparable understanding of topological phases. One direction, described

in Sec. III.G, is to analyze models in which the interactions encode some combinatorial relations, such as those associated with string nets or loop gases (Fendley and Fradkin, 2005; Freedman *et al.*, 2005a; Levin and Wen, 2005b; Fidkowski *et al.*, 2006; Fendley, 2007). However, we only have a few examples of microscopic interactions which give rise to these intermediate-scale structures. We need more general guidelines which enable us to look at a given Hamiltonian and determine if it is likely to have a non-Abelian topological phase; a more detailed analysis or experimental study could then be carried out. This is an important direction for future research because, although nature has given us the quantum Hall regime as a promising hunting ground for topological phases, the energy scales are very low. A topological phase in a transition metal oxide might have a much larger gap and therefore be much more robust.

An important problem on the mathematical side is a complete classification of topological phases. In this review, we have focused on a few examples of topological phases: those associated with $\text{SU}(2)_k$ Chern-Simons theory, especially the $k=2,3$ cases. These are part of a more general class associated with an arbitrary semi-simple Lie group G at level k . Another class is associated with discrete groups, such as phases whose effective field theories are lattice gauge theories with discrete gauge group. New topological phases can be obtained from both of these by coset constructions and/or tensoring together different effective field theories. However, a complete classification is not known. With a complete classification in hand, if we were to observe a topological phase in nature, we could identify it by comparing it against the list of topological phases. Since we have observed relatively few topological phases in nature, we have not needed a complete classification. If, however, many more are lurking, waiting to be observed, then a complete classification could be useful in the way that the closely related problem of classifying rational conformal field theories has proved useful in understanding classical and quantum critical points.

We refer here, and throughout this article, to topological phases as defined in Sec. III (and which we recapitulate below). There are many other possible exotic phases which share some characteristics of topological phases, such as the emergence of gauge fields in their low-energy theories (Wen, 2004), but do not satisfy all criteria. These do not appear to be useful for quantum computation.

Finally, the three-dimensional frontier must be mentioned. Most theory (and experiment) pertains to 2D or quasi-2D systems. In 3+1 dimensions, even the underlying mathematical structure of TQFTs is quite open. Little is known beyond finite group gauge theories. For example, we do not know if quantum information can (in the thermodynamic limit) be permanently stored at finite temperature in any three-dimensional system. [According to Dennis *et al.* (2002), this is possible in 4+1 dimensions, not possible in 2+1 dimensions, and is an open question in 3+1 dimensions.] The case of 2+1 dimensions has been the playground of anyons for

30 years. Will looplike “particles” in 3+1 dimensions be as rich a story 30 years from now?

It is fitting to end this review with a statement of the definition of a topological phase: the ground state in the presence of multiple quasiparticles or in a nontrivial topology has a stable degeneracy which is immune to weak (but finite) local perturbations. Note that the existence of an excitation gap is not needed as a part of this definition although the stability of the ground state degeneracy to local perturbations almost always necessitates the existence of an excitation gap. We have three comments about this definition. (i) Incompressible FQH states satisfy our definition and they are, so far, the only experimentally established topological phases. (ii) The existence of a topological phase does not, by itself, enable topological quantum computation—one needs quasiparticles with non-Abelian braiding statistics, and for *universal* topological quantum computation, these quasiparticles’ topological properties must belong to a class which includes $SU(2)_k$, with $k=3,5,6,7,8,9,\dots$, as discussed. (iii) Possible non-Abelian quantum Hall states, such as $\nu=5/2$ and $12/5$, are the first among several possible candidates, including Sr_2RuO_4 , which has been shown to be a chiral p -wave superconductor (Kidwingira *et al.*, 2006; Xia *et al.*, 2006), and p -wave paired cold atom superfluids.

Note added in proof

Dolev *et al.* (2008) have recently measured the low-frequency current noise (“shot noise”) at a point contact in the $\nu=5/2$ state. They find the noise to be consistent with charge- $e/4$ quasiparticles, and inconsistent with $e/2$. A quasiparticle charge of $e/4$ is consistent with paired states at $\nu=5/2$, including both the Moore-Read (Pfaffian) state and the anti-Pfaffian state, and also Abelian paired states. sdfgsdfgsdfg

In another recent experiment, Radu *et al.* (2008) measured the dependence on voltage and temperature of the tunneling current at a point contact in the $\nu=5/2$ state. They find that the current is well fit by the form $I = T^\alpha F(e^*V/k_B T)$ where $e^*=e/4$, and the exponent α and scaling function $F(x)$ appear to be consistent with predictions based on the anti-Pfaffian state, although it is premature to rule out other possible states.

In a recent paper, Peterson *et al.* (2008) have performed finite-system exact diagonalization studies which find the correct ground state degeneracy on the torus at $\nu=5/2$ and also observe the expected degeneracy between Pfaffian and anti-Pfaffian states. The key new ingredient in their calculation is the inclusion of the effects of the finite thickness of the 2D layer which also appears to enhance the overlap between the non-Abelian states and the exact numerical finite-system wave function at $\nu=5/2$.

The first two papers provide the first direct experimental evidence in support of the $5/2$ state being non-Abelian while the third paper strengthens the case from numerics.

ACKNOWLEDGMENTS

The authors are grateful for support from Microsoft Station Q, the National Science Foundation under Grant No. DMR-0411800, the Army Research Office under Grant No. W911NF-04-1-0236, LPS-NSA-CMTC, the Minerva Foundation, the Israel Science Foundation, the U.S.-Israel Binational Science Foundation, and Alcatel-Lucent Bell Labs.

APPENDIX: CONFORMAL FIELD THEORY FOR NONEXPERTS

We consider chiral conformal field theories (CFTs) in two dimensions. Chiral means that all of our fields will be functions of $z=x+iy$ only and not functions of \bar{z} . [For a good introduction to CFT, see Belavin *et al.* (1984) and Di Francesco *et al.* (1997)].

1. OPE

To describe a CFT we give its “conformal data,” including a set of primary fields, each with a conformal dimension Δ , a table of fusion rules of these fields, and a central charge c (which we will not need here, but is fundamental to defining each CFT). Data for three CFTs are given in Table II.

The operator product expansion (OPE) describes what happens to two fields when their positions approach each other. We write the OPE for two arbitrary fields ϕ_i and ϕ_j as

$$\lim_{z \rightarrow w} \phi_i(z) \phi_j(w) = \sum_k C_{ij}^k (z-w)^{\Delta_k - \Delta_i - \Delta_j} \phi_k(w), \quad (\text{A1})$$

where the structure constants C_{ij}^k are only nonzero as indicated by the fusion table. [We assume that all fields ϕ_k are primary fields. So-called “descendant” fields, which are certain types of “raising operators” applied to the primary fields, can also occur on the right-hand side, with the dimension of the descendant being greater than that of its primary by an integer. Since we are concerned only with leading singularities in the OPE, we ignore descendants. For all CFTs considered, the coefficient of the primary on the right-hand side will not vanish, although this can happen (Ardonne and Schoutens, 2007).] Note that the OPE works *inside* a correlator. For example, in the \mathbb{Z}_3 parafermion CFT (see Table II), since $\sigma_1 \times \psi_1 = \epsilon$, for arbitrary fields ϕ_i we have

$$\begin{aligned} & \lim_{z \rightarrow w} \langle \phi_1(z_1) \cdots \phi_M(z_M) \sigma_1(z) \psi_1(w) \rangle \\ & \sim (z-w)^{2/5-1/15-2/3} \langle \phi_1(z_1) \cdots \phi_M(z_M) \epsilon(w) \rangle. \end{aligned} \quad (\text{A2})$$

In addition to the OPE, there is also an important “neutrality” condition: a correlator is zero unless all fields can fuse together to form the identity field $\mathbf{1}$. For example, in the \mathbb{Z}_3 parafermion field theory $\langle \psi_2 \psi_1 \rangle \neq 0$ since $\psi_2 \times \psi_1 = \mathbf{1}$, but $\langle \psi_1 \psi_1 \rangle = 0$ since $\psi_1 \times \psi_1 = \psi_2 \neq \mathbf{1}$.

2. Conformal blocks

We look at what happens when a fusion has more than one possible result. For example, in the Ising CFT, $\sigma \times \sigma = \mathbf{1} + \psi$. Using the OPE, we have

$$\lim_{w_1 \rightarrow w_2} \sigma(w_1)\sigma(w_2) \sim \mathbf{1}/(w_1 - w_2)^{1/8} + (w_1 - w_2)^{3/8}\psi, \tag{A3}$$

where we neglected the constants C_{ij}^k . If we consider $\langle \sigma\sigma \rangle$, the neutrality condition picks out only the first term in Eq. (A3) where the two σ 's fuse to form $\mathbf{1}$. Similarly, $\langle \sigma\sigma\psi \rangle$ results in the second term of Eq. (A3) where the two σ 's fuse to form ψ which then fuses with the additional ψ to make $\mathbf{1}$.

Fields may also fuse to form the identity in more than one way. For example, in the correlator $\langle \sigma(w_1)\sigma(w_2)\sigma(w_3)\sigma(w_4) \rangle$ of the Ising CFT, the identity is obtained via two possible fusion paths—resulting in two different so-called “conformal blocks.” On the one hand, one can fuse $\sigma(w_1)$ and $\sigma(w_2)$ to form $\mathbf{1}$ and similarly fuse $\sigma(w_3)$ and $\sigma(w_4)$ to form $\mathbf{1}$. On the other hand, one can fuse $\sigma(w_1)$ and $\sigma(w_2)$ to form ψ and fuse $\sigma(w_3)$ and $\sigma(w_4)$ to form ψ , and then fuse the two resulting ψ fields together to form $\mathbf{1}$. The correlator generally gives a linear combination of the possible resulting conformal blocks. We thus think of such a correlator as living in a vector space rather than having a single value. (If we instead choose to fuse 1 with 3, and 2 with 4, we obtain two blocks that are linear combinations of the ones found by fusing 1 with 2 and 3 with 4. The resulting vector space, however, is independent of the order of fusion.) Crucially, transporting the coordinates w_i around each other makes a rotation within this vector space.

To be clear about the notion of conformal blocks, look at the explicit form of the Ising CFT correlator,

$$\lim_{w \rightarrow \infty} \langle \sigma(0)\sigma(z)\sigma(1)\sigma(w) \rangle = a_+ F_+ + a_- F_-, \tag{A4}$$

$$F_{\pm}(z) \sim [wz(1-z)]^{-1/8} \sqrt{1 \pm \sqrt{1-z}}, \tag{A5}$$

where a_+ and a_- are arbitrary coefficients. [Equations (A4) and (A5) are results of calculations not given here (Di Francesco *et al.*, 1997).] When $z \rightarrow 0$ we have $F_+ \sim z^{-1/8}$, whereas $F_- \sim z^{3/8}$. Comparing to Eq. (A3) we conclude that F_+ is the result of fusing $\sigma(0) \times \sigma(z) \rightarrow \mathbf{1}$ whereas F_- is the result of fusing $\sigma(0) \times \sigma(z) \rightarrow \psi$. As z is taken in a clockwise circle around the point $z=1$, the inner square root changes sign, switching F_+ and F_- . Thus this “braiding” (or “monodromy”) operation transforms,

$$\begin{pmatrix} a_+ \\ a_- \end{pmatrix} \rightarrow e^{2\pi i/8} \begin{pmatrix} 0 & 1 \\ 1 & 0 \end{pmatrix} \begin{pmatrix} a_+ \\ a_- \end{pmatrix}. \tag{A6}$$

Having a multiple-valued correlator (i.e., multiple conformal blocks) is a result of having such branch cuts.

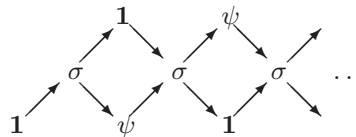


FIG. 22. Bratteli diagram for fusion of multiple σ fields in the Ising CFT.

Braiding the coordinates (w 's) around each other results in the correlator changing values within its allowable vector space.

A useful technique for counting conformal blocks is the Bratteli diagram. In Fig. 22 we give the Bratteli diagram for the fusion of multiple σ fields in the Ising CFT. Starting with $\mathbf{1}$ at the lower left, at each step moving from the left to the right, we fuse with one more σ field. At the first step, the arrow points from $\mathbf{1}$ to σ since $\mathbf{1} \times \sigma = \sigma$. At the next step σ fuses with σ to produce either ψ or $\mathbf{1}$ and so forth. Each conformal block is associated with a path through the diagram. Thus to determine the number of blocks in $\langle \sigma\sigma\sigma\sigma \rangle$ we count the number of paths of four steps in the diagram starting at the lower left and ending at $\mathbf{1}$.

3. Changing bases

As mentioned above, the space spanned by the conformal blocks resulting from the fusion of fields is independent of the order of fusion (which field is fused with which field first). However, fusing fields together in different orders results in a different basis for that space. A convenient way to denote fusion of fields in a particular order is by using fusion tree diagrams as shown in Fig. 23. Both diagrams show the fusion of three initial fields ϕ_i , ϕ_j , and ϕ_k . The diagram on the left shows ϕ_j and ϕ_k fusing together first to form ϕ_p which then fuses with ϕ_i to form ϕ_m . One could equally well have chosen to fuse together ϕ_i and ϕ_j together first before fusing the result with ϕ_k , as shown on the right of Fig. 23. The mathematical relation between these two bases is given in the equation shown in Fig. 23 in terms of the so-called F matrix (for “fusion”), which is an important property of any given CFT or TQFT. An example of using the F matrix is given in Sec. IV.B.

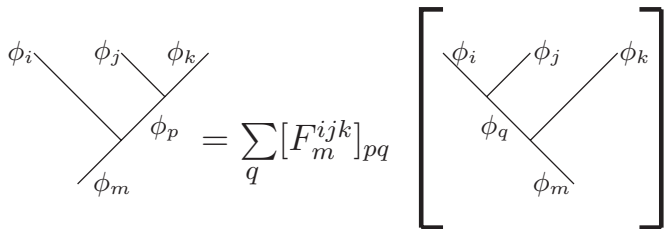


FIG. 23. Basis states obtained by fusing fields together depends on the order of fusion (although the space spanned by these states is independent of the order). The F matrix converts between the possible bases.

4. The chiral boson

A particularly important CFT is obtained from a free Bose field theory in 1+1 dimension by keeping only the left-moving modes (Di Francesco *et al.*, 1997). The free chiral Bose field $\phi(z)$, which is a sum of left-moving creation and annihilation operators, has a correlator $\langle \phi(z)\phi(z') \rangle = -\ln(z-z')$. We then define the normal ordered chiral vertex operator $:e^{i\alpha\phi(z)}:$, which is a conformal field. Note that we will typically not write the normal ordering indicators as $::$. Since ϕ is a free field, Wick's theorem can be used to obtain (Di Francesco *et al.*, 1997)

$$\begin{aligned} \langle e^{i\alpha_1\phi(z_1)} \cdots e^{i\alpha_N\phi(z_N)} \rangle &= \exp\left(-\sum_{i<j} \alpha_i\alpha_j \langle \phi(z_i)\phi(z_j) \rangle\right) \\ &= \prod_{i<j} (z_i - z_j)^{\alpha_i\alpha_j} \end{aligned} \quad (A7)$$

(strictly speaking this identity holds only if the neutrality condition $\sum_i \alpha_i = 0$ is satisfied, otherwise the correlator vanishes).

REFERENCES

- Abo-Shaer, J. R., C. Raman, J. Vogels, and W. Ketterle, 2001, "Observation of vortex lattices in Bose-Einstein condensate," *Science* **292**, 476.
- Aharonov, D., and M. Ben-Or, 1997, *Proceedings of the Twenty-Ninth Annual ACM Symposium on Theory of Computing* (ACM, New York), pp. 176-188.
- Alford, M. G., K. Benson, S. R. Coleman, J. March-Russell, and F. Wilczek, 1990, "The interactions and excitations of non-Abelian vortices," *Phys. Rev. Lett.* **64**, 1632; **65**, 668(E) (1990).
- Anderson, P. W., 1973, "Resonating valence bonds: A new kind of insulator?," *Mater. Res. Bull.* **8**, 153.
- Anderson, P. W., 1987, "The resonating valence bond state in La_2CuO_4 and superconductivity," *Science* **235**, 1196.
- Aneziris, C., A. P. Balachandran, M. Bourdeau, S. Jo, T. R. Ramadas, and R. D. Sorkin, 1989, "Statistics and general relativity," *Mod. Phys. Lett. A* **4**, 331.
- Ardonne, E., 2002, "Parafermion statistics and the application to non-Abelian quantum Hall states," *J. Phys. A* **35**, 447.
- Ardonne, E., P. Bouwknegt, and K. Schoutens, 2001, "Non-Abelian quantum Hall states—Exclusion statistics, k -matrices and duality," *J. Stat. Phys.* **102**, 421.
- Ardonne, E., and E.-A. Kim, 2008, "Hearing non-Abelian statistics from a Moore-Read double point contact interferometer," *J. Stat. Mech.: Theory Exp.* **2008**, L04001.
- Ardonne, E., and K. Schoutens, 1999, "New class of non-Abelian spin-singlet quantum Hall states," *Phys. Rev. Lett.* **82**, 5096.
- Ardonne, E., and K. Schoutens, 2007, "Wavefunctions for topological quantum registers," *Ann. Phys. (N.Y.)* **322**, 221.
- Arovas, D., J. R. Schrieffer, and F. Wilczek, 1984, "Fractional statistics and the quantum Hall effect," *Phys. Rev. Lett.* **53**, 722.
- Bais, F. A., 1980, "Flux metamorphosis," *Nucl. Phys. B* **170**, 32.
- Bais, F. A., A. Morozov, and M. de Wild Propitius, 1993, "Charge screening in the Higgs phase of Chern-Simons electrodynamics," *Phys. Rev. Lett.* **71**, 2383.
- Bais, F. A., P. van Driel, and M. de Wild Propitius, 1992, "Quantum symmetries in discrete gauge theories," *Phys. Lett. B* **280**, 63.
- Bais, F. A., P. van Driel, and M. de Wild Propitius, 1993, "Anyons in discrete gauge theories with Chern-Simons terms," *Nucl. Phys. B* **393**, 547.
- Bakalov, B., and A. Kirillov, 2001, *Lectures on Tensor Categories and Modular Functors*, University Lecture Series Vol. 21 (American Mathematical Society, Providence).
- Balatsky, A., and E. Fradkin, 1991, "Singlet quantum Hall effect and Chern-Simons theories," *Phys. Rev. B* **43**, 10622.
- Balents, L., M. P. A. Fisher, and S. M. Girvin, 2002, "Fractionalization in an easy-axis kagome antiferromagnet," *Phys. Rev. B* **65**, 224412.
- Balents, L., M. P. A. Fisher, and C. Nayak, 1998, "Nodal liquid theory of the pseudo-gap phase of high- T_c superconductors," *Int. J. Mod. Phys. B* **12**, 1033.
- Balents, L., M. P. A. Fisher, and C. Nayak, 1999, "Dual order parameter for the nodal liquid," *Phys. Rev. B* **60**, 1654.
- Balents, L., M. P. A. Fisher, and C. Nayak, 2000, "Dual vortex theory of strongly interacting electrons: A non-Fermi liquid with a twist," *Phys. Rev. B* **61**, 6307.
- Bantay, P., 1997, "The Frobenius-Schur indicator in conformal field theory," *Phys. Lett. B* **394**, 87.
- Baskaran, G., Z. Zou, and P. W. Anderson, 1987, "The resonating valence bond state and high- T_c superconductivity—A mean field theory," *Solid State Commun.* **63**, 973.
- Belavin, A. A., A. M. Polyakov, and A. B. Zamolodchikov, 1984, "Infinite conformal symmetry in two-dimensional quantum field theory," *Nucl. Phys. B* **241**, 333.
- Bena, C., and C. Nayak, 2006, "Effects of non-Abelian statistics on two-terminal shot noise in a quantum Hall liquid in the Pfaffian state," *Phys. Rev. B* **73**, 155335.
- Bergholtz, E. J., J. Kailasvuori, E. Wikberg, T. H. Hansson, and A. Karlhede, 2006, "Pfaffian quantum Hall state made simple: Multiple vacua and domain walls on a thin torus," *Phys. Rev. B* **74**, 081308.
- Berry, M. V., 1984, "Quantal phase factors accompanying adiabatic changes," *Proc. R. Soc. London, Ser. A* **392**, 45.
- Bishara, W., G. A. Fiete, and C. Nayak, 2008, "Quantum Hall states at $\nu=2/(k+2)$," *Phys. Rev. B* **77**, 241306.
- Bishara, W., and C. Nayak, 2007, "Non-Abelian anyon superconductivity," *Phys. Rev. Lett.* **99**, 066401.
- Bishara, W., and C. Nayak, 2008, "Edge states and interferometers in the Pfaffian and anti-Pfaffian states of the $\nu=5/2$ quantum Hall system," *Phys. Rev. B* **77**, 165302.
- Blanchet, C., N. Habegger, G. Masbaum, and P. Vogel, 1995, "Topological quantum field theories derived from the Kauffman bracket," *Topology* **34**, 883.
- Blok, B., and X. G. Wen, 1990, "Effective theories of the fractional quantum Hall effect: Hierarchy construction," *Phys. Rev. B* **42**, 8145.
- Blok, B., and X.-G. Wen, 1992, "Many-body systems with non-Abelian statistics," *Nucl. Phys. B* **374**, 615.
- Boeinger, G., H. Stomer, D. Tsui, A. Chang, J. Hwang, A. Cho, C. Tu, and G. Weimann, 1987, "Activation energies and localization in the fractional quantum Hall effect," *Phys. Rev. B* **36**, 7919.
- Bonderson, P., A. Kitaev, and K. Shtengel, 2006, "Detecting non-Abelian statistics in the $\nu=5/2$ fractional quantum Hall state," *Phys. Rev. Lett.* **96**, 016803.
- Bonderson, P., K. Shtengel, and J. K. Slingerland, 2006, "Probing non-Abelian statistics with quasiparticle interferometry,"

- Phys. Rev. Lett. **97**, 016401.
- Bonderson, P., K. Shtengel, and J. K. Slingerland, 2007, “Decoherence of anyonic charge in interferometry measurements,” Phys. Rev. Lett. **98**, 070401.
- Bonesteel, N. E., 1989, “Valence bonds and the Lieb-Schultz-Mattis theorem,” Phys. Rev. B **40**, 8954.
- Bonesteel, N. E., 2000, “Chiral spin liquids and quantum error-correcting codes,” Phys. Rev. A **62**, 062310.
- Bonesteel, N. E., L. Hormozi, G. Zikos, and S. H. Simon, 2005, “Braid topologies for quantum computation,” Phys. Rev. Lett. **95**, 140503.
- Bonesteel, N. E., I. A. McDonald, and C. Nayak, 1996, “Gauge fields and pairing in double-layer composite fermion metals,” Phys. Rev. Lett. **77**, 3009.
- Bonesteel, N. E., and K. Yang, 2007, “Infinite-randomness fixed points for chains of non-Abelian quasiparticles,” Phys. Rev. Lett. **99**, 140405.
- Bouwknegt, P., and K. Schoutens, 1999, “Exclusion statistics in conformal field theory—Generalized fermions and spinons for level-1 wzw theories,” Nucl. Phys. B **547**, 501.
- Bravyi, S., 2006, “Universal quantum computation with the $\nu = 5/2$ fractional quantum Hall state,” Phys. Rev. A **73**, 042313.
- Bravyi, S., and A. Kitaev, 2001, “Quantum invariants of 3-manifolds and quantum computation,” unpublished.
- Bremner, M. J., C. M. Dawson, J. L. Dodd, A. Gilchrist, A. W. Harrow, D. Mortimer, M. A. Nielsen, and T. J. Osborne, 2002, “Practical scheme for quantum computation with any two-qubit entangling gate,” Phys. Rev. Lett. **89**, 247902.
- Brennen, G. K., and J. K. Pachos, 2007, “Why should anyone care about computing with anyons?,” Proc. R. Soc. London, Ser. A **464**, 1.
- Bretin, V., S. Stock, Y. Seurin, and J. Dalibard, 2004, “Fast rotation of a Bose-Einstein condensate,” Phys. Rev. Lett. **92**, 050403.
- Calderbank, A. R., and P. W. Shor, 1996, “Good quantum error-correcting codes exist,” Phys. Rev. A **54**, 1098.
- Camino, F. E., W. Zhou, and V. J. Goldman, 2005, “Realization of a Laughlin quasiparticle interferometer: Observation of fractional statistics,” Phys. Rev. B **72**, 075342.
- Cappelli, A., L. S. Georgiev, and I. T. Todorov, 1999, “A unified conformal field theory description of paired quantum Hall states,” Commun. Math. Phys. **205**, 657.
- Cappelli, A., L. S. Georgiev, and I. T. Todorov, 2001, “Parafermion Hall states from coset projections of Abelian conformal theories,” Nucl. Phys. B **599**, 499.
- Cardy, J. L., 1986, “Operator content of two-dimensional conformally invariant theories,” Nucl. Phys. B **270**, 186.
- Cattaneo, A. S., P. Cotta-Ramusino, J. Froehlich, and M. Martellini, 1995, “Topological BF theories in 3 and 4 dimensions,” J. Math. Phys. **36**, 6137.
- Chang, C.-C., and J. K. Jain, 2004, “Microscopic origin of the next-generation fractional quantum Hall effect,” Phys. Rev. Lett. **92**, 196806.
- Chayes, J. T., L. Chayes, and S. A. Kivelson, 1989, “Valence bond ground states in a frustrated two-dimensional spin-1/2 Heisenberg antiferromagnet,” Commun. Math. Phys. **123**, 53.
- Chen, H.-D., and J. Hu, 2007, “Exact mapping between classical and topological orders in two-dimensional spin systems,” Phys. Rev. B **76**, 193101.
- Chen, Y., F. Wilczek, E. Witten, and B. Halperin, 1989, “On anyon superconductivity,” Int. J. Mod. Phys. B **3**, 1001.
- Choi, H., W. Kang, S. Das Sarma, L. N. Pfeiffer, and K. W. West, 2008, “Activation gaps of fractional quantum Hall effect in the second Landau level,” Phys. Rev. B **77**, 081301.
- Chung, S. B., and M. Stone, 2006, “Proposal for reading out anyon qubits in non-Abelian $\nu=12/5$ quantum Hall state,” Phys. Rev. B **73**, 245311.
- Chung, S. B., and M. Stone, 2007, “Explicit monodromy of Moore-Read wavefunctions on a torus,” J. Phys. A **40**, 4923.
- Coldea, R., D. Tennant, and Z. Tylczynski, 2003, “Observation of extended scattering continua characteristic of spin fractionalization in the two-dimensional frustrated quantum magnet Cs_2CuCl_4 by neutron scattering,” Phys. Rev. B **68**, 134424.
- Collins, G., 2006, “Computing with quantum knots,” Sci. Am. (Int. Ed.) **294** (4), 57.
- Cooper, N. R., and E. H. Rezayi, 2007, “Competing compressible and incompressible phases in rotating atomic Bose gases at filling factor $\nu=2$,” Phys. Rev. A **75**, 013627.
- Cooper, N. R., N. K. Wilkin, and J. M. F. Gunn, 2001, “Quantum phases of vortices in rotating Bose-Einstein condensates,” Phys. Rev. Lett. **87**, 120405.
- Das Sarma, S., M. Freedman, and C. Nayak, 2005, “Topologically protected qubits from a possible non-Abelian fractional quantum Hall state,” Phys. Rev. Lett. **94**, 166802.
- Das Sarma, S., M. Freedman, and C. Nayak, 2006, “Topological quantum computation,” Phys. Today **59** (7), 32.
- Das Sarma, S., C. Nayak, and S. Tewari, 2006, “Proposal to stabilize and detect half-quantum vortices in Strontium Ruthenate thin films: Non-Abelian braiding statistics of vortices in a $p_x + ip_y$ superconductor,” Phys. Rev. B **73**, 220502.
- Das Sarma, S., and A. Pinczuk, 1997, Eds., *Perspectives in Quantum Hall Effects: Novel Quantum Liquids in Low-Dimensional Semiconductor Structures* (Wiley, New York).
- Dean, C. R., B. A. Piot, P. Hayden, S. Das Sarma, G. Gervais, L. N. Pfeiffer, and K. W. West, 2008, “Intrinsic gap of the $\nu = 5/2$ fractional quantum Hall state,” Phys. Rev. Lett. **100**, 146803.
- de C. Chamon, C., D. E. Freed, S. A. Kivelson, S. L. Sondhi, and X. G. Wen, 1997, “Two point-contact interferometer for quantum Hall systems,” Phys. Rev. B **55**, 2331.
- Dennis, E., A. Kitaev, A. Landahl, and J. Preskill, 2002, “Topological quantum memory,” J. Math. Phys. **43**, 4452.
- De Picciotto, R., M. Reznikov, M. Heiblum, V. Umansky, G. Bunin, and D. Mahalu, 1997, “Direct observation of a fractional charge,” Nature (London) **389**, 162.
- Deser, S., R. Jackiw, and S. Templeton, 1982, “Three-dimensional massive gauge theories,” Phys. Rev. Lett. **48**, 975.
- Deutsch, D., 1985, “Quantum theory, the Church-Turing principle and the universal quantum computer,” Proc. R. Soc. London, Ser. A **400**, 97.
- Di Francesco, P., P. Mathieu, and D. Sénéchal, 1997, *Conformal Field Theory* (Springer, New York).
- Dijkgraaf, R., and E. Witten, 1990, “Topological gauge theories and group cohomology,” Commun. Math. Phys. **129**, 393.
- Dimov, I., B. I. Halperin, and C. Nayak, 2008, “Spin order in paired quantum Hall states,” Phys. Rev. Lett. **100**, 126804.
- DiVincenzo, D. P., 2000, “The physical implementation of quantum computation,” Fortschr. Phys. **48**, 771.
- Dolev, M., M. Heiblum, V. Umansky, A. Stern, and D. Mahalu, 2008, “Observation of a quarter of an electron charge at the $\nu=5/2$ quantum Hall state,” Nature (London) **452**, 829–834.
- Doplicher, S., R. Haag, and J. E. Roberts, 1971, “Local observables and particle statistics. I,” Commun. Math. Phys. **23**, 199.
- Doplicher, S., R. Haag, and J. E. Roberts, 1974, “Local observ-

- ables and particle statistics. II,” *Commun. Math. Phys.* **35**, 49.
- Douçot, B., M. V. Feigel’man, L. B. Ioffe, and A. S. Iosevich, 2005, “Protected qubits and Chern-Simons theories in Josephson junction arrays,” *Phys. Rev. B* **71**, 024505.
- Douçot, B., L. B. Ioffe, and J. Vidal, 2004, “Discrete non-Abelian gauge theories in Josephson-junction arrays and quantum computation,” *Phys. Rev. B* **69**, 214501.
- Du, R. R., H. L. Stormer, D. C. Tsui, L. N. Pfeiffer, and K. W. West, 1993, “Experimental evidence for new particles in the fractional quantum Hall effect,” *Phys. Rev. Lett.* **70**, 2944.
- Duan, L.-M., E. Demler, and M. D. Lukin, 2003, “Controlling spin exchange interactions of ultracold atoms in optical lattices,” *Phys. Rev. Lett.* **91**, 090402.
- Dyakonov, M. I., 2007, in *Future Trends in Microelectronics. Up the Nano Creek*, edited by S. Luryi, J. Xu, and A. Zaslavsky (Wiley, New York), pp. 4–18.
- Eisenstein, J. P., K. B. Cooper, L. N. Pfeiffer, and K. W. West, 2002, “Insulating and fractional quantum Hall states in the first excited Landau level,” *Phys. Rev. Lett.* **88**, 076801.
- Eisenstein, J. P., R. L. Willett, H. L. Stormer, L. N. Pfeiffer, and K. W. West, 1990, “Activation energies for the even-denominator fractional quantum Hall effect,” *Surf. Sci.* **229**, 31.
- Eliitzur, S., G. Moore, A. Schwimmer, and N. Seiberg, 1989, “Remarks on the canonical quantization of the Chern-Simons-Witten theory,” *Nucl. Phys. B* **326**, 108.
- Farhi, E., J. Goldstone, S. Gutmann, and M. Sipser, 2000, “Quantum computation by adiabatic evolution,” e-print arXiv:quant-ph/0001106.
- Fateev, V. A., and A. B. Zamolodchikov, 1985, “Parafermionic currents in the two-dimensional conformal quantum field theory and selfdual critical points in $z(n)$ invariant statistical systems,” *Sov. Phys. JETP* **62**, 215.
- Feiguin, A., P. Fendley, M. P. A. Fisher, and C. Nayak, 2008, “Non-equilibrium transport through a point contact in the $\nu = 5/2$ non-Abelian quantum Hall state,” e-print arXiv:0809.1415.
- Feiguin, A., S. Trebst, A. W. W. Ludwig, M. Troyer, A. Kitaev, Z. Wang, and M. H. Freedman, 2007, “Interacting anyons in topological quantum liquids: The golden chain,” *Phys. Rev. Lett.* **98**, 160409.
- Feiguin, A. E., E. Rezayi, C. Nayak, and S. Das Sarma, 2008, “Density matrix renormalization group study of incompressible fractional quantum Hall states,” *Phys. Rev. Lett.* **100**, 166803.
- Feldman, D. E., Y. Gefen, A. Kitaev, K. T. Law, and A. Stern, 2007, “Shot noise in anyonic Mach-Zehnder interferometer,” *Phys. Rev. B* **76**, 085333.
- Feldman, D. E., and A. Kitaev, 2006, “Detecting non-Abelian statistics with an electronic Mach-Zehnder interferometer,” *Phys. Rev. Lett.* **97**, 186803.
- Fendley, P., 2007, “Quantum loop models and the non-Abelian toric code,” e-print arXiv:0711.0014.
- Fendley, P., M. P. A. Fisher, and C. Nayak, 2006, “Dynamical disentanglement across a point contact in a non-Abelian quantum Hall state,” *Phys. Rev. Lett.* **97**, 036801.
- Fendley, P., M. P. A. Fisher, and C. Nayak, 2007a, “Edge states and tunneling of non-Abelian quasiparticles in the $\nu = 5/2$ quantum Hall state and $p + ip$ superconductors,” *Phys. Rev. B* **75**, 045317.
- Fendley, P., M. P. A. Fisher, and C. Nayak, 2007b, “Topological entanglement entropy from the holographic partition function,” *J. Stat. Phys.* **126**, 1111.
- Fendley, P., and E. Fradkin, 2005, “Realizing non-Abelian statistics in time-reversal-invariant systems,” *Phys. Rev. B* **72**, 024412.
- Fendley, P., R. Moessner, and S. L. Sondhi, 2002, “Classical dimers on the triangular lattice,” *Phys. Rev. B* **66**, 214513.
- Fetter, A., C. Hanna, and R. Laughlin, 1989, “Random-phase approximation in the fractional-statistics gas,” *Phys. Rev. B* **39**, 9679.
- Feynman, R. P., 1982, “Simulating physics with computers,” *Int. J. Theor. Phys.* **21**, 467.
- Feynman, R. P., 1986, “Quantum mechanical computers,” *Found. Phys.* **16**, 507.
- Fidkowski, L., 2007, “Double point contact in the $k=3$ Read-Rezayi state,” e-print arXiv:0704.3291.
- Fidkowski, L., M. Freedman, C. Nayak, K. Walker, and Z. Wang, 2006, “From string nets to non-Abelions,” e-print arXiv:cond-mat/0610583.
- Fiete, G. A., W. Bishara, and C. Nayak, 2008, “Multi-channel Kondo models in non-Abelian quantum Hall droplets,” e-print arXiv:0803.4205.
- Fradkin, E., M. Huerta, and G. Zemba, 2001, “Effective Chern-Simons theories of Pfaffian and parafermionic quantum Hall states, and orbifold conformal field theories,” *Nucl. Phys. B* **601**, 591.
- Fradkin, E., and L. P. Kadanoff, 1980, “Disorder variables and para-fermions in two-dimensional statistical mechanics,” *Nucl. Phys. B* **170**, 1.
- Fradkin, E., C. Nayak, and K. Schoutens, 1999, “Landau-Ginzburg theories for non-Abelian quantum Hall states,” *Nucl. Phys. B* **546**, 711.
- Fradkin, E., C. Nayak, A. Tsvetlik, and F. Wilczek, 1998, “A Chern-Simons effective field theory for the Pfaffian quantum Hall state,” *Nucl. Phys. B* **516**, 704.
- Fradkin, E., and S. H. Shenker, 1975, “Phase diagrams of lattice gauge theories with Higgs fields,” *Phys. Rev. D* **19**, 3682.
- Fredenhagen, K., K. H. Rehren, and B. Schroer, 1989, “Superselection sectors with braid group statistics and exchange algebras,” *Commun. Math. Phys.* **125**, 201.
- Freedman, M., A. Kitaev, M. Larsen, and Z. Wang, 2003, “Topological quantum computation,” *Bull., New Ser., Am. Math. Soc.* **40**, 31.
- Freedman, M., C. Nayak, and K. Shtengel, 2003, “Non-Abelian topological phases in an extended Hubbard model,” e-print arXiv:cond-mat/0309120.
- Freedman, M., C. Nayak, and K. Shtengel, 2005a, “Extended Hubbard model with ring exchange: A route to a non-Abelian topological phase,” *Phys. Rev. Lett.* **94**, 066401.
- Freedman, M., C. Nayak, and K. Shtengel, 2005b, “Line of critical points in 2+1 dimensions: Quantum critical loop gases and non-Abelian gauge theory,” *Phys. Rev. Lett.* **94**, 147205.
- Freedman, M., C. Nayak, K. Shtengel, K. Walker, and Z. Wang, 2004, “A class of P, T -invariant topological phases of interacting electrons,” *Ann. Phys. (N.Y.)* **310**, 428.
- Freedman, M., C. Nayak, and K. Walker, 2006, “Towards universal topological quantum computation in the $\nu = 5/2$ fractional quantum Hall state,” *Phys. Rev. B* **73**, 245307.
- Freedman, M. H., 2001, “Quantum computation and the localization of modular functors,” *Found. Comput. Math.* **1**, 183.
- Freedman, M. H., 2003, “A magnetic model with a possible Chern-Simons phase,” *Commun. Math. Phys.* **234**, 129.
- Freedman, M. H., M. J. Larsen, and Z. Wang, 2002a, “A modular functor which is universal for quantum computation,” *Commun. Math. Phys.* **227**, 605.

- Freedman, M. H., M. J. Larsen, and Z. Wang, 2002b, "The two-eigenvalue problem and density of Jones representation of braid groups," *Commun. Math. Phys.* **228**, 177.
- Fröhlich, J., and F. Gabbiani, 1990, "Braid statistics in local quantum theory," *Rev. Math. Phys.* **2**, 251.
- Fröhlich, J., and P. A. Marchetti, 1988, "Quantum field theory of anyons," *Lett. Math. Phys.* **16**, 347.
- Fröhlich, J., and P. A. Marchetti, 1989, "Quantum field theories of vortices and anyons," *Commun. Math. Phys.* **121**, 177.
- Fröhlich, J., and P. A. Marchetti, 1991, "Spin-statistics theorem and scattering in planar quantum field theories with braid statistics," *Nucl. Phys. B* **356**, 533.
- Fubini, S., 1991, "Vertex operators and quantum Hall effect," *Mod. Phys. Lett. A* **6**, 347.
- Fubini, S., and C. A. Lutken, 1991, "Vertex operators in the fractional quantum Hall effect," *Mod. Phys. Lett. A* **6**, 487.
- Fuchs, J., 1992, *Affine Lie Algebras and Quantum Groups* (Cambridge University Press, Cambridge, England).
- Funar, L., 1999, "On TQFT representations," *Pac. J. Math.* **188**, 251.
- Gaebler, J. P., J. T. Stewart, J. L. Bohn, and D. S. Jin, 2007, "*p*-wave feshbach molecules," *Phys. Rev. Lett.* **98**, 200403.
- Gawędzki, K., and A. Kupiainen, 1988, "G/H conformal field theory from gauged WZW model," *Phys. Lett. B* **215**, 119.
- Georgiev, L. S., 2006, "Topologically protected gates for quantum computation with non-Abelian anyons in the Pfaffian quantum Hall state," *Phys. Rev. B* **74**, 235112.
- Georgiev, L. S., and M. R. Geller, 2006, "Aharonov-Bohm effect in the non-Abelian quantum Hall fluid," *Phys. Rev. B* **73**, 205310.
- Gepner, D., and Z.-a. Qiu, 1987, "Modular invariant partition functions for parafermionic field theories," *Nucl. Phys. B* **285**, 423.
- Gepner, D., and E. Witten, 1986, "String theory on group manifolds," *Nucl. Phys. B* **278**, 493.
- Girvin, S. M., and A. H. MacDonald, 1987, "Off-diagonal long-range order, oblique confinement and the fractional quantum Hall effect," *Phys. Rev. Lett.* **58**, 1252.
- Godfrey, M. D., P. Jiang, W. Kang, S. H. Simon, K. W. Baldwin, L. N. Pfeiffer, and K. W. West, 2007, "Aharonov-Bohm-like oscillations in quantum Hall corrals," e-print arXiv:0708.2448.
- Goerbig, M. O., P. Lederer, and C. M. Smith, 2004, "Second generation of composite fermions and the self-similarity of the fractional quantum Hall effect," *Int. J. Mod. Phys. B* **18**, 3549.
- Goldin, G. A., R. Menikoff, and D. H. Sharp, 1981, "Representations of a local current algebra in nonsimply connected space and the Aharonov-Bohm effect," *J. Math. Phys.* **22**, 1664.
- Goldman, V. J., and B. Su, 1995, "Resonant tunneling in the quantum Hall regime: Measurement of fractional charge," *Science* **267**, 1010.
- Goldstone, J., and F. Wilczek, 1981, "Fractional quantum numbers of solitons," *Phys. Rev. Lett.* **47**, 986.
- Gómez, C., M. Ruiz-Altaba, and G. Sierra, 1996, *Quantum Groups in Two-Dimensional Physics*, Cambridge Monographs on Mathematical Physics (Cambridge University Press, Cambridge, England).
- Gottesman, D., 1998, "Theory of fault-tolerant quantum computation," *Phys. Rev. A* **57**, 127.
- Greiter, M., X.-G. Wen, and F. Wilczek, 1991, "Paired Hall state at half filling," *Phys. Rev. Lett.* **66**, 3205.
- Greiter, M., X. G. Wen, and F. Wilczek, 1992, "Paired Hall states," *Nucl. Phys. B* **374**, 567.
- Grosfeld, E., N. R. Cooper, A. Stern, and R. Ilan, 2007, "Predicted signatures of *p*-wave superfluid phases and Majorana zero modes of fermionic atoms in rf absorption," *Phys. Rev. B* **76**, 104516.
- Grosfeld, E., S. H. Simon, and A. Stern, 2006, "Switching noise as a probe of statistics in the fractional quantum Hall effect," *Phys. Rev. Lett.* **96**, 226803.
- Grosfeld, E., and A. Stern, 2006, "Electronic transport in an array of quasiparticles in the $\nu=5/2$ non-Abelian quantum Hall state," *Phys. Rev. B* **73**, 201303.
- Gurarie, V., and C. Nayak, 1997, "A plasma analogy and Berry matrices for non-Abelian quantum Hall states," *Nucl. Phys. B* **506**, 685.
- Gurarie, V., L. Radzihovsky, and A. V. Andreev, 2005, "Quantum phase transitions across a *p*-wave Feshbach resonance," *Phys. Rev. Lett.* **94**, 230403.
- Haldane, F. D. M., 1983, "Fractional quantization of the Hall effect: A hierarchy of incompressible quantum fluid states," *Phys. Rev. Lett.* **51**, 605.
- Halperin, B. I., 1982, "Quantized Hall conductance, current-carrying edge states, and the existence of extended states in a two-dimensional disordered potential," *Phys. Rev. B* **25**, 2185.
- Halperin, B. I., 1983, "Theory of the quantized Hall conductance," *Helv. Phys. Acta* **56**, 75.
- Halperin, B. I., 1984, "Statistics of quasiparticles and the hierarchy of fractional quantized Hall states," *Phys. Rev. Lett.* **52**, 1583.
- Halperin, B. I., P. A. Lee, and N. Read, 1993, "Theory of the half-filled Landau level," *Phys. Rev. B* **47**, 7312.
- Hansson, T. H., V. Oganesyan, and S. L. Sondhi, 2004, "Superconductors are topologically ordered," *Ann. Phys. (N.Y.)* **313**, 497.
- Harrow, A., 2001, "Quantum compiling," B.Sc. thesis (MIT, Cambridge, MA), available online at <http://www.media.mit.edu/physics/publications/theses/01.05.aram.pdf>
- He, S., S. Das Sarma, and X. C. Xie, 1993, "Quantized Hall effect and quantum phase transitions in coupled two-layer electron systems," *Phys. Rev. B* **47**, 4394.
- He, S., X. C. Xie, S. Das Sarma, and F. C. Zhang, 1991, "Quantum Hall effect in double-quantum-well systems," *Phys. Rev. B* **43**, 9339.
- Heinonen, O., 1998, *Composite Fermions* (World Scientific, Singapore).
- Henley, C. L., 1997, "Relaxation time for a dimer covering with height representation," *J. Stat. Phys.* **89**, 483.
- Hormozi, L., G. Zikos, N. E. Bonesteel, and S. H. Simon, 2007, "Topological quantum compiling," *Phys. Rev. B* **75**, 165310.
- Hou, C.-Y., and C. Chamon, 2006, "'Wormhole' geometry for entrapping topologically protected qubits in non-Abelian quantum Hall states and probing them with voltage and noise measurements," *Phys. Rev. Lett.* **97**, 146802.
- Ilan, R., E. Grosfeld, and A. Stern, 2008, "Coulomb blockade as a probe for non-Abelian statistics in Read-Rezayi states," *Phys. Rev. Lett.* **100**, 086803.
- Imbo, T. D., C. S. Imbo, and E. C. G. Sudarshan, 1990, "Identical particles, exotic statistics and braid groups," *Phys. Lett. B* **234**, 103.
- Imbo, T. D., and J. March-Russell, 1990, "Exotic statistics on surfaces," *Phys. Lett. B* **252**, 84.
- Ioffe, L. B., M. Feigel'man, V. A. Ioselevich, D. Ivanov, M. Troyer, and G. Blatter, 2002, "Topologically protected quan-

- tum bits using Josephson junction arrays,” *Nature (London)* **415**, 503.
- Ivanov, D. A., 2001, “Non-Abelian statistics of half-quantum vortices in p -wave superconductors,” *Phys. Rev. Lett.* **86**, 268.
- Jackiw, R., and C. Rebbi, 1976, “Solitons with fermion number $1/2$,” *Phys. Rev. D* **13**, 3398.
- Jackiw, R., and J. R. Schrieffer, 1981, “Solitons with fermion number $1/2$ in condensed matter and relativistic field theories,” *Nucl. Phys. B* **190**, 253.
- Jacob, P., and P. Mathieu, 2000, “Parafermionic character formulae,” *Nucl. Phys. B* **587**, 514.
- Jacob, P., and P. Mathieu, 2002, “Parafermionic quasi-particle basis and fermionic-type characters,” *Nucl. Phys. B* **620**, 351.
- Jain, J. K., 1989, “Composite-fermion approach for the fractional quantum Hall effect,” *Phys. Rev. Lett.* **63**, 199.
- Jaksch, D., and P. Zoller, 2005, “The cold atom Hubbard toolbox,” *Ann. Phys. (N.Y.)* **351**, 52.
- Ji, Y., Y. Chung, D. Sprinzak, M. Heiblum, D. Mahalu, and H. Shtrikman, 2003, “An electronic MachZehnder interferometer,” *Nature (London)* **422**, 415.
- Jolicoeur, T., 2007, “Non-Abelian states with negative flux: A new series of quantum Hall states,” *Phys. Rev. Lett.* **99**, 036805.
- Jones, V. F. R., 1985, “A polynomial invariant for knots via von Neumann algebras,” *Bull., New Ser., Am. Math. Soc.* **12**, 103.
- Kalmeyer, V., and R. B. Laughlin, 1987, “Equivalence of the resonating-valence-bond and fractional quantum Hall states,” *Phys. Rev. Lett.* **59**, 2095.
- Karabali, D., Q.-H. Park, H. J. Schnitzer, and Z. Yang, 1989, “A GKO construction based on a path integral formulation of gauged Wess-Zumino-Witten actions,” *Phys. Lett. B* **216**, 307.
- Kassel, C., 1995, *Quantum Groups* (Springer-Verlag, New York).
- Kauffman, L., 1987, “State models and the Jones polynomial,” *Topology* **26**, 395.
- Kauffman, L., and S. Lins, 1994, *Temperley-Lieb Recoupling Theory and Invariants of 3-manifolds*, Ann. Math. Stud. Vol. 134 (Princeton University Press, Princeton, NJ).
- Kauffman, L. H., 2001, *Knots and Physics*, 3rd ed. (World Scientific, Singapore).
- Kauffman, L. H., and S. J. Lomonaco, Jr., 2004, “Braiding operators are universal quantum gates,” *New J. Phys.* **6**, 134.
- Kauffman, L. H., and S. J. Lomonaco, Jr., 2007, “ q -deformed spin networks, knot polynomials and anyonic topological quantum computation,” *J. Knot Theory Ramif.* **16**, 267.
- Kawamura, T., and S. Das Sarma, 1992, “Phonon-scattering-limited electron mobilities in $\text{Al}_x\text{Ga}_{1-x}\text{As}/\text{GaAs}$ heterojunctions,” *Phys. Rev. B* **45**, 3612.
- Kidwingira, F., J. D. Strand, D. J. Van Harlingen, and Y. Maeno, 2006, “Dynamical superconducting order parameter domains in Sr_2RuO_4 ,” *Science* **314**, 1267.
- Kirtley, J. R., C. Kallin, C. W. Hicks, E. A. Kim, Y. Liu, K. A. Moler, Y. Maeno, and K. D. Nelson, 2007, “Upper limit on spontaneous supercurrents in Sr_2RuO_4 ,” *Phys. Rev. B* **76**, 014526.
- Kitaev, A. Y., 2003, “Fault-tolerant quantum computation by anyons,” *Ann. Phys. (N.Y.)* **303**, 2.
- Kitaev, A. Y., 2006, “Anyons in an exactly solved model and beyond,” *Ann. Phys. (N.Y.)* **321**, 2.
- Kitaev, A. Y., and J. Preskill, 2006, “Topological entanglement entropy,” *Phys. Rev. Lett.* **96**, 110404.
- Kitaev, A. Y., A. Shen, and M. Vyalii, 1999, *Classical and Quantum Computation* (American Mathematical Society, Providence).
- Kivelson, S. A., 1989, “Statistics of holons in the quantum hard-core dimer gas,” *Phys. Rev. B* **39**, 259.
- Kivelson, S. A., and D. S. Rokhsar, 1990, “Bogoliubov quasiparticles, spinons, and spin-charge decoupling in superconductors,” *Phys. Rev. B* **41**, 11693.
- Kivelson, S. A., D. S. Rokhsar, and J. P. Sethna, 1987, “Topology of the resonating valence-bond state: solitons and high- T_c superconductivity,” *Phys. Rev. B* **35**, 8865.
- Klein, D. J., 1982, “Exact ground states for a class of antiferromagnetic Heisenberg models with short-range interactions,” *J. Phys. A* **15**, 661.
- Knill, E., R. Laflamme, and W. H. Zurek, 1998, “Resilient quantum computation: Error models and thresholds,” *Proc. R. Soc. London, Ser. A* **454**, 365.
- Knizhnik, V. G., and A. B. Zamolodchikov, 1984, “Current algebra and Wess-Zumino model in two dimensions,” *Nucl. Phys. B* **247**, 83.
- Kogut, J. B., 1979, “An introduction to lattice gauge theory and spin systems,” *Rev. Mod. Phys.* **51**, 659.
- Koulakov, A. A., M. M. Fogler, and B. I. Shklovskii, 1996, “Charge density wave in two-dimensional electron liquid in weak magnetic field,” *Phys. Rev. Lett.* **76**, 499.
- Kuperberg, G., 1996, “Spiders for rank 2 Lie algebras,” *Commun. Math. Phys.* **180**, 109.
- Larsen, M. J., E. C. Rowell, and Z. Wang, 2005, “The n -eigenvalue problem and two applications,” *Int. Math. Res. Notices* **64**, 3987.
- Laughlin, R. B., 1981, “Quantized Hall conductivity in two dimensions,” *Phys. Rev. B* **23**, 5632.
- Laughlin, R. B., 1983, “Anomalous quantum Hall effect: An incompressible quantum fluid with fractionally charged excitations,” *Phys. Rev. Lett.* **50**, 1395.
- Laughlin, R. B., 1988a, “The relationship between high-temperature superconductivity and the fractional quantum Hall effect,” *Science* **242**, 525.
- Laughlin, R. B., 1988b, “Superconducting ground state of non-interacting particles obeying fractional statistics,” *Phys. Rev. Lett.* **60**, 2677.
- Lee, D.-H., G.-M. Zhang, and T. Xiang, 2007, “Edge solitons of topological insulators and fractionalized quasiparticles in two dimensions,” *Phys. Rev. Lett.* **99**, 196805.
- Lee, S.-S., S. Ryu, C. Nayak, and M. P. Fisher, 2007, “Particle-hole symmetry and the $\nu=5/2$ quantum Hall state,” *Phys. Rev. Lett.* **99**, 236807.
- Lee, T., and P. Oh, 1994, “Non-Abelian Chern-Simons quantum mechanics,” *Phys. Rev. Lett.* **72**, 1141.
- Leggett, A. J., 1975, “A theoretical description of the new phases of liquid ^3He ,” *Rev. Mod. Phys.* **47**, 331.
- Leinaas, J. M., and J. Myrheim, 1977, “On the theory of identical particles,” *Nuovo Cimento Soc. Ital. Fis., B* **37B**, 1.
- Levin, M., B. I. Halperin, and B. Rosenow, 2007, “Particle-hole symmetry and the Pfaffian state,” *Phys. Rev. Lett.* **99**, 236806.
- Levin, M. A., and X.-G. Wen, 2005a, “*Colloquium*: Photons and electrons as emergent phenomena,” *Rev. Mod. Phys.* **77**, 871.
- Levin, M. A., and X.-G. Wen, 2005b, “String-net condensation: A physical mechanism for topological phases,” *Phys. Rev. B* **71**, 045110.
- Levin, M. A., and X.-G. Wen, 2006, “Detecting topological order in a ground state wave function,” *Phys. Rev. Lett.* **96**,

- 110405.
- Levinson, J., N. Cooper, and V. Gurarie, 2007, “Strongly-resonant p -wave superfluids,” *Phys. Rev. Lett.* **99**, 210402.
- Lilly, M. P., K. B. Cooper, J. P. Eisenstein, L. N. Pfeiffer, and K. W. West, 1999a, “Anisotropic states of two-dimensional electron systems in high Landau levels: Effect of an in-plane magnetic field,” *Phys. Rev. Lett.* **83**, 824.
- Lilly, M. P., K. B. Cooper, J. P. Eisenstein, L. N. Pfeiffer, and K. W. West, 1999b, “Evidence for an anisotropic state of two-dimensional electrons in high Landau levels,” *Phys. Rev. Lett.* **82**, 394.
- Lo, H.-K., and J. Preskill, 1993, “Non-Abelian vortices and non-Abelian statistics,” *Phys. Rev. D* **48**, 4821.
- López, A., and E. Fradkin, 1991, “Fractional quantum Hall effect and Chern-Simons gauge theories,” *Phys. Rev. B* **44**, 5246.
- López, A., and E. Fradkin, 2004, “Fermion Chern-Simons theory of hierarchical fractional quantum Hall states,” *Phys. Rev. B* **69**, 155322.
- Mackenzie, A. P., and Y. Maeno, 2003, “The superconductivity of Sr_2RuO_4 and the physics of spin-triplet pairing,” *Rev. Mod. Phys.* **75**, 657.
- Manfra, M. J., R. de Picciotto, Z. Jiang, S. H. Simon, L. N. Pfeiffer, K. W. West, and A. M. Sergent, 2007, “Impact of spin-orbit coupling on quantum Hall nematic phases,” *Phys. Rev. Lett.* **98**, 206804.
- Manin, Y. I., 1980, *Computable and Uncomputable* (Sovetskoye Radio, Moscow), Vol. 21.
- Marzouli, A., and M. Rasetti, 2005, “Spin network setting of topological quantum computation,” *Int. J. Quantum Inf.* **3**, 65.
- McKay, W., and J. Patera, 1981, *Tables of Dimensions, Indices, and Branching Rules for Representations of Simple Lie Algebras*, Lecture Notes in Pure and Applied Mathematics Vol. 69 (Dekker, New York).
- Miller, J. B., I. P. Radu, D. M. Zumbuhl, E. M. Levenson-Falk, M. A. Kastner, C. M. Marcus, L. N. Pfeiffer, and K. W. West, 2007, “Fractional quantum Hall effect in a quantum point contact at filling fraction $5/2$,” *Nat. Phys.* **3**, 561.
- Milovanović, M., and N. Read, 1996, “Edge excitations of paired fractional quantum Hall states,” *Phys. Rev. B* **53**, 13559.
- Misguich, G., C. Lhuillier, B. Bernu, and C. Waldtmann, 1999, “Spin-liquid phase of the multiple-spin exchange Hamiltonian on the triangular lattice,” *Phys. Rev. B* **60**, 1064.
- Mochon, C., 2003, “Anyons from nonsolvable finite groups are sufficient for universal quantum computation,” *Phys. Rev. A* **67**, 022315.
- Mochon, C., 2004, “Anyon computers with smaller groups,” *Phys. Rev. A* **69**, 032306.
- Moessner, R., and S. L. Sondhi, 2001, “Resonating valence bond phase in the triangular lattice quantum dimer model,” *Phys. Rev. Lett.* **86**, 1881.
- Moessner, R., S. L. Sondhi, and P. Chandra, 1999, “Two-dimensional periodic frustrated Ising models in a transverse field,” *Phys. Rev. Lett.* **84**, 4457.
- Moller, G., and S. H. Simon, 2008, “Paired composite fermion wavefunctions,” *Phys. Rev. B* **77**, 075319.
- Moore, G., and N. Read, 1991, “Non-Abelions in the fractional quantum Hall effect,” *Nucl. Phys. B* **360**, 362.
- Moore, G., and N. Seiberg, 1988, “Polynomial equations for rational conformal field theories,” *Phys. Lett. B* **212**, 451.
- Moore, G., and N. Seiberg, 1989, “Classical and quantum conformal field theory,” *Commun. Math. Phys.* **123**, 177.
- Morf, R., and N. d’Ambrumenil, 2003, “Disorder in fractional quantum Hall states and the gap at $\nu=5/2$,” *Phys. Rev. B* **68**, 113309.
- Morf, R. H., 1998, “Transition from quantum Hall to compressible states in the second Landau level: New light on the $\nu=5/2$ enigma,” *Phys. Rev. Lett.* **80**, 1505.
- Morf, R. H., and N. d’Ambrumenil, 1995, “Stability and effective masses of composite fermions in the first and second Landau level,” *Phys. Rev. Lett.* **74**, 5116.
- Morf, R. H., N. d’Ambrumenil, and S. Das Sarma, 2002, “Excitation gaps in fractional quantum Hall states: An exact diagonalization study,” *Phys. Rev. B* **66**, 075408.
- Motrunich, O. I., 2003, “Bosonic model with z_3 fractionalization,” *Phys. Rev. B* **67**, 115108.
- Motrunich, O. I., and T. Senthil, 2002, “Exotic order in simple models of bosonic systems,” *Phys. Rev. Lett.* **89**, 277004.
- Mudry, C., and E. Fradkin, 1994a, “Mechanism of spin and charge separation in one-dimensional quantum antiferromagnets,” *Phys. Rev. B* **50**, 11409.
- Mudry, C., and E. Fradkin, 1994b, “Separation of spin and charge quantum numbers in strongly correlated systems,” *Phys. Rev. B* **49**, 5200.
- Mueller, E. J., 2004, “Artificial electromagnetism for neutral atoms: Escher staircase and Laughlin liquids,” *Phys. Rev. A* **70**, 041603.
- Murthy, G., and R. Shankar, 2003, “Hamiltonian theories of the fractional quantum Hall effect,” *Rev. Mod. Phys.* **75**, 1101.
- Nayak, C., and K. Shtengel, 2001, “Microscopic models of two-dimensional magnets with fractionalized excitations,” *Phys. Rev. B* **64**, 064422.
- Nayak, C., and F. Wilczek, 1996, “ $2n$ -quasihole states realize 2^{n-1} -dimensional spinor braiding statistics in paired quantum Hall states,” *Nucl. Phys. B* **479**, 529.
- Nielsen, M. A., and I. L. Chuang, 2000, *Quantum Computation and Quantum Information* (Cambridge University Press, Cambridge, England).
- Niu, Q., D. J. Thouless, and Y.-S. Wu, 1985, “Quantized Hall conductance as a topological invariant,” *Phys. Rev. B* **31**, 3372.
- Ortalano, M. W., S. He, and S. Das Sarma, 1997, “Realistic calculations of correlated incompressible electronic states in $\text{GaAs-Al}_x\text{Ga}_{1-x}\text{As}$ heterostructures and quantum wells,” *Phys. Rev. B* **55**, 7702.
- Oshikawa, M., Y. B. Kim, K. Shtengel, C. Nayak, and S. Tewari, 2007, “Topological degeneracy of non-Abelian states for dummies,” *Ann. Phys. (N.Y.)* **322**, 1477.
- Overbosch, B. J., and F. A. Bais, 2001, “Inequivalent classes of interference experiments with non-Abelian anyons,” *Phys. Rev. A* **64**, 062107.
- Overbosch, B. J., and X.-G. Wen, 2007, “Dynamical and scaling properties of $\nu=5/2$ interferometer,” e-print arXiv:0706.4339.
- Pachos, J. K., 2006, “Quantum computation with Abelian anyons on the honeycomb lattice,” *Int. J. Quantum Inf.* **4**, 947–954.
- Pachos, J. K., 2007, “The wavefunction of an anyon,” *Ann. Phys. (N.Y.)* **322**, 1254–1264.
- Pan, W., R. R. Du, H. L. Stormer, D. C. Tsui, L. N. Pfeiffer, K. W. Baldwin, and K. W. West, 1999, “Strongly anisotropic electronic transport at Landau level filling factor $\nu=9/2$ and $\nu=5/2$ under a tilted magnetic field,” *Phys. Rev. Lett.* **83**, 820.

- Pan, W., H. L. Stormer, D. C. Tsui, L. N. Pfeiffer, K. W. Baldwin, and K. W. West, 2001, "Experimental evidence for a spin-polarized ground state in the $\nu=5/2$ fractional quantum Hall effect," *Solid State Commun.* **119**, 641.
- Pan, W., J.-S. Xia, V. Shvarts, D. E. Adams, H. L. Stormer, D. C. Tsui, L. N. Pfeiffer, K. W. Baldwin, and K. W. West, 1999, "Exact quantization of the even-denominator fractional quantum Hall state at $\nu=5/2$ Landau level filling factor," *Phys. Rev. Lett.* **83**, 3530.
- Peterson, M. R., and S. Das Sarma, 2008, "Orbital Landau level dependence of the fractional quantum Hall effect in quasi-two-dimensional electron layers: Finite thickness effects," e-print arXiv:0801.4819.
- Peterson, M. R., Th. Jolicoeur, and S. Das Sarma, 2008, "Finite layer thickness stabilizes the Pfaffian state for the $\nu=5/2$ fractional quantum Hall effect: Wavefunction overlap and topological degeneracy," e-print arXiv:0803.0737v1.
- Pfeiffer, L., 2007, private communication.
- Popp, M., B. Paredes, and J. I. Cirac, 2004, "Adiabatic path to fractional quantum Hall states of a few bosonic atoms," *Phys. Rev. A* **70**, 053612.
- Prange, R., and S. M. Girvin, 1990, Eds., *The Quantum Hall Effect* (Springer-Verlag, New York).
- Preskill, J., 2004, "Lecture notes for physics 219: Quantum computation," available at http://www.theory.caltech.edu/~preskill/ph219/ph219_2004.html
- Radu, I. P., J. B. Miller, C. M. Marcus, M. A. Kastner, L. N. Pfeiffer, and K. W. West, 2008, "Quasiparticle tunneling in the fractional quantum Hall state at $\nu=5/2$," e-print arXiv:0803.3530v1.
- Read, N., 1989, "Order parameter and Ginzburg-Landau theory for the fractional quantum Hall effect," *Phys. Rev. Lett.* **62**, 86.
- Read, N., 1990, "Excitation structure of the hierarchy scheme in the fractional quantum Hall effect," *Phys. Rev. Lett.* **65**, 1502.
- Read, N., 2003, "Non-Abelian braid statistics versus projective permutation statistics," *J. Math. Phys.* **44**, 558.
- Read, N., 2006, "Wavefunctions and counting formulas for quasiholes of clustered quantum Hall states on a sphere," *Phys. Rev. B* **73**, 245334.
- Read, N., and B. Chakraborty, 1989, "Statistics of the excitations of the resonating-valence-bond state," *Phys. Rev. B* **40**, 7133.
- Read, N., and D. Green, 2000, "Paired states of fermions in two dimensions with breaking of parity and time-reversal symmetries and the fractional quantum Hall effect," *Phys. Rev. B* **61**, 10267.
- Read, N., and E. Rezayi, 1996, "Quasiholes and fermionic zero modes of paired fractional quantum Hall states: The mechanism for non-Abelian statistics," *Phys. Rev. B* **54**, 16864.
- Read, N., and E. Rezayi, 1999, "Beyond paired quantum Hall states: Parafermions and incompressible states in the first excited Landau level," *Phys. Rev. B* **59**, 8084.
- Rezayi, E. H., and F. D. M. Haldane, 2000, "Incompressible paired Hall state, stripe order, and the composite fermion liquid phase in half-filled Landau levels," *Phys. Rev. Lett.* **84**, 4685.
- Rezayi, E. H., and N. Read, 2006, "Non-Abelian quantized Hall states of electrons at filling factors $12/5$ and $13/5$ in the first excited Landau level," e-print arXiv:cond-mat/0608346.
- Rezayi, E. H., N. Read, and N. R. Cooper, 2005, "Incompressible liquid state of rapidly rotating bosons at filling factor $3/2$," *Phys. Rev. Lett.* **95**, 160404.
- Rokhsar, D. S., 1990, "Solitons in chiral-spin liquids," *Phys. Rev. Lett.* **65**, 1506.
- Rokhsar, D. S., and S. A. Kivelson, 1988, "Superconductivity and the quantum hard-core dimer gas," *Phys. Rev. Lett.* **61**, 2376.
- Rosenow, B., and B. I. Halperin, 2007, "Influence of interactions on flux and back-gate period of quantum Hall interferometers," *Phys. Rev. Lett.* **98**, 106801.
- Rosenow, B., B. Halperin, S. Simon, and A. Stern, 2008, "Bulk-edge coupling in the non-Abelian $\nu=5/2$ quantum Hall interferometer," *Phys. Rev. Lett.* **100**, 226803.
- Saminadayar, L., D. C. Glattli, Y. Jin, and B. Etienne, 1997, "Observation of the $e/3$ fractionally charged Laughlin quasiparticle," *Phys. Rev. Lett.* **79**, 2526.
- Scarola, V. W., J. K. Jain, and E. H. Rezayi, 2002, "Possible pairing-induced even-denominator fractional quantum Hall effect in the lowest Landau level," *Phys. Rev. Lett.* **88**, 216804.
- Schwarz, A. S., 1978, "The partition function of degenerate quadratic functional and Ray-Singer invariants," *Lett. Math. Phys.* **2**, 247.
- Schweikhard, V., I. Coddington, P. Engels, V. P. Mogendorff, and E. A. Cornell, 2004, "Rapidly rotating Bose-Einstein condensates in and near the lowest Landau level," *Phys. Rev. Lett.* **92**, 040404.
- Seidel, A., and D.-H. Lee, 2006, "Abelian and non-Abelian Hall liquids and charge-density wave: Quantum number fractionalization in one and two dimensions," *Phys. Rev. Lett.* **97**, 056804.
- Semenoff, G. W., and P. Sodano, 2006, "Stretching the electron as far as it will go," *Electron. J. Theor. Phys.* **10**, 157.
- Semenoff, G. W., and P. Sodano, 2007, "Stretched quantum states emerging from a Majorana medium," *J. Phys. B* **40**, 1479.
- Senthil, T., and M. P. A. Fisher, 2000, " z_2 gauge theory of electron fractionalization in strongly correlated systems," *Phys. Rev. B* **62**, 7850.
- Senthil, T., and M. P. A. Fisher, 2001a, "Fractionalization in the cuprates: Detecting the topological order," *Phys. Rev. Lett.* **86**, 292.
- Senthil, T., and M. P. A. Fisher, 2001b, "Fractionalization, topological order, and cuprate superconductivity," *Phys. Rev. B* **63**, 134521.
- Senthil, T., and O. Motrunich, 2002, "Microscopic models for fractionalized phases in strongly correlated systems," *Phys. Rev. B* **66**, 205104.
- Shimizu, Y., K. Miyagawa, K. Kanoda, M. Maesato, and G. Saito, 2003, "Spin liquid state in an organic Mott insulator with a triangular lattice," *Phys. Rev. Lett.* **91**, 107001.
- Shor, P. W., 1994, *Proceedings of the 35th Annual Symposium on Foundations of Computer Science*, edited by Shafi Goldwasser (IEEE Computer Society Press, Los Alamitos, CA), pp. 124–134.
- Shor, P. W., 1995, "Scheme for reducing decoherence in quantum computer memory," *Phys. Rev. A* **52**, R2493.
- Simon, S. H., 2000, "Proposal for a quantum Hall pump," *Phys. Rev. B* **61**, R16327.
- Simon, S. H., 2008, "Effect of Landau level mixing on braiding statistics," *Phys. Rev. Lett.* **100**, 116803.
- Simon, S. H., N. E. Bonesteel, M. H. Freedman, N. Petrovic, and L. Hormozi, 2006, "Topological quantum computing with only one mobile quasiparticle," *Phys. Rev. Lett.* **96**, 070503.

- Simon, S. H., E. H. Rezayi, and N. R. Cooper, 2007a, “Generalized quantum Hall projection Hamiltonians,” *Phys. Rev. B* **75**, 075318.
- Simon, S. H., E. H. Rezayi, and N. R. Cooper, 2007b, “Pseudopotentials for multiparticle interactions in the quantum Hall regime,” *Phys. Rev. B* **75**, 195306.
- Simon, S. H., E. H. Rezayi, N. R. Cooper, and I. Berdnikov, 2007, “Construction of a paired wave function for spinless electrons at filling fraction $\nu=2/5$,” *Phys. Rev. B* **75**, 075317.
- Slingerland, J. K., and F. A. Bais, 2001, “Quantum groups and non-Abelian braiding in quantum Hall systems,” *Nucl. Phys. B* **612**, 229.
- Sørensen, A. S., E. Demler, and M. D. Lukin, 2005, “Fractional quantum Hall states of atoms in optical lattices,” *Phys. Rev. Lett.* **94**, 086803.
- Steane, A., 1996a, “Multiple particle interference and quantum error correction,” *Proc. R. Soc. London, Ser. A* **452**, 2551.
- Steane, A. M., 1996b, “Error correcting codes in quantum theory,” *Phys. Rev. Lett.* **77**, 793.
- Steane, A. M., 1996c, “Simple quantum error-correcting codes,” *Phys. Rev. A* **54**, 4741.
- Stern, A., 2008, “Anyons and the quantum Hall effect—A pedagogical review,” *Ann. Phys. (N.Y.)* **323**, 204–249.
- Stern, A., and B. I. Halperin, 2006, “Proposed experiments to probe the non-Abelian $\nu=5/2$ quantum Hall state,” *Phys. Rev. Lett.* **96**, 016802.
- Stern, A., F. von Oppen, and E. Mariani, 2004, “Geometric phases and quantum entanglement as building blocks for non-Abelian quasiparticle statistics,” *Phys. Rev. B* **70**, 205338.
- Stone, M., and S.-B. Chung, 2006, “Fusion rules and vortices in p_x+ip_y superconductors,” *Phys. Rev. B* **73**, 014505.
- Stormer, H. L., L. N. Pfeiffer, K. W. Baldwin, and K. W. West, 1990, “Observation of a Bloch-Grüneisen regime in a two-dimensional electron transport,” *Phys. Rev. B* **41**, 1278.
- Su, W. P., and J. R. Schrieffer, 1981, “Fractionally charged excitations in charge-density-wave systems with commensurability 3,” *Phys. Rev. Lett.* **46**, 738.
- Su, W. P., J. R. Schrieffer, and A. J. Heeger, 1980, “Soliton excitations in polyacetylene,” *Phys. Rev. B* **22**, 2099.
- Sutherland, B., 1988, “Systems with resonating-valence-bond ground states: Correlations and excitations,” *Phys. Rev. B* **37**, 3786.
- Tao, R., and Y.-S. Wu, 1984, “Gauge invariance and fractional quantum Hall effect,” *Phys. Rev. B* **30**, 1097.
- Tewari, S., S. Das Sarma, and D. H. Lee, 2007, “An index theorem for the majorana zero modes in chiral p -wave superconductors,” *Phys. Rev. Lett.* **99**, 037001.
- Tewari, S., S. Das Sarma, C. Nayak, C. Zhang, and P. Zoller, 2007, “Quantum computation using vortices and Majorana zero modes of a p_x+ip_y superfluid of fermionic cold atoms,” *Phys. Rev. Lett.* **98**, 010506.
- Tewari, S., C. Zhang, S. Das Sarma, C. Nayak, and D.-H. Lee, 2008, “Testable signatures of quantum nonlocality in a two-dimensional chiral p -wave superconductor,” *Phys. Rev. Lett.* **100**, 027001.
- Thouless, D. J., and Y. Gefen, 1991, “Fractional quantum Hall effect and multiple Aharonov-Bohm periods,” *Phys. Rev. Lett.* **66**, 806.
- Toke, C., and J. K. Jain, 2006, “Understanding the $5/2$ fractional quantum Hall effect without the Pfaffian wave function,” *Phys. Rev. Lett.* **96**, 246805.
- Toke, C., N. Regnault, and J. K. Jain, 2007, “Nature of excitations of the $5/2$ fractional quantum Hall effect,” *Phys. Rev. Lett.* **98**, 036806.
- Tracy, L. A., J. P. Eisenstein, L. N. Pfeiffer, and K. W. West, 2007, “Spin transition in the half-filled Landau level,” *Phys. Rev. Lett.* **98**, 086801.
- Trebst, S., P. Werner, M. Troyer, K. Shtengel, and C. Nayak, 2007, “Breakdown of a topological phase: Quantum phase transition in a loop gas model with tension,” *Phys. Rev. Lett.* **98**, 070602.
- Tserkovnyak, Y., and S. H. Simon, 2003, “Monte Carlo evaluation of non-Abelian statistics,” *Phys. Rev. Lett.* **90**, 016802.
- Tsui, D. C., H. L. Stormer, and A. C. Gossard, 1982, “Two-dimensional magnetotransport in the extreme quantum limit,” *Phys. Rev. Lett.* **48**, 1559.
- Turaev, V. G., 1994, *Quantum Invariants of Knots and 3-Manifolds* (Walter de Gruyter, Berlin).
- Turaev, V. G., and O. Y. Viro, 1992, “State sum invariants of 3-manifolds and quantum $6j$ -symbols,” *Topology* **31**, 865902.
- Verlinde, E., 1988, “Fusion rules and modular transformations in 2D conformal field theory,” *Nucl. Phys. B* **300**, 360.
- Verlinde, E., 1990, *Proceedings of the International Colloquium on Modern Quantum Field Theory* (World Scientific, Singapore).
- Volovik, G. E., 1994, *The Universe in a Helium Droplet* (Oxford University Press, New York).
- Walker, K., 1991, “On Witten’s 3-manifold invariants,” available at <http://canyon23.net/math/1991TQFTNotes.pdf>
- Wan, X., Z.-X. Hu, E. H. Rezayi, and K. Yang, 2007, “Fractional quantum Hall effect at $\nu=5/2$: Ground states, non-Abelian quasiholes, and edge modes in a microscopic model,” e-print arXiv:0712.2095.
- Wan, X., K. Yang, and E. H. Rezayi, 2006, “Edge excitations and non-Abelian statistics in the Moore-Read state: A numerical study in the presence of coulomb interaction and edge confinement,” *Phys. Rev. Lett.* **97**, 256804.
- Wen, X. G., 1990, “Topological orders in rigid states,” *Int. J. Mod. Phys. B* **4**, 239.
- Wen, X. G., 1991a, “Mean-field theory of spin-liquid states with finite energy gap and topological orders,” *Phys. Rev. B* **44**, 2664.
- Wen, X. G., 1991b, “Non-Abelian statistics in the fractional quantum Hall states,” *Phys. Rev. Lett.* **66**, 802.
- Wen, X. G., 1992, “Theory of the edge states in fractional quantum Hall effects,” *Int. J. Mod. Phys. B* **6**, 1711.
- Wen, X.-G., 1999, “Projective construction of non-Abelian quantum Hall liquids,” *Phys. Rev. B* **60**, 8827.
- Wen, X.-G., 2004, *Quantum Field Theory of Many-body Systems* (Oxford University Press, New York).
- Wen, X. G., and Q. Niu, 1990, “Ground-state degeneracy of the fractional quantum Hall states in the presence of a random potential and on high-genus Riemann surfaces,” *Phys. Rev. B* **41**, 9377.
- Wen, X.-G., and Y.-S. Wu, 1994, “Chiral operator product algebra hidden in certain fractional quantum Hall wave functions,” *Nucl. Phys. B* **419**, 455.
- Wen, X. G., and A. Zee, 1992, “Classification of Abelian quantum Hall states and matrix formulation of topological fluids,” *Phys. Rev. B* **46**, 2290.
- Wen, X.-G., and A. Zee, 1998, “Topological degeneracy of quantum Hall fluids,” *Phys. Rev. B* **58**, 15717.
- Wess, J., and B. Zumino, 1971, “Consequences of anomalous ward identities,” *Phys. Lett.* **37B**, 95.
- Wilczek, F., 1982a, “Magnetic flux, angular momentum, and statistics,” *Phys. Rev. Lett.* **48**, 1144.

- Wilczek, F., 1982b, "Quantum mechanics of fractional-spin particles," *Phys. Rev. Lett.* **49**, 957.
- Wilczek, F., 1990, *Fractional Statistics and Anyon Superconductivity* (World Scientific, Singapore).
- Wilkin, N. K., J. M. F. Gunn, and R. A. Smith, 1998, "Do attractive bosons condense?," *Phys. Rev. Lett.* **80**, 2265.
- Willett, R., J. P. Eisenstein, H. L. Stormer, D. C. Tsui, A. C. Gossard, and J. H. English, 1987, "Observation of an even-denominator quantum number in the fractional quantum Hall effect," *Phys. Rev. Lett.* **59**, 1776.
- Willett, R., H. Stormer, D. Tsui, A. Gossard, and J. English, 1988, "Quantitative experimental test for the theoretical gap energies in the fractional quantum Hall effect," *Phys. Rev. B* **37**, 8476.
- Willett, R. L., M. J. Manfra, L. N. Pfeiffer, and K. W. West, 2007, "Confinement of fractional quantum Hall states in narrow conducting channels," *Appl. Phys. Lett.* **91**, 052105.
- Witten, E., 1983, "Global aspects of current algebra," *Nucl. Phys. B* **223**, 422.
- Witten, E., 1989, "Quantum field theory and the Jones polynomial," *Commun. Math. Phys.* **121**, 351.
- Witzel, W. M., and S. Das Sarma, 2006, "Quantum theory for electron spin decoherence induced by nuclear spin dynamics in semiconductor quantum computer architectures: Spectral diffusion of localized electron spins in the nuclear solid-state environment," *Phys. Rev. B* **74**, 035322.
- Wojs, A., 2001, "Electron correlations in partially filled lowest and excited Landau levels," *Phys. Rev. B* **63**, 125312.
- Wojs, A., and J. J. Quinn, 2002, "Electron correlations in a partially filled first excited Landau level," *Physica E (Amsterdam)* **12**, 63.
- Wojs, A., and J. J. Quinn, 2006, "Landau level mixing in the $\nu=5/2$ fractional quantum Hall state," *Phys. Rev. B* **74**, 235319.
- Wojs, A., D. Wodzinski, and J. J. Quinn, 2006, "Second generation of Moore-Read quasiholes in a composite-fermion liquid," *Phys. Rev. B* **74**, 035315.
- Wojs, A., K.-S. Yi, and J. J. Quinn, 2004, "Fractional quantum Hall states of clustered composite fermions," *Phys. Rev. B* **69**, 205322.
- Wu, Y.-S., 1984, "General theory for quantum statistics in two dimensions," *Phys. Rev. Lett.* **52**, 2103.
- Wynn, J. C., D. A. Bonn, B. W. Gardner, Y.-J. Lin, R. Liang, W. N. Hardy, J. R. Kirtley, and K. A. Moler, 2001, "Limits on spin-charge separation from $h/2e$ fluxoids in very underdoped $\text{YBa}_2\text{Cu}_3\text{O}_{6+x}$," *Phys. Rev. Lett.* **87**, 197002.
- Xia, J., Y. Maeno, P. T. Beyersdorf, M. M. Fejer, and A. Kapitulnik, 2006, "High resolution polar Kerr effect measurements of Sr_2RuO_4 : Evidence for broken time-reversal symmetry in the superconducting state," *Phys. Rev. Lett.* **97**, 167002.
- Xia, J. S., W. Pan, C. L. Vicente, E. D. Adams, N. S. Sullivan, H. L. Stormer, D. C. Tsui, L. N. Pfeiffer, K. W. Baldwin, and K. W. West, 2004, "Electron correlation in the second Landau level: A competition between many nearly degenerate quantum phases," *Phys. Rev. Lett.* **93**, 176809.
- Zhang, C., V. Scarola, S. Tewari, and S. Das Sarma, 2008, "Anyonic braiding in optical lattices," *Proc. Natl. Acad. Sci. U.S.A.* **105**, 5945.
- Zhang, C., S. Tewari, and S. Das Sarma, 2007, "Bell's inequality and universal quantum gates in a cold atom chiral fermionic p-wave superfluid," *Phys. Rev. Lett.* **99**, 220502.
- Zhang, F., and S. Das Sarma, 1986, "Excitation gap in the fractional quantum Hall effect: Finite layer thickness corrections," *Phys. Rev. B* **33**, 2903.
- Zhang, S. C., T. H. Hansson, and S. Kivelson, 1989, "Effective-field-theory model for the fractional quantum Hall effect," *Phys. Rev. Lett.* **62**, 82.